

# **Ventricular myocyte sarcolemmal K<sub>ir</sub>6.1/SUR2B potassium channels; A potential effector of cardioprotection**

Thesis submitted for the degree of  
Doctor of Philosophy  
at the University of Leicester

by

Shen Chen (MSc)  
Department of Cardiovascular Sciences  
University of Leicester

2018

## Abstract

$K_{ATP}$  channels are ubiquitously expressed and are said to couple cellular metabolic state and electrical excitability. The  $K_{ATP}$  channel complex is composed of two subunits in a hetero-octameric structure, with  $K_{ir}6$  subunit form the pore and sulphonylurea receptors (SUR) as  $\beta$ -subunits. In the heart,  $K_{ATP}$  channels are considered to be composed of the  $K_{ir}6.2/SUR2A$  combination and play a key role in responding to metabolic stress as well as in cardioprotection. It is hypothesised that opening of the cardiac Sarco $K_{ATP}$  channel shortens the action potential duration so reducing the ATP consumption during an ischaemic event to preserve energy and so limit  $Ca^{2+}$  overload.

Previous data (unpublished) suggested there was a  $K_{ir}6.1$ -like current, with constitutive activity, on the rat cardiomyocyte sarcolemmal membrane. In this study, firstly, the  $K_{ir}6.1$ -like channel was formally identified by using electrophysiology patch clamp and specific pharmacological inhibitors. Secondly, further evidence was acquired using specific knockdown the pore-forming and  $\beta$ -subunits using adenoviral-introduced shRNA. Finally, for Sarco $K_{ir}6.1$  current was investigated in control cardiomyocytes and in IPC, adenosine-induced cardioprotection and sex-specific cardioprotection.

In this study, a new small-conductance  $K_{ATP}$  channel was identified at the cardiac sarcolemmal surface along with the large-conductance channel. These findings suggest that there are two components to  $I_{KATP}$  in the heart,  $I_{KATP-SC}$ , composed of  $K_{ir}6.1/SUR2B$  subunits, and  $I_{KATP-LC}$  which is the classically thought of cardiac  $K_{ir}6.2/SUR2A$  complex. It is suggested the newly discovered  $I_{KATP-SC}$  plays an important role in regulating action potential duration as well as mediating cardioprotection. This  $I_{KATP-SC}$  may help explain the role that cardiac sarcolemmal  $K_{ATP}$  plays in cardioprotection.

## Acknowledgements

This PhD thesis is the culmination of my 4 years of research during my PhD period. This would never have been accomplished without the great help and guidance from my supervisor Dr Richard Rainbow, in both academic and my life during these 4 years. Also, my co-supervisors, Dr Noel Davies and Dr Dave Lodwick, without your support, I could not have got this far in my PhD project. Special thanks go to the post-doc in the lab group, also my associate supervisor, Dr Sean Brennan, for all the advice and help with my thesis and my experiments.

I would also like to thank Dr Nina Storey, Dr John Mitcheson and Mrs Sonja Khemiri, whose generous advice and help in my experiments allowed me to complete this work. I would also like to thank Dr Lory Francescut, for her generous help and support when using the lab equipment. In addition, thanks to anyone who has helped me and given advice in the lab who I have forgotten! Thank you all.

Thank you to Dr Karl Herbert and Kim Mason for your help in the administration and nagging me when I've forgotten my paperwork so I can have a better chance of focusing on my study.

Finally, thanks to my parents and family, without your support I could not have possibly finished my PhD. Big thanks to my Mom and Dad, I could have never accomplished my PhD without your love and your support. Also, special thanks to Qi Yue, who selflessly motivated me and helps and encourages me through the days and nights at the end of my writing stage.

# Table of Contents

<b>Abstract</b>	<b>i</b>
<b>Acknowledgements</b>	<b>ii</b>
<b>Table of Contents</b>	<b>iii</b>
<b>List of Figures</b>	<b>xii</b>
<b>List of Tables</b>	<b>xvii</b>
<b>Abbreviations</b>	<b>xviii</b>
<b>Chapter 1 Introduction</b>	<b>1</b>
1.1 Whole heart structure and physiological roles	2
1.2 Cardiomyocytes	3
1.2.1 Structural components	3
1.2.2 Sarcomeres	4
1.2.3 T-tubule system	5
1.2.4 Excitation contraction coupling	5
1.3 Membrane transport in cardiomyocytes	6
1.3.1 Ion channels	7
1.3.1.1 Sodium currents	9
1.3.1.2 Calcium currents	9
1.3.1.3 Potassium currents	10
1.3.1.3.1 $I_{to}$	10
1.3.1.3.2 $I_{kr}$	11

1.3.1.3.3	$I_{ks}$	12
1.3.1.3.4	$I_{kl}$	13
1.3.2	Intracellular ion channels and their role in excitation contraction coupling	13
1.3.3	ATPases	14
1.3.4	Carriers and transporters	15
1.3.5	Gap junctions	15
1.4	ATP-sensitive Potassium ( $K_{ATP}$ ) channels	16
1.4.1	Distribution of $K_{ATP}$ channels and its diverse roles	21
1.4.1.1	Pancreas	21
1.4.1.2	Smooth muscle	22
1.4.1.3	Skeletal muscle	23
1.4.1.4	Brain	23
1.4.1.5	Heart	24
1.4.2	Pharmacology of $K_{ATP}$ channels	24
1.4.3	$K_{ATP}$ channels and their role in diseases	27
1.4.3.1	Cardiac $K_{ATP}$ channels in diseases	28
1.4.4	$K_{ATP}$ channel knockout models and what they tell us	28
1.5	The cardiac action potential	29
1.5.1	The human ventricular cardiac action potential and the Ion channels underlying phases 0 to IV	29
1.5.1.1	The electrical conduction system in the heart:	30
1.5.1.1.1	Sinoatrial node	30
1.5.1.1.2	Atrioventricular Node	31

1.5.1.1.3	Ventricular action potentials and regional variations	32
1.5.1.1.3.1	Purkinje fibres	32
1.5.1.1.3.2	base to apex	33
1.5.1.1.3.3	endo to epicardial	33
1.5.2	Modulation of the cardiac action potential	34
1.5.2.1	Modulation of the cardiac action potential by parasympathetic nervous system (PSNS) control	34
1.5.2.2	Modulation of the cardiac action potential by sympathetic nervous system (SNS) drive	35
1.5.2.3	Pharmacological modulation of the action potential	35
1.5.3	Species variation in the cardiac action potential	38
1.5.4	Diseases altering the cardiac action potential	39
1.1.1.1	Long QT syndrome	39
1.5.4.1	Arrhythmias	40
1.5.4.1.1	Ventricular arrhythmias	41
1.5.4.1.2	Atrial arrhythmias	41
1.6	Metabolism in the heart	41
1.6.1	Substrate utilisation	42
1.6.1.1	Fatty acid metabolism	42
1.6.1.2	Glycolytic metabolism	42
1.6.2	Metabolic changes in disease states	43
1.7	Ischaemic damage	44
1.7.1	Acute coronary syndromes	45

1.7.1.1	Myocardial infarction and unstable angina	46
1.7.2	Heart failure	46
1.8	Cardioprotection	47
1.8.1	Overview of cardioprotection	47
1.8.2	Cell signalling in cardioprotection	47
1.8.3	Ischaemic preconditioning	50
1.8.4	Ischaemic post-conditioning	52
1.8.5	Remote conditioning	52
1.8.6	Pharmacological preconditioning	53
1.8.7	K <sub>ATP</sub> channels and cardioprotection	54
1.8.7.1	The mitochondrial K <sub>ATP</sub> in cardioprotection	54
1.8.7.2	The role of the sarcolemmal K <sub>ATP</sub> (K <sub>ir</sub> 6.2/SUR2A) in cardioprotection	57
1.9	The use of RNA interference in electrophysiology	58
1.9.1	RNAi, background and mechanism	58
1.9.2	Advantages and disadvantages of the RNAi technique over conventional knockout, inducible knockout or CRISPR animal models	60
1.10	Aims and hypotheses	62
<b>Chapter 2 Materials and Methods</b>		<b>64</b>
2.1	Introduction	65
2.2	Solutions	65
2.2.1	Cardiomyocyte isolation and extracellular perfusion solutions	65
2.2.2	Western Blotting	66
2.2.3	Electrophysiology solutions	69

2.3	Cardiomyocyte isolation protocol	69
2.3.1	Ischaemic preconditioning protocol	70
2.4	Cell culture & infection	71
2.4.1	HEK 293 A culturing protocol	71
2.4.2	HEK 293 A transfection	71
2.4.3	Adenovirus replication protocol	72
2.4.4	Cardiomyocyte culture & infection protocol	73
2.4.4.1	Adenovirus infection efficiency	74
2.5	Protein Extraction and Bradford Protein Assay	74
2.6	Western blotting	75
2.7	Electrophysiology	76
2.7.1	Apparatus for patching	76
2.7.2	Electrode preparation	77
2.7.3	Membrane potentials & ionic flux	77
2.7.4	Patch-Clamp: Cell-attached Configuration	78
2.7.4.1	Voltage-step measurement protocol	80
2.7.5	Patch-Clamp: Whole-cell Recording Configuration	80
2.8	Phenotypic screening	82
2.9	Fluorescent imaging	82
2.10	Statistical Analysis	84
<b>Chapter 3 The identification of a ~39 pS-conductance SarcoK<sub>ATP</sub> in cardiomyocyte</b>		<b>85</b>
3.1	Introduction	86

3.2	Results	87
3.2.1	Identification of a channel active under resting conditions with a single channel current amplitude of ~5 pA	87
3.2.2	Determination of the single channel conductance of the recorded currents using cell attached patch on cardiomyocytes	89
3.2.3	The effect of glibenclamide, a non-selective $K_{ATP}$ inhibitor, on the ~39 pS-conductance channel	91
3.2.4	The effect of PNU37883A (a $K_{ir}6.1$ specific blocker) on the ~39 pS-current	93
3.2.5	Calcium transients in cardiomyocyte are prolonged by PNU37883A treatment.	99
3.2.6	Effect of rosiglitazone on the ~39 pS-conductance channel in rat cardiomyocytes	101
3.2.7	Identification of the ~39 pS-conductance channel in cardiomyocytes of other species	103
3.2.8	Calcium transients in guinea pig cardiomyocyte can be prolonged by PNU37883A treatment in calcium fluorescence imaging.	105
3.3	Discussion	107
<b>Chapter 4 Identification of the molecular nature of the ~39 pS-current expressed at the cardiomyocyte membrane using shRNA</b>		<b>114</b>
4.1	Introduction	115
4.2	Results	116
4.2.1	The $K_{ir}6.1$ -like channel remains functional in cardiomyocytes following 24 h culture	116

4.2.2	The open probability of the ~39 pS-conductance channel was reduced following adenoviral infection with a $K_{ir}6.1$ -specific targeting shRNA	118
4.2.3	Western blot analysis in fresh isolated, 24 h cultured and $K_{ir}6.1$ knockdown cardiomyocyte.	123
4.2.4	The open probability of the $K_{ir}6.1$ channel was reduced following adenoviral infection with a specific SUR2B, but not SUR2A, targeting shRNA	125
4.2.5	Infection with a shRNA against the $K_{ir}6.2$ subunit causes a reduction in the MI-activated currents measured using whole-cell recording.	128
4.2.6	Knocking down $K_{ir}6.1$ prolongs the cardiac action potential in rat and guinea pig cultured cardiomyocytes	131
4.2.7	Functional effects of SUR knockdown on cardiac action potential duration and resting membrane potential in rat cultured cardiomyocytes	138
4.3	Discussion	142
4.3.1	The functional role of $K_{ir}6.1$ /SUR2B in cardiomyocytes	145
<b>Chapter 5</b>	<b>The physiological role of <math>K_{ir}6.1</math>/SUR2B channel at the cardiomyocyte cell surface.</b>	<b>148</b>
5.1	Introduction	149
5.2	Results	150
5.2.1	The effect of pharmacological inhibition of $K_{ir}6.1$ /SUR2B currents in freshly isolated cardiomyocytes in a metabolic inhibition and reperfusion (MI/R) protocol	150
5.2.2	The effect of isoform-specific subunit knockdown on cardiomyocyte contractile recovery and survival in MI/R.	154

5.2.3	$K_{ir}6.1$ knockdown causes early calcium and magnesium accumulation during metabolic inhibition.	158
5.3	Discussion	162
<b>Chapter 6 A role for cardiomyocyte sarcolemmal <math>K_{ir}6.1</math>/SUR2B in cardioprotection</b>		<b>167</b>
6.1	Introduction	168
6.2	Results	169
6.2.1	3 $\mu$ M PNU37883A reduces the protection imparted by ischaemic preconditioning.	169
6.2.2	The increasing whole-cell residual leak current and APD shortening in IPC myocyte can be reversed by 3 $\mu$ M PNU treatment.	175
6.2.3	Increasing in Sarco $K_{ir}6.1$ /SUR2B channel activity following a metabolic stress/reperfusion cycle in cell-attached recording, in both rat and guinea pig cardiomyocytes.	179
6.2.4	Cardioprotection imparted by a 5 min pre-treatment with adenosine is abolished by 3 $\mu$ M PNU37883A.	182
6.2.5	Differences in Sarco $K_{ir}6.1$ /SUR2B open probability on cardiomyocytes between male and female littermates.	186
6.3	Discussion	188
<b>Chapter 7 General Discussion</b>		<b>194</b>
7.1	$K_{ir}6.1$ /SUR2B: an unexpected finding at the cardiac sarcolemmal membrane surface	195
7.1.1	Evidence for a $K_{ir}6.1$ /SUR2B at the sarcolemmal membrane	196

7.1.2	Evidence in the literature that $K_{ir}6.1/SUR2B$ is expressed in cardiomyocytes	197
7.2	A role for $K_{ir}6.1$ in cardiac function?	199
7.2.1	The differences in function and activity of $K_{ir}6.1/SUR2B$ and $K_{ir}6.2/SUR2A$	200
7.2.2	Pharmacological and electrophysiological function	201
7.2.3	Does $K_{ir}6.1/SUR2B$ explain the disconnection between $K_{ATP}$ function and observable pharmacological modulation of the heart?	202
7.3	Is cardiac sarcolemmal $K_{ir}6.1/SUR2B$ a key effector of cardioprotection?	203
7.3.1	Hypothesis for a role of $K_{ir}6.1/SUR2B$ and not $K_{ir}6.2/SUR2A$ in cardioprotection	203
7.3.2	What mechanism might be modulating $K_{ir}6.1/SUR2B$ ?	206
7.4	Future directions for research	208
7.5	Conclusions	209
	<b>References</b>	<b>211</b>

## List of Figures

Figure 1.1: A diagram of whole heart structure.....	2
Figure 1.2: A diagram of sarcomere. ....	4
Figure 1.3: The unique channel kinetics for hERG channel.....	12
Figure 1.4: Structure of $K_{ir}6.x$ $K_{ATP}$ channel. ....	19
Figure 1.5: $K_{ATP}$ channel regulates the secretion of insulin in $\beta$ -pancreatic cells. ....	22
Figure 1.6: Diagram showing the point of action of different classes of antiarrhythmic drugs.....	36
Figure 1.7: Action potential in distinct species, recorded from guinea pig, rat, rabbit and human ventricular myocyte.....	38
Figure 1.8: An example ECG from Lead II. ....	40
Figure 1.9: Brief diagram of cardiac emerge metabolism, with substrates of fatty acid, lactate and glucose. ....	44
Figure 1.10: A diagram of NO/PKG, RISK and SAFE cardioprotective signal pathway. ....	48
Figure 2.1: A brief diagram for cell-attached configuration and whole-cell recording configuration. ....	81
Figure 3.1: Identification of a small conductance, metabolically insensitive, current in cell- attached patch recording from rat cardiomyocytes. ....	88
Figure 3.2: A $\sim 39$ pS current is active in rat cardiomyocytes in normal Tyrode's solution and metabolic inhibition activates a $\sim 78$ pS $K_{ir}6.2$ channel. ....	90
Figure 3.3: $10 \mu\text{M}$ Glibenclamide treatment supresses the small-conductance current at the cardiac sarcolemmal membrane.....	92

Figure 3.4: PNU37883A, a $K_{ir}6.1$ specific channel blocker, suppresses the small conductance current at the cardiac sarcolemmal membrane.....	93
Figure 3.5: The $K_{ir}6.1$ specific blocker PNU37883A (PNU) partially inhibits the glibenclamide sensitive current activated by pinacidil. ....	95
Figure 3.6: 3 $\mu$ M PNU37883A blocks glibenclamide sensitive leak current. ....	96
Figure 3.7: 3 $\mu$ M PNU37883A prolonged action potential duration as well as depolarize resting membrane potential. ....	98
Figure 3.8: Measuring rat cardiomyocyte $Ca^{2+}$ transient in action potential duration using the single wavelength $Ca^{2+}$ indicator, Fluo-4.....	100
Figure 3.9: Rosiglitazone suppressed the $\sim 39$ pS-conductance currents on cardiac sarcolemmal membrane. ....	102
Figure 3.10: The 39 pS-conductance channel current recorded from other species cardiomyocytes. ....	104
Figure 3.11: Measuring guinea pig cardiomyocyte $Ca^{2+}$ transient in action potential duration by single wavelength $Ca^{2+}$ indicator, Fluo-4. ....	106
Figure 4.1: Both small-conductance ( $K_{ir}6.1$ -like) and known sarcolemmal $K_{ATP}$ channel ( $K_{ir}6.2$ ) are expressed in cardiomyocytes after 24 h in culture.....	117
Figure 4.2: $K_{ir}6.1$ specific targeting shRNA ( $K_{ir}6.1A$ ) reduces the small-conductance channel activity following 24 h adenoviral infection. ....	119
Figure 4.3: $K_{ir}6.1$ specific targeting shRNA $K_{ir}6.1B$ reduced the small-conductance channel activity following 24 h adenoviral infection. ....	120
Figure 4.4: $K_{ir}6.1$ specific targeting shRNA $K_{ir}6.1$ A&B reduced the small-conductance channel activity. ....	121

Figure 4.5: $K_{ir}6.1$ current is unaltered in both negative control virus and $K_{ir}6.2$ knockdown, compared with 24 h culture cardiomyocyte.....	122
Figure 4.6: Analysis of $K_{ir}6.1$ protein expression in freshly isolated, 24 h cultured and $K_{ir}6.1$ KD cardiomyocyte by western blot.....	124
Figure 4.7: SUR2B specific targeting shRNA reduced the $K_{ir}6.1$ -containing channel activity following 24 h adenoviral infection. ....	126
Figure 4.8: SUR2A specific targeting shRNA has no reduction effect on the $K_{ir}6.1$ -containing channel activity following 24 h adenoviral infection.....	127
Figure 4.9: Measuring both whole cell leak currents and MI induce currents in whole-cell recording configuration in all 24 h culture, negative control and $K_{ir}6.2$ knockdown.....	130
Figure 4.10: $K_{ir}6.1$ knockdown & PNU mediate to change action potential duration in 24 h culture rat cardiomyocyte. ....	132
Figure 4.11: $K_{ir}6.2$ knockdown & negative control infection does not change the action potential duration in 24 h culture rat cardiomyocyte. ....	133
Figure 4.12: PNU37883A prolonged the action potential duration in 24 h cultured guinea pig cardiomyocytes. ....	135
Figure 4.13: $K_{ir}6.1$ targeting shRNA ( $K_{ir}6.1$ A&B) prolonged the action potential duration in 24 h cultured guinea pig cardiomyocytes. ....	137
Figure 4.14: Effect of infect both of SUR specific targeting shRNA (SUR2A/SUR2B) on action potential duration in 24 h culture cardiomyocyte. ....	139

Figure 4.15: PNU and Glibenclamide treatments alter the action potential duration in both 24 h cultured and SUR2A knockdown cardiomyocyte but not SUR2B knockdown.....	141
Figure 5.1: 3 $\mu$ M PNU treatment leads to early contractile failure, decreased contractile recovery and decreased cell survival with a metabolic inhibition and reperfusion (MI/R) protocol.....	151
Figure 5.2: The cardiotoxic effect of 3 $\mu$ M PNU treatments is more clearly revealed using a modified MI/R protocol. ....	153
Figure 5.3: Contractile recovery and percentage cell survival was reduced in $K_{ir}6.1$ KD and $K_{ir}6.2$ KD infected cells compared with 24 h cultured and negative control. .	155
Figure 5.4: Decreasing in contractile recovery rate and percentage cell survival after MI/R protocol on SUR2B KD myocytes compared with 24 h control and negative control. ....	156
Figure 5.5: 3 $\mu$ M PNU treatments reduce contractile recovery following a MI/R protocol as well as percentage cell survival in 24 h control, negative control and $K_{ir}6.2$ KD. ....	157
Figure 5.6: The effect of $K_{ir}6.1$ KD on $Ca^{2+}$ during metabolic inhibition. ....	159
Figure 5.7: The effects of subunit knockdown on the changes in Magnesium Green fluorescence intensity on 24 h cultured, $K_{ir}6.1$ knockdown and SUR2B knockdown cardiomyocyte. ....	161
Figure 6.1: 3 $\mu$ M treatments attenuate the cardioprotective effect in ischemia preconditioning cardiomyocyte. ....	170

Figure 6.2: An increased open probability of cardiac sarcolemmal $K_{ir}6.1$ channels following IPC. ....	172
Figure 6.3: PNU37883A inhibits the up-regulated $K_{ir}6.1$ activity in IPC cells, as well as shortening the time to $K_{ir}6.2$ activation during MI. ....	174
Figure 6.4: Glibenclamide sensitive leak current was also sensitive to 3 $\mu$ M PNU37883 A in IPC cardiomyocyte. ....	176
Figure 6.5: 3 $\mu$ M PNU treatment reverses the shortening of the APD seen following IPC. ....	178
Figure 6.6: Increasing Sarco $K_{ir}6.1$ /SUR2B channel activity after a metabolic stress/reperfusion cycle in cell-attached recording from rat cardiomyocytes. .	180
Figure 6.7: Increasing expression of Sarco $K_{ir}6.1$ /SUR2B current after a metabolic stress/reperfusion cycle in cell-attached recording from guinea pig (GP) cardiomyocytes. ....	181
Figure 6.8: 3 $\mu$ M PNU treatment attenuates the enhanced cell survival following adenosine pre-treatment. ....	183
Figure 6.9: Adenosine pre-treatment up-regulates cardiac sarcolemmal $K_{ir}6.1$ currents and delays the activation of $K_{ir}6.2$ currents during MI. ....	185
Figure 6.10: Up-regulation of cardiac sarcolemmal $K_{ir}6.1$ currents in female Wister rat, with delayed activation of $K_{ir}6.2$ currents during MI. ....	187

## List of Tables

Table 1.1: Approximate ionic concentrations for the intracellular and extracellular environment in cardiac tissue. ....	7
Table 1.2: Distribution of functional $K_{ATP}$ channel in the body. ....	17
Table 1.3: Sensitivity of ATP and ADP on major $K_{ATP}$ channels. ....	20
Table 1.4: $IC_{50}$ for pharmacological inhibitors on major $K_{ATP}$ channels. ....	26
Table 1.5: $EC_{50}$ for pharmacological activators on major $K_{ATP}$ channels. ....	27
Table 1.6: Cardiac cell types displaying pacemaker behaviour. ....	32
Table 1.7: The Vaughan-Williams Classification of Antiarrhythmic Drugs. ....	36
Table 2.1: Solution constituents for Normal Tyrode's, $Ca^{2+}$ free Tyrode's (0CaT), Substrate-free Tyrode's (SFT), and Substrate-free Tyrode's metabolic inhibition (SFT-MI). ....	66
Table 2.2: 12% SDS-PAGE gel constituents. ....	67
Table 2.3: Constituents for RIPA buffer. ....	67
Table 2.4: 6× Laemmli Buffer constituents. ....	68
Table 2.5: 10× TBS constituents. ....	68
Table 2.6: Running Buffer constituents. ....	68
Table 2.7: Transfer Buffer constituents. ....	68
Table 2.8: Table constituents of both cell-attached solution and whole cell-recording solution. ....	69
Table 2.9: shRNA targeted sequences for $K_{ir}6.1A$ , $K_{ir}6.1B$ , SUR2A and SUR2B. ....	72

## Abbreviations

Abbreviations used in this thesis:

[Ca <sup>2+</sup> ] <sub>i</sub>	intracellular Ca <sup>2+</sup> concentration
[K <sup>+</sup> ] <sub>o</sub>	extracellular K <sup>+</sup> concentration
°C	degrees centigrade
0CaT	Ca <sup>2+</sup> free Tyrode's
ABC	ATP binding cassette
Acetyl-CoA	acetylcoenzyme
Ach	acetylcholine
Acyl-CoA	palmitoyltransferase
ADP	adenosine diphosphate
AF	atrial fibrillation
Akt	protein kinase B
AMISTAD	Acute Myocardial Infarction Study of Adenosine
AMP	adenosine monophosphate
AMPK	cyclic adenosine monophosphate-activated kinase
ANOVA	analysis of variance
ANS	autonomic nervous system
AP	action potentials
APD	action potential duration
APS	ammonium persulphate
ATP	adenosine-5'-triphosphate
AVN	atrioventricular node
bp	base pairs
BSA	bovine serum albumin
BPM	beats per minute
cAMP	cyclic adenosine monophosphate
cGMP	cyclic guanosine monophosphate

CICR	calcium-induced calcium release
CK	creatine kinase
C <sub>m</sub>	membrane capacitance
CN	cyanide
CPT	carnitine palmitoyltransferase
C-terminus	carboxy terminus
DAD	delayed afterdepolarization
DAG	diacylglycerol
dH <sub>2</sub> O	distilled water
DNA	deoxyribonucleic acid
DNP	protonophore 2,4-dinitrophenol
DTT	dithiothreitol
EAD	early afterdepolarizations
EC Coupling	excitation contraction coupling
EC <sub>50</sub>	half maximal effective concentration
ECG	electrocardiogram
EDTA	ethylenediaminetetraacetic acid
EFS	electric field stimulation
EGFP	enhanced green fluorescent protein
EGTA	ethyleneglycoltetraacetic acid
E <sub>K</sub>	K <sup>+</sup> equilibrium potential
E <sub>Na</sub>	Na <sup>+</sup> equilibrium potential
eNOS	endothelial nitric oxide synthase
ER	endoplasmic reticulum
ERK	extracellular regulated kinase
ERP	effective refractory period
FA	fatty acid
FABP	fatty acid binding protein
FAT	fatty acid translocase

g	gram
G6P	glucose 6-phosphate
GLUT	glucose transporter
GP	guinea pig
gp130	glycoprotein 130
GPCR	G protein-coupled receptor
GSK3 $\beta$	glycogen synthase kinase 3 $\beta$
GTP	guanosine triphosphate
HCN	hyperpolarization-activated cyclic nucleotide-gated
HEK	human embryonic kidney
HEPES	(4-(2-hydroxyethyl)-1-piperazineethanesulfonic acid
hERG	human ether-a-go-go related gene
IAA	iodoacetate acid
IC <sub>50</sub>	half maximal inhibitory concentration
I <sub>f</sub>	'funny' currents
I <sub>kr</sub>	cardiac rapid delayed rectifier K <sup>+</sup> current
I <sub>ks</sub>	cardiac slow delayed rectifier current
IPC	ischemic preconditioning
I <sub>to</sub>	cardiac transient outward K <sup>+</sup> current
JAK	Janus kinase
K <sub>Ach</sub>	Ach-dependent K <sup>+</sup> channel
K <sub>ATP</sub>	potassium channel ATP-sensitive potassium
kb	kilo-base pairs
KchiP2	K <sub>v</sub> potassium interacting protein 2
KCO	potassium channel opener
KD	knockdown
K <sub>ir</sub>	inwardly rectifying potassium channel
K <sub>v</sub>	voltage-dependent K <sup>+</sup>
KO	knockout
LC	large conductance

LQTS	long QT syndrome
M	mole
MI	metabolic inhibition
MI/R	metabolic inhibition/reperfusion
min	minutes
MIP	post-conditioning
mitoK <sub>ATP</sub>	mitochondrial K <sub>ATP</sub>
MPC	mitochondrial pyruvate transporter
mRNA	messenger ribonucleic acid
ms	milliseconds
mV	millivolts
Na <sub>v</sub>	voltage-gated Na <sup>+</sup> channel
NBF	nucleotide binding Folder
NCX	Na <sup>+</sup> /Ca <sup>2+</sup> exchanger
NO	nitric oxide
NSTEMI	non-ST-segment elevation myocardial infraction
NT	normal tyrode's
N-terminus	amino terminus
P1075	N-cyano-N'-(1,1-dimethylpropyl)-N''-3-pyridylguanidine
p70S6K	p70 S6 kinase
PAGE	polyacrylamide gel electrophoresis
PBS	phosphate buffered saline
PCr	phosphocreatine
PDH	pyruvate dehydrogenase
PI3K	phosphatidylinositol (4,5)-bisphosphate 3-kinase
PIP2	phosphatidylinositol-4, 5-bisphosphate
PKA	cAMP activated protein kinase
PKC	calcium activated protein kinase
PKCi	PKC inhibitor peptide

PKG	protein kinase G
PLC	phospholipase C
P-loop	pore loop
PMCA	plasma membrane $\text{Ca}^{2+}$ ATPase
PNU37883A	N-Cyclohexyl-N'-tricyclo[3.3.1.1 <sup>3,7</sup> ]dec-1-yl-4morpholine carboximidamide
$P_o$	open probability
PSNS	parasympathetic nervous system
PTCA	percutaneous transluminal coronary angioplasty
RA	right atrium
RICS	RNA-induced silencing complex
RIPA	radioimmunoprecipitation (lysis buffer)
RIPC	Remote ischaemic preconditioning
RISK	Reperfusion Injury Salvage Kinase
RMP	resting membrane potential
ROMK	renal outer medullary potassium channel
ROS	reactive oxygen species
RyR	ryanodine receptors
s	second
S.E.M	standard error of the mean
SA	sinoatrial node
SAFE	Survivor Activating Factor Enhancement
SarcoK <sub>ATP</sub>	sarcolemmal K <sub>ATP</sub>
SC	small conductance
SDS	Sodium dodecyl sulfate
SDS-PAGE	sodium dodecyl sulphate polyacrylamide gel electrophoresis
SERCA	sarcoplasmic-endoplasmic $\text{Ca}^{2+}$ -ATPase
SFT	substrate-free Tyrode's
sGC	soluble guanylate cyclase
siRNA	small interfering RNA

SNS	sympathetic nervous system
SR	sarcoplasmic reticulum
STAT	signal transducer and activator of transcription
STEMI	ST-segment elevation myocardial infarction
SUR	sulphonylurea receptor
SVC	superior vena cava
TBS	Tris-buffered saline
TEMED	N,N,N',N'-Tetramethyl-1-,2-diaminomethane
TMD	transmembrane domain
TNF $\alpha$	tumor necrosis factor $\alpha$
Tris	Tris(hydroxymethyl)aminomethane
T-tubules	Transverse tubules
TTX	tetrodotoxin
UDP	uridine diphosphate
VF	ventricular fibrillation
VSMC	vascular smooth muscle cells

# **Chapter 1**

## **Introduction**

**1.1 Whole heart structure and physiological roles**

The heart is a biological pump that moves blood through the vascular circulatory system of the body. The heart is located behind the sternum and in front of thoracic vertebra, with 2/3 in the left thoracic cavity and 1/3 in the right thoracic cavity (Ho & Nihoyannopoulos, 2006). In higher species such as mammals, the heart usually consists of 4 chambers, two small atria and two larger ventricles (Figure 1.1). In most mammalian species, the heart can be separated into two halves; the right, which pumps blood around the pulmonary circulation to allow gaseous exchange, and the left that pumps the re-oxygenated blood around the systemic circulation. As the left side of the heart pumps blood into the systemic circulation, requiring a greater pressure than the pulmonary system, it is usually more muscular than the right (Figure 1.1). The heart efficiently drives this blood transportation system to provide the organism with the substrates (e.g. oxygen and glucose) for cellular respiration and to remove the metabolic by-products of this process (e.g. CO<sub>2</sub>).

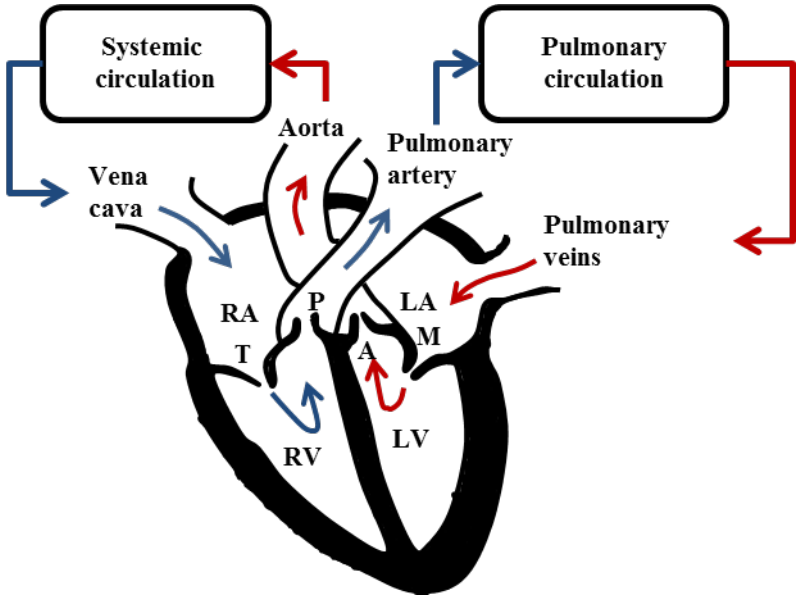


**Figure 1.1: A diagram of whole heart structure.** Arrows indicate the direction of blood flow. Blue arrows represent the blood with low oxygen and carries CO<sub>2</sub>. Red arrows represent the blood enriched with oxygen. RA: right atria; LA: left atria; RV: right ventricle; LV, left ventricle; T: tricuspid valve; M: mitral valve; P: pulmonary valve; A: aortic valve.

## 1.2 Cardiomyocytes

Cardiomyocytes are contractile cells that form the muscular structure of the heart. Cardiomyocytes have an ordered intracellular structure that is separated into discrete sarcomeres that allow the cells, and so the heart, to efficiently pump in a coordinated manner. The heart provides the pumping force required for the circulation of blood in response to an intrinsic stimulation; the cardiomyocytes are unable to trigger action potentials themselves (Woodcock & Matkovich, 2005). Cardiac pacemaker cells are a specialized form of cardiomyocyte that are a key constituent of the cardiac conduction system (Irisawa, 1978). The cardiac pacemaker cells have the ability to generate, and receive modulatory electric impulses, that allow the cardiac conduction system to control the rhythmic myocardial contractions (Woodcock & Matkovich, 2005). The cardiac conduction system includes: sino-atrial node, intermodal tract, atrioventricular junction, atrioventricular bundle, left/right bundle branch and Purkinje fibres (Liang *et al.*, 2015). The sino-atrial node is the primary pacemaker in normal conditions in most mammalian species (Boyett *et al.*, 2000).

### 1.2.1 Structural components

In general, cardiomyocytes are formed from the same constituent as most muscle cells; a sarcolemmal membrane, myofibril structures, myoplasm, organelles and multiple nuclei. Cardiomyocytes are similar to the muscle cells found in skeletal muscle, with a striated appearance; however, there are also some features specific to cardiomyocytes. Cardiomyocytes are rod shaped and are normally binucleate (Raulf *et al.*, 2015). Between the cardiomyocytes, there are intercalated discs that act as cellular bridges that electrically connect each cardiomyocyte. These are low resistance connections that allow  $\text{Na}^+$ ,  $\text{K}^+$  and  $\text{Ca}^{2+}$  to move between cells therefore conducting electrical impulses (Kleber & Saffitz, 2014). In the whole heart, although the atrial and ventricular cells are separated into different regions of the myocardium, the intercalated discs allow the flow of electrical stimulation through the whole heart allowing the contraction to occur in an ordered fashion.

### 1.2.2 Sarcomeres

The cardiomyocyte contains large amounts of myofibrils that are assembled into bunches of myofilaments. Myofibrils show a distinct and repeating structure that are separated by several Z-lines. Between two Z-lines, the myofibrils are termed a sarcomere which is the basic contractile unit in cardiomyocytes (Winslow *et al.*, 2011). The myofibrils are connected each side of intercalated discs and provide length-wise contractile force (Sparrow & Schöck, 2009). Under light microscope illumination, the sarcomeres give the myocyte a striated appearance with dark and light bands. The light bands are mostly comprised of actin, or thin filaments. The thick filaments that comprise the dark bands are formed by myosin, which has binding sites for the thin filament,  $\text{Ca}^{2+}$  and ATP on a globular head (Sparrow & Schöck, 2009). The thin filament has one side connected to thick filament and the other side bound with Z-disks (Figure 1.2). The area near Z-disks where has no thick filament overlapping, called the I-band. The thin filaments extended from I-bands and with one side going in and overlapping with thick filaments, connected with A-bands that is only comprised by the entire length of myosin filament. A region called H-zone is located in the A-bands, with no actin filament overlapping but only myosin filament. When contracting, the myosin filament do not change their length, with shortening in I-bands and H-zone, therefore the Z lines come closer to each other (Huxley, 1974).

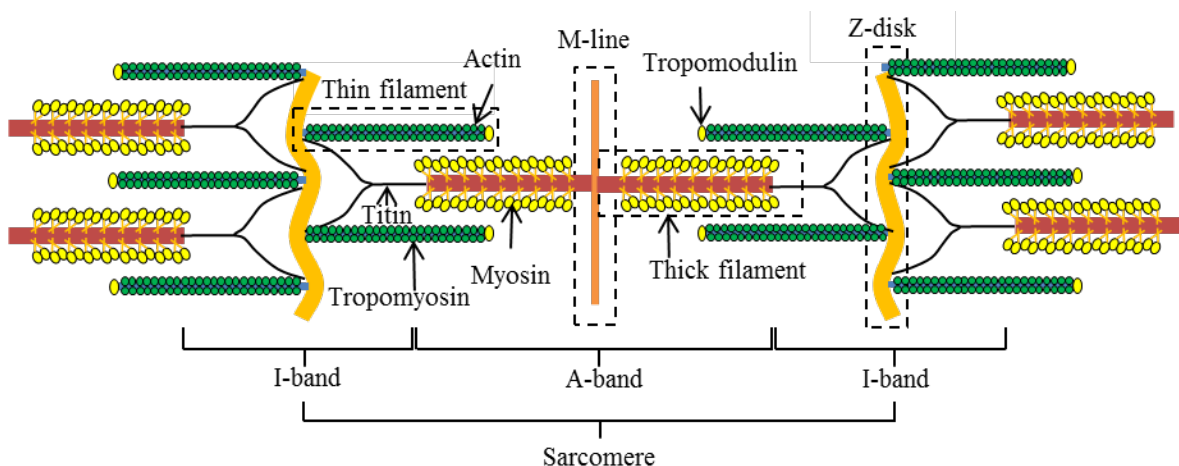


**Figure 1.2: A diagram of sarcomere.** The thin filaments are mostly composed by actin and tropomyosin, with one end anchored on Z-disk and the other end able to bind the myosin and produce contraction when presence of  $\text{Ca}^{2+}$ . The area near Z-disks with no overlapping of actin and myosin, called I-band. The thick filaments are form by myosin that occupied A-band, with one end anchored on M-line and the other end binds titin which connect the thick filament to the Z-disk. The M-line is the middle of sarcomere that anchors and crosslinks multiple thick filaments. Z-disk connected adjacent sarcomeres, which anchors and crosslinks thin filaments between sarcomeres.

### 1.2.3 T-tubule system

Transverse tubules (T-tubules) are an extension of the sarcolemmal membrane that penetrate into cardiomyocytes and run along the length of the sarcomeres. In mammals, the directions of T-tubules are always vertical with axial radiations on the sarcomeres. L-type  $\text{Ca}^{2+}$  channels are found within the T-tubule system and are located near the ryanodine receptors (RyR) on the SR. Thus, electrical stimulation rapidly induces  $\text{Ca}^{2+}$  influx and so intracellular  $\text{Ca}^{2+}$  release from RyR (Ibrahim *et al.*, 2011). In cardiomyocytes, the T-tubule system is different from skeletal muscle cells, which are short and broad and forms diads with longitudinal tubules in cardiomyocyte instead of triads in skeleton muscle cells (Ibrahim *et al.*, 2011). In addition, different to the skeletal muscle cells, the T-tubules in cardiomyocyte encircle the sarcomeres at the Z-disks rather than the thick/thin filament overlapping zone (Guo *et al.*, 2013).

### 1.2.4 Excitation contraction coupling

Excitation contraction coupling is a process which connects the depolarisation of the membrane potential with the activation of the contractile machinery (SANDOW, 1952; Huxley, 1974). There are three main drivers of this process; firstly, the electrical impulse that conducts into the cardiomyocyte through T-tubules system; secondly, the release of  $\text{Ca}^{2+}$  from the sarcoplasmic reticulum (SR) and its ultimate removal and finally, the contraction and relaxation of the cardiomyocytes. In cardiomyocytes, the excitation-contraction coupling relies on a mechanism termed  $\text{Ca}^{2+}$ -induced  $\text{Ca}^{2+}$  release (CICR). In the absence of extracellular  $\text{Ca}^{2+}$ , cardiomyocytes lose the ability to contract and remain in a diastolic state (Katz, 2001). The action potential is triggered in the cardiac pacemaker (see section 1.5.1.1) and conducts through heart via gap junctions, where the action potential spreads from the membrane surface into the T-tubule system. The voltage-gated L-type  $\text{Ca}^{2+}$  channel in the T-tubules open due to the depolarization, allowing a  $\text{Ca}^{2+}$  influx into the cell so causing a regional increase in  $\text{Ca}^{2+}$  concentration (Bodi, 2005). The increasing  $\text{Ca}^{2+}$  concentration leads a positive feedback of  $\text{Ca}^{2+}$  release from the SR due to binding of  $\text{Ca}^{2+}$  to RyR in the SR membrane. As is described in section 1.2.2, 2 different filaments exist in the sarcomere, with myosin (thick) filament and actin (thin) filament. It has been previously described (Huxley, 1974), in resting conditions, tropomyosin covers the binding site for

myosin filaments on actin filaments. The structure of this is altered by  $\text{Ca}^{2+}$  binding on troponin-C molecules which reveals the binding site for myosin. Once revealed, the myosin filaments are able to bind the actin filaments. Then, by hydrolysis of ATP on the myosin filaments, the actin filaments are pulled (slide) inward to the centre (M-line) of myosin filaments; therefore the whole sarcomere is shortened. This complex, and contracture, is maintained until a new ATP binds the myosin filament, and is termed *rigor* stage. Once a new ATP binds to the myosin, the hydrolysis provides the energy required for the release of actin and therefore, the sarcomere relaxes. To trigger relaxation, the diastolic period, the intracellular  $\text{Ca}^{2+}$  concentration ( $[\text{Ca}^{2+}]_i$ ) must be reduced.  $\text{Ca}^{2+}$  can be taken up by the Sarcoplasmic/Endoplasmic reticulum ATPase (SERCA), be sequestered in the mitochondria, or removed to the extracellular environment via the plasma membrane  $\text{Ca}^{2+}$ -ATPase (PMCA) or removed via the  $\text{Na}^+/\text{Ca}^{2+}$  exchanger (NCX).

### 1.3 Membrane transport in cardiomyocytes

The internal and external environment of all cells is separated by a membrane; the structure of which is comprised of phospholipids and proteins. The membrane is not simply a static bag that separates the intracellular and extracellular environment, but is a functional organelle that acts as a permeability barrier, regulating the flow of ions and molecules. The membrane is formed of a bilayer of phospholipids. Each phospholipid is an amphiphilic molecule with hydrophilic “head” group facing outward to both intracellular and extracellular environment and their hydrophobic tails in between. This hydrophobicity at the core of the lipid bilayer makes it an impermeable barrier to charged or polar moieties and therefore ions, charged or polar molecules cannot passively cross. Only lipid soluble small molecules can pass through due to its hydrophobicity. Cells, therefore, have the ability to maintain an internal environment that differs from the extracellular environment. Despite this requirement for differential environments, cells still require the membrane to be partially permeable to allow oxygen and other essential metabolites to enter the cell for normal metabolic processes to occur. The membrane is, therefore, said to be selectively permeable as cells allow these to cross the membrane in a regulated manner. This is achieved via membrane proteins that are integral to the structure. These proteins may form

pores that allow facilitated diffusion of ions down their concentration gradients, termed ion channels. Ion channels allow the passive movement of ions down their concentration gradient, but in order to set up and maintain the gradient energy, in the form of ATP, must be expended. Membrane transport requiring energy is referred to as an active process. Active transport is often used to describe the transport of molecules or ions against their concentration gradient using the energy released from the hydrolysis of ATP to ADP. An example of such a transport mechanism are the family of ATPase pumps, an example of which is the Na<sup>+</sup>/K<sup>+</sup>/ATPase that moves Na<sup>+</sup> and K<sup>+</sup> ions against their concentration gradient. In addition, the potential energy in a concentration gradient for an ion may be used to transport ions or molecules in or out of the cells. An example of this is the NCX which uses the potential energy in the Na<sup>+</sup> gradient to extrude Ca<sup>2+</sup> ions from the cell. Such transport, using the potential energy in the Na<sup>+</sup> gradient, is referred to as secondary active transport. The ionic gradients across the cell membrane are of fundamental importance. The normal distribution of ions is shown below for cardiac cells in Table 1.1

Ion	[Intracellular] mM	[Extracellular] mM
Na <sup>+</sup>	10 -12	130 -140
K <sup>+</sup>	140 -150	4 - 5
Ca <sup>2+</sup>	~0.0001	1.8 - 2
Cl <sup>-</sup>	10 - 20	95 - 110

**Table 1.1: Approximate ionic concentrations for the intracellular and extracellular environment in cardiac tissue.**

Finally, for large molecules, transport in or out of the cell relies on the formation of vesicles, exocytosis and endocytosis with outward and inward respectively.

**1.3.1 Ion channels**

Ion channels are proteins that span the lipid bilayer and so can transmit information between the extracellular and intracellular environment of the cell. In general, the common feature of ion channels is an aqueous pore through the membrane which is surrounded by  $\alpha$ -helices. The aqueous pore facilitates movement of ions down their electrochemical gradient

therefore allowing a pathway through which charged ions can pass through the hydrophobic core of the bilayer membrane. Each type of ion channel differs in its selectivity for the ions that pass through, with selectivity motifs embedded in the amino acid structure as well as the size of the pores determining the permeability. In addition, ion channels not only allow the facilitated diffusion of ions but, rather than being a constant free-flow of ions, also regulate the movement by gating mechanisms that regulate the open/close/inactivated state. Such regulatory mechanisms can vary, but include voltage and ligand sensitivity. Furthermore, the duration of channel opening is often time limited by inactivation gates or intracellular modifying interacting molecules. Ion channels are widely distributed in tissues and organs due to the ubiquity of these mechanisms in electrical signalling which by opening ion channels the charge between membranes can be altered. To change the channel opening state, ion channels alter their conformation to allow ions pass through the aqueous pore.

The gating system for ion channels can be classified as voltage-gated, ligand-gated, mechanical force and signalling molecules. Voltage-gated ion channels sense the potential difference across the membrane and therefore alter the conformation to open or close the ion channel. In general, the voltage-gated ion channels are closed at the resting membrane potential and activate in response to depolarization. When the membrane potential reaches the threshold for activation, the voltage sensor shifts so changing the channel conformation to the open state, allowing the influx or efflux of ions. The structures for most voltage-gated channels are similar, with 4 contributing subunits each comprising 6 transmembrane domains, where transmembrane segments 1 – 4 make up the voltage sensor and 5 to 6 are pore forming units (Bezanilla & Perozo, 2003).

Ligand-gated ion channels rely on chemical messengers, or ligands, binding the channel structure to cause activation. Some of the ligand-gated channel can be regulated by intracellular ligands, such as the ATP sensitive potassium channel ( $K_{ATP}$ ) which can be blocked by intracellular ATP. In cardiomyocytes, ion channels are important in establishing resting membrane potential, shaping the action potential, controlling its duration and the spread of electrical excitability in the myocardium.

### ***1.3.1.1 Sodium currents***

In cardiomyocytes, Na<sup>+</sup> channels have rapid kinetics that causes channel activation within the first millisecond and are subsequently inactivated within a few milliseconds. The most abundantly expressed Na<sup>+</sup> channel underlying the cardiac I<sub>Na</sub> current is Na<sub>v</sub>1.5. The channel can exist in 3 states, closed, open and inactivated. The equilibrium potential for Na<sup>+</sup> is ~+60 mV therefore activation of Na<sup>+</sup> currents causes a substantial depolarisation, and are responsible for the initial depolarisation (phase 1) of the cardiac action potential. At the peak of action potential, 1–2 ms, all Na<sub>v</sub> channels will be inactive, therefore Na<sup>+</sup> influx ceases. Na<sub>v</sub> channels only recover from inactivation at repolarised potentials. Therefore, these channels do not contribute further to the action potential in cardiomyocytes in normal physiological conditions.

### ***1.3.1.2 Calcium currents***

In the cardiac sarcolemmal membrane, there are two types of Ca<sup>2+</sup> channels, T-type and L-type Ca<sup>2+</sup> channels, and play important roles in regulating action potential as well as EC coupling. Both channels are named after their channel kinetics with rapidly inactivating or “transient” (T-type) and “long lasting” (L-type) respectively (Perez-Reyes, 2003). Both passing inward Ca<sup>2+</sup> currents that depolarise the membrane potential. T-type Ca<sup>2+</sup> channels have a more negative membrane potential threshold compared that in L-type Ca<sup>2+</sup> channels. In cardiac pacemaker cells, the T-type Ca<sup>2+</sup> channels are important in providing rapid depolarization in addition to the Na<sup>+</sup> channel. Compared to the L-type Ca<sup>2+</sup> channel, the T-type Ca<sup>2+</sup> channels are more active at negative potentials and rapidly inactivate during sustained depolarization (Colquhoun & Hawkes, 1982). Previous literature demonstrated that selective block of the T-type Ca<sup>2+</sup> currents by nickel and tetramethrin significantly decreased the heart rate via slowing the depolarization at the potential voltage of ~-50 mV (Hagiwara *et al.*, 1988).

T-type Ca<sup>2+</sup> channels are not largely expressed in ventricular cardiomyocyte, where the L-type Ca<sup>2+</sup> channel has a more important role (Perez-Reyes, 2003). The L-type Ca<sup>2+</sup> channel is primarily responsible for the prolonged plateau of the action potential and activates rapidly with channel time constant of 6.7 ms (Wang *et al.*, 2001) however, the Na<sub>v</sub>1.5 time constant is 0.81 ms (Beyder *et al.*, 2010) meaning the I<sub>Na</sub> current has a more prominent role

in the initial depolarisation. The large, sustained inward  $\text{Ca}^{2+}$  current produced during the plateau phase triggers an increase in  $[\text{Ca}^{2+}]_i$  via CICR, essential for efficient excitation-contraction coupling (section 1.2.4). The plateau phase ends as the L-type  $\text{Ca}^{2+}$  channels move into an inactive state which, with increasing  $\text{K}^+$  currents, leads to a repolarisation of the membrane potential.

### ***1.3.1.3 Potassium currents***

Activation of  $\text{K}^+$  currents drives the membrane potential more negative, and contributes to the repolarization of an action potential, due to  $E_K$  being  $\sim -95$  mV in physiological conditions. There are 4 main  $\text{K}^+$  currents involved in repolarization, they are  $I_{to}$ ,  $I_{kr}$ ,  $I_{ks}$  and  $I_{kl}$ .  $I_{to}$ ,  $I_{kr}$ , and  $I_{ks}$  are all voltage-gated  $\text{K}^+$  currents, whilst  $I_{kl}$  is formed from inwardly rectifying channel subunits. The transient outward  $\text{K}^+$  current,  $I_{to}$ , is important the early repolarization of the action potential, imparting a ‘notch’ following phase 0 of the action potential, due to its rapidly activating and inactivating kinetics. In phase 3 repolarization, the rapidly and slowly activating delayed rectifier potassium current,  $I_{kr}$  and  $I_{ks}$ , together with inward rectifier current  $I_{kl}$ , are the major repolarizing currents that restore the membrane potential to the resting level.

#### ***1.3.1.3.1 $I_{to}$***

Between different species, the expression of  $I_{to}$  currents varies and so its contribution to the action potential can differ. In some rodents, such as mice and rats,  $I_{to}$  plays a large part in the repolarization and so forms a near triangular action potential with no distinct plateau (Xu *et al.*, 1999; Workman *et al.*, 2001, 2012; Sah *et al.*, 2002; Workman, 2010; Madhvani *et al.*, 2011).  $I_{to}$  currents shape the phase 1 repolarisation, which affects the activation time course of L-type  $\text{Ca}^{2+}$  channel as well as the driving force for  $\text{Ca}^{2+}$  ions, resulting in a regulation in plateau phase amplitude and the action potential duration (Sun & Wang, 2005; Workman *et al.*, 2012).  $I_{to}$  currents are inactivated with the maintained depolarization, with the time constant on the order of  $\sim 30$ -100 ms in human or ferret subepicardial myocyte (Patel & Campbell, 2005), or around 10 ms in isolated canine ventricular myocytes (Calloe *et al.*, 2009). The  $I_{to}$  current is formed by voltage-dependent  $\text{K}^+$  ( $\text{K}_v$ ) channels, with  $\text{K}_v4.2$  channels involved into the  $I_{to,fast}$  currents and the  $\text{K}_v1.4$  channels into  $I_{to,slow}$  currents (Patel & Campbell, 2005). Previous literature revealed that native  $I_{to,fast}$  currents mimicked by

recombinant expression of  $K_v4.2$  and  $K_v$  potassium interacting protein 2 (KchiP2) (An *et al.*, 2000; Deschênes & Tomaselli, 2002). The  $I_{to, slow}$  currents are formed from  $K_v1.4$  channel which have slow recovery kinetics and was regulated by  $K_v\beta$  proteins (Morales *et al.*, 1995).

The differential expression of  $I_{to}$  currents in different areas of the myocardium causes regional differences in action potential, with more  $K_v1.4$  channel expression in the ventricular wall and the atria (Calloe *et al.*, 2009; CALLOE *et al.*, 2011). In the clinic, the reduction of  $I_{to}$  can be seen in the most common cardiac arrhythmia, atrial fibrillation, where the  $I_{to}$  currents were significantly reduced by electrophysiological remodelling (Workman *et al.*, 2012). That is probably because the reduction of  $I_{to}$  elevates the plateau phase of action potential, prolonging the L-type  $Ca^{2+}$  channel opening time and resulting in a significant prolongation or even early afterdepolarisations of the action potential (Xu *et al.*, 1999; Sah *et al.*, 2002).

#### **1.3.1.3.2 $I_{kr}$**

$I_{kr}$  currents have been shown to be expressed throughout the heart, including the nodal tissue, atria, Purkinje fibres and ventricles. In human,  $I_{kr}$  is encoded by the ether-a-go-go related gene (hERG); in other species referred to as ERG, and the channel itself is  $K_v11.1$  (Sanguinetti *et al.*, 1995; Trudeau *et al.*, 1995). Similar to the  $K_v4.1$  and  $K_v1.4$ , the  $K_v11.1$  channel is a voltage-gated  $K^+$  channel with 6-transmembrane domains which from transmembrane 1 to 4 are the voltage-sensing domains and the transmembrane 5 to 6, including the P-loop, as pore-forming units (Bezaniilla & Perozo, 2003). The  $\beta$ -subunits for the  $K_v11.1$  have been suggested to be KCNE1 or KCNE2, which the  $K_v11.1$ -KCNE1 interaction was more robust than that with KCNE2 in the HEK heterologous expression system (Um & McDonald, 2007). Moreover, dominant-negative mutant KCNE1 in the heterologous cell line can also significantly reduce hERG currents (Bennett *et al.*, 1995). The physiological role of  $K_v11.1$  is highly related to the membrane potential, Figure 1.3 illustrates the unique channel biophysical characteristics of relatively slow kinetics from the closed to open state but moves 10 times more rapidly from the open to inactive state (Piper *et al.*, 2005). This property makes the  $K_v11.1$  pivotal in the cardiac action potential where the channel moves from the closed state to the open state when the membrane potential is depolarized above its threshold for activation, but rapidly moves into the inactive state.

Thus, the  $K_v11.1$  only conducts a small potassium current in the initial depolarization and the plateau phase. With membrane potential repolarization the  $K_v11.1$  channel is rapidly released from the inactivated state and slowly deactivates to the closed state (Piper *et al.*, 2005), providing a strong outward  $K^+$  current that accelerates repolarization. Thus, the  $I_{kr}$  currents play a key role in shaping the repolarisation of the action potential in phase 3.

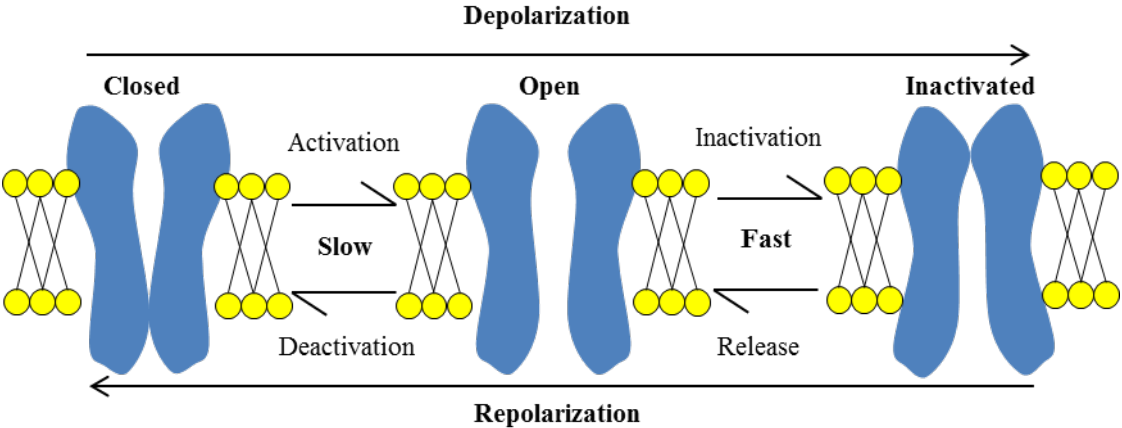


**Figure 1.3: The unique channel kinetics for hERG channel.** hERG channels have a slow kinetics in transferring the conformation between closed state and open state but move rapidly between open and inactivated state.

**1.3.1.3.3  $I_{ks}$**

In the recombinant system, co-expression of  $K_v7.1$  and KCNE1 subunits forms a channel with similar electrophysiological characteristics of the native  $I_{ks}$  current (Barhanin *et al.*, 1996; Sanguinetti *et al.*, 1996; Jespersen *et al.*, 2005; Amin *et al.*, 2010). This current is also known as  $K_vLQT1$  due to having been cloned from a Long QT syndrome patient by using linkage analysis (Wang *et al.*, 1996). The  $K_v7.1$   $\alpha$ -subunit forms the pore of the channel, and has 6-transmembrane domains as a standard voltage-gated structure (Sansom *et al.*, 2002). The  $\beta$ -subunits for the  $K_v7.1$  channel is KCNE1 which only has 1-transmembrane domain and has recently been suggested to interact with the  $K_v7.1$  in a ratio of 2 KCNE:4  $K_v7.1$  (Nakajo *et al.*, 2010; Kobertz, 2014; Plant *et al.*, 2014). When the membrane depolarises to the threshold, the slow activation of  $K_v7.1$ /KCNE1 complex gives a steadily increasing  $K^+$  current throughout the action potential.

The  $K_v7.1$  subunit when expressed alone shows rapidly activating kinetics, but interacting with KCNE1 slows the movement of S4 segments down, which is the voltage-sensor

segments, and resulting in a slow channel kinetics on  $K_v7.1/KCNE1$  channel (Ruscic *et al.*, 2013). In addition,  $I_{ks}$  currents also can modulate the heart rate. To increase the heart, rat sympathetic nervous system (SNS) mediates the  $\beta$ -adrenergic receptor activation, which alters the  $K_v7.1$  channel kinetics that accelerates channel activation and slow down the deactivation kinetics (see section 1.5.2.2). The relatively slow deactivation of  $I_{ks}$  currents are the key in this modulation, where if the phase 4 diastolic period is not long enough to allow  $K_v7.1$  channel deactivation, the increasing  $I_{ks}$  currents can be ‘carried over’ into the next action potential (Rocchetti *et al.*, 2001; Diness *et al.*, 2006). Therefore, the summation of  $I_{ks}$  current can result in more rapid action potential repolarization as well as the increasing heart rate (Marx *et al.*, 2002).

#### 1.3.1.3.4 $I_{k1}$

The  $I_{k1}$  current is not voltage-gated *per se*, but shows inward rectification that allows more currents to pass when the membrane potential is close to the resting potential. This property is due to the underlying channel proteins being blocked at more depolarized potentials by intracellular polyamines, such as spermine. Thus,  $I_{k1}$  currents stabilise the cardiac resting membrane potential between -70 mV to -90 mV, depending on the species.  $I_{k1}$  currents are formed by  $K_{ir2.x}$  proteins, with 4  $K_{ir2.x}$  forming the pore structure (Ivanov *et al.*, 2004). Three members of the  $K_{ir2.x}$  family have been identified in cardiac tissue so far,  $K_{ir2.1}$ ,  $K_{ir2.2}$  and  $K_{ir2.3}$  (Kubo *et al.*, 1993; Bond *et al.*, 1994; Takahashi *et al.*, 1994; Bredt *et al.*, 1995; Töpert *et al.*, 1998; Veldhuis, 2015). The  $K_{ir2.x}$  channel can express as homomeric or heteromeric tetramers (Lu, 2004).  $PIP_2$  is an important regulator of  $K_{ir2.x}$ , which binds directly to the channel and stabilises the open state. The high affinity that  $PIP_2$  has for binding to  $K_{ir2.x}$  helps explain the  $I_{k1}$  constitutive activity (Lopes *et al.*, 2002).

### 1.3.2 Intracellular ion channels and their role in excitation contraction coupling

In cardiomyocytes, the excitation contraction coupling relies on CICR (see section 1.2.4). The  $Ca^{2+}$  ions influx via L-type  $Ca^{2+}$  channels and activates the nearby RyR to produce  $Ca^{2+}$  sparks. RyR are located in the SR membrane, which are response to the increased intracellular  $Ca^{2+}$  to release  $Ca^{2+}$  from the SR stores. In cardiomyocytes, the main isoform of RyR is RyR2 which was found in in the junctional SR that near the T-tubules in the diad. In addition, the RyR2 shows slow and weak inactivation kinetics so for step increases in

$[Ca^{2+}]_i$  the RyR2 open probability increases (Györke & Fill, 1993; Jones *et al.*, 2017). Furthermore, the RyR2 can also be regulated by the luminal  $Ca^{2+}$  in the SR; with more  $Ca^{2+}$  content in SR the RyR2 demonstrates an increased open probability (Györke & Györke, 1998). Finally, the RyR2 distributed in clusters in the diad (Marx *et al.*, 2001). Once activated, the release of  $Ca^{2+}$  must be stopped to prevent intracellular  $[Ca^{2+}]_i$  overload. There are 2 hypotheses; Firstly, it was proposed that the RyR2 channel is inactivated by the increasing  $[Ca^{2+}]_i$  via a cytoplasmic binding site (Fabiato, 1985), however evidence from other literature suggests this mechanism was too slow to stop  $Ca^{2+}$  release (Györke & Fill, 1993). S. Györke (1998) later suggested a second hypothesis where the decreasing luminal  $Ca^{2+}$  in the SR caused a further decrease in RyR2 open probability due to its dependence on the luminal SR  $Ca^{2+}$ . Together with the coupled channel kinetics (Marx *et al.*, 2001; Jones *et al.*, 2017), if one channel closed due to the lower open probability induced by falling luminal  $Ca^{2+}$  level, all RyR2s close due to the coupling gating (Marx *et al.*, 2001). Finally, following a contraction, cytosolic  $Ca^{2+}$  is removed by re-uptake to the SR via SERCA, with additional  $Ca^{2+}$  extruded from the cardiomyocyte through the sarcolemmal membrane PMCA and the NCX (Jafri, 2012).

### 1.3.3 ATPases

ATPases are the enzymes that catalyse the hydrolysis of intracellular ATP into ADP and a free phosphate ion, which releases energy that can be used elsewhere. Some enzymes are transmembrane proteins that allows ions move in or out of the plasma membrane against their concentration gradients, often termed membrane pumps. In the last stage of excitation-contraction coupling, the SERCA and PMCA are important to restore the  $[Ca^{2+}]_i$  to resting levels in diastole by sequestering  $Ca^{2+}$  into the network of the SR or extruded from the cell (Jafri, 2012). The  $Na^+/K^+$ -ATPase is important in maintaining concentration gradients for both  $Na^+$  and  $K^+$ , where both ions are moved across the membrane against their concentration gradients. Each molecule of ATP hydrolysed pumps 2  $K^+$  ions into the cell and 3  $Na^+$  ions out, maintaining a high concentration of  $K^+$  and low concentration of  $Na^+$  in the intracellular environment. In addition, the functional  $Na^+/K^+$ -ATPase also plays a key role in maintaining osmolality therefore maintaining the cell volume.

### 1.3.4 Carriers and transporters

Besides ion channels, there are other routes for facilitated diffusion of ions without the direct consumption of ATP through carrier proteins. The differences between carriers and ion channels is that carriers transport the substances across the membrane by binding and changing conformation to move a group of ions or molecules from one side of the membrane to the other side. Carriers do not have any recognisable pore structure. There are three categories of carriers, firstly, uniport, which allows one ion or molecule through the membrane; secondly, symport, which allows multiple ions or molecules through the membrane in the same direction; thirdly, antiport, which moves ions or molecules in the opposite direction across the membrane. Mostly, the molecules and ions transport across membrane through carriers passively, from a high to low concentration. In some cases, carriers can transport the ions or molecules via secondary active transport which means the carrier utilize the  $\text{Na}^+$  concentration gradients that maintained by ATPase, e.g. NCX.

### 1.3.5 Gap junctions

Gap junctions are special intercellular structures that are important in conducting electrical signals. Each gap junction is formed by 12 connexin molecules which form 2 connexions that equally shared by the 2 participating cells. Three types of connexin proteins, which are Cx40, Cx43 or Cx45, have been identified that are involved in forming cardiomyocyte gap junctions (Van Veen *et al.*, 2001). Gap junctions together connected cytoplasm of adjacent cell therefore allows multiple molecules, ions and electrical impulses to direct transmit from cell to cells. In cardiomyocytes, due to connection of cytoplasmic between each adjacent myocyte, both electrical signal and the metabolites can be coupled between cells. In the heart, one of the important roles the gap junctions play is the propagation of action potential (Rohr, 2004). Gap junctions can transport all polar molecules with the molecules weight up to 1.2 kD (Van Veen *et al.*, 2001; Berg *et al.*, 2002), such molecules as ATP, ADP,  $\text{Ca}^{2+}$ , cAMP, adenosine and even siRNA can all move through gap junctions so coupling the intercellular metabolic and electrical state (Nielsen *et al.*, 2012). Thus, this property may progress and spread cell damage and death from ischemic regions. For example, Cx43 null mutations (Cx43<sup>+/-</sup>) mice have smaller infarct size compared with the wild-type mice after coronary artery ligation (Kanno *et al.*, 2003). However, the use of gap

junction activity enhancers has also been reported to reduce infarct size after acute ischaemia/reperfusion (Hennan *et al.*, 2009). The permeability of gap junctions are complex due to there are more than 20 different connexin isoforms and all able to form heteromeric channels, with each type of connexin has different pore properties (Nielsen *et al.*, 2012). Gap junctions can be regulated by several conditions, such as voltage,  $\text{Ca}^{2+}$  concentration, pH, phosphorylation, and protein interactions (Nielsen *et al.*, 2012). Among them, voltage-dependent inactivation is the most salient channel feature. Similar to the voltage-gated channel, gap junctions tend to conduct a large current independent to the voltage gradient, but gradually inactivated during the increasing voltage gradients (Nielsen *et al.*, 2012).

#### 1.4 ATP-sensitive Potassium ( $\text{K}_{\text{ATP}}$ ) channels

ATP-sensitive potassium ( $\text{K}_{\text{ATP}}$ ) channels are a subgroup of the Inwardly Rectifying Potassium channel ( $\text{K}_{\text{ir}}$ ) family and are weak inwardly rectifying  $\text{K}^+$  channels regulated by the intracellular ATP/ADP level. This sensitivity to intracellular nucleotides has led to the hypothesis that they couple cellular metabolism to membrane electrical activity or membrane potential (Antcliff *et al.*, 2005; Nichols, 2006; Ortiz *et al.*, 2013; Sun & Feng, 2013).  $\text{K}_{\text{ATP}}$  channels are blocked by normal physiological concentrations of ATP, and therefore open under conditions of metabolic stress or ATP depletion.  $\text{K}_{\text{ATP}}$  channels, unlike other members of the inward rectifier family, are hetero-octameric in structure with four pore-forming subunits ( $\text{K}_{\text{ir}6.x}$ ) with four sulfonylurea receptors ( $\text{SUR}_x$ ) (Shyng & Nichols, 1997; Li *et al.*, 2017).

Following the first identification of an ATP-sensitive  $\text{K}^+$  channel in guinea pig cardiac cells (Noma, 1983),  $\text{K}_{\text{ATP}}$  channels have been identified in various tissues. In mammals, the channel is ubiquitously expressed, however the distribution of the different  $\text{K}_{\text{ATP}}$  channel subunits varies depending on tissue type (Shieh *et al.*, 2000). Three  $\text{K}_{\text{ir}6}$  family members have been identified,  $\text{K}_{\text{ir}6.1-6.3}$  (Inagaki *et al.*, 1995; Zhang *et al.*, 2006). Both  $\text{K}_{\text{ir}6.1}$  and  $\text{K}_{\text{ir}6.2}$  channels are expressed in most species, which share 70% homology in their amino acid sequence (Kono *et al.*, 2000), however  $\text{K}_{\text{ir}6.3}$  has only been identified in zebrafish (Zhang *et al.*, 2006). The nucleotide binding domains, and so the metabolic sensor of  $\text{K}_{\text{ATP}}$  channels, have contributions from both  $\text{K}_{\text{ir}6}$  and SUR subunits. Each  $\text{K}_{\text{ir}6}$  subunit has two

transmembrane domains with four  $K_{ir}6$  subunits coming together to form the pore of channel. Both the N- and C-termini are located on the cytoplasmic side of the membrane, and on the binding of intracellular ATP to the C-termini (Figure 1.2), inhibits channel opening (Nichols *et al.*, 2013). Three SUR accessory subunits have been identified, SUR1 and SUR2 with 2 splice variants, SUR2A and SUR2B (Kloor *et al.*, 1999; Ashfield *et al.*, 2000; Fujita *et al.*, 2006; Flagg *et al.*, 2008). In  $K_{ATP}$  channels, the SUR subunit increases the sensitivity to ATP and also confers activation by nucleotide diphosphates.

The  $K_{ir}6.2/SUR1$  combination has been shown to form the  $K_{ATP}$  channel complex in mammalian pancreatic tissue (Inagaki *et al.*, 1997; Tarasov *et al.*, 2004; Li *et al.*, 2017). Using immunocytochemistry, the expression of  $K_{ir}6.1$  in rat and mice vascular smooth muscle cell, coronary arteries smooth muscle cell and endothelial cells has been observed. The  $K_{ATP}$  channel isoform expressed in ventricular myocytes has been described as  $K_{ir}6.2/SUR2A$ , however there is evidence that  $K_{ir}6.1$ , SUR2B and SUR1 subunits expressed in ventricular and atrial myocytes (Morrissey *et al.*, 2005*b*, 2005*a*).

<i>Isoforms</i>	<i>SUR1</i>	<i>SUR2A</i>	<i>SUR2B</i>
<i>K<sub>ir</sub>6.1</i>	<i>Neuronal</i> (Lee <i>et al.</i> , 1999) <i>Cochlea Hensen cells</i> (Reiken <i>et al.</i> , 2003)	<i>Smooth Muscle?*</i>	<i>Vascular Smooth muscle</i> (Teramoto, 2006a) <i>Cardiac sarcolemmal membrane?</i>
<i>K<sub>ir</sub>6.2</i>	<i>Pancreatic islet cells</i> (Hattersley & Ashcroft, 2005) <i>Neuronal</i> (Karschin <i>et al.</i> , 1997)	<i>Cardiac and Skeletal muscle</i> (Jovanović <i>et al.</i> , 2016)	<i>Smooth muscle</i> (Teramoto, 2006a)

**Table 1.2: Distribution of functional  $K_{ATP}$  channel in the body.** \* Isoform not currently identified *in vivo* but can express in HEK 293 cells (Lodwick *et al.*, 2014).

$K_{ir}6.1$  is encoded by  $K^+$  inwardly-rectifying channel, subfamily J, member 8 (*KCNJ8* (Delaney *et al.*, 2012));  $K_{ir}6.2$  is encoded by *KCNJ11* (Fedele *et al.*, 2013). In addition to the  $K_{ir}6$  subunits, the features of the three known SUR subunits are essential for channel

function. Two isoforms of SUR have been reported to date, SUR1 and SUR2, with two splice variants of SUR2, SUR2A and SUR2B, encoded by *ABCC9* but differing by alternative use of exon 38 encoding an additional 42 amino acids in C-terminal tail of SUR2A (Isomoto *et al.*, 1996; Aguilar-Bryan *et al.*, 1998; Pu *et al.*, 2008; Kefaloyianni *et al.*, 2012). The different usage of exon 38 and the alternation in the C-terminal 42 amino acids can be than used for designing specific targeting shRNA and antibodies between SUR2A and SUR2B. As it was shown in Figure 1.4, The SUR have 1 L0 as a linker region to link with other SUR subunits, and each SUR subunits contains 3 transmembrane segments termed TMD0 to TMD2, with 5, 6, 6 transmembrane helices respectively (Nichols, 2006; Burke *et al.*, 2008). SUR subunits are part of the ATP-binding cassette (ABC) family of proteins and have 2 nucleotide-binding domains, NBF1 and NBF2. These 2 nucleotide-binding domains have Walker A and Walker B structures which can enhance the ability of ATP binding and hydrolysis in these regions (Seino & Miki, 2004).

The SUR subunits primary functional role is to control the open and closed state of the channel by sensing the intracellular ATP/ADP level (Nichols, 2006). To achieve this goal, the SUR subunits broaden the ATP binding site on  $K_{ir}6$  subunits, enhancing the sensitivity so maintaining the  $K_{ATP}$  channel in the closed state in normal physiological conditions due to the presence of ATP. SUR subunits can also mediate the channel opening with MgADP to counter the inhibitory effect of binding ATP. To activate the  $K_{ATP}$  channel, MgADP can bind on the 2 nucleotide binding sites on SUR subunits, NBF1 and NBF2, so causing the channel to open (Pelletier *et al.*, 2000). Lastly, the co-assembly of SUR subunits with  $K_{ir}6$  subunits allows the channel to be released from the ER. Both SUR and  $K_{ir}6$  subunits contain an ER retention sequence (RXR) that inhibits trafficking of the protein until these sequences are masked (Zerangue *et al.*, 1999). Like the  $K_{ir}6$  subunits, the distribution of SUR also varies in expression in different tissues. Expression of SUR1 is associated with the pancreas and neuronal tissue. SUR2A is predominantly expressed in cardiac and skeletal muscle, whilst SUR2B is predominantly thought to be vascular (Bryan & Aguilar-Bryan, 1999; Suzuki *et al.*, 1999; Campbell *et al.*, 2003; Shi *et al.*, 2005). Therefore, the different function and roles for  $K_{ATP}$  in different tissues can be altered according to the combination of subunits.

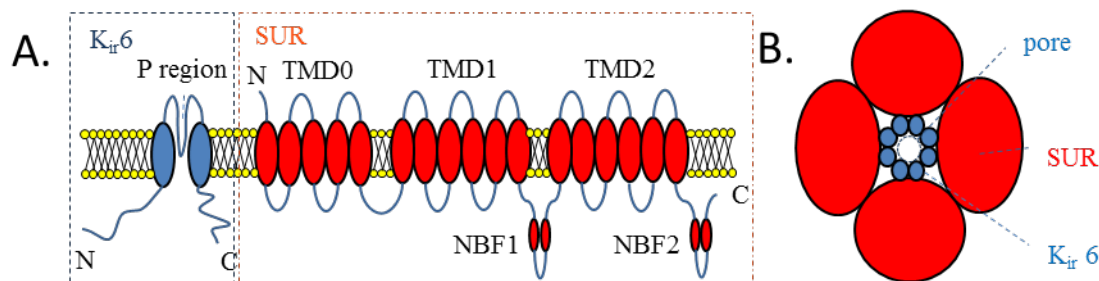


**Figure 1.4: Structure of  $K_{ir6.x}$   $K_{ATP}$  channel.** A, Diagram of a typical  $K_{ATP}$  ion channel structure. Channel's pore has formed by  $K_{ir6}$  subunits, with M1 and M2 2-transmembrane segments in each  $K_{ir6}$  subunit; the N- and C-termini located at cytoplasm side. TMD0-TMD2 represent 3 SUR transmembrane segments, with NBF1 and NBF2 nucleotide-binding domains in cytoplasmic side. B, The octamer structure of  $K_{ATP}$  channel.

Recently, by using cryoelectron microscopy, the structure of the pancreatic  $K_{ATP}$  channel,  $K_{ir6.2}/SUR1$ , including its binding sites for both ATP and ADP was elucidated (Gregory *et al.*, 2017; Lee *et al.*, 2017; Li *et al.*, 2017). At the resolution of 3.9 Å and 5.6 Å, the ATP binding sites on  $K_{ir6.2}$  was revealed on the surface of the C-terminal cytoplasmic domain, which was formed by 14 residues and specifically 2 neighbouring residues N48 and R50 form hydrogen bonds with Watson-Crick edge that specifically recognize ATP over GTP (Lee *et al.*, 2017). Interpreting the architecture of the  $K_{ir6.2}/SUR1$  channel, the L0 of TMD0 on SUR1 was suggested to be the major mediator between SUR1 and  $K_{ir6.2}$  with L0 physically connecting the 2 subunits so allowing SUR1 and  $K_{ir6.2}$  functional crosstalk (Li *et al.*, 2017). Gregory *et al.* (2017) proposed that when ATP binds on the  $K_{ir6.2}$ , the C-terminal cytoplasmic domain of  $K_{ir6.2}$  is locked with L0 of SUR1, which blocks the movement between L0 and the N-terminal of  $K_{ir6.2}$  that is essential to open the channel. This model is supported by the finding of crosslinks of L0 with the  $K_{ir6.2}$  N-terminal near the ATP binding site that closes the channel without the presence of ATP (Pratt *et al.*, 2012). Moreover, the binding site of glibenclamide on SUR1 has also been elucidated, which was next to the L0 and interacted with TM6, 7, 8, 11 in TMD1 and TM16 and 17 from TMD2 (Gregory *et al.*, 2017). Thus, the putative inhibitory mechanism for glibenclamide was proposed that, similar to ATP, stabilized the movement between the N-terminal of  $K_{ir6.2}$  and SUR1 and prevents the  $K_{ATP}$  channel from opening (Gregory *et al.*, 2017; Li *et al.*, 2017). Additionally for sulphonylurea drugs, SUR1 provides binding sites for both ATP and ADP, with a closed catalytically inactive degenerate site for  $Mg^{2+}$ -ATP

on NBD1 and an open catalytically competent consensus ATPase site of  $Mg^{2+}$ -ADP on NBD2, resulting in functionally asymmetric NBD dimer in terms of nucleotide-binding (Lee *et al.*, 2017). In addition, the degenerate nucleotide-binding site for  $Mg^{2+}$ -ATP is less selective to ATP but allows  $Mg^{2+}$ -ADP to bind as well; the consensus site for  $Mg^{2+}$ -ADP is highly selective to ADP, a property that allows SUR1 to be more sensitive to ADP compared that with ATP (Lee *et al.*, 2017). After intracellular ATP depletion/rise of ADP, ATP then dissociates from the  $K_{ir}6.2$  and the channel is then released from its inhibitory state. The rise of intracellular ADP binding on the NBDs of SUR1 leads NBD transformation from two monomers into one NBD dimer, which further causes the conformational changes of TMDs and L0 of SUR1 and rotates  $K_{ir}6.2$ 's C-terminal cytoplasmic domain clockwise to drive the pore open (Li *et al.*, 2017). Thus, a plausible mechanistic model was provided by the high-resolution channel structure that explains the regulation of pancreatic  $K_{ATP}$  by intracellular ATP/ADP concentration. The sensitivity to ATP or ADP of major  $K_{ATP}$  channel in each combination is outlined in Table 1.3.

	ATP	ADP
$K_{ir}6.1/SUR1$	$IC_{50} \sim 337.8 \mu M$ (Takano <i>et al.</i> , 1998)	Not Found
$K_{ir}6.1/SUR2A$	$IC_{50} \sim 190 \mu M$ (Aggarwal <i>et al.</i> , 2013)	Not Found
$K_{ir}6.1/SUR2B$	$EC_{50} \sim 68.3 \mu M$ * $IC_{50} \sim 251 \mu M$ * (Satoh <i>et al.</i> , 1998)	$EC_{50} \sim 96 \mu M$ $IC_{50} \sim 1.9 mM$ (Davies <i>et al.</i> , 2010)
$K_{ir}6.2/SUR1$	$IC_{50} \sim 7 \sim 22 \mu M$ (Ashcroft, 2005) (Ribalet <i>et al.</i> , 2003) (Kang <i>et al.</i> , 2008)	$IC_{50} \sim 64 \sim 115 \mu M$ ** (Ribalet <i>et al.</i> , 2003) (Dabrowski <i>et al.</i> , 2003)
$K_{ir}6.2/SUR2A$	$IC_{50} \sim 18 \sim 26 \mu M$ (Lodwick <i>et al.</i> , 2014) (Babenko <i>et al.</i> , 1998) (Babenko <i>et al.</i> , 1999)	$EC_{50} \sim 250 \mu M$ *** (Matsushita <i>et al.</i> , 2002) $IC_{50} \sim 275 \mu M$ ** (Lederer & Nichols, 1989)
$K_{ir}6.2/SUR2B$	$IC_{50} \sim 57 \sim 300 \mu M$ (Isomoto <i>et al.</i> , 1996) (Aziz <i>et al.</i> , 2012)	$EC_{50} \sim 28 \mu M$ *** (Matsushita <i>et al.</i> , 2002)

**Table 1.3: Sensitivity of ATP and ADP on major  $K_{ATP}$  channels.** \*Presence of 10  $\mu M$  pinacidil.  
\*\*Absence with  $Mg^{2+}$ . \*\*\*Presence with  $Mg^{2+}$ .

### 1.4.1 Distribution of $K_{ATP}$ channels and its diverse roles

As shown in Table 1.2 the  $K_{ATP}$  channel is ubiquitously expressed and the subunit combination in each tissue determines the channel function.

#### 1.4.1.1 *Pancreas*

$K_{ir}6.2$  containing channels have been most widely studied in pancreatic cells and cardiac ventricular myocytes (Flagg & Nichols, 2011), where mutation of these channel may cause defects in these two organs. The role of  $K_{ATP}$  in pancreatic  $\beta$  cells was identified by using transgenic mice carrying dominant-negative  $K_{ir}6.2$  that generated by substituting the glycine of the G-Y-G selectivity motif of the pore with serine (Miki *et al.*, 1997). In these experiments, hypoglycaemia was observed with hyperinsulinemia in new-born mice, whilst adults presented a downward trend in numbers of  $\beta$  cells while developing hyperglycaemia. These results suggest that the  $K_{ATP}$  channel function was impaired in the  $\beta$  cell so might play an important role in the regulation of insulin secretion (outlined in Figure 1.5). In the pancreatic  $\beta$  cell, the  $K_{ATP}$  channel is comprised of  $K_{ir}6.2/SUR1$  subunits (Bennett *et al.*, 2010). As a metabolic sensor, the  $K_{ATP}$  is closed in response to the increasing concentration of ATP (Tarasov *et al.*, 2004). When there is an increase in glucose, or intracellular ATP, the  $K_{ATP}$  channel will be closed causing a depolarization of the membrane potential, resulting in the voltage-gated  $Ca^{2+}$  channel activation (Tarasov *et al.*, 2004).

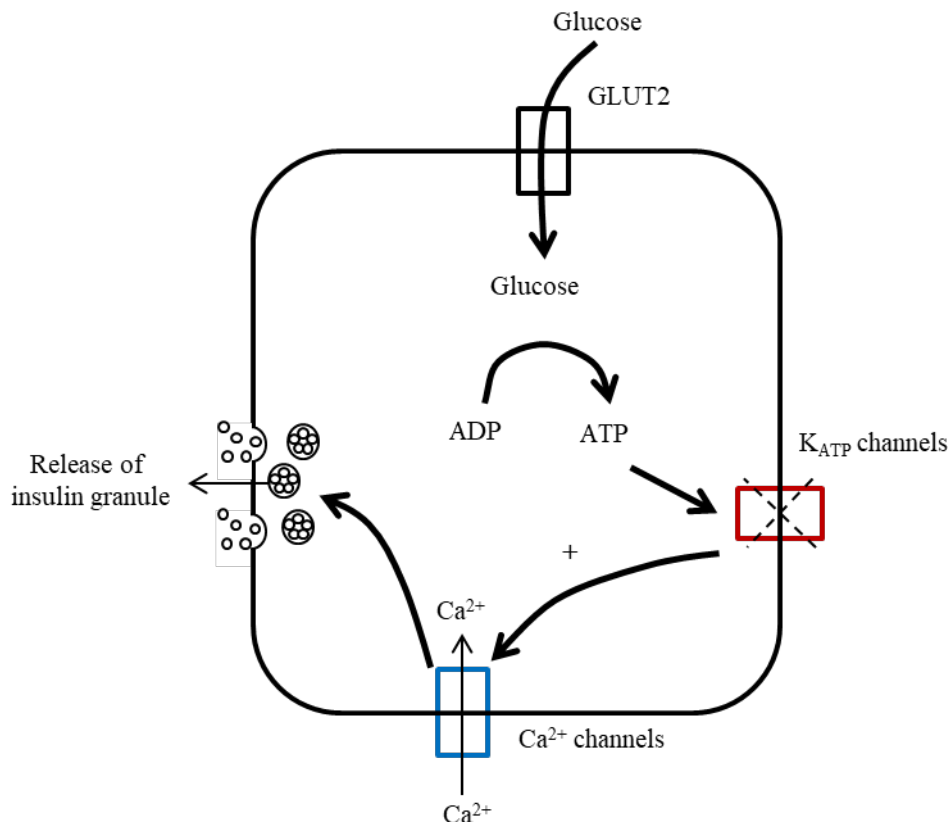


**Figure 1.5:  $K_{ATP}$  channel regulates the secretion of insulin in  $\beta$ -pancreatic cells.** Blood glucose enters the  $\beta$ -pancreatic cells via GLUT2 and increases the intracellular ATP, which inhibits the  $K_{ATP}$  channel and depolarise the membrane potential. The voltage-gated  $Ca^{2+}$  channel opened in response to the membrane depolarization and therefore resulting in insulin release.

#### 1.4.1.2 Smooth muscle

In vascular smooth muscle cells (VSMC), the accepted main isoform of  $K_{ATP}$  contains both  $K_{ir}6.1$  and SUR2B subunits and modulated by many vasodilators and vasoconstrictors so plays an important role in regulating the vascular tone (Yamada *et al.*, 1997; Yang *et al.*, 2008; Tang *et al.*, 2010; Shi *et al.*, 2012; Tian *et al.*, 2014). The VSMC type  $K_{ATP}$  channel is regulated by vasoactive hormones and neurotransmitters, such as  $\alpha$  and  $\beta$ -adrenergic receptor agonists, angiotensin II, arginine vasopressin and adenosine. In addition, as a member of the  $K_{ATP}$  channel family, metabolites such as ATP, ADP and pH can also regulate the VSMC  $K_{ir}6.1$  channel. Kakkar *et al* (2006) suggested that knockout the  $K_{ir}6.1$  gene in mouse induced spontaneous coronary vasospasm and sudden death. The vasculature isoform of  $K_{ATP}$  is relatively ATP insensitive, but has been shown to require intracellular ATP to open as it is hypothesized that this allows the  $K_{ir}6.1$ /SUR2B channel to

maintain a basal level of activity (Yamada *et al.*, 2011). The  $K_{ir}6.1$  channel activity is increased by vasodilators, so causing membrane potential hyperpolarization and reduced L-type  $Ca^{2+}$  channel activity, and decreased by vasoconstrictors causing an increase in  $[Ca^{2+}]_i$ .  $K_{ir}6.1$ , therefore, plays an important role in regulating vasoconstriction and so control of blood pressure. In animals expressing a gain-of-function mutant  $K_{ir}6.1$  channel, mice consistently have lower blood pressure (Li *et al.*, 2013a). In contrast, with conditional knockout of the gene, the lack of functional  $K_{ir}6.1$  leads to hypertension (Aziz *et al.* 2014).

#### **1.4.1.3 Skeletal muscle**

The  $K_{ir}6.2/SUR2A$  combination is considered as the  $K_{ATP}$  channel complex in skeletal muscle cells, demonstrated by loss of  $K_{ATP}$  activity in skeletal muscle cells in  $K_{ir}6.2$ -null animal (Miki *et al.*, 2002a) and SUR2-null animals (Chutkow *et al.*, 2001). Similar to the  $K_{ATP}$  channels within cardiomyocyte, the  $K_{ATP}$  channel remain in a closed state in the resting conditions, and is activated in response to metabolic inhibition (Hussain *et al.*, 1994; Matar *et al.*, 2000).

#### **1.4.1.4 Brain**

$K_{ATP}$  channels are widely expressed in the brain, where they are hypothesized to play a crucial role in preventing epilepsy and in neuroprotection. All known  $K_{ATP}$  channel subunits have been identified in the brain (Karschin *et al.*, 1997; Zhou *et al.*, 1999; Eaton *et al.*, 2002; Thomzig *et al.*, 2003; Ballanyi, 2004). The  $K_{ATP}$  channel composition in brain is region-dependent, where  $K_{ir}6.2$  containing channels are found in the hypothalamus, basal forebrain and striatum and probably associated with SUR1  $\beta$ -subunits (Karschin *et al.*, 1997; Miki *et al.*, 2001; Avshalumov & Rice, 2003; Chen *et al.*, 2003; Allen & Brown, 2004). In contrast,  $K_{ir}6.1$  was also found to co-express with SUR1 at peri-synaptic sites in the hippocampus, which regulating the release of glutamate (Soundarapandian *et al.*, 2007). It is suggested that the mechanism of neuroprotection is similar to that in cardiac tissue (Miki *et al.*, 2002a) and similarly, the  $K_{ATP}$  channel plays an important role by delaying the intracellular  $Ca^{2+}$  rise in Purkinje neurons as well as the dorsal vagal neurons (Ballanyi, 2004). Furthermore, the stimulation of adenosine A1 receptors or using the  $K_{ATP}$  opener nicorandil leads to a protection of the brain against the deleterious effect of hypoxia, which can be reversed by glibenclamide (Heurteaux *et al.*, 1995). Using  $K_{ir}6.2$ -null mice, Yamada

*et al* (2001) identified that these mice were susceptible to seizures after hypoxia, suggesting the  $K_{ir}6.2$  play a protective role in hypoxia-induced seizures. In addition, silencing the  $K_{ir}6.1$  gene in mice's hippocampus via RNAi also increases the susceptibility to seizures induced by kainic acid injection, suggesting the  $K_{ir}6.1$  type  $K_{ATP}$  channel may also play a vital role in the brain (Soundarapandian *et al.*, 2007).

#### **1.4.1.5 Heart**

The cardiac ventricular  $K_{ATP}$  channel complex has long been considered as  $K_{ir}6.2/SUR2A$ , however there is evidence to suggest that all  $K_{ATP}$  subunits can be identified in myocardial cells (Suzuki *et al.*, 1999; Singh *et al.*, 2003; van Bever *et al.*, 2004; Morrissey *et al.*, 2005*b*). Current opinion suggests that there are two locations where  $K_{ATP}$  channels are expressed in cardiomyocyte, sarcolemmal membrane and inner mitochondrial membrane (Bajgar *et al.*, 2001; Singh *et al.*, 2003; van Bever *et al.*, 2004; Morrissey *et al.*, 2005*b*, 2005*a*; Zhang *et al.*, 2010).  $K_{ATP}$  channels are highly important in the heart as they have been hypothesised to play an important role in coupling the metabolic state to the electrical activity. In the cardiomyocyte, the  $K_{ATP}$  channels are normally considered to only open in response to metabolic stress where their activity would hyperpolarise the membrane potential and shortening the action potential to preserve the intracellular ATP. Moreover, by using the  $K_{ATP}$  channel opener SR44866 (Bimakalim), Faivre & Findlay (1990) suggested that the action potential duration can be shortened to half by activating just 1% of the total available  $K_{ATP}$  channels.

### **1.4.2 Pharmacology of $K_{ATP}$ channels**

The pharmacological modulation of  $K_{ATP}$  channels usually occurs via the NBFx or TMDx of the SUR subunits, such as the sulphonylurea drug glibenclamide, where binding sites are located at TMD0 (Li *et al.*, 2017) or NBF1 (Mikhailov *et al.*, 2001; Pu *et al.*, 2008; Gregory *et al.*, 2017). The activator, pinacidil, has a binding site located on TMD2 and partly NBF2 (Moreau *et al.*, 2000; Flagg *et al.*, 2010). There also other types of drug which directly act on the pore structure of  $K_{ATP}$  channel, such as the  $K_{ir}6.1$  specific blocker PNU37883A, (Cui *et al.*, 2003; Kovalev *et al.*, 2004; Teramoto, 2006*b*; Ekman *et al.*, 2012). Among the  $K_{ATP}$  openers, as shown in Table 1.5, some show partial selectivity for SUR2

subunits over SUR1, such as pinacidil, P1075, cromakalim and nicorandil (Grover & Garlid, 2000; M. Ashcroft & M. Gribble, 2000; Gribble & Reimann, 2002).

Multiple binding sites on TMD0-3 and NBF1-2 for both pharmacological agents and nucleotides on SUR<sub>x</sub> subunits and some of the drugs can modulate sensitivity to nucleotides, or their own activity be modulated by the presence of nucleotides. Diazoxide has great affinity for SUR1 and SUR2B on its own, however it will also activate the SUR2A containing K<sub>ATP</sub> channels in the presence of MgADP (Grover & Garlid, 2000; Rodrigo *et al.*, 2004).

Unlike sulphonylurea drugs, PNU37883A (4-morpholinecarboxamidine-N-1-adamantyl-N0-cyclohexyl-hydrochloride) was developed as a non-sulphonylurea drug and shows a selective inhibitory effect on vascular K<sub>ATP</sub> channels with limited influence in other organs (Wellman *et al.*, 1999). As described in previous reports (Teramoto *et al.*, 2004; Kovalev *et al.*, 2004), PNU37883A is a pore blocker that blocks the pore directly from the cytoplasmic side and its sensitivity was linked to an 81 amino-acid section located at the C-terminal. PNU37883A can inhibit the K<sub>ir</sub>6.1 channel irrespective of the SUR subunits type and has been demonstrated to be a high affinity K<sub>ir</sub>6.1 blocker in vascular smooth muscle (Cui *et al.*, 2003; Hanna *et al.*, 2005; Teramoto, 2006*b*; Tan *et al.*, 2007). Similar to PNU, the PPAR $\gamma$  agonist, rosiglitazone, also shows a direct inhibitory effect on K<sub>ir</sub>6.x subunits regardless of the SUR subunits involved in the channel complex. Both PNU and rosiglitazone show selectivity for K<sub>ir</sub>6.1 over K<sub>ir</sub>6.2 (Yu *et al.*, 2012). However, unlike PNU, rosiglitazone acts from the cytoplasmic side of K<sub>ir</sub>6.x subunits (Yu *et al.*, 2012). The IC<sub>50</sub> for some common pharmacological inhibitors are outlined in table 1.4 for most major K<sub>ATP</sub> channel subunit combinations.

	Glibenclamide	PNU 37883A	Rosiglitazone	5-HD	HMR1098
K <sub>ir</sub> 6.1 /SUR1	Not Found	IC <sub>50</sub> =32 μM * (Surah-Narwal <i>et al.</i> , 1999)	Not Found	IC <sub>50</sub> =66 μM *** (Liu <i>et al.</i> , 2001)	IC <sub>50</sub> =100 μM *** (Liu <i>et al.</i> , 2001)
K <sub>ir</sub> 6.1 /SUR2A	IC <sub>50</sub> ~6 nM **** (Lodwick <i>et al.</i> , 2014)	Not Found	Not Found	NE ** (Liu <i>et al.</i> , 2001)	NE ** (Liu <i>et al.</i> , 2001)
K <sub>ir</sub> 6.1 /SUR2B	IC <sub>50</sub> ~56 nM ** (Stephan <i>et al.</i> , 2006)	IC <sub>50</sub> ~5 μM **** (Cui <i>et al.</i> , 2003; Kovalev <i>et al.</i> , 2004)	IC <sub>50</sub> ~10 μM **** (Yu <i>et al.</i> , 2012)	NE ** (Liu <i>et al.</i> , 2001)	NE ** (Liu <i>et al.</i> , 2001)
K <sub>ir</sub> 6.2 /SUR1	IC <sub>50</sub> ~0.48 nM ** (Stephan <i>et al.</i> , 2006)	NE * (Surah-Narwal <i>et al.</i> , 1999)	IC <sub>50</sub> ~45 μM **** (Yu <i>et al.</i> , 2012)	IC <sub>50</sub> =81 μM ** (Liu <i>et al.</i> , 2001)	IC <sub>50</sub> =5 μM ** (Liu <i>et al.</i> , 2001)
K <sub>ir</sub> 6.2 /SUR2A	IC <sub>50</sub> ~3 nM **** (Lodwick <i>et al.</i> , 2014)	IC <sub>50</sub> >100 μM **** (Cui <i>et al.</i> , 2003)	IC <sub>50</sub> ~37 μM **** (Yu <i>et al.</i> , 2012)	NE** (Liu <i>et al.</i> , 2001)	IC <sub>50</sub> =1.5 μM ** (Liu <i>et al.</i> , 2001)
K <sub>ir</sub> 6.2 /SUR2B	IC <sub>50</sub> ~42 nM ** (Dörschner <i>et al.</i> , 1999)	IC <sub>50</sub> ~15 μM **** (Cui <i>et al.</i> , 2003) / IC <sub>50</sub> >100 μM **** (Kovalev <i>et al.</i> , 2004)	IC <sub>50</sub> ~50 μM **** (Yu <i>et al.</i> , 2012)	NE** (Liu <i>et al.</i> , 2001)	IC <sub>50</sub> =100 μM** (Liu <i>et al.</i> , 2001)

**Table 1.4: IC50 for pharmacological inhibitors on major KATP channels.** NE indicates no effect. \*Currents were induced by 200 μM diazoxide. \*\* Currents were induced by 100 μM P-1075. \*\*\*Currents were induced by 100 μM diazoxide. \*\*\*\* Currents were induced by 100 μM pinacidil.

	Pinacidil	P-1075	Diazoxide	Nicorandil
K <sub>ir</sub> 6.1/SUR1	Not Found	NE (Liu <i>et al.</i> , 2001)	EC <sub>50</sub> =10 μM (Liu <i>et al.</i> , 2001)	Not Found
K <sub>ir</sub> 6.1/SUR2A	EC <sub>50</sub> ~45 μM (Lodwick <i>et al.</i> , 2014)	EC <sub>50</sub> ~1 μM (Liu <i>et al.</i> , 2001)	NE (Liu <i>et al.</i> , 2001)	Not Found
K <sub>ir</sub> 6.1/SUR2B	EC <sub>50</sub> ~0.21 μM (Suzuki <i>et al.</i> , 2001)	EC <sub>50</sub> =0.16 μM (Liu <i>et al.</i> , 2001)	EC <sub>50</sub> ~30 μM (Liu <i>et al.</i> , 2001)	EC <sub>50</sub> ~10-15 μM * (Fujiwara & Angus, 1996; Hsieh <i>et al.</i> , 2001)
K <sub>ir</sub> 6.2/SUR1	NE at 1 mM (Yunoki <i>et al.</i> , 2003)	EC <sub>50</sub> ~5 μM (Liu <i>et al.</i> , 2001)	EC <sub>50</sub> ~10 μM (Liu <i>et al.</i> , 2001)	Not Found
K <sub>ir</sub> 6.2/SUR2A	EC <sub>50</sub> ~10-32 μM (Shindo <i>et al.</i> , 1998) (Lodwick <i>et al.</i> , 2014)	EC <sub>50</sub> ~5 μM (Liu <i>et al.</i> , 2001)	NE (Liu <i>et al.</i> , 2001) EC <sub>50</sub> ~10 μM ** (D'hahan <i>et al.</i> , 1999)	EC <sub>50</sub> >500 μM (Shindo <i>et al.</i> , 1998)
K <sub>ir</sub> 6.2/SUR2B	EC <sub>50</sub> ~2 μM (Shindo <i>et al.</i> , 1998)	EC <sub>50</sub> =0.16 μM (Liu <i>et al.</i> , 2001)	NE (Liu <i>et al.</i> , 2001)	EC <sub>50</sub> ~10 μM (Shindo <i>et al.</i> , 1998)

**Table 1.5: EC50 for pharmacological activators on major K<sub>ATP</sub> channels.** NE indicates no effect. \*EC<sub>50</sub> were obtained by measuring the percentage vascular relaxation. \*\*\*Presence with 100 μM ADP.

### 1.4.3 K<sub>ATP</sub> channels and their role in diseases

As K<sub>ATP</sub> channels are ubiquitously expressed, a disruption of normal K<sub>ATP</sub> channel activity that occurs in diseases show several physiological consequences. In the pancreas, a decreased K<sub>ATP</sub> current due to mutation has been identified to be associated with congenital hyperinsulinism, with excessive amounts of insulin secretion (Akrouh *et al.*, 2011). In the vasculature, when the K<sub>ATP</sub> currents are inhibited, the membrane potential is depolarized so aberrantly activating the L-type Ca<sup>2+</sup> channel which enhances vasoconstriction (Nichols *et al.*, 2013).

### 1.4.3.1 Cardiac $K_{ATP}$ channels in diseases

In cardiac tissues, the  $K_{ATP}$  channels are strongly associated with some disease states. Recently, a  $K_{ir}6.1$  encoding gene (*KCNJ8*) mutation (S422L) demonstrated a clear connection with the sinus rhythm, which was found in a patient suffer from both idiopathic VF and prominent sinus rhythm (HAÏSSAGUERRE *et al.*, 2009). From the same S422L mutation in  $K_{ir}6.1$  encoding gene, Brugada syndrome, atrial fibrillation and early repolarization syndrome is also reported (HAÏSSAGUERRE *et al.*, 2009; Medeiros-domingo *et al.*, 2010; Delaney *et al.*, 2012). Among those diseases, the  $K_{ATP}$  channels in Brugada syndrome and early repolarization syndrome show and increased expression. By comparing this  $K_{ir}6.1$ -S422L channel with the wild-type, the ATP sensitivity of the mutant is reduced, perhaps explaining the gain-of-function (Barajas-Martínez *et al.*, 2012). In terms of the SUR subunits, there are no SUR1 mutations associated with cardiac disease, which complements the hypothesis that SUR1 is not expressed in the ventricular tissue. However, in the loss-of-function mutation of *ABCC9*, or SUR2, the long-standing AF and idiopathic dilated cardiomyopathy have been found to be associated with the mutation (Bienengraeber *et al.*, 2004; Olson *et al.*, 2007). Analysis of the mutation of *ABCC9* in Cantu syndrome, the mutation was found as gain-of-function (Grange *et al.*, 2006; Van Bon *et al.*, 2012).

### 1.4.4 $K_{ATP}$ channel knockout models and what they tell us

$K_{ir}6.2$ /SUR2A has been generally considered as the cardiac sarcolemmal  $K_{ATP}$  (Sarco $K_{ATP}$ ). This hypothesis was further confirmed by studying  $K_{ir}6.2$  gene knockdown mice, where Suzuki *et al* (2002) demonstrated that the  $K_{ATP}$  channel opener (KCO) pinacidil was unable to shorten the APD compared with a significant effect in WT mice. Furthermore, the Sarco $K_{ATP}$  was absent in sino-atrial node cells in the  $K_{ir}6.2$  knockout animal (Fukuzaki *et al.*, 2008). A further experiment was conducted by Yamada *et al* (2006), using an aortic constriction model in  $K_{ir}6.2$  knockout mice to investigate the role of cardiac  $K_{ATP}$  channels in HF. After several hours of aortic constriction,  $K_{ir}6.2$ -KO mice presents features of congestive HF, such as decreased cardiac heart function, fluid retention, ventricular conduction block and progressive sinus bradycardia. 50% of  $K_{ir}6.2$ -KO mice were dead after 48 h. In contrast, none of the wild-type mice demonstrates signs of HF or increase

mortality. In ECG recording, one of the classical standards in ischaemic measurement is the elevation of the ST-segment. In wild type mice, when creating anterior wall myocardial infarction with the ligation of coronary arteries, the ST-segment was elevated in ECG recordings as soon as the ligation occurs. From Li *et al* (2000) research in  $K_{ir}6.2$ -deficient mice, after anterior wall myocardial infarction by ligation of coronary arteries, ST-segment showed no change on ECG recordings which suggests the involvement of  $K_{ATP}$  channels in myocardial infarction. Although it is generally accepted that  $K_{ir}6.1$  is not the dominant  $K_{ATP}$  channel expressed in cardiac myocytes, the findings from  $K_{ir}6.1$  null animal suggest this channel should not be ignored. In knockdown of the  $K_{ir}6.1$  gene, mice illustrated a high mortality rate of a sudden, premature death (Miki *et al.*, 2002). Minami *et al* (2004) suggested that the sudden death of  $K_{ir}6.1$  null mice was due to myocardial ischemia. This finding suggested that  $K_{ir}6.2$  was not the only  $K_{ir}6$  subunit in cardiac cells.

## 1.5 The cardiac action potential

An action potential occurs in excitable cells after an electrical impulse is received that is substantial enough to cause a rapid depolarisation from resting membrane potential. An action potential can be propagated from cell to cell through gap junctions in cardiomyocytes. In cardiomyocytes, action potentials are initiated by the cardiac pacemaker cells rather than from central nervous system activity as in skeletal muscle.

### 1.5.1 The human ventricular cardiac action potential and the Ion channels underlying phases 0 to IV

The cardiac action potential is typically separated into five phases. In phase 4, the ventricular myocyte is in diastole with a stable resting membrane potential. In this phase ions are still moving in and out of the cardiomyocyte however there is a dynamic balance that allows for maintains of a stable potential difference. In order to maintain the resting membrane potential in this phase, several ion channels are involved, specifically the  $K_{ir}2.1$  channel (Miake *et al.*, 2003); as well as some ion pumps and exchangers which regulate the ionic gradients. In human ventricular myocyte, the resting membrane potential is around -90 mV (Santana *et al.*, 2010) The resting membrane potential is close to the  $E_K$ , suggesting

that  $K^+$  is the dominant ion moving across the membrane in this phase (Ivanov *et al.*, 2004). In addition, due to the slow deactivation kinetics, both  $K_v11.1$  and  $K_v7.1$  remain active in the initial of phase 4 (Schmitt *et al.*, 2014). In phase 0 of the cardiac action potential a rapid depolarisation from resting membrane potential is seen, from around -90 mV to approximately +50 mV in human ventricular myocytes (Santana *et al.*, 2010), close to  $E_{Na}$ , suggesting the  $Na^+$  channel plays a substantial role in the phase. After the influx  $Na^+$  ions raise the membrane potential to the peak, the depolarization is terminated due to the inactivation of  $Na_v1.5$  currents and the activation of  $I_{to}$  currents and NCX (Santana *et al.*, 2010). The action potential enters phase 2, with a sustained plateau from the influx  $Ca^{2+}$  ions (Bourgonje *et al.*, 2013). Taken together, all the movements of these ions reach a relative balance so that allows the membrane potential remains constant. In phase 3, the action potential rapidly repolarises due to the inactivation of L-type  $Ca^{2+}$  channels and the increasing activity of  $I_{ks}$ ,  $I_{kr}$  and  $I_{kl}$  currents. Therefore, the action potential terminates as the resting membrane potential is restored, returning to phase 4.

#### ***1.5.1.1 The electrical conduction system in the heart:***

The electrical conduction system within the heart is important in regulating the excitation and contraction of cardiomyocytes by coordinating spread of excitation throughout the heart. The electrical impulse is initiated in the sinoatrial node (SAN) in the right atrium, which is firstly transmitted into the atria, and then to the atrioventricular node (AVN) which located in the interatrial septum. To ensure the ventricular contraction occurs after the atria, the conduction of the electrical signal is delayed for up to 0.12 s in the AVN. Additionally, there is a marked difference in the action potential between ventricular and atrial myocytes which is most clear in phase 2, where the atrial myocyte has a smaller  $Ca^{2+}$  influx therefore demonstrates shorter plateau phase, compared with ventricular myocytes. Following the AVN, the stimulus passes through the Purkinje fibres and into the cells in the ventricles, where the electrical impulse continues to be transmitted via gap junctions throughout the myocardium.

##### ***1.5.1.1.1 Sinoatrial node***

As a cardiac pacemaker, the sinoatrial node can continually trigger action potentials that propagate throughout the heart. Unlike ventricular cardiomyocytes, the SAN does not have

a stable resting phase between action potentials. The membrane potential gradually depolarises until reaching the threshold for triggering of another action potential. This pacemaker potential begins as soon as phase 4 completes and so the membrane potential begins to depolarise again. The ‘funny’ currents ( $I_f$ ) underlie the pacemaker potential due to the hyperpolarization-activated cyclic nucleotide-gated (HCN) current. The  $I_f$  currents are non-selective  $\text{Na}^+$  and  $\text{K}^+$  currents and slowly activate in the voltage range of diastole; then rapidly deactivate on depolarisation (DiFrancesco, 2010). In addition, cAMP significantly increases the  $I_f$  currents via direct interaction with the f/HCN channel (DiFrancesco, 1995). Altering  $I_f$  current therefore modulates the spontaneous activity in the SAN so controls heart rate. For example,  $\beta$ -adrenergic agonists (sympathetic drive) stimulate  $I_f$  currents, which leads a more rapid depolarization phase to increase heart rate, but with only modest alteration in the shape of action potential (DiFrancesco, 2010). Conversely, parasympathetic drive slows the pacemaker potential and so slows heart rate.

Once the  $I_f$  currents raises the membrane potential to the threshold value, the L-type calcium channels fully open and action potential occurs. The L-type  $\text{Ca}^{2+}$  channels inactivate and the  $\text{K}^+$  channels dominate triggering the repolarization of the pacemaker cell. Within the heart, the SAN has the highest automaticity (Table 1.3) compared with other rhythmic cells.

#### ***1.5.1.1.2 Atrioventricular Node***

The AVN is located at the lower back of the interatrial septum, which connects the atria and ventricle. In order to allow the atrial contraction to occur independently of the ventricle, so that the blood in left and right atrium can be ejected into ventricle, the AVN delays the electrical impulse from SAN for up to 0.12 s. The delayed in conducting electrical impulse received from atria was probably due to the gap junctions that connected AV cells were composed by Cx40, which conducts signals in a much slower velocity (Saksena & Marchlinski, 2015). This property also protect the ventricles from contracting in excessively speed that caused by atrial arrhythmia. Similar to the SA cells, the AV cells also have  $I_f$  currents in response of the repetitive depolarization. However, as the absence of  $I_{k1}$  currents, the resting membrane potential for AV cells is higher, helping the cells

reaching the threshold potentials (Saksena & Marchlinski, 2015). Within the heart, the AVN generate slower electrical impulses (Table 1.6) compared with the SAN.

<b>Pacemaker</b>	<b>Location</b>	<b>Inherent rate (beats per minute, BPM)</b>
Sinoatrial (SA) node	Right atrium (RA) at junction with superior vena cava (SVC)	~100 BPM (Verkerk <i>et al.</i> , 2007)
Atrioventricular (AV) node	RA at posteroinferior area of interatrial septum	~50 BPM (Shaffer <i>et al.</i> , 2014)
Purkinje fibres	Throughout the ventricles	~30 BPM (Shaffer <i>et al.</i> , 2014)

**Table 1.6: Cardiac cell types displaying pacemaker behaviour.**

### ***1.5.1.1.3 Ventricular action potentials and regional variations***

As the cardiac action potential is dependent on the ion channel activity, the different distribution of ion channels in the heart causes regional variations in action potentials. A major cause of the regional variations are outward  $K^+$  channels (Fedida & Giles, 1991). By studying the rat cardiac action potential duration (APD) in endocardial trabeculae and papillary muscle from left and right ventricle, the APD was found to be different between the left and right ventricles (Watanabe *et al.*, 1983). Similar result were also found in canine ventricles, between epicardium and endocardium, where some action potential properties, such as amplitude and APD, were altered (Litovsky & Antzelevitch, 1988). Fedida & Giles (1991) demonstrated that the transient outward currents were reduced in density, from epicardium to endocardium and papillary muscle cells (Fedida & Giles, 1991). By calculating the outward transient  $K^+$  channel density, Fedida & Giles (1991) suggested the epicardial cells have the largest channels density and followed by endocardial cells, with the lowest channel density in papillary myocyte.

#### ***1.5.1.1.3.1 Purkinje fibres***

Purkinje fibres are important components of the cardiac conduction system, which are enriched with mitochondria and  $Na^+$  channels so that the electrical impulse can be conducted rapidly. Purkinje fibres in the subendocardium transmit electrical activity from the SAN and are arranged in longitudinal direction to the ventricle walls. Due to the

specialized structure for conducting the impulse, the Purkinje fibres are larger than cardiomyocytes but have fewer myofibrils. In normal physiological conditions, the Purkinje fibres conduct the action potential from both side bundle branches to the ventricles, maintaining cardiac rhythmicity with the pace generated at the SAN. However, if both SAN and AVN malfunction the Purkinje fibres generate a slow, ~25 BPM electrical pulse.

#### *1.5.1.1.3.2 base to apex*

The action potential duration is known to differ in duration from base to apex, with a longer duration at base than that at the apex (NOBLE & COHEN, 1978). The apex area needs to contract earlier and for longer than that in the base region. In addition, the epicardial action potentials begin at the left ventricle apex and are propagated to the right atrio-ventricular groove (Laurita *et al.*, 1996). In the basal area,  $I_{ks}$  has been shown to be the dominant repolarising current, demonstrating slow activation/inactivation kinetics (described in section 1.3.2.3.3) so causing a slow repolarization (Cheng *et al.*, 1999). The shorter action potential duration within the apex myocyte is due to their repolarizing currents being predominantly  $I_{kr}$ . As described in section 1.3.2.3.2, the unique channel kinetics allow this channel to be rapidly released from an inactivated state on repolarization and therefore provides a substantial repolarising current (Cheng *et al.*, 1999).

#### *1.5.1.1.3.3 endo to epicardial*

Differences have also been found in the action potential between endocardial and epicardial cells, with endocardial action potential duration being longer than that in epicardia (Bryant *et al.*, 1998; Burton & Cobbe, 2001). Another population of cells, termed M cells, have the longest action potential duration in the transmural gradient, and are located in the middle of endocardial and epicardial cells (Sicouri & Antzelevitch, 1991; Bryant *et al.*, 1998). Although the  $I_{to}$  currents are large and shape the early repolarization in Phase 1 to a spike-and-dome configuration in epicardial and M cells, the rapid inactivation kinetics excludes  $I_{to}$  currents from Phase 3 repolarization (Liu & Antzelevitch, 1995). Bryant (1998) demonstrated that the transmural dispersion was caused by different  $I_{ks}$  and  $I_{kr}$  current densities in each region. In guinea pig ventricle, both  $I_{kr}$  and  $I_{ks}$  currents are significantly lower in endocardial cells than the epicardial cells, which is hypothesised to explain why the APD in endocardial cells are longer than that in epicardial cells (Bryant *et al.*, 1998).

## 1.5.2 Modulation of the cardiac action potential

Sodium currents are primarily responsible for cardiac action potential depolarization, changing the membrane potential from  $-80$  mV to  $\sim +25$  mV in 5-10 ms (Petitprez *et al.*, 2008). Although the  $\text{Na}^+$  currents are only sustained for 1–3 ms, the  $\text{Na}^+$  currents can still modulate the action potential. By using tetrodotoxin (TTX), a  $\text{Na}^+$  channel inhibitor, the rate of depolarization in the action potential was decreased by 10% (Brette & Orchard, 2006). Additional application of TTX to the Purkinje fibres resulted in a loss of propagation of the action potential (Carmeliet, 1987). T-type  $\text{Ca}^{2+}$  channel and L-type  $\text{Ca}^{2+}$  channels play different roles in different regions of the heart (Perez-Reyes, 2003). By inhibiting the T-type  $\text{Ca}^{2+}$  channel, the SAN firing rate was significantly reduced in rabbit heart (Doerr *et al.*, 1989; Satoh, 1995). L-type  $\text{Ca}^{2+}$  channels play the largest role in phase 2, and tend to cause bradycardia if they are inhibited or if there is a partial loss-of-function mutation (Ivanov *et al.*, 2004). Potassium currents perhaps have the most important role in modulating the repolarization in cardiac action potential, which is described in section 1.3.2.3 and in section 1.4.3.

### 1.5.2.1 Modulation of the cardiac action potential by parasympathetic nervous system (PSNS) control

Heart rate is modulated by both parasympathetic and sympathetic nerve activity from the autonomic nervous system (ANS). The ANS modulates the unconscious functions, for example the heart rate, digestion, respiratory rate, pupillary response, urination, and sexual arousal. PSNS also been referred as ‘rest-and-digest’ system. PSNS innervation to the heart from vagal branches, with the efferent component of preganglionic fibres connected between vagal branches and the heart. Furthermore, the PSNS makes synaptic connections with ganglion cells in the cardiac plexus or intracardiac ganglia. In the cardiac action potential innervation, the major neurotransmitter produced from PSNS activity is Acetylcholine (ACh) which is released by the stimulated preganglionic neurons and acts on postganglionic neurons to stimulate the nicotinic receptors. Finally, the ACh released by postganglionic neuron stimulates the muscarinic receptors of the target organ. Stimulation of the parasympathetic branch results in a suppression effect that decreases heart rate and contractility. In humans, the loss-of-function in parasympathetic was often associated with

severe heart failure (Marmar & Shivkumar, 2008). To suppress the SAN activity, the PSNS activates an Ach-dependent  $K^+$  channel ( $K_{ACH}$ ) which hyperpolarizes the membrane potential in the SAN, causing the resting membrane potential to be more hyperpolarized. This causes a suppression of  $I_f$  currents and so slows the heart rate (DiFrancesco, 2010).

### ***1.5.2.2 Modulation of the cardiac action potential by sympathetic nervous system (SNS) drive***

The Sympathetic nervous system (SNS) innervates the heart from both cervical and thoracic sympathetic ganglia. Although some of the SNS is located in central nervous system, the SNS is normally considered as peripheral. Sympathetic cardiac nerves arise in the sympathetic trunk ganglia. The sympathetic nerves follow the course of the common pulmonary artery, which goes into the plexus that innervates the main left coronary artery, finally, extending into the superficial epicardial of the heart, which enter the myocardium with the coronary arteries. The SNS regulate the body's 'fight-or-flight' response. The released Ach from preganglionic sympathetic neuron then activates the postsynaptic neuron so that it secretes noradrenaline; which also causes hormonal secretion of adrenaline from adrenal medulla if under extended stimulation. Together, both adrenaline and noradrenaline act on adrenergic receptors in the cardiovascular system, which increases cardiac output, cardiac contractile force, cardiac conduction and heart rate. The  $\beta$ -adrenergic receptor is the mostly found adrenergic receptor within the heart, which is activated by both adrenaline and noradrenaline.  $\beta$ -adrenergic receptors downstream signalling includes cAMP and PKA which can phosphorylate a wide range of membrane proteins (Chen *et al.*, 2014). The stimulation of  $\beta$ -adrenergic receptor can lead to an increased  $I_f$  currents in SAN, which are activated via direct binding of cAMP resulting more rapid pacemaker potential so increasing firing rate of the action potential (DiFrancesco, 2010).

### ***1.5.2.3 Pharmacological modulation of the action potential***

As there are many compounds that can alter cardiac ion channel behavior, pharmacological modulation of the cardiac action potential is possible in disease states, such as arrhythmia. The classification of antiarrhythmic drugs is using the Vaughan-Williams Classification of Antiarrhythmic Drugs (Table 1.7), where drugs are categorized by their effect on cardiac electrophysiology.

<b>Drug Class</b>	<b>Mechanism of action:</b>	
<b>Class I</b>	Na <sup>+</sup> channel modulators	
	<b>A.</b>	Na <sup>+</sup> channel blockers (intermediate dis/association rates) (alter QRS complex) e.g. procainamide
	<b>B.</b>	Na <sup>+</sup> channel blockers (fast dis/association rates) (can prolong QRS on overdose) e.g. lidocaine
	<b>C.</b>	Na <sup>+</sup> channel blockers (slow dis/association rates) e.g. flecainide
<b>Class II</b>	Anti-sympathetic nervous system agents – most β-blockers e.g. propranolol, atenolol	
<b>Class III</b>	K <sup>+</sup> efflux modulators – most blockers currently). sotalol (a β-blocker) and amiodarone show class III activity	
<b>Class IV</b>	Class IV agents (Ca <sup>2+</sup> channel blockers and AVN modulators). e.g. verapamil, diltiazem	
<b>Class V</b>	Class V agents (other or unknown mechanisms). e.g. digoxin, adenosine.	

**Table 1.7: The Vaughan-Williams Classification of Antiarrhythmic Drugs.**

As is outlined in Figure 1.6, Class I antiarrhythmic Na<sup>+</sup> channel blockers can slow the conduction velocity of the heart, blocking reentry excitability and so limit arrhythmias. According to the different electrophysiological effects, Na<sup>+</sup> channel blockers are divided into IA, IB and IC three categories. Class IA drugs inhibit the opening of Na<sup>+</sup> channels and

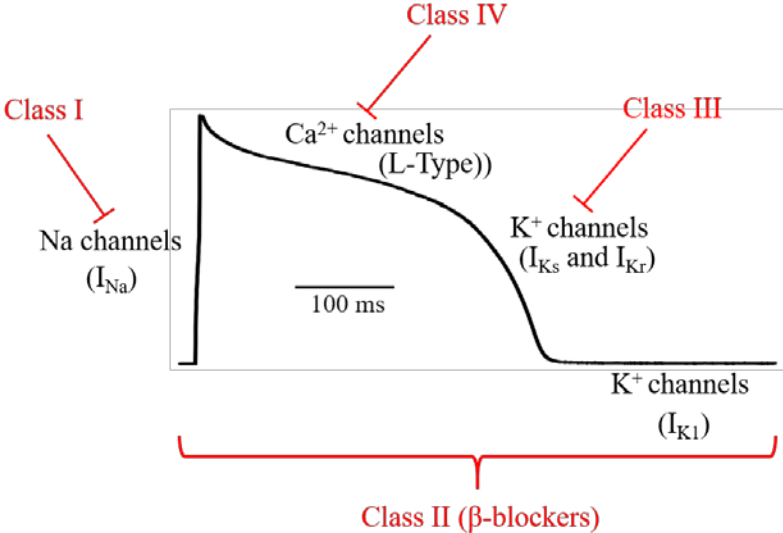


**Figure 1.6: Diagram showing the point of action of different classes of antiarrhythmic drugs**

delay the recovery of channel inactivation. Class IB drugs inhibit the  $\text{Na}^+$  channel and promote  $\text{K}^+$  efflux from the cell to shorten the APD, so extending the refractory period. Class IC drugs strongly inhibit  $\text{Na}^+$  channels, resulting in effective refractory period (ERP) extension, slowed conduction and a reduction in aberrant early activation.

Class II drugs are  $\beta$ -adrenoceptor blockers and so have indirect ion channel effects (Figure 1.6). Blocking the  $\beta$ -adrenoceptors decreases cAMP concentration so inhibiting L-type  $\text{Ca}^{2+}$  channel activity but reduced activity of PKA (Szentmiklosi *et al.*, 2015). Furthermore, the decreasing in intracellular cAMP can also reduce the  $I_f$  current in the pacemaker cells so reducing heart rate (Baruscotti *et al.*, 2005).

Class III drugs are  $\text{K}^+$  channel blockers, so prolonging APD and suppressing tachyarrhythmia from reentry (Figure 1.6). The  $I_{kr}$  channel kinetics are closely related to  $[\text{K}^+]_o$  that with increasing  $[\text{K}^+]_o$  the open probability of  $I_{kr}$  channel is increased; decreasing  $[\text{K}^+]_o$  reduces the open probability of  $I_{kr}$  (Sanguinetti *et al.*, 1995). Therefore, if medication was accompanied with low  $[\text{K}^+]_o$ , APD prolongation may occur and produce arrhythmia (Sanguinetti *et al.*, 1995). Amiodarone has blocking effects on both  $I_{kr}$  and  $I_{ks}$  current as well as  $\text{Na}^+$  channels (Ghovanloo *et al.*, 2016),  $\text{Ca}^{2+}$  channels (Kobayashi *et al.*, 2014) and  $\beta$ -adrenoceptors (Ghovanloo *et al.*, 2016), resulting in APD prolongation, ERP extension and slowed heart rate.

Class IV drugs are  $\text{Ca}^{2+}$  channel blockers. These are used to block the L-type  $\text{Ca}^{2+}$  channel in sinoatrial and atrioventricular node to slow the heart rate. Due to the negative effects that the decreasing  $\text{Ca}^{2+}$  influx causes in terms of reducing contractile force, Verapamil is not the first chose in arrhythmia treatment. However, Verapamil is important in treating angina due to the reduced oxygen demand in the myocardium as well as relief of coronary vasospasm.

Cardiac ion channels may also be modulated by off target effects of drugs. For example, glibenclamide, an early therapeutic given to type II diabetics to promote insulin secretion via blockade of the ATP-sensitive  $\text{K}^+$  ( $\text{K}_{ATP}$ ) channel, was also found to block the same channel family in the heart (Karck *et al.*, 2001; Sanada *et al.*, 2001; Pu *et al.*, 2008).

Furthermore, a number of drugs have been withdrawn from the market because of their effect of blocking the  $I_{kr}$  current in cardiac cells, causing a prolonged APD which could lead to arrhythmias and even sudden cardiac death (Ackerman & Clapham, 1997; Vincent *et al.*, 1999; Shieh *et al.*, 2000; Brown, 2004; Lu *et al.*, 2012).

### 1.5.3 Species variation in the cardiac action potential

As it was described in section 1.3.1.3, the different properties of ion channel cause action potential variation, so between species the cardiac action potential can be different due to the differential expression of channels. As shown in Figure 1.7, the cardiac action potential between rabbit and guinea pig is similar, except the rapid early repolarization, or notch, in phase 1 due a lack of  $I_{to}$  currents in guinea pigs. Rat ventricular myocyte action potentials are significantly shorter, demonstrating a prominent phase 1 with a lack of distinct plateau phase and finally with a relatively slow repolarization to terminate the action potential. Compared to the rabbit, smaller rodents have a larger  $I_{to}$  current which rapidly repolarises the membrane potential (Varró *et al.*, 1993). In terms of the relatively slow repolarization at the phase 4 of rat action potential, the possible reason is the smaller  $I_{k1}$  currents the rat express (Varró *et al.*, 1993).

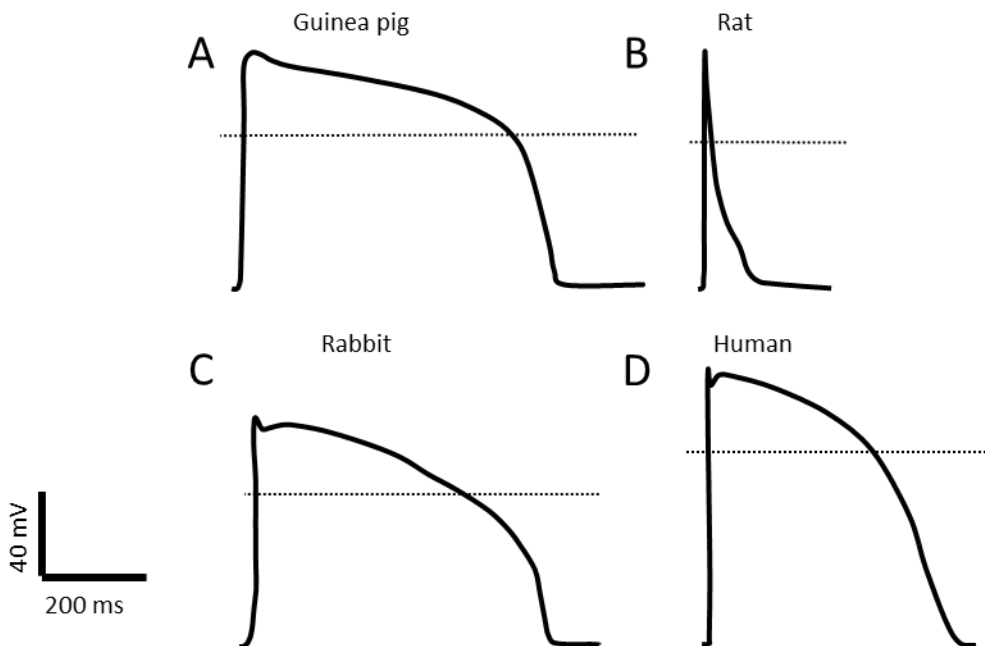


**Figure 1.7: Action potential in distinct species, recorded from guinea pig, rat, rabbit and human ventricular myocyte.** All action potential was stimulated in 0.5 Hz and recorded in room temperature, from isolated guinea pig, rat, rabbit and human ventricular myocyte. Figures were adapted from Varró (1993) and Li (1999).

In comparisons, the human cardiac action potential is more like that in rabbit, with one noticeable notch in phase 1 repolarization, but demonstrates a more negative resting potential of  $\sim -90$  mV (Santana *et al.*, 2010)) compared with that rat ( $\sim -70$  mV (Kavak *et al.*, 2008)), guinea pig ( $\sim -80$  mV (Vandenberg *et al.*, 1997) and rabbit ( $\sim -80$  mV (Fedida & Giles, 1991)). This is perhaps due to the larger expression of  $I_{K1}$  in human cardiomyocytes (Miake *et al.*, 2003).

#### 1.5.4 Diseases altering the cardiac action potential

In cardiac diseases, perturbations in ion channel function can cause marked changes in the action potential.

##### 1.1.1.1 Long QT syndrome

Long QT syndrome (LQTS) is caused by a delayed repolarization in ventricle action potential, is characterized by a prolonged QT interval in electrocardiogram (ECG, see figure 1.8) and can lead to fatal arrhythmias. The origin of the long QT syndrome can be separated into different ion channel genes and so alterations in currents. Two of the repolarising  $K^+$  currents underlie most LQT syndromes. Mutations of the  $K_v7.1$  protein, that underlies  $I_{Ks}$ , can cause an LQT syndrome (LQT1) that is often subclinical, as  $I_{Ks}$  is not the main repolarising current in most of the myocardium (Wang *et al.*, 1996). The loss-of-function in hERG channel, that underlies the  $I_{Kr}$  current, cause a more pronounced form of LQT syndrome (LQT2) that has a high incidence of ventricular arrhythmias, often leading to sudden cardiac death (Sanguinetti *et al.*, 1996), Mutations in these channels account for  $\sim 90\%$  of all cases of LQT syndrome. LQT3 syndrome is a much less common, but equally dangerous condition affecting  $\sim 5\%$  patients with LQT syndromes. LQT3 is associated with mutations in *SCN5A* which increases the  $Na^+$  current in early depolarization, resulting in longer repolarization and therefore a prolonged QT interval in ECG (Bennett *et al.*, 1995; Medeiros-Domingo *et al.*, 2007). Moreover, the mutation on the other gene and protein, such as *SCN4B* (Medeiros-Domingo *et al.*, 2007; Tan *et al.*, 2010) and  $\alpha 1$ -syntrophin (Medeiros-Domingo *et al.*, 2007; Wu *et al.*, 2008; Cheng *et al.*, 2009), significantly increase the  $Na_v1.5$  open time in depolarization and leading a long QT syndrome as well as sudden infant death syndrome.

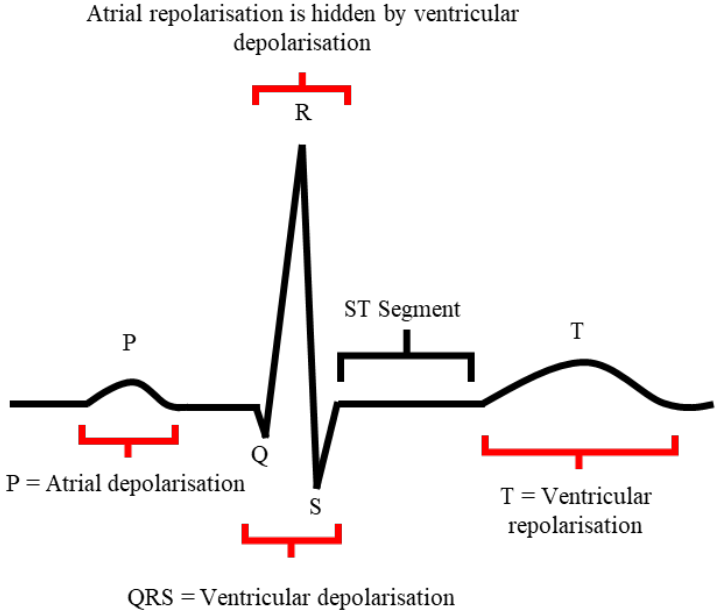


**Figure 1.8: An example ECG from Lead II.** Lead II ECG recorded the depolarization/repolarization vectors (between left leg and right arm) in the heart, begins from the ‘P’ wave: depolarization of atrial, from right atrial to the left. The ‘QRS’ complex represents to the ventricular depolarization. The ST-segment represents the phase 2 repolarization in ventricular, almost no activity from isoelectric line due to ventricular isoelectric. ‘T’ wave represents the repolarization in left and right ventricular.

**1.5.4.1 Arrhythmias**

Heart arrhythmia occurs when the regular heart rhythm is disrupted or there is a loss of coordination in the spread of electrical excitability which may cause the heart rate to be either too fast (tachycardia) or too slow (bradycardia). This can also be variable, from a transient palpitation to complete fibrillation that may lead to cardiac arrest or sudden death. The trigger for arrhythmia can vary; one such trigger is the atypical automaticity of pacemaker AVN or SAN driven by enhanced sympathetic or ion channel remodelling (Imanishi & Surawicz, 1976; Zicha *et al.*, 2005). Additionally, an increase in extracellular  $K^+$  can also lead to arrhythmia due to the reduction of  $I_{kr}$  and  $I_{kl}$  (Katzung & Morgenstern, 1977). Atypical depolarizations may occur and can be categorized as early afterdepolarizations (EAD) which often result in an aberrant reactivation of  $Na^+$  channels during the plateau phase giving a second depolarization spike, or delayed afterdepolarization (DAD) where the additional depolarization occurs either late in repolarization or after complete repolarization. The DAD is often triggered by excessive activity of NCX at the resting membrane potential, which depolarizes the membrane potential and triggers the  $Ca^{2+}$  release from SR (Marban *et al.*, 1986; Boyden *et al.*, 2000).

#### ***1.5.4.1.1 Ventricular arrhythmias***

Ventricular arrhythmias occur when abnormal electrical impulses start in the ventricular conduction system, and include ventricular tachycardia and ventricular fibrillation (VF). Among them, VF is more dangerous and life-threatening. When VF occurs, the disorganised electrical activity in ventricles causes the heart to “quiver” without pumping blood into the circulation. By studying the  $I_{K1}$  gain-of-function mouse model, a hyperpolarised resting membrane potential was observed in both atrial and ventricular tissue, leading them to be prone to re-entry for  $Na^+$  channel and so increased the frequency of VF (Samie *et al.*, 2000; Warren *et al.*, 2003). Conversely, inhibition of  $I_{K1}$  has an anti-arrhythmic effect (Samie *et al.*, 2000; Warren *et al.*, 2003).

#### ***1.5.4.1.2 Atrial arrhythmias***

Atrial fibrillation (AF) is an atypical heart rhythm that includes the feature of rapid and irregular beating of the atria. AF can be induced by mutation of a number of different genes including *SCN1B* and *SCN2B*, resulting in the reduction of the  $Na^+$  current in the early depolarization (Watanabe *et al.*, 2008, 2009). Furthermore, as  $I_{K1}$  contributes the most during phase 3 repolarization, the upregulation of  $I_{K1}$  has been suggested associated with AF (Workman *et al.*, 2001; Tang *et al.*, 2015).

### **1.6 Metabolism in the heart**

Under normal physiological conditions, oxidative phosphorylation in the mitochondria produces more than 95% of the ATP in the heart, with the last 5% generated from glycolytic metabolism. Around 60% to 70% of the total ATP produced is used for the myocardial contraction, with the remaining 30% to 40% for the various ATPases, such as  $Ca^{2+}$ -ATPase in the SR. Within the heart, both intracellular ATP and phosphocreatine provides the energy in myocardial activity, in which the latter one is used for ATP transportation and buffering. Furthermore, mitochondrial creatine kinase (CK) catalyzes the reaction that transferring of high-energy phosphate bond in ATP into creatine, which produces phosphocreatine (PCr) and ADP. When the energy demand exceeds the energy supply, the level of PCr is reduced, keeping ATP at a normal level.

In normal physiological condition, the heart has a high hydrolysis rate of ATP due to the continuous mechanical work. Correspondingly, the high-energy-phosphate pool in the heart is relatively small and can be depleted in a few seconds; therefore, the ATP generation is crucial to maintain the myocardial activity. In the heart, the substrate that utilized for the ATP generation includes fatty acid (FA), glucose, lactate acid and pyruvate. Within the heart, the approximately 70% to 90% of total ATP is generated by oxidation of FA, with the remaining 10% to 30% provided by the glucose, lactate acid and pyruvate. Both glucose and lactate acid yields pyruvate which is then oxidized to Acetyl-CoA in the mitochondria. The Acetyl-CoA then joins into the Krebs cycle and generates energy.

### **1.6.1 Substrate utilisation**

#### ***1.6.1.1 Fatty acid metabolism***

In the normal cardiac metabolism, the energy requires for cardiomyocyte is highly dependent on extrinsic sources of FA that must be transported to the mitochondria. Multiple transport proteins are involved in the transporting the FA from the blood vessels into the cardiomyocyte, including, the fatty acid translocase (FAT/CD36) and fatty acid binding protein (FABP). In the cytosol, the FA is esterified to fatty Acyl-CoA, which is esterified to triglyceride or further converted into long-chain acylcarnitine by the carnitine palmitoyltransferase I (CPT-1). CPT I is a key point in regulating the rate of  $\beta$ -oxidation as the conversion from Acyl-CoA to long-chain acylcarnitine is required before transport to the mitochondria. In the mitochondrial matrix, CPT II then converts the long-chain acylcarnitine back to long-chain Acyl-CoA that enters the  $\beta$ -oxidation generating Acetyl-CoA and the reducing equivalents NADH and FADH<sub>2</sub> (Figure 1.9).

#### ***1.6.1.2 Glycolytic metabolism***

The heart can use ingested exogenous glucose or the glycogen stores, which, within the myocyte are negligible. The glucose transporters GLUT1 and GLUT4 are used for the majority of glucose transportation with GLUT4 is the major glucose transporter in adult myocytes, where the surface expression is increased by the actions of insulin. After entering the cytoplasm, as outlined in Figure 1.9, the glucose is rapidly phosphorylated to

glucose 6-phosphate (G6P), which then enters glycolysis to generate pyruvate, NADH and a small amount of ATP.

### 1.6.2 Metabolic changes in disease states

During conditions of hypoxia the metabolism shifts from primarily fatty acid metabolism (aerobic) to glycolytic metabolism (anaerobic) (Smith & Bigham, 2013). This is a comparatively inefficient form of ATP synthesis as glycolysis would need to be increased 20-fold to match the energy demand of the myocardium. During mild ischaemia, the ratio of fatty acid to glucose metabolism does not significantly change, however in prolonged ischemia, the oxygen supply is decreased but the glucose uptake and glycolytic rate is increased. Additionally, lactate dehydrogenase catalyses the reduction of pyruvate to lactate, which requires  $H^+$  and NADH to regenerate  $NAD^+$ . If the increased lactate can be removed by the coronary circulation in time there will be no serious consequences, however, if lactate accumulates, the intracellular pH will decrease and NADH will accumulate which inhibits glycolysis. In addition, the  $Ca^{2+}$  binding protein, troponin T, that regulates myofibril contraction is sensitive to pH, so at low pH myofibril contractile function is inhibited (Morimoto *et al.*, 1999). In severe ischemia, the oxidation of both free fatty acids and glucose is inhibited, and the small amount of ATP provided by the glucose glycolysis is the only source that supports cardiomyocyte survival. Therefore, oxidation of free fatty acid will aggravate the myocardial hypoxia and intracellular acidosis, which may further damage the myocyte and cause cardiomyocyte death (Kibos *et al.*, 2014).

In the development of HF, the heart mainly depends on glycolysis as the energy source, with decreased use of fatty acids as an energy source. Recchia *et al* (1998) found that in pacing-induced heart failure, the primary energy course changed from fatty acid oxidation to glucose metabolism. Razeghi *et al* (2001) suggested that a more embryonic-type of energy metabolism was present during HF due to the down-regulation of 'adult' gene (*GLUT4*, *mGS*, *mCPT-1*) transcription and increased embryonic gene (*GLUT1*, *IGS*, and *lCPT-1*) transcription. Casademont (2002) found that, in the stage between the developments of dilated cardiomyopathy to heart failure, genes that encodes electron transfer chain was defected so that the function of electron transfer chain was abnormal.

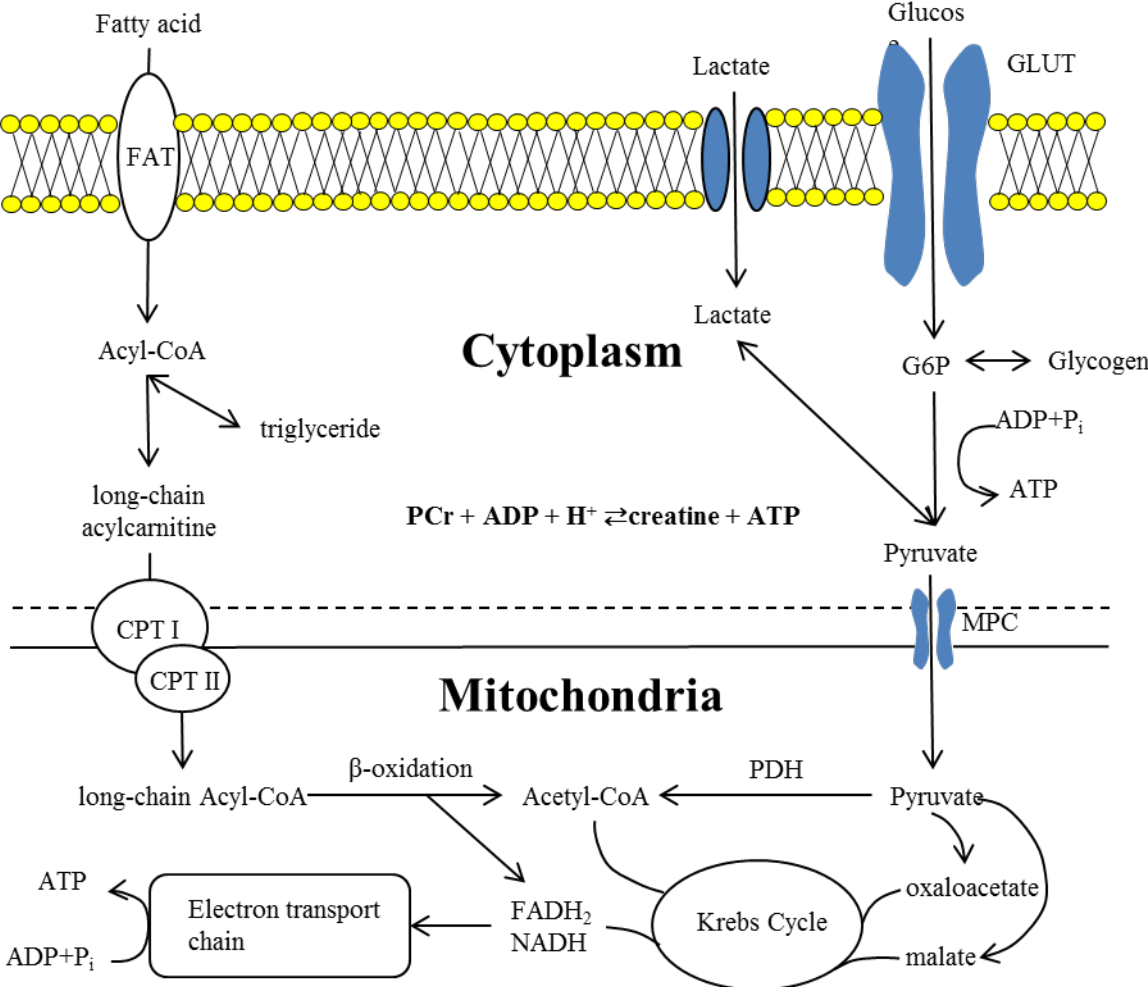


**Figure 1.9: Brief diagram of cardiac energy metabolism, with substrates of fatty acid, lactate and glucose.** PCr indicates phosphocreatine; Acetyl-CoA, acetylcoenzyme A; CPT, palmitoyltransferase; Acyl-CoA, acylcoenzyme A; G6P, glucose 6-phosphate; PDH, pyruvate dehydrogenase; GLUT, glucose transporter; FAT, fatty acid transporter; MPC, mitochondrial pyruvate transporter.

**1.7 Ischaemic damage**

Ischaemia *in vivo* is defined as a lack of blood flow resulting in a reduced supply of oxygen and nutrients to a tissue. Myocardial ischaemic damage is, therefore, caused by anything that causes a marked reduction of blood flow to the myocardial tissue. Ischaemic damage to the myocardium can occur during two periods, the period of full ischaemia and on reperfusion where local ischaemia may exist if the microvasculature is still blocked due to microemboli or vasoconstriction. During ischaemia, cardiomyocytes can be damaged by

several factors, such as depletion in intracellular energy, dysregulation of metabolism, inflammatory responses and  $\text{Ca}^{2+}$  overload. During ischaemia, aerobic metabolism is rapidly switched to anaerobic glycolysis to continue ATP synthesis. In addition, the decreasing ATP reduces the  $\text{Na}^+/\text{K}^+$  ATPase, SERCA and PMCA activity, all which further increase  $\text{Ca}^{2+}$  and  $\text{H}^+$  via NCX and  $\text{Na}^+-\text{H}^+$  exchange (Gho *et al.*, 1997). Furthermore, there is an inflammatory response, where tumour necrosis factor TNF- $\alpha$  plays a key role in damage the cardiomyocyte, which in turn induces mononuclear macrophage and T lymphocyte infiltration into the myocardium leading to cardiomyocyte mortality and fibrosis (Bodi, 2012).

On the relief of the ischaemia, termed reperfusion, some cardiomyocytes can regain normal function, however some become further damaged, contributing to the area of infarction. In the mitochondria it is hypothesised that this induces the openings of mitochondrial permeability transition pore (mPTP) due to oxidative stress, causing mitochondrial swelling, release of proteins and uncoupling of oxidative phosphorylation; often termed ischemia/reperfusion injury (Budas *et al.*, 2007; Ovize *et al.*, 2010; Rana *et al.*, 2014; Yuan *et al.*, 2014). The rapid increase in oxygen on reperfusion may result in a large amount ROS generation, the consequences of which are further damage of membrane permeability, via peroxidation, resulting in cellular oedema. Furthermore, the ROS can also suppress the function of membrane proteins and damage the electron transport chain (ETC), so disrupting ATP synthesis and contribute to the  $\text{Ca}^{2+}$  overload.

### **1.7.1 Acute coronary syndromes**

Acute Coronary Syndromes (ACS) are caused by the insufficient blood flow to the heart due to sudden blockage in coronary arteries. These syndromes cause common symptoms that can include chest pain, shortness of breath, nausea and sweating. The outcomes of the ACS depend on the degree and the location of the blockage, which can be as severe as a sudden and complete blockage or a transient temporary clot. The term ACS can include unstable angina (UA), myocardial infarction (MI) and sudden cardiac death.

### ***1.7.1.1 Myocardial infarction and unstable angina***

Myocardial infarction is caused by a rapid reduction in part of the myocardial coronary blood flow, resulting in necrosis. The dysfunction of the tissue within the area of infarct is permanent; however, there are some potentially reversible ischaemic areas near the damaged tissue. Myocardial infarction mainly affects the left ventricle, but the lesion can extend to the right ventricle or atrium. The severity of a myocardial infarction is judged on how large the infarct is and how much the damaged tissue affects myocardial function. Broadly, myocardial infarction can be categorised into two categories. The first, ST-segment elevation myocardial infarction (STEMI) which, as the name suggests, gives a characteristic elevation in the baseline between the S and T segment in the II, III and aVF leads of ECG (Figure 1.8). This is indicative of the movement of electrical current around an area of damaged tissue. The second, non-ST-segment elevation myocardial infarction (NSTEMI), which does not show any perturbation of the ECG signal. Due to their relative severities, STEMI is often described as being caused by a near complete occlusion, whereas NSTEMI is caused by a severe narrowing or incomplete block which causes ischaemia, but not enough to cause large areas of infarct.

An unstable angina is induced by a transient vasospasm on an already narrowed artery. The vasospasm may be caused by platelet activation release thromboxane A<sub>2</sub> and serotonin; or coronary thrombosis that spontaneously resolves so restoring the blood flow. No manifestations of necrosis can be seen in UA, in terms of histology, biochemical markers or the corresponding ECG changes.

### **1.7.2 Heart failure**

Heart Failure (HF) is a clinical syndrome that is usually caused by coronary artery disease, and often results from the damage caused by myocardial infarction. The clinical symptoms are pulmonary congestion, dyspnea and fatigue.

“Compensative hypertrophy” is the most common symptom in the early stages of development of HF due to the long-term overloading in cardiomyocyte to compensate the inadequate generation of ATP. During the development of HF, the T-tubule can remodelling their structure which causes Ca<sup>2+</sup> handling dysfunction and loss of the

synchronous  $\text{Ca}^{2+}$  release, leading to defective EC coupling (Guo *et al.*, 2013). In addition, PKA can be activated during the development of HF due to the SNS activation which attempts to improve the cardiac function (Marks, 2013). The stimulation of PKA in HF can hyperphosphorylate RyR2 on the SR and creates the 'leaky' RyR2 channel and reduce the SR  $\text{Ca}^{2+}$  content as well as reduces the amplitude of SR  $\text{Ca}^{2+}$  release (Reiken *et al.*, 2003). Furthermore, the increased activation of PKA also stimulate the L-type  $\text{Ca}^{2+}$  channel to open, resulting in an increased  $\text{Ca}^{2+}$  influx via L-type  $\text{Ca}^{2+}$  channels (Marks, 2013). Pumping the cytoplasmic  $\text{Ca}^{2+}$  back to SR through SERCA2a requires ATP, therefore increasing ATP consumption contributing to the early fatigue observed in HF patients (Reiken *et al.*, 2003). Finally, the  $\text{K}_{\text{ir}}6.1/\text{SUR2B}$  selective opener, natakalin and iptakalin, demonstrated a protective effect in the failing heart, which prevented ventricular remodelling and reducing endothelial dysfunction (Wang *et al.*, 2016). Finally, the metabolic substrates used in cardiac metabolism during HF were changed, from predominantly fatty acid to glycolytic (section 1.6.2).

## 1.8 Cardioprotection

### 1.8.1 Overview of cardioprotection

Cardioprotection is a broad term used to describe any process that imparts protection to the heart from ischemic damage. Damage to the myocardium can occur in two phases, during the ischaemia and on reperfusion. Cardioprotection is any stimulus given to the heart or cardiomyocytes that triggers the endogenous mechanisms to limit ischaemic or reperfusion injury and improve myocyte survival.

### 1.8.2 Cell signalling in cardioprotection

In the cardioprotective signalling pathways, there are numerous signalling molecules involved in transmitting the protective signals from the trigger to the effectors. The mechanism of acute ischemia-reperfusion injury has suggested involving ROS generation, reduction of nitric oxide (NO) supply,  $\text{Ca}^{2+}$  overload and mPTP opening leading to cell death. In addition, nuclear factor (NF $\kappa$ B) and other transcription factor activation will further enhance the expression of cell adhesion molecules, leukocyte infiltration, and more

aggravating tissue damage. Conversely, the activation of several signalling pathways has been demonstrated to attenuate these damaging events to reduce the ischemia/reperfusion injury. Part of the cardioprotective signalling pathway is outlined in Figure 1.10 below.

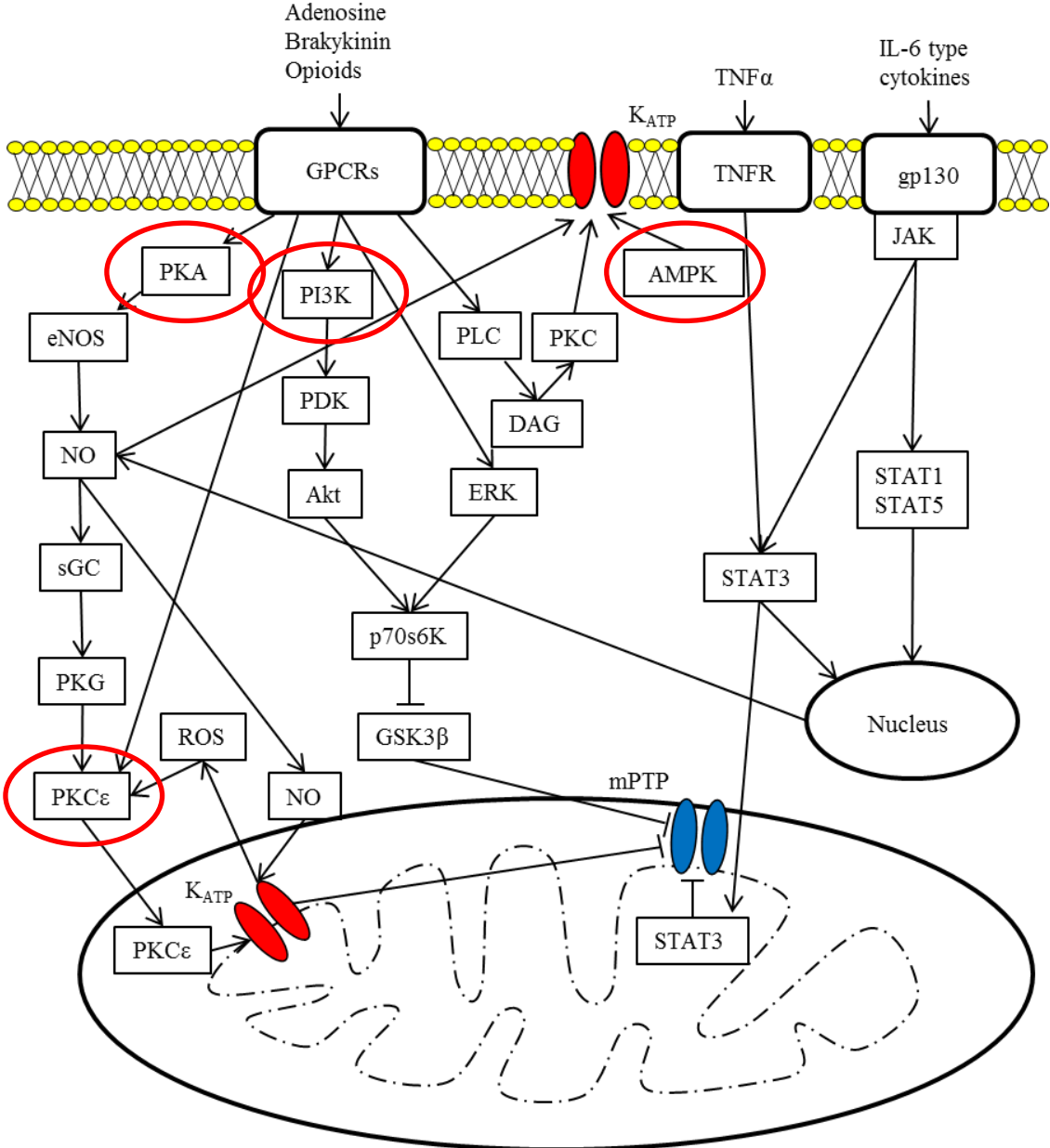


**Figure 1.10: A diagram of NO/PKG, RISK and SAFE cardioprotective signal pathway.** Akt indicates protein kinase B; AMPK, cyclic adenosine monophosphate-activated kinase; DAG, diacylglycerol; ERK, extracellular regulated kinase; GPCR, G protein-coupled receptor; gp130, glycoprotein 130; GSK3 $\beta$ , glycogen synthase kinase 3  $\beta$ ; JAK, Janus kinase; K<sub>ATP</sub>, ATP-dependent potassium channel; NO, nitric oxide; eNOS, endothelial nitric oxide synthase; PI3K, phosphatidylinositol (4,5)-bisphosphate 3-kinase; PKC, protein kinase C; PKG, protein kinase G; PLC, phospholipase C; ROS, reactive oxygen species; sGC, soluble guanylate cyclase; STAT, signal transducer and activator of transcription; and TNF $\alpha$ , tumor necrosis factor  $\alpha$ .

Previous studies have shown that the increase in cAMP levels in IPC myocyte activates PKA, which can trigger the NO-PKG signalling pathway via endothelial nitric oxide synthase (eNOS) activation (Lochner *et al.*, 1999; Sanada *et al.*, 2004). Pharmacological inhibition of PKA using H89 abolished the cardioprotection as well as the activation of eNOS, demonstrating PKA as an important upstream signal of the NO-PKG signalling pathway (Yang *et al.*, 2013). In addition, the PKA can also phosphorylate a small heat-shock protein Hsp20 which imparted cardioprotection (Edwards *et al.*, 2012). Furthermore, PKA may also important in activating  $K_{ATP}$ , including  $K_{ir6.1/SUR2B}$ , which will be further discussed in discussion section 7.3.2.

PKC has been shown to play a vital role in IPC. PKC was hypothesised to mediate cardioprotection due to activation of the “conventional” cardiac sarcolemmal  $K_{ATP}$  (Light *et al.*, 2000). Furthermore, the same key isoform, PKC $\epsilon$ , plays an important role in sex-specific cardioprotection, where Edwards *et al* (2009) found that the blockage of PKC $\epsilon$  by chelerythrine reversed the enrichment of sarcolemmal  $K_{ATP}$  protein in females, suggesting the PKC $\epsilon$ -mediated regulation of sarcolemmal  $K_{ATP}$ . Another key potential site for the action of PKC is the mitochondria. Studies have demonstrated that activation of PKC $\epsilon$  causes a translocation to the mitochondria and it is suggested causes an activation of the mito $K_{ATP}$  channel (Novalija *et al.*, 2003; Ludwig *et al.*, 2004; Zatta *et al.*, 2006). It was hypothesised that opening of the mito $K_{ATP}$  was beneficial to the mitochondria causing hyperpolarisation of the mitochondrial inner membrane to close the mPTP and protect the mitochondria from swelling and apoptosis (Hausenloy & Yellon, 2004; Lacerda *et al.*, 2009). In addition, it was hypothesised that the opening of mito $K_{ATP}$  may promote a small amount of reactive oxygen species (ROS) that may back activate PKC $\epsilon$  and create a positive feedback loop (Budas *et al.*, 2007).

AMP-activated kinase (AMPK) is activated by ATP depletion as well as increased AMP/ATP ratio, which plays a role in coordinating metabolism (Mihaylova & Shaw, 2011). Knockdown of AMPK in mice, Sukhodub *et al* (2007) discovered that mice lost the preconditioning-induced cardioprotection, suggesting the AMPK plays a key role in the preconditioning mechanism. Furthermore, investigation of resveratrol-induced cardioprotection, Du *et al* (2014) found that resveratrol exerted a cardioprotective effect via

AMPK-K<sub>ir</sub>6.2 K<sub>ATP</sub> pathway, which increases K<sub>ATP</sub> channel activity by the enhanced AMPK phosphorylation, but either suppressed AMPK or knockdown of K<sub>ir</sub>6.2 subunits attenuated the cardioprotection.

PI3K/Akt are components of Reperfusion Injury Salvage Kinase (RISK) signalling pathway, that can be triggered by acetylcholine via transactivation EGF receptors by GPCR (Krieg *et al.*, 2002). In addition, the GPCR also activate PI3K by the Gβγ that derived from the stimulation of Gq-coupled receptors (Naga Prasad *et al.*, 2000). Overexpression of Gβγ sequestering peptide in mice, βARKct attenuated the ischemia preconditioning, although did not inhibit the preconditioning-induced phosphorylation of downstream p70 S6 kinase (p70S6K), which suggested the p70S6K also be a downstream signal in other ischemia preconditioning-induced pathway (Tong *et al.*, 2004). It was suggested that the downstream signal of PI3K/Akt is GSK3β. In post-conditioning the GSK3β phosphorylated via PI3K/GSK3β signalling pathway, PI3K inhibition by wortmannin reduces the phosphorylation of GSK3β and therefore abolished the protective effect (Wu *et al.*, 2012). In addition, PI3K also been reported as upstream signal of PKC. Inhibition the PI3K by wortmannin causes suppression of phosphorylation of Akt as well as the translocation of PKCε plus the NO generation (Tong *et al.*, 2000).

### 1.8.3 Ischaemic preconditioning

Ischaemic precondition (IPC) is an endogenous mechanism which is triggered by a series of brief periods of ischaemia, resulting in an improved cardiomyocyte survival and contractile function when exposed to a major ischaemic insult (O'Rourke, 2000; Suzuki *et al.*, 2002; Gross & Peart, 2003; Sasaki *et al.*, 2003). Murry *et al.* (1986) identified this cardioprotective mechanism with two windows of protection; the first continues for several hours after the initial period of reperfusion and the second from 24 h to 72 h. Receptors and signalling pathway have been investigated that are involved in IPC, such as GPCRs, nitric oxide (NO) and cGMP pathway, along with the generation of reactive oxygen species (ROS). The adenosine, opioid and bradykinin GPCRs have been suggested to be involved in the activation of IPC. Among them, adenosine directly couples PKC through phospholipases, which is a pivotal point in many signalling pathways, coordinating the signalling to the mitochondria (Das, 2004; Solenkova, 2005). However, the signalling

pathways for opioid and bradykinin receptors are more complicated, where the opioid receptors need transactivation of the epidermal growth factor receptor before the activation of downstream PI3K/Akt signalling pathway. For the bradykinin receptor, the pathway was suggested that through coupling G proteins and activates the downstream eNOS/PKG pathway and RISK pathway (Keusch *et al.*, 2008).

Research on adrenoceptors suggests that the  $\alpha$ -adrenoceptors are also involved in the IPC mechanism. By using the  $\alpha$ -agonist, phenylephrine, the cardioprotective effect was mimicked, demonstrating a significant reduction in infarct size following a 10 min pre-treatment with phenylephrine prior to the ischemia, but the protective effect abolished by use of  $\alpha$ -receptor blocker, phenoxybenzamine (Tsuchida *et al.*, 1994). Research using transgenic mice further distinguished that it is the  $\alpha_{1A}$  but not  $\alpha_{1B}$  receptors that protect the heart from ischemia injury (Rorabaugh *et al.*, 2005).

NO has also been demonstrated to protect the heart via the reduction of inflammation and prevent the ventricular remodelling, which is dependent on the cGMP signalling pathway (Yin *et al.*, 2008). Moreover, evidence suggests NO can also protect the heart in a cGMP-independent way by the inhibition of downstream glycogen synthase kinase 3 $\beta$  (Yin *et al.*, 2008), resulting in the closure of mPTP, suggesting the mitoK<sub>ATP</sub> open to modulate cardioprotection (Ovize *et al.*, 2010).

In adenosine-mediated cardiac preconditioning, the  $[Ca^{2+}]_i$  is important in the activation of PKC (Node *et al.*, 1997). It is well documented that both  $[Ca^{2+}]_i$  overload and stress-induced ROS worsen the ischaemia/reperfusion injury (Turrens *et al.*, 1991; Aldakkak *et al.*, 2008). However, controversially, a brief exposure of  $Ca^{2+}$  and ROS in the ischemia reperfusion can actually induce cardioprotection (Oldenburg *et al.*, 2004; Yang *et al.*, 2010). It perhaps due to the fact that  $Ca^{2+}$  is essential for the activation of the PKC signalling pathway (Gopalakrishna & Anderson, 1989; Huang, 1989), which triggers the IPC.

The K<sub>ATP</sub> channels are also highly associated with IPC, which will be discussed in section 1.8.6.

#### 1.8.4 Ischaemic post-conditioning

Although IPC can significantly reduce I/R damage to the myocardium, the requirement to give these brief periods of ischaemia before the major ischaemic insult means that it is of limited use clinically. Previous literature demonstrates that after 60 mins of left anterior descending occlusion followed by 3 cycles of 30 s of occlusion and 30 s reperfusion, the infarct size was significantly reduced (Zhao *et al.*, 2003). This phenomenon then was then called myocardial ischemic post-conditioning (MIP) as the stimulus is after the major insult and was also shown in other species (Yang *et al.*, 2004; Skyschally *et al.*, 2009; Ovize *et al.*, 2010). In addition, the MIP has already shown beneficial outcomes in some clinical diseases such as STEMI (Mewton *et al.*, 2013). Both RISK and Survivor Activating Factor Enhancement (SAFE) pathways were found to be involved in triggering MIP, with both pathways inhibiting formation of the mPTP so preventing apoptosis induced by I/R (Hausenloy & Yellon, 2004; Lacerda *et al.*, 2009). Occultation

#### 1.8.5 Remote Ischaemic Preconditioning (RIPC)

RIPC imparts cardioprotection via a series of brief periods of ischaemia in remote organs or tissues, resulting in reduction of infarct size during a prolonged ischaemic insult in the heart (Schoemaker & van Heijningen, 2000; Liem *et al.*, 2002; Tokuno, 2002). For example, ligation of anterior mesenteric artery or the left renal artery have both been reported to impart protection to the myocardium (Gho *et al.*, 1996; Lang *et al.*, 2006). Further examination of RIPC has shown that ischaemia in multiple tissues triggers cardioprotection, including femoral blood restriction, pacing the gastrocnemius muscle by electrical stimulation (Birnbaum *et al.*, 1997) and suppressing the blood flow in the hind-limb. These prevented the heart going into tachyarrhythmia following ischemia/reperfusion (Oxman *et al.*, 1997). The  $K_{ATP}$  channel was suggested to have a role in mediating the protective effect in RIPC due to diazoxide mimicking the protective effect of RIPC (Kristiansen *et al.*, 2005). In cerebral RIPC, pre-treatment with the  $K_{ATP}$  blocker 5-HD attenuated the protective effect and further indicates that  $K_{ATP}$  channels play an important role in RIPC (Nakamura *et al.*, 2002; Yoshida *et al.*, 2004b).  $K_{ATP}$  channels are also suggested to be a key mediator in RIPC in the myocardium, where glibenclamide abolished the protective effect on the myocardium of occlusion of one hindlimb (Schmidt *et al.*, 2007). Furthermore, NO

(described in section 1.8.3) was also suggested to play an important role in RIPC. The stimulation of NO was shown to be involved with activation of  $K_{ATP}$  channels via NO-cGMP-PKG pathway (Yasuda *et al.*, 2009). Additionally, NO can also mediate the activation of  $K_{ATP}$  channels via decreasing their ATP sensitivity as well as increasing the affinity of  $K_{ATP}$  openers (Shinbo & Iijima, 1997; Kawano *et al.*, 2009). In mice, a series of hyperemia in femoral artery activates eNOS and releases NO which is oxidized to nitrite and transported to the myocardium and reduced back to NO by cardiac myoglobin. Thus, genetic or pharmacological suppression of eNOS at the remote hypoxia site, or directly inhibiting the synthesis of NO in the target organ, results in the protective effect given by RIPC being abolished (Rassaf *et al.*, 2014).

RIPC potentially has many advantages in the clinic, as it can impart cardioprotection and attenuates cardiac injury without an intrusive operation. Several clinical trials have been done. RIPC on STEMI patients before primary percutaneous coronary intervention attenuated reperfusion injury and therefore salvaged the myocardium from infarction (Bøtker *et al.*, 2010). Including RIPC prior to children undergo operations on congenital heart defect repair also illustrated a cardioprotective potential with reduced troponin I in the myocardium, less resistance in the airway and reduction of inotropic score (Cheung *et al.*, 2006). However, RIPC in clinics for the patients undergoing coronary-artery by-pass graft surgery, in some cases, did not show significant differences in terms of cardiac outcomes, compared with the control sham group (Rahman *et al.*, 2009; Karuppasamy *et al.*, 2011; Lucchinetti *et al.*, 2012; Young *et al.*, 2012; Ahmad *et al.*, 2014; Hausenloy *et al.*, 2015).

### **1.8.6 Pharmacological preconditioning**

Previous studies demonstrated that applying adenosine A1/A2-receptor agonists or bradykinin before ischaemia mimics the IPC protection (Feng *et al.*, 2000; Yang *et al.*, 2010). Moreover, both IPC and pharmacological activation of the  $\delta$ -Opioid receptors by  $\delta$ -Opioid agonist D-Ala<sup>2</sup>-D-Leu<sup>5</sup> enkephalin in rat heart significantly improved the aortic flow after ischaemia, but both protective effect can be antagonised by the non-selective Opioid antagonist naloxone (Karck *et al.*, 2001). Additionally, dogs, pre-treated with diazoxide, show a slowed metabolism during ischaemia, with less ATP consumption as well as less lactate production, suggesting that diazoxide mimics IPC via preservation of

intracellular ATP (Schwartz *et al.*, 2007). Atrial natriuretic peptide also demonstrates cardioprotective effect in rabbit heart via the activation of PKG, which protective effect can be inhibited the putative mitoK<sub>ATP</sub> blocker 5-HD, suggested the PKG activated the mitoK<sub>ATP</sub> and finally the RISK (Yang *et al.*, 2006). Additional protective drugs include sildenafil and vardenafil, which are Phosphodiesterase-5 inhibitors, showing a significant reduction in infarct size and reperfusion injury via the activation of cGMP and PKG (Yang *et al.*, 2006). However, despite many drugs show protection in the lab, currently none are approved by FDA (Wojtovich *et al.*, 2012). In terms of clinic trials, adenosine has been most thoroughly investigated. Infusion of adenosine into the peripheral intravenous of myocardial infarction patients, the Acute Myocardial Infarction Study of Adenosine (AMISTAD) trials I and II demonstrated patients infarct size following thrombolytic-treatment were significantly reduced but was only limited in the patients with anterior wall infarction (Mahaffey *et al.*, 1999; Ross *et al.*, 2005). Moreover, applying adenosine during percutaneous transluminal coronary angioplasty (PTCA) also illustrated benefits such as ischaemic area reduction, isovolumetric contraction improvement and a decrease in left ventricular ejection fraction (Heidland *et al.*, 2000).

### **1.8.7 K<sub>ATP</sub> channels and cardioprotection**

#### ***1.8.7.1 The mitochondrial K<sub>ATP</sub> in cardioprotection***

Unlike the SarcoK<sub>ATP</sub>, the subunits that comprise the mitochondrial K<sub>ATP</sub> (mitoK<sub>ATP</sub>) are not clearly identified. K<sub>ir</sub>6.1 was considered as a mitoK<sub>ATP</sub> as it showed close pharmacological properties to the K<sub>ir</sub>6.1 channel, which can be inhibited by Acyl-CoA and activated by GTP, GDP, and diazoxide (Garlid *et al.*, 1997; Bajgar *et al.*, 2001), having distinct pharmacological features to K<sub>ir</sub>6.2 (Grover & Garlid, 2000). Miki *et al.* (2002) identified that after K<sub>ir</sub>6.1 gene knockdown in mice there was sudden death accompanied by vasospasm and Prinzmetal angina, however, the mitoK<sub>ATP</sub> still showed activation when treated with diazoxide. Furthermore, when a dominant negative K<sub>ir</sub>6.1 construct was delivered to adult myocytes the diazoxide activated mitochondrial matrix redox state was not altered compared to the wild type animal. These findings suggest that the K<sub>ir</sub>6.1 protein may not be part of the mitoK<sub>ATP</sub> (Seharaseyon *et al.*, 2000a).

By treating IPC cells with a proposed mitoK<sub>ATP</sub> opener and inhibitor, Garlid *et al* (1997) found that the protective effect can be enhanced by the opener diazoxide, but was abolished using the proposed blocker 5-HD or glibenclamide. To support these findings, a method to detect the redox state of mitochondria was developed. Liu *et al* (1998) found that either a mitoK<sub>ATP</sub> opener or blocker had the ability to active or reverse the oxidation of mitochondria without influencing SarcoK<sub>ATP</sub> current. This provided strong evidence that mitoK<sub>ATP</sub> channels contributed to ischemia preconditioning. However, the selectivity of 5-HD was questioned by Li *et al* (2010b), by performing inside-out patch recordings. 5-HD actually blocked K<sub>ir</sub>6.2/SUR2A recombinant channel with an IC<sub>50</sub>=28.7 μM with 1 μM ATP and showed further efficacy in higher ATP concentrations. In addition, the expression of K<sub>ir</sub>6.2 is essential for the proper function of the heart. In K<sub>ir</sub>6.2 knockout mice, the protective function induced by IPC was abolished. K<sub>ir</sub>6.2-null mice failed to shorten the APD during ischaemia as well as had increased infarct size following ischemia/reperfusion, compared with wild-type mice (Suzuki *et al.*, 2002). By using K<sub>ir</sub>6.2-null mice, Yamada *et al* (2006) illustrated the heart is more vulnerable when suffering from ischaemia, with prolonged APD, intracellular calcium overload and ATP depletion as well as compromised myocardial performance after 30 min aortic constriction, compared with wild-type. Ischaemically preconditioned K<sub>ir</sub>6.2-null animals fail to efficiently regulate ATP consumption compared with IPC wild-type mice, with inferior ATP turnover rate, ATP synthesis rate and ATP utilization rate (Gumina *et al.*, 2003). The opening of mitoK<sub>ATP</sub> was also suggested to increase mitochondrial matrix volume via K<sup>+</sup> influx accompanied with weak acids to keep electroneutrality as well as the movement of water by osmotic forces (Grover & Garlid, 2000; O'Rourke, 2000). However, neither the selective mitoK<sub>ATP</sub> activator diazoxide nor mitoK<sub>ATP</sub> blocker 5-HD/glibenclamide changes the mitochondrial matrix volume in experimental conditions (Das *et al.*, 2003); another reports suggesting 5-HD increases the mitochondrial matrix volume (Lim *et al.*, 2002). Both reports argue that the commonly used, and considered selective agents, lack an effect on the putative mitoK<sub>ATP</sub> channel. Moreover, both 5-HD and diazoxide have the ability to exert their effect through alternative pathways, where 5-HD can be converted to 5-HD-CoA on outer membrane, and a small amount can enter the mitochondria and be oxidized (Lim *et al.*, 2002). Secondly, the accumulation of cytosol 5-HD-CoA increases the activity of CPT I

and results in the stimulation of endogenous fatty acid oxidation which worsens the cell recovery after ischaemia (Lopaschuk, 1997). Thirdly, 300  $\mu\text{M}$  5-HD, a concentration conventionally used in experiments suppressing ascorbate oxidation, was suggested to cause mitochondrial outer membrane rupture and cytochrome c loss (Lim *et al.*, 2002). Finally, flavoprotein fluorescence signals used to indicate the mitoK<sub>ATP</sub> opening state can be reduced by 5-HD metabolic substrate, a medium-chain fatty acid decanoate, suggesting the signal reduction may not reflect the mitoK<sub>ATP</sub> opening state but a cellular switch from glucose to fatty acid metabolism (Dröse *et al.*, 2006). In terms of diazoxide, it has been shown to activate the K<sub>ir</sub>6.2/SUR2A in the similar manner with K<sub>ir</sub>6.2/SUR1 (Table 1.5) when presence with 100  $\mu\text{M}$  ADP (D'hahan *et al.*, 1999). Thus, the side effect on K<sub>ir</sub>6.2 inhibition of 5-HD provides another possible explanation that how 5-HD negating preconditioning experiments. Secondly, diazoxide is able to oxidize the mitochondrial flavoproteins via inhibiting succinate dehydrogenase activity and followed on the blockage of citric cycle (Kowaltowski *et al.*, 2001; Hanley *et al.*, 2002). Taking these two points together, mimicking preconditioning by diazoxide may not occur through the opening of mitoK<sub>ATP</sub>. Suzuki *et al* (2002) showed that diazoxide can no longer induce cardioprotection in K<sub>ir</sub>6.2 knockout animals.

It should be noted that up-to-date experiments have not measured the mitoK<sub>ATP</sub> currents directly; measurements of mitoK<sub>ATP</sub> channel currents have proven impossible to date and so researchers assume that the mitochondrial redox state is a consequence of the activation of mitoK<sub>ATP</sub>. Recently, Foster *et al* (2012) identified expression of ROMK (K<sub>ir</sub>1.2) in the inner mitochondria membrane of bovine heart and its location was confirmed by cell imaging. ROMK channels share some of the common features with the identified properties of hypothesized mitoK<sub>ATP</sub>, such as can be activated by PIP<sub>2</sub> and suppressed by pH, PKC and show sensitivity to glibenclamide (Braun *et al.*, 2002; Zeng *et al.*, 2003; Lee *et al.*, 2008; Wojtovich *et al.*, 2010; Foster *et al.*, 2012). This result may help to explain the lack of effect of K<sub>ir</sub>6.1 gene knockdown on mitochondrial function and the pharmacological features that mitoK<sub>ATP</sub> retain in these animals. More work is still needed in the future to validate this discovery.

### ***1.8.7.2 The role of the sarcolemmal $K_{ATP}$ ( $K_{ir}6.2/SUR2A$ ) in cardioprotection***

The role of the accepted Sarco $K_{ATP}$  channel ( $K_{ir}6.2/SUR2A$ ) in cardioprotection is unclear, however there is evidence suggesting that the  $K_{ir}6.2$  channel plays an important role. In normal physiological conditions, Sarco $K_{ATP}$  remains predominantly in the closed state and so does not have a significant effect on membrane potential or APD. However, during metabolic stress, such as ischaemia, cardiac  $K_{ATP}$  channels will normally open and shorten the APD to decrease the contraction to preserve ATP (Lederer *et al.*, 1989). During metabolic inhibition, the reduction of intracellular ATP and the increase of MgADP can result in the opening of Sarco $K_{ATP}$  channel. Opening of Sarco $K_{ATP}$  activates a hyperpolarizing  $K^+$  current which accelerates repolarization of the action potential plateau therefore limiting  $Ca^{2+}$  influx, which reduces the  $Ca^{2+}$  overload in cardiac myocyte (Brunner *et al.*, 2003). This idea was supported by McPherson *et al* (1993), where cardioprotection could be afforded to cells using the  $K_{ATP}$  opener pinacidil, which shortened APD and depressed the contractility to preserve intracellular energy. These channels are also potentially involved in the beneficial effects of IPC. To date, the established cardiac Sarco $K_{ir}6.2/SUR2A$  channel, is considered as the functional Sarco $K_{ATP}$  channel in cardiomyocytes (Suzuki *et al.*, 2002; Wojtovich *et al.*, 2013). However, in cardiomyocytes that exhibited a cardioprotected phenotype imparted by several different protocols, Brennan *et al* (2015) demonstrated the activation of  $K_{ir}6.2/SUR2A$  was delayed in MI, suggesting this channel did not *impart* cardioprotection. Furthermore, by comparing the timing between contractile failure and  $K_{ir}6.2/SUR2A$  activation during MI, the timing suggests the MI-induced  $K_{ir}6.2$  currents caused contractile failure (Brennan *et al.*, 2015). Finally, a significantly longer duration to  $K_{ir}6.2/SUR2A$  activation in cardioprotected myocyte compared with control cells, suggests there is another protective factor in IPC cells other than  $K_{ir}6.2/SUR2A$  (Brennan *et al.*, 2015).

From the description above, the opening of  $K_{ATP}$  seems to help cardiac cells to activate cardioprotection. However, the maintained opening of  $K_{ATP}$  channel also leads to early repolarization of cells APD, which causes a reduction of QT interval and refractory period and can lead to re-entrant arrhythmias with ST-segment elevate on ECG (Tinker *et al.*, 2014). Moreover, In early reports, early repolarisation is commonly considered as a

physiological change in human however this can be associated with a susceptibility to ventricular fibrillation (Burashnikov & Antzelevitch, 2011).

Lawrence *et al* (2002) demonstrated the mRNA and the expression of  $K_{ir}6.1$  can be enhanced by ischaemia and after transfection of  $K_{ir}6.1$  dominant negative subunits into cardiomyocytes, the increasing mortality was shown when cells exposed to ischaemia. Further evidence supporting this idea, by ligating the coronary arteries, Isidoro *et al* (2007) found that the expression level of  $K_{ir}6.1$  was up-regulated and the expression level of  $K_{ir}6.1$  near infarct zone was even higher. From those previous data,  $K_{ir}6.1$  seems to be a crucial part of IPC.

## **1.9 The use of RNA interference in electrophysiology**

The identification of ion channel subunits or their physiological role is important to understanding physiological processes. To investigate the loss-of-function, some pharmacological agents can be used to inhibit the ion channel, however, the pharmacological agents may not specific enough to some types of ion channels (i.e Glibenclamide inhibits both  $K_{ir}6.1$  and  $K_{ir}6.2$   $K_{ATP}$  channels (Russ *et al.*, 1999; Kovalev *et al.*, 2004)) or is not efficient in certain circumstance (i.e Glibenclamide in metabolic stress (Findlay, 1993)). Compared to the pharmacological methods, the RNA interference (RNAi) technology provides a specific knockdown of selected channel subunits. Furthermore, RNAi technology avoids activating/inactivating the alternative signalling pathway that can be induced by pharmacological inhibitors. RNAi exhibits a rapid effect on gene silencing, showing a significant attenuation of gene expression in 24 h to 48 h. Finally, unlike the conventional knockout animal, the RNAi technology does not interference with cellular genomic expression until RNAi, which prevent the animal from developing compensatory mechanisms.

### **1.9.1 RNAi, background and mechanism**

In normal physiological conditions, RNAi is a vital component in the immune system which responds to the invasion of foreign genetic material to play a vital role in antiviruses (Li *et al.*, 2013; Maillard *et al.*, 2013). Fire *et al* (1998) demonstrated that the degradation

of mRNA was involved in the mechanism of RNAi-induced gene silencing, which led to the understanding that RNAi does not suppress gene expression by inhibiting transcription, rather it inhibits translation. Transfection with double stranded (ds) RNA, Hammond *et al* (2000) detected a ~25 nucleotide fragment from the drosophila cells that underwent RNAi, suggesting the injected dsRNA induced ~25 nucleotide fragments to specifically degrade the targeted mRNA. In a further research, Zamore *et al* (2000) found these ~25 nucleotide fragments were degraded from dsRNA and these nucleotide fragments were small interfering RNA (siRNA). Bernstein *et al* (2001) purified the nuclease that cuts dsRNA into small fragments or siRNA, terming this 'Dicer', from the RNase III family. However, Dicer only cuts dsRNA into siRNA and induces siRNA untwisting, the degrading of target mRNA is by another nuclease that found in RNA-induced silencing complex (RISC).

The mechanism of action of RNAi can therefore be broken down into 3 steps; First, in the initiation step the introduced dsRNA in cell will be recognized and bound by Dicer, then dsRNA is cleaved into siRNA with the length of ~22 nucleotide to act as guide sequences which with contains homologous sequences to the targeting mRNA (Bernstein *et al.*, 2001).

There are limitations in inducing RNAi by dsRNA in mammal cells. dsRNA has a low efficiency in silencing gene expression in mammal tissue due to interferons that can be generated by immunological responses to delete dsRNA (Rao *et al.*, 2009). Specifically, RNA-dependent protein kinase (PKR), an antiviral response, plays a regulatory role in RNAi mechanism, which phosphorylates EIF-2 $\alpha$  to suppress the general translation (Paddison *et al.*, 2002). The PKR activation occurs as the inserted dsRNA exceeds the length of 30 bp, so that triggers the antiviral response and causes translational repression and apoptosis (Clarke & Mathews, 1995). A new method that induces RNAi with smaller than 30 bp RNA has been discovered, short-hairpin RNA (shRNA) that was designed to achieve stable gene silencing through a DNA template mechanism in mammal cells. RNA polymerase III (pol III) or pol II has used as the promoter, as has U6, H1 promoter and tRNA<sup>Val</sup> promoters. In particular, the pol III promoter generates transcription termination at the second or third residue of a stretch of 4 'TTTT' as well as generate ~2 nt 'UU' overhang at 3'-terminus (Cullen, 2006; Rao *et al.*, 2009). Two short complementary sequences that were separated by a loop will be inserted in after the promoter. Normally the

sequence is about 19-29 nucleotide with the 2 short complementary sequences are designed based on the target mRNA (Kim, 2003). Once the shRNA that generated from pol III promoter to terminator is similar to siRNA, Dicer will degrade the shRNA to siRNA. After the degradation of shRNA into siRNA, the mechanism will follow the same behaviour of dsRNA in the second step, at which mRNA will be degraded by a cellular mechanism (Rao *et al.*, 2009). Therefore, by using shRNA, we can build up a model that shows a constant target gene inhibition that provide a continual and much more efficiency gene knockdown effect (Rao *et al.*, 2009). By showing this feature, RNAi is becoming more popular and as a standard laboratory technique to research and for the understanding of one single gene in mammal cells.

### **1.9.2 Advantages and disadvantages of the RNAi technique over conventional knockout, inducible knockout or CRISPR animal models**

Conventional knockout is one of the most important technologies in modelling genetic disorders and identifying the role a specific gene has in normal physiological function. To achieve the conventional knockout, several technologies were used. The first technology is gene targeting, by using homologous recombination, the targeted gene can be altered in a predetermined way (Bronson & Smithies, 1994). The second technology is mouse embryonic stem (ES) cell system, which ES cells were derived from the inner cell mass of a mouse blastocyst. The ES cells remain undifferentiated under suitable tissue culture conditions. The mouse chimeras then can be produced by introducing the culture cells into a blastocyst and continue its development *in utero*, which is able to pass the ES cell genome to their offspring. Therefore, by breeding the mouse chimeras and screening the ES genotype on their offspring, the altered genome in ES cells can be passed into living mice. The advantages in conventional transgenic technologies are: firstly, the ES cells are convenient in culture and manipulated by homologous recombination. Secondly, the introduction of the genetically modified ES cells into blastocysts causes the development of mouse chimeras, which provide both wild-type and the genetically modified phenotype (Bronson & Smithies, 1994). However, altering genome can cause developmental problem such as embryonic lethality (Ryding *et al.*, 2001). Furthermore, conventional knockout

affected the whole animal with every tissue and organ, so that may result in a complex phenotype that hard to interpret.

Compared with the conventional knockout animals, the inducible gene knockout provides more *in vivo* control on the gene expression. An inducible knockout allows activation or inactivation on targeting gene in different development time points, which is normally accomplished by the control of transcriptional activation via the usage of antibiotic (Zeng *et al.*, 2008). For example, tamoxifen induces or inhibits a gene, so this can be “switched on” by application of the antibiotic to the animal. The benefits of inducible knockout are two-fold; the gene function can be investigated in multiple or distinct tissues and any developmental time point. Furthermore, due to the time points of gene expression regulation can be controlled, the drawbacks in conventional knockdown, such as embryonic lethality and compensatory mechanisms can be bypassed and are useful for age-dependent research (Zeng *et al.*, 2008).

Clustered Regularly Interspaced Short Palindromic Repeats (CRISPR) and CRISPR-associated proteins 9 (Cas9) system has been demonstrated to be a powerful tool in genetic manipulation. The study of CRISPR/Cas9 system began only few years ago, however CRISPR/Cas9 system already shown advantages compared with conventional knockout and inducible knockout. The CRISPR/Cas system is the immune response against non-self DNA invasions, such as virus and plasmids, in the prokaryotes. The CRISPR/Cas system is functional from the first encounter of the invading non-self DNA and phage DNA segments into CRISPR loci (spacer). Then the host prokaryotic organism will transcribe and process the CRISPR loci, generating the mature CRISPR RNA that contains the CRISPR repeat sequence, and the spacer segment generated from the previous invading DNA. Finally, the next time the system encounters the foreign DNA that contains the homologous sequences, the CRISPR RNA will clip the invading non-self DNA through a complex nucleic acid (Unniyampurath *et al.*, 2016). Base on this mechanism, a new gene knockdown/knockout technology was developed. Editing genome by CRISPR/Cas9 system already shown advantages in being highly specific at gene targeting (Tu *et al.*, 2015), as the system is based on 23 base pair matches so that the CRISPR/Cas9 can target any gene sequence. Moreover, the CRISPR/Cas9 system can target two alleles and therefore causes a null-

mutation in animals, which is hard to produce in large animals due to the difficulty in the mating of heterozygous mutant large animals (Tu *et al.*, 2015). Another advantage is, compare to the conventional knockout animal, the producing of knockout animals are much quicker by use CRISPR/Cas9 system due to the CRISPR/Cas9 system bypass the ES cell targeting stage but can directly inject the Cas9 protein into zygotes instead (Hsu *et al.*, 2014).

In this project, the use of genetic manipulation of channel subunits was limited to shRNA. The use of this technology allowed for specific knockdown of channel subunits in otherwise wild-type cells. This allowed for direct comparison of wild-type and knockdown cells from the same animal. The use of shRNA also bypassed any developmental issues that knockdown may have introduced.

### **1.10 Aims and hypotheses**

Although the  $K_{ir}6.2/SUR2A$  channel is widely accepted as the cardiac sarcolemmal  $K_{ATP}$  channel and plays an important role in cardioprotection, evidence suggests the  $K_{ir}6.1-K_{ATP}$  channel is also expressed and plays an important role in regulating cardiac physiology. Previous data (unpublished) from the host laboratory suggested a  $K_{ir}6.1$ -like current is constitutively active on the cardiac sarcolemmal membrane surface.

The project aims were to:

- 1) Investigate electrophysiological properties of these  $K_{ir}6.1$ -like channels.
- 2) Identify the channel subunits and  $\beta$ -subunits using pharmacological means and shRNA gene knockdown
- 3) Investigating what role the  $K_{ir}6.1$ -like current play in physiological conditions.
- 4) Investigate the impact on the cardiomyocyte of selective knockdown of the  $K_{ir}6.1$  channel by pharmacological inhibition or gene knockdown.
- 5) Investigate the role of  $K_{ir}6.1$ -like currents in cardioprotection.

The following three hypotheses will be tested:

Cardiac sarcolemmal  $K_{ir}6.1$  channels play a role in the modulation of the action potential duration and the resting potential. This regulates  $Ca^{2+}$  influx during metabolic inhibition, slowing the rate of ATP depletion and so limiting the potential damage by  $Ca^{2+}$  overload.

The channel complex that shows constitutive activity at the sarcolemmal membrane surface is comprised of the accepted vascular subunits,  $K_{ir}6.1/SUR2B$ .

Following cardioprotection,  $K_{ir}6.1$  channel activity is increased, shortens the action potential duration so protects the cell from excessive  $Ca^{2+}$  loading that is damaging during ischaemia.

## **Chapter 2**

### **Materials and Methods**

## **2.1 Introduction**

In this thesis, the methods can be categorized into two main areas of research: molecular biology and electrophysiology. Molecular biology provides tools to manipulate ion channels at the molecular level. By using such techniques, the expression level of a specific protein can be modulated. In addition, using cloning techniques, ion channels can be expressed in a cell line system so that the properties of a channel can be studied without other influence from other native channels or signalling. For characterisation of ion channel properties, patch clamp was used in this project. In particular, the cell-attached and whole cell-recording configurations were used to measure single channel activity on the cardiomyocyte membrane surface and the whole cell current respectively. Using a combination of molecular and electrophysiological techniques the cellular response to changing ion channel expression, or a channels activity using pharmacological agents, can be measured.

## **2.2 Solutions**

### **2.2.1 Cardiomyocyte isolation and extracellular perfusion solutions**

The perfusion solutions used in this project were based around a modified Tyrode's solution. In this project, four types of modified Tyrode's solutions were used to enzymatically digest the heart to obtain freshly isolated cardiomyocytes, as well as perform contractile function and electrophysiological experiments. Table 2.1 outlines the composition of each solution.

<b>Chemicals</b>	<b>Normal Tyrode's (mM)</b>	<b>Ca<sup>2+</sup> free Tyrode's (mM)</b>	<b>Substrate-free Tyrode's (mM)</b>	<b>Substrate-free Tyrode's metabolic inhibition (mM)</b>
KCl	5	5	5	5
NaCl	135	135	140	140
NaH <sub>2</sub> PO <sub>4</sub>	0.33	0.33	0.33	0.33
Na Pyruvate	5	5	--	--
HEPES	10	10	10	10
Mannitol	5	5	--	--
Glucose	5	5	--	--
Sucrose	--	--	10	10
CaCl <sub>2</sub>	2	--	2	2
MgCl <sub>2</sub>	1	1	1	1
EGTA	0	0.4	--	--
Sodium Cyanide	--	--	--	2
Iodoacetic acid	--	--	--	1
pH to 7.4 with NaOH				

**Table 2.1: Solution constituents for Normal Tyrode's, Ca<sup>2+</sup> free Tyrode's (0CaT), Substrate-free Tyrode's (SFT), and Substrate-free Tyrode's metabolic inhibition (SFT-MI).**

### 2.2.2 Western Blotting

Western blot is used in this study for detecting target protein, in terms of the molecular weight and the expression level. In this study western blot was used to reveal the alteration of interested protein between control and knockdown group. The constituents of the resolving and stacking gel that form the 12% SDS-PAGE gel used in this study are shown in Table 2.2. The stacking gel, which lies on top of the resolving gel, assembles the protein into narrow bands so that all proteins enter the resolving gel at the same time. The resolving gel then separates the proteins contained with the sample by their molecular mass.

Chemicals	12% Resolving Gel (10 ml)	Stacking Gel (5 ml)
dH <sub>2</sub> O	3.3 ml	0.85 ml
1.5 M Tris (pH at 8.8 with HCl)	2.5 ml	--
1 M Tris (pH at 6.8 with HCl)	--	0.625 ml
30% Acrylamide (Bio-Rad)	4 ml	0.85 ml
10% SDS	0.1 ml	0.05 ml
10% APS	0.1 ml	0.05 ml
TEMED	4 µl	5 µl

**Table 2.2: 12% SDS-PAGE gel constituents.**

The lysis buffer (RIPA; Table 2.3), is used to break up the cell membrane, increase the yield protein and prevent protein degradation.

Lysis Buffer (RIPA)	5 ml
NaCl	150 mM
EDTA	1 mM
1 M Tris-HCl (pH at 7.5 with HCl)	25 mM
Na-deoxycholate	0.025 g
10% NP-40	500 µl
10% SDS	50 µl
1 x Protease cocktail (Roche)*	700 µl

**Table 2.3: Constituents for RIPA buffer.** \*cOmplete, Mini, Ethylenediaminetetraacetic acid (EDTA)-free protease cocktail (Roche)

Laemmli Buffer (Table 2.4) is beneficial in protein loading. First, DDT as a reducing agent breaks apart the disulfide bonds that remove secondary and tertiary structure. Secondly, the SDS denatures the proteins and provides a negative charge so that the proteins are separated based on their size. Thirdly, bromophenol blue and glycerol aids protein loading by adding colour and density to the samples, respectively.

<b>6× Laemmli Buffer</b>	<b>10 ml</b>
SDS	1.2 g
Bromophenol blue	6 mg
Glycerol	5.875 g
0.5 M Tris (pH at 6.8 with HCl)	1.2 ml
dH <sub>2</sub> O	2.1 ml
DTT	0.93 g

**Table 2.4: 6× Laemmli Buffer constituents.**

Tris-buffered saline buffer (TBS; Table 2.5) was used for washing immobilon-P PVDF membrane (Millipore, UK) or to dilute antibodies.

<b>10× TBS (pH 7.6)</b>	<b>1 litre</b>
Trizma HCl	24.23 g
NaCl	80.06 g
dH <sub>2</sub> O	1 liter

**Table 2.5: 10× TBS constituents.** Solution was used at pH 7.6.

The running buffer (Table 2.6) was used during protein electrophoresis.

<b>Running Buffer (pH 8.3)</b>	<b>1 litre</b>
Tris base	3.03 g
Glycine	14.4 g
10% SDS	10 ml
dH <sub>2</sub> O	990 ml

**Table 2.6: Running Buffer constituents.** Solution was used at pH 8.3.

The transfer buffer (Table 2.7), was used to transfer the proteins to an immobilon-P PVDF membrane (Millipore, UK) from 12% SDS-PAGE gel.

<b>Transfer Buffer</b>	<b>1 litre</b>
Tris base	3.03 g
Glycine	14.4 g
Methanol	200 ml
dH <sub>2</sub> O	800 ml

**Table 2.7: Transfer Buffer constituents.**

All chemicals listed above were purchased from Sigma-Aldrich unless stated otherwise.

### 2.2.3 Electrophysiology solutions

In patch-clamp experiments, the extracellular NT or SFT-MI solutions (Table 2.1) were perfused into the cell chamber by Gilson Evolution peristaltic pump (Gilson) with a perfusion rate of 2.4 ml/min. Solutions were heated to  $32\pm 2^\circ\text{C}$  by Dagan Heatwave before perfused into cell chamber. The solution was changed by manually quick swap inlet from one to another. The pipette solutions were used to conduct the electrical signal between the cell and the electrode.

Cell-attached pipette solution (Table 2.8) with 140 mM  $\text{K}^+$  was used in cell-attached patch configuration achieving a reversal potential of 0 mV for  $\text{K}^+$  channel recording (assuming 140 mM intracellular  $\text{K}^+$ ). During the whole cell-recording, the pipette solution and cytosol as considered as one continuous solution. 5 mM EGTA with 0.61 mM  $\text{Ca}^{2+}$  was used in whole cell-recoding solution (Table 2.8) giving a calculated 20 nM free  $\text{Ca}^{2+}$  during whole cell-recording patching.

Chemicals	Cell-attached (mM)	Whole cell-recoding (mM)
KCl	140	110
KOH	--	30
HEPES	10	10
$\text{CaCl}_2$	1	0.61 (~20 nM free $\text{Ca}^{2+}$ )
$\text{MgCl}_2$	0.5	1
ATP	--	1
ADP	--	0.1
GTP	--	0.1
EGTA	--	5
pH	pH 7.2 with KOH	pH to 7.2 with HCl

**Table 2.8: Table constituents of both cell-attached solution and whole cell-recording solution.**

### 2.3 Cardiomyocyte isolation protocol

Rat cardiomyocytes were prepared from adult male Wistar rat (400-450 g) excised hearts using retrograde perfusion via a Langendorff canulae. Typically, 70-90% healthy rod-shaped myocytes were harvested in each isolation.

Animals were culled by stunning and cervical dislocation following the Home Office UK animals (Scientific Procedures) Act 1986 (2012 amendment) regulations. The heart was rapidly excised and placed into 4°C nominally 0CaT (Table 2.1). The heart was rapidly cannulated via the aorta and perfused for ~6 min with 0CaT at 37°C. Perfusion solution was exchanged to 0CaT containing enzyme mixture (1.6 mg/ml BSA, 0.66 mg/ml protease and 0.46 mg/ml collagenase). During the enzyme perfusion, after initially swelling, the heart returns to being soft to the touch as the digestion progresses. The heart was periodically massaged to monitor excessive pressure build up. Following the relaxation of the heart, the presence of rod-shaped cardiomyocytes in the perfusate identified that digestion was complete. Solution was swapped to 0CaT to remove residual enzyme from the tissue. The heart was then cut to increase the surface area and the remaining tissue transferred into a flask containing 2 mM NT (Table 2.1). Cardiac tissue was shaken in a 37°C water bath for 5 mins to release cardiomyocytes. The solution containing isolated cardiomyocytes was removed and the tissue re-suspended in fresh NT and this process repeated until no further viable cardiomyocytes were harvested. Any undigested tissue was removed and the cell suspension filtered to remove residual intact tissue. The cell suspension allowed settle for 15 min, the supernatant removed, pellet re-suspended with fresh NT and allowed to settle for a further 10 min. Finally, the pellet was re-suspended and the cell suspension maintained in 3–5 ml of fresh NT solution in 75 mm petri dishes until use.

### **2.3.1 Ischaemic preconditioning protocol**

Cardioprotection can be imparted to isolated cardiomyocytes by using an ischaemic preconditioning protocol applied to the whole heart prior to cell isolation. This method of imparting cardioprotection was developed by Rodrigo *et al* (2008) and is routinely used by the host laboratory (Sims *et al.*, 2014; Brennan *et al.*, 2015). Briefly, the heart was excised and perfused via the Langendorff cannula with a modified NT solution that contained no pyruvate, for 5 min. Perfusion was then halted for 5 min, and followed by 5 min of reperfusion. This cycle was repeated 3 times to mimic several brief periods of hypoxia to trigger cardiac ischaemia preconditioning (IPC). Following the final reperfusion, the solution was exchanged with 0CaT and the cardiomyocyte isolation protocol was followed as described above.

## 2.4 Cell culture & infection

### 2.4.1 HEK 293 A culturing protocol

For HEK 293A cell culture, Minimum Essential Medium Eagle supplemented with 10% foetal calf serum and 2 mM L-glutamine was used. HEK (Human embryonic kidney) 293A were cultured in 75 cm<sup>2</sup> flasks with complete medium (constituents shown above), and maintained in a 37°C incubator supply with 5% CO<sub>2</sub>. HEK 293A were split when cells reached approximately 90% confluence in flasks.

### 2.4.2 HEK 293 A transfection

Plasmids encoding *Rattus KCNJ8* (GenBank accession number: D42145), *KCNJ11* (GenBank accession number: D86039) and *Abcc9* (uses exon 38A, SUR2A variant, Genbank accession number: D83598; uses exon 38B, SUR2B variant, GenBank accession number: AF087838) were kindly provided by Dr Dave Lodwick. To obtain K<sub>ir</sub>6.1 and K<sub>ir</sub>6.2 proteins for the positive control for western blotting, combinations of K<sub>ir</sub>6.1/SUR2B and K<sub>ir</sub>6.2/SUR2A were co-transfected into HEK 293A cells, with transfection ratio of 1:2 in each combination.

Before transfection, 1.5x10<sup>5</sup> cells with 2 ml complete medium were seeded in each well in 6-well-plates for 48 h. Cells were then washed with PBS then treated with 5 ml trypsin (with 0.02% EDTA in PBS) at 37°C for 3-5 min. 10 ml complete medium was added into each flask. The cell suspension was removed and centrifuged at 180 g for 5 min, the supernatant discarded and the pellet re-suspended in 10 ml complete medium. 50 µl of cell suspensions was mixed with 50 µl trypan blue to assess viability. One third of the cell suspension was added into new flasks with fresh complete medium for growth.

For transfection, using FuGENE HD (Promega), complete medium was removed and replaced with 2 ml Opti-MEM (serum free). Maximum 2 µg DNA samples were diluted into 100 µl Opti-MEM with 5 µl FuGENE HD, the mixture incubated in room temperature for 5 min and then added into each well. The 6-well-plates were maintained in an incubator at 37°C with 5% CO<sub>2</sub> for 48 h.

### 2.4.3 Adenovirus replication protocol

The adenoviral vectors containing shRNA (targeted sequences sorted in Table 2.9) used in this project has previously produced as recombinant-defective adenovirus by Dr Dave Lodwick. A total of 5 different shRNA sequences were used in this study (Table 2.9). This recombinant-defective adenovirus can only replicate in a HEK 293A cell line. Infected HEK 293A cells will adhere for to the flask longer and so provide a marker of maximal adenoviral replication once the cells begin to float in the media. HEK 293A were seeded into 175 cm<sup>2</sup> flasks, incubated for 48 h to reach approximately 70% to 80% confluence. On the day of infection, the medium was replaced with 1 ml of the required adenovirus in 30 ml fresh complete medium. Once the replication was complete in HEK 293A cell, the HEK 293A cells lyse and detach from the bottom of the flask. The released virus then infects other cells in the flask. Once ~90% of HEK 293A cells were lysed, the medium was transferred into universal tubes and centrifuged for 5 min at 350 g. The resulting supernatant, containing the harvested adenovirus, was stored at -80°C. The infection efficiency of every batch of virus was calculated by the ability to infect cardiomyocytes. 4 different shRNA were used in this project, with each one packaged into the adenovirus. The shRNA targeted sequences were listed below in the table:

shRNA	Targeted Sequences
K <sub>ir</sub> 6.1A	ccaatgctcaggtcattcac
K <sub>ir</sub> 6.1B	acctgctccagcacaagaa
SUR2A	acctgctccagcacaagaa
SUR2B	ccatagctcatcggttca

**Table 2.9: shRNA targeted sequences for K<sub>ir</sub>6.1A, K<sub>ir</sub>6.1B, SUR2A and SUR2B.** The control shRNA is a proprietary product which is a none-targeting shRNA that comes with the virus construction kit (Ambion).

All shRNA were designed and packaged by Dr. Dave Lodwick. Targeted sequences were chosen using software provided by Ambion (now Thermo/Life Tech) for designing shRNAs except for SUR2B shRNA which target sequences can only be placed on the splice junction. Verification of sequences targeting K<sub>ir</sub>6.2 is published (Storey *et al.*, 2013). Other than K<sub>ir</sub>6.2 shRNA, all K<sub>ir</sub>6.1, SUR2A and SUR2B shRNA sequences were verified by luciferase or fluorescence gene expression assays. K<sub>ir</sub>6.1 and SUR2A were verified by electrophysiology. Both K<sub>ir</sub>6.1A and K<sub>ir</sub>6.1B shRNA knockdown efficiency were verified

using a flow cytometry method by previous students. By co-transfection of each shRNA with pcDNA3.1-K<sub>ir</sub>6.1-EGFP and pcDNA3.1-SUR2A into HEK cells (recombinant K<sub>ir</sub>6.1/SUR2A channel), the EGFP fluorescence intensity was measured by flow cytometry and the reduction in EGFP fluorescence in K<sub>ir</sub>6.1A or K<sub>ir</sub>6.1B group represent their knockdown efficiency. K<sub>ir</sub>6.1A reduces the mean EGFP fluorescence to 14% and K<sub>ir</sub>6.1B reduces the mean EGFP fluorescence to 25%. A modified plasmid pENTR-1A was used as vector, which contained an U6 (pol III) promoter for shRNA expressing as well as either mCherry or EGFP under the control of a CMV promoter. The designed shRNA sequences were cloned into this customized pENTR-1A vector. All constructs were verified by sequencing and by functional assays described above. Clones in the modified pENTR-1A were recombined in vitro with pAd/PI-Dest (Thermo/Life Tech) which contains the adenoviral backbone.

#### **2.4.4 Cardiomyocyte culture & infection protocol**

For cardiomyocyte culture, media 199 (Life Technologies) was used as basal media and was supplemented with ITS+3 (2 mg/100 ml), Carnitine (2 mM), Creatine (5 mM), Taurine (5 mM), T3 (1.5 pM), Pen/Strep (100 Units) and Sodium pyruvate (100 mM). All chemicals were from Sigma-Aldrich unless stated otherwise.

For culturing, freshly isolated myocytes were re-suspended and settled in complete medium 199 twice, then transferred into 3 ml (with  $2 \times 10^5$  cells/ml) medium 199 into each well of a 6-well plates and maintained in a 37°C incubator with 5% CO<sub>2</sub> for 24 h. In order to maintain physiological morphology in short-term culture, the medium had no foetal calf serum added (Mitcheson, 1998).

Adenovirus-containing cell lysate (described in section 2.3.3) was added to freshly isolated cardiomyocytes incubated in 6-well plates. For each virus, the amount of virus-containing lysate was calculated based on the infection efficiency in cardiomyocytes calculated following harvesting of the virus. Typically, 100–250 µl of virus-containing lysate was added to cardiomyocytes. The plates were maintained in an incubator supplied with 5% CO<sub>2</sub> at 37°C for 24 h after viral infection. After 24 h, cells were collected from each well and washed twice with normal Tyrode's solution and settled in 75 mm petri dishes for experimentation.

#### **2.4.4.1 Adenovirus infection efficiency**

Each shRNA adenoviral construct was tagged with a fluorescent reporter gene (mCherry or GFP). The infection efficiency was tested using fluorescence imaging after each adenovirus preparation. The optimum amount of each adenovirus-containing cell lysate was calculated for each batch. 24 h after infection, the infection efficiency was calculated by randomly picking 6 fields of view containing ~30 cells and, using the fluorescence from infected cardiomyocytes, calculating the percentage infection efficiency. The amount of virus added to the cultured cardiomyocytes that gave 50% to 60% infection efficiency was used in all experiments to limit the potential toxicity of the virus.

### **2.5 Protein Extraction and Bradford Protein Assay**

For HEK 293 A cells that were transfected with K<sub>i</sub>6.1/SUR2B, proteins were extracted after 48 h incubation in 6-well-plates in a 5% CO<sub>2</sub> incubator at 37°C. 6-well plates were kept on ice during extraction processing. Wells were washed 3 times with 20 mM Tris (pH 7.5)/0.9% NaCl, and cells were lysed using RIPA buffer. Cells were scraped off the well and pipetted into Eppendorfs. Samples were vortexed and centrifuged for 30 s at 16500 g at 4°C. The supernatants were pipetted into clean tubes and ready for Bradford assay.

For cardiomyocyte protein extraction, 500 µl lysis buffer (Table 2.3) was applied to a cardiomyocyte pellet following acute isolation (or culture). Samples were then transferred into Eppendorfs and kept on ice. Samples were vortexed and centrifuged for 30 s at 16500 g at 4°C. The supernatants were pipetted into clean tubes and ready for Bradford assay.

To perform a standard curve for the Bradford assay, Bovine Serum Albumin (BSA) was prepared at concentrations of 0 to 30 µg in a total volume of 200 µl in lysis buffer. Protein samples with unknown concentrations were diluted in lysis buffer to a volume of 200 µl, in the ratio of 1:10, 1:100 and 1:200. An Ultrospec III UV/Vis Spectrophotometer (Pharmacia LKB) at 595 nm was used to determine absorbance. 1 ml 1 × 1 ml Protein Assay Dye Reagent Concentrate (Bio-Rad) was added in to each BSA standard and experimental protein samples, incubated in room temperature for 10 min before measurement. After measurement, the absorbance values of BSA standards were used to draw the standard curve, to which the concentration of unknown protein samples would then be extrapolated.

## 2.6 Western blotting

Freshly isolated or 24 h cultured cardiomyocytes were allowed to settle for 10 min in normal Tyrode's solution to remove cell debris and dead cardiomyocytes. To extract protein, Tyrode's was replaced with 500  $\mu$ l of ice cold radio immune precipitation assay (RIPA; Table 2.3) lysis buffer. Samples were agitated by vortexing and passed through a 22-gauge syringe needle several times to shear genomic DNA. Samples were centrifuged at 16500 g for 30 s with the resulting supernatant frozen at  $-80^{\circ}\text{C}$ . The total protein concentration of each lysate was determined by measuring the absorbance of each sample mixture with 1 ml 1 $\times$  Protein Assay Dye Reagent Concentrate (Bio-Rad) at 595 nm, using an Ultrospec III UV/Vis Spectrophotometer and comparing it with a standard curve constructed with known concentrations of BSA.

Supernatants were boiled for 5 min at  $95^{\circ}\text{C}$  with 1x laemmli loading buffer (Table 2.4). Protein samples and the Blue Protein Standard marker (Broad Range from 11-190kDa, New England) were separated by 12% SDS-PAGE for 3 h at 100 V using the Mini-PROTEAN<sup>®</sup> 3 Cell electrophoresis apparatus (Bio-Rad, UK). 12% resolving gel and stacking gel were prepared followed the constituents (Table 2.2) along with running buffer (Table 2.6). Protein samples were then transferred by electrophoresis for 1 h at 110 V, using the Trans-blot<sup>®</sup> Cell apparatus (Bio-Rad, UK), onto an immobilon-P PVDF membrane (Millipore, UK) with pre-chilled transfer buffer (Table 2.7).

Following protein transfer, membranes were washed 3 times (5 min per wash) in Tris-buffered saline (TBS), containing 0.1% Tween (TBS-T), before being incubated in blocking buffer (10% marvel milk in TBS-T) overnight at  $4^{\circ}\text{C}$  (or 1 h in room temperature).

After blocking, following another 3 $\times$  5 min washes in TBS-T, membranes were incubated for 2 h at room temperature with the appropriate primary antibody, diluted in 1% milk powder (w/v) in TBS-T. Primary antibodies used in this study were developed by Prof Norman (University of Leicester) corresponding to the rat  $K_{ir}6.1$  (Singh *et al.*, 2003). This primary antibody was used at a 1:250 dilution in TBS-T with 5% (w/v) dry milk solution. Additionally, the primary antibodies, anti- $K_{ir}6.2$  (Alomone lab; Cat #: APC-020), diluted into 1:500 in TBS-T with 5% (w/v) milk solution was also used.

Following incubation in primary antibody, membranes were washed in TBS-T for  $3 \times 5$  min and then incubated for 2 h at room temperature with the appropriate horseradish peroxidase-conjugated secondary antibody (Jackson Immuno Research, 1:10000 in TBS-T). The membrane was washed with TBS-T for  $3 \times 5$  min. Membranes were then incubated with SuperSignal West Pico or Femto Chemiluminescent Substrate kit (Thermo Scientific, UK). Immunoreactivity proteins were detected using the FUJIFILM LAS-4000 (FUJIFILM)

## **2.7 Electrophysiology**

Electrophysiology allows the electrical properties of cells or whole tissues to be measured directly using microelectrodes. In this project, patch clamp was used to investigate the relationship between expression of ion channel subunits, such as  $K_{ir}6.1$ , and the physiological changes it caused to action potential duration (APD) and resting membrane potential (RMP) in cardiomyocytes. To investigate the physiological regulatory role of  $K_{ir}6.1$  activity on cardiomyocyte function, action potentials (AP) were recorded. A small current (normally 1-2 nA) was applied via the patch pipette, to depolarise the resting membrane potential between 8 mV to 12 mV (~130% the stimulus required to generate a response), to stimulate the cardiac AP. The calculated APD at 90% repolarization ( $APD_{90}$ ) was measured throughout my project. In each condition, such as control, drug treatments and gene knockdown, a minimum of 60 action potential sweeps were measured individually for their  $APD_{90}$  as well as RMP that was taken from the mean baseline prior to AP trigger. The mean  $APD_{90}$  and RMP were then calculated in excel and be used as 1 data point in the analysis.

### **2.7.1 Apparatus for patching**

Cells were visualised using a Nikon TiU microscope with a 20 $\times$  objective. All signals were collected by an Axopatch 200B amplifier (Axon Instruments, Foster City, CA) coupled to digital interface (Digidata 1440, Axon Instruments). Lowpass filter was set on 2 kHz. Sampling rate was set on 10 kHz. Data was acquired by Clampex software (Axon Instruments), which was analysed by Clampfit software (Axon Instruments). A two-stage vertical electrode puller (Narishige/model: PC-10) was used to prepare electrodes. A micromanipulator (Siskiyou) was used position the electrode in the rig.

### 2.7.2 Electrode preparation

1.2-mm borosilicate glass capillaries (Warner Instruments) were used to produce electrodes. Typically, electrodes with a resistance of between 3-6 MΩ were used in both whole cell recording and the cell-attached recording configurations. All electrodes were used on the day of preparation.

### 2.7.3 Membrane potentials & ionic flux

The resting membrane potential of a cell is the potential difference across the cell membrane and can be measured using patch clamp recording. The external membrane potential (i.e. the bathing solution) was used as a reference potential, equal to 0 mV. The potential differences across the external and interior phospholipid bilayer are a relative value due to interior membrane potential being expressed relative to the external potential arbitrarily set to 0 mV as a reference membrane potential. At the 'resting' membrane potential in normal physiological conditions, K<sup>+</sup> ions predominantly, although not exclusively, move across the membrane and so contribute the most to the resting membrane potential. Normally, the concentration gradient is maintained by the Na-K-ATPase so that there is a high concentration of intracellular K<sup>+</sup> and a lower extracellular K<sup>+</sup> concentration. Potassium ions therefore diffuse in an outward direction. In an idealised, perfectly selective, cell membrane that could only allow K<sup>+</sup> ions to pass; the membrane potential will 'rest' when the concentration gradient moves out and electrical gradient pulling positively charged potassium ions back in is equal. This theoretical membrane potential is termed the equilibrium potential. The equilibrium potential can be calculated for any ion using the Nernst equation below:

Equation 1

$$E_x = \frac{RT}{zF} \ln \frac{[X]_o}{[X]_i}$$

Briefly,  $E_x$  represents the equilibrium potential for the particular ion. X is the ionic concentration outside (<sub>o</sub>) and inside (<sub>i</sub>). R is the gas constant (8.314 J K<sup>-1</sup>mol<sup>-1</sup>), F is Faradays constant (96500 C mol<sup>-1</sup>), T is the temperature in °K and z is the valency and charge of the ion.

To fully characterise the membrane potential of the cell by calculation, knowledge of the relative permeability of the membrane to each ion would be required. With this information, the Goldman, Hodgkin and Katz (GHK) equation could be used. This is a more complex form of the Nernst equation that includes the relative permeabilities:

$$V_m = \frac{RT}{zF} \ln \left( \frac{p[K]_o + p[Na]_o + p[Ca]_o + p[Cl]_o}{p[K]_i + p[Na]_i + p[Ca]_i + p[Cl]_i} \right)$$

Equation 2, the GHK equation.

In the equation, the  $V_m$  is the membrane potential.  $R$  is the gas constant ( $8.314 \text{ J K}^{-1} \text{ mol}^{-1}$ ),  $F$  is Faradays constant ( $96500 \text{ C mol}^{-1}$ ),  $T$  is the temperature in Kelvins and  $z$  is the half number of electrons (in mol) transferred in the cell reaction, or the valency of the ion.  $p$  is the permeability for that ion (in m/s).  $[ion]_o$  is the extracellular concentration of that ion (in  $\text{mol/m}^3$ ).  $[ion]_i$  is the intracellular concentration of that ion (in  $\text{mol/m}^3$ ).

#### 2.7.4 Patch-Clamp: Cell-attached Configuration

In the cell-attached configuration, current is only recorded from the area of membrane in the tip of the patch electrode. Typically,  $K_{ir6.1}$ -containing channels can be resolved with up to three open levels with electrodes of 3–6  $\text{M}\Omega$ . For the cell-attached configuration, the sampling rate was set at 10 kHz with 2 kHz frequency set for Lowpass filter.

Cardiomyocytes were allowed to adhere in the perfusion chamber for 5-10 min prior to experimentation. Cell-attached pipette solution (section 2.6.1) was loaded into electrode. The electrode was gently pushed onto the cell membrane, and suction applied if necessary to achieve a gigaohm seal. All analysis was done on recordings that showed no fluctuation in the baseline or evidence of early activation of  $K_{ir6.2}$  in the absence of MI. These observations were used as exclusion criteria to identify unhealthy cells. Similar exclusion criteria were applied in whole-cell recording configuration.

In the cell attached configuration, the pipette voltage was always held at +40 mV. Assuming the cardiomyocyte resting membrane potential was -70 mV, the recording was acquired at an equivalent holding potential of -110 mV (Figure 2.1). Channel event

detection was processed by Clampfit software. All channel open probabilities were acquired from traces duration longer than 180 s in cell-attached patch configuration.

In the cell-attached configuration, the channel open probability ( $P_o$ ) was calculated. The open probability was used as a measure of channel activity and the effect of various pharmacological agents. To calculate the ion channels opening probabilities in the recording,

Equation 3

$$P_o = \frac{t_o}{T}$$

Or

$$P_o = \frac{T_o}{NT}$$

$P_o$  represents the opening probability for the ion channel which calculated by the ratio between  $t_o$ , the opening time for single ion channel, and  $T$ , the whole recording duration.  $T_o$  represents the total opening duration of one certain type of channels opening on different levels.  $N$  equals the number of ion channels opening in the recording, when there was only one channel opening in the patch,  $N$  equals one.

For the sum of more than one ion channels opening in multiple levels,  $T_o$  is,

Equation 4

$$T_o = \sum_{L=1}^N t_o L$$

In this equation,  $L$  represents the different open levels, for example  $L=1, 2, 3$ .  $t_{oL}$  was the opening time for this type of ion channels in different opening levels. For example, Therefore, in a recording with  $N=4$  ion channels open and 3 opening levels with opening duration in each level of 700 ms ( $t_{o1}$ ), 90 ms ( $t_{o2}$ ) and 10 ms ( $t_{o3}$ ), in a recording with the total recording length  $T=1000$  ms. Therefore,  $T_o=t_{o1}+t_{o2}+t_{o3}=800$  ms. The single channel

open probability is  $P_o = 700 + 90 + 10 / (1000 \times 4) = 0.2$ . Same equation has been used to measure the channel open probability in previous studies (Fenwick *et al.*, 1982; Sollini *et al.*, 2002).

However, the number of channels contributing to a recording cannot be measured because of the stochastic behaviour, ion channels can alternately go into activation or closed state (assuming they were two-state channel) during 1 recording. Therefore, the opening probability of the channel can only be presented in NP<sub>o</sub>, calculated by following equation.

Derived from Equation 3,

$$NP_o = \frac{T_o}{T}$$

This equation has been used for measuring multiple channel open probability in previous studies (Zhang & McMahon, 2000; Roh *et al.*, 2007).

#### **2.7.4.1 Voltage-step measurement protocol**

The current-voltage (I-V) relationship of each sarcolemmal K<sub>ATP</sub> and K<sub>ir2</sub> current was measured by a series of voltage steps in the cell-attached configuration. Voltage steps, with duration of 4 s, were recorded in 10 mV increments from an equivalent of -180 mV to +10 mV. The conductance of the channel was calculated from the slope of the single channel I-V relationship.

#### **2.7.5 Patch-Clamp: Whole-cell Recording Configuration**

To record in the whole-cell ruptured patch configuration, gentle suction was applied to the patch pipette once the cell-attached configuration (section 2.7.4) had been achieved. The range of series resistance values for whole-cell configuration recordings was 8-20 MΩ and the capacitance from recorded cardiomyocyte was 80-120 pF. Any recordings did not meet the criteria of series resistance and capacitance was aborted. Series resistance and membrane capacitance were measured using the membrane test function in pCLAMP. Each capacitance for the cell was recorded and used to normalize the whole-cell currents during the analysis.

The pipette potential was changed to -80 mV prior to patch rupture to ensure that the holding potential, once the whole cell configuration had been achieved, was close to the resting membrane potential of cardiomyocytes.

The total membrane capacitance ( $C_m$ ) of the lipid bilayer represented the membrane surface area, which  $C_m$  and the cell membrane surface area are in linear relationship in the cells in spherical or cylindrical shape, such as cardiomyocyte. Therefore, the measured  $C_m$  can be used to reference the membrane surface area. In my whole-cell recordings, the measured capacitance of the lipid bilayer can be used to normalize the recorded whole-cell leak currents. The whole-cell leak currents can be normalized by divide the measured  $C_m$ , with the units of pA/pF.

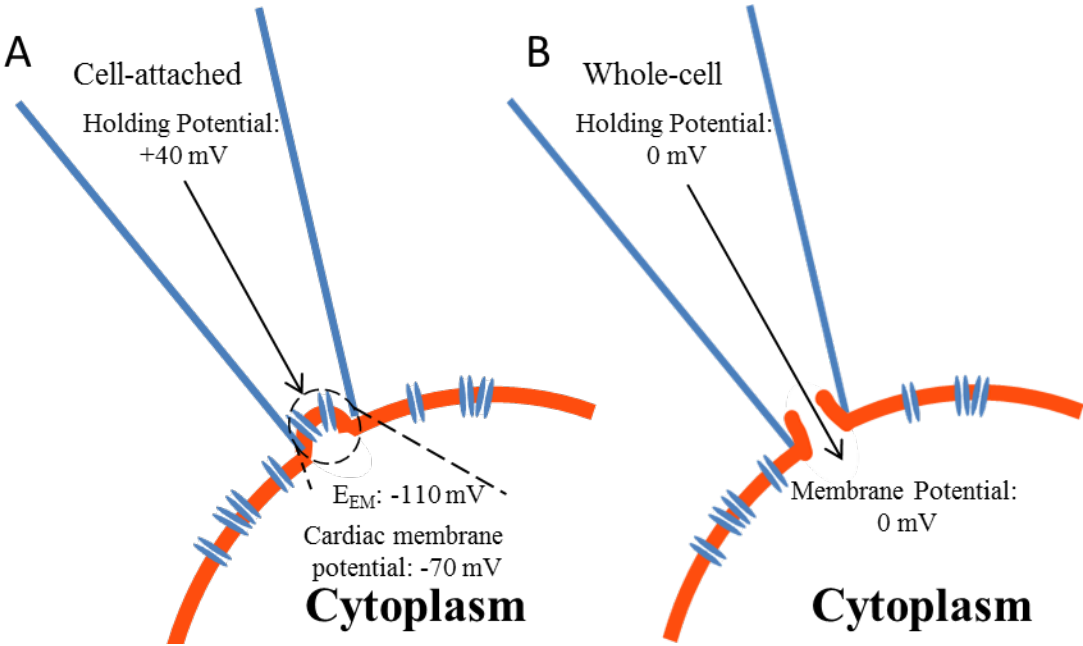


**Figure 2.1: A brief diagram for cell-attached configuration and whole-cell recording configuration.** A. In cell-attached configuration the holding voltage from electrode was +40 mV. In resting condition, the cardiomyocytes' membrane potential in cytoplasm side is assumed to be -70 mV in rat ventricular myocyte. Referencing the extracellular-environment as 0 mV, the equivalent membrane potential in the clamping area  $E_{EM} = -110$  mV. B. In whole-cell recording configuration, the cell membrane was ruptured, allowing the electrode directly clamp the whole cell membrane potential. Thus, the holding voltage from electrode equals the membrane potential in whole-cell recording configuration.

## 2.8 Phenotypic screening

To assess the effect of the channel of interest on cardiomyocyte contractile function, a metabolic inhibition and simulated reperfusion (MI/R) protocol was used in isolated cardiomyocytes. Briefly, cardiomyocytes were initially perfused with NT solution at  $32\pm 2^{\circ}\text{C}$  for 3 min. 1 Hz electric field stimulation was used to trigger contractions throughout the protocol. The solution was exchanged for a metabolic inhibition (MI) solution (Table 2.1) for 7 min, followed by 10 min of simulated reperfusion with NT solution. To pharmacologically inhibit  $\text{K}_{\text{ir}}6.1$ -containing  $\text{K}_{\text{ATP}}$  channels, 3  $\mu\text{M}$  PNU37883A was added into both NT solution and MI solution. The times to contractile failure and percentage of contractile recovery were recorded in addition to the cell survival (determined by hypercontracted cells being unable to exclude trypan blue). The percentages of contractile recovery and cell survival were used as marker of cardioprotection with a contractile recovery of less than 40% and a cell survival of  $\sim 70\%$  demonstrating a control, non-cardioprotected phenotype.

## 2.9 Fluorescent imaging

Fluorescent imaging was used in this study to measure changes in intracellular ATP (or ADP) and changes in calcium during simulated ischaemia and reperfusion. Two dyes were used to measure  $\text{Ca}^{2+}$  changes, with Fura-2-AM Cell Permeant (Invitrogen) ratiometric  $\text{Ca}^{2+}$  indicator used in the measurement of intracellular  $\text{Ca}^{2+}$  concentration and Fluo-4-AM (Invitrogen)  $\text{Ca}^{2+}$  indicator used in  $\text{Ca}^{2+}$  transient recording. Magnesium Green (Invitrogen) was used as an ADP indicator used in the measurement of whole-cell ADP level during metabolism inhibition. For Fura-2-AM Cell Permeant  $\text{Ca}^{2+}$  dye, the excitation wavelengths were 340 ( $\text{Ca}^{2+}$  bound)/380 ( $\text{Ca}^{2+}$  free) nm and emissions were collected at wavelengths above 520 nm. For Fluo-4-AM  $\text{Ca}^{2+}$  dye, the excitation wavelength was 488 nm with the emissions collected at wavelengths above 520 nm. For  $\text{Mg}^{2+}$  green dye, the excitation wavelength was 506 nm and the emission wavelength was 531 nm.

In order to obtain the details of  $\text{Ca}^{2+}$  transient, the exposure time and shutter speed were kept as low as possible to increase the data acquisition rate. A single wavelength  $\text{Ca}^{2+}$  dye was used to detect and measure the  $\text{Ca}^{2+}$  transient recordings as a dual excitation dye, such as Fura-2 would require two images to be collected for one ratio data point. However, a

single wavelength dye has its limitations, which is due to the lack of a reference fluorescence signal for the background; the fluorescence intensity can be altered by the changing volumes of a cell, particularly in a contractile myocyte. The ratiometric dye overcomes the problem, as the calculated ratio between the  $\text{Ca}^{2+}$  bound and free dye can be independent from cell's volume change. However, because of the CCD camera used in these experiments is not fast enough, the single wavelength dye was chosen to indicate  $\text{Ca}^{2+}$  change during transient.

In order to statistically analysis the  $\text{Ca}^{2+}$  transients, the following parameters were measured in this project: the  $\text{Ca}^{2+}$  transient duration at 50% of peak to baseline and  $\text{Ca}^{2+}$  transient duration at 90% its return to from peak to baseline. All raw fluorescence intensity data was collected from the imaging software Winfluor (John Dempster, University of Strathclyde), with the region of interest drawn around each cardiomyocyte. Minimum 6 cells  $\text{Ca}^{2+}$  transients' fluorescence signals were measured in each experiment and the signals were averaged from each experiment by excel. To allow each drug to exert their maximum effect, only  $\text{Ca}^{2+}$  transients fluorescence signals at the end of each treatment were measured. Due to a non-ratiometric dye being used in the  $\text{Ca}^{2+}$  transients measurement, the baseline and the peak fluorescence intensity was uneven in each  $\text{Ca}^{2+}$  transients, which was unable to measure the parameters in an excel spreadsheet. The solution used was to normalize each  $\text{Ca}^{2+}$  transient fluorescence intensity from 0 (baseline) to 1 (peak), A minimum of 15  $\text{Ca}^{2+}$  transients were measured in each drug treatment as 1 data points used in statistical analysis. Example traces in Figure 3.11 shown the averaged and normalized signals for 1 experiment.

Cells were incubated in a lightproof tube with fluorescent indicators at a concentration of 5  $\mu\text{M}$  for minimum 30 min. Cells were then settled for 10 min in the perfusion chamber prior to experimentation. The protocol outlined in the phenotypic screening section (section 2.7) was used to investigate changes in ATP and  $\text{Ca}^{2+}$ .

The fluorescence imaging system was built on a Nikon 200 inverted microscope with a 20 $\times$  objective used to observe cells via a Roper Cascade CCD camera. The DeltaRAM X monochromator (PTI, New Jersey, USA) was used as a fluorescent illuminator. 79001 - ET - Fura 2 filter (Chroma Technology Corp, Vermont, USA) was installed to allow detection

and quantification of ratiometric signal intensities. EasyRatio Pro was used to control the CCD camera. All images were analyzed in Winfluor (John Dempster, University of Strathclyde).

## 2.10 Statistical Analysis

One-way ANOVA/Two-way with Holm-Sidak post-test test was used to compare the statistical difference for the multiple comparisons between control group and drug treatment/gene knockdown groups. Electrophysiology data was collected by Clampfit 10.3 (Axon Instruments) software and Student's paired or unpaired t-test was used to compare statistical difference in single cell-attached or whole-cell recording data. For IC<sub>50</sub>/EC<sub>50</sub> calculations, concentration–response curves were fitted using the Hill equation:

Equation 5

$$I/I_A = \frac{1}{1 + \left(\frac{[x]}{IC_{50}}\right)^n}$$

Where I is the current in the test compound, I<sub>A</sub> is the current in the absence of the test compound, [X] is the concentration of the compound, IC<sub>50</sub> (or EC<sub>50</sub>) is the concentration that produces half maximal block and n is the slope factor (Hill coefficient). All phenotypic screen data were collected from > 3 animals and > 6 experiments. Data are presented as means±S.E.M. unless stated otherwise. All data was analysed using Microsoft Excel 2016 and statistical analysis was calculated by Prism (version 6; Graphpad Software, SanDiego, CA). P<0.05 was considered as a significant difference in statistical analysis.

## **Chapter 3**

**The identification of a ~39 pS-conductance**

**SarcoK<sub>ATP</sub> in cardiomyocyte**

### 3.1 Introduction

In the literature, the dogma states that  $K_{ATP}$  channels expressed at the cardiomyocyte membrane surface (Sarco $K_{ATP}$ ) are inhibited by intracellular ATP and opened by increasing concentrations of ADP. This property has led to the description of the Sarco $K_{ATP}$  as a metabolic sensor on the cardiomyocyte membrane. The inhibition by ATP causes the Sarco $K_{ATP}$  to remain closed in normal physiological conditions. During periods of metabolic stress, the Sarco $K_{ATP}$  will be activated by an increase in ADP and decrease in ATP, which hyperpolarises the membrane potential and shortens the action potential to limit further ATP depletion and reduce  $Ca^{2+}$  overload. The cardiac  $K_{ATP}$  current ( $I_{KATP}$ ) has been widely studied on the cardiac sarcolemmal membrane and has been demonstrated to be activated by metabolic inhibition or by pharmacological agents. The activity of the known cardiac  $K_{ATP}$  channel can be readily identified on the cardiac sarcolemmal membrane surface using the channel conductance, which is  $\sim 80$  pS for  $K_{ir}6.2/SUR2A$  isoform. The  $K_{ir}6.2/SUR2A$  complex has been considered as the sole Sarco $K_{ATP}$  channel complex expressed at the cardiomyocyte membrane surface.

By using cell-attached patch recording, a second small-conductance  $K^+$  channel was identified on the cardiac sarcolemmal membrane that was open in normal resting conditions. This channel had a larger conductance than the  $K_{ir}2.1$  channel (expected to be  $\sim 20$  pS (Fischer-Lougheed *et al.*, 2001)), with a conductance of around  $\sim 39$  pS.

It was hypothesised that, given the similarity in conductance to  $K_{ir}6.1$ -containing channels expressed in other cells, such as smooth muscle (as described in section 1.4.1 of the introduction), the inhibition by glibenclamide (shown in Figure 3.3B) and that the channel exhibits a bursting pattern of opening similar to other  $K_{ATP}$  channel family members that this  $\sim 39$  pS-current may be from a  $K_{ir}6.1$ -containing ion channel.

## 3.2 Results

### 3.2.1 Identification of a channel active under resting conditions with a single channel current amplitude of ~5 pA

In the cell-attached patch configuration, cardiomyocytes were perfused with NT at  $32 \pm 2^\circ\text{C}$  to record channel activity. Following this, the solution was exchanged for SFT-MI for the rest of the recording. This was done to assess the metabolic sensitivity of a  $\sim 39$  pS-conductance and to distinguish it from the  $\text{K}_{\text{ir}6.2}/\text{SUR}2\text{A}$  complex. The pipette potential was held at +40 mV with 140 mM  $\text{K}^+$  in pipette solution, which, assuming a resting membrane potential of -70 mV, gives an approximate membrane potential of around -110 mV across the cell-attached patch. These parameters were applied in all cell-attached recordings unless stated otherwise. In every patch, a channel with a single channel current of  $\sim 5$  pA can be observed in normal physiological resting conditions (Figure 3.1 A(ii)). In contrast, Figure 3.1A (iii) shows the activation of the  $\text{K}_{\text{ir}6.2}/\text{SUR}2\text{A}$  current ( $\sim 10$  pA) after metabolic inhibition due to the depletion of ATP and the elevation of intracellular ADP. Figure 3.1B shows an amplitude histogram of the single channel current where this small-conductance potassium channel opened at  $\sim 5$  pA (Figure 3.1B) in resting conditions compared with  $\text{K}_{\text{ir}6.2}$  with  $\sim 10$  pA openings after MI stimulation (Figure 3.1C).

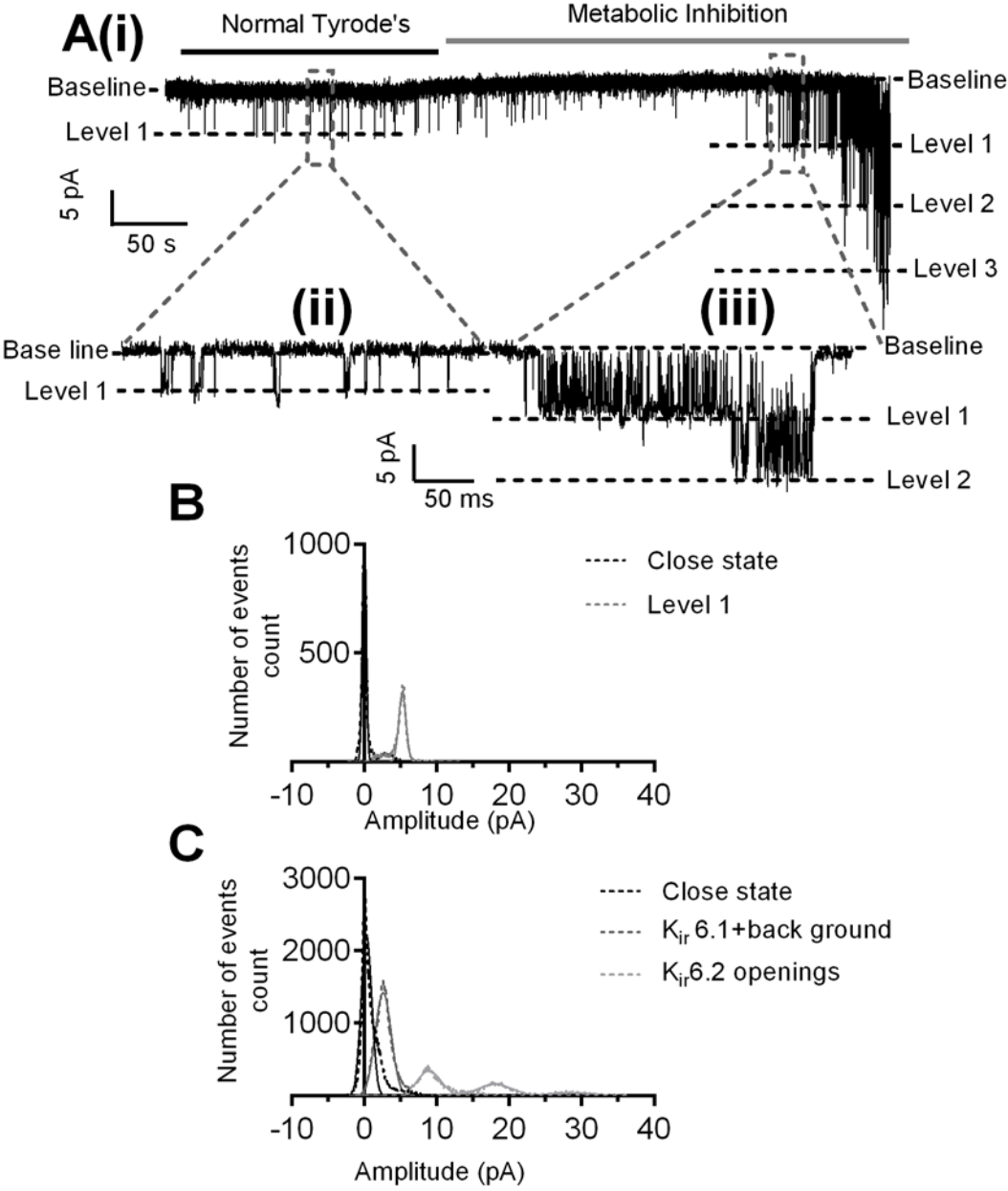


**Figure 3.1: Identification of a small conductance, metabolically insensitive, current in cell-attached patch recording from rat cardiomyocytes.** A(i), Example recording of cardiac sarcolemmal currents recorded by cell-attached patch from acutely isolation cardiomyocytes. Cells were held at a pipette potential of -40 mV with 140 mM  $K^+$  in the patch pipette solution, giving an equivalent membrane potential of  $\sim$ 110 mV. (ii), expanded trace showing a channel passing  $\sim$ 5 pA of current for each opening in resting conditions. (iii), Expanded trace showing a conventional cardiac sarcolemmal  $K_{ATP}$  channel ( $K_{ir}6.2/SUR2A$ ) current ( $\sim$ 10 pA in amplitude) in cell-attached recording activated by metabolic inhibition. B and C, Amplitude histograms showing mean opening amplitudes from different opening levels in NT solution (B) and in metabolic inhibition (C).

### 3.2.2 Determination of the single channel conductance of the recorded currents using cell attached patch on cardiomyocytes

The cell-attached configuration was used to measure the single channel conductance of the small (~5 pA) current and the  $K_{ir}6.2/SUR2A$  current for comparison. The membrane potential was held at increasing potentials stepping from -180 mV to 10 mV, recording for 4 s in 10 mV increments. The small-conductance channel currents reversed at around 0 mV, consistent with this being a  $K^+$  current which showed a linear inward current voltage relationship (Figure 3.2A). The slope of the line was used to calculate the conductance, which was  $38.71 \pm 0.92$  pS ( $n=10$  and  $n>3$  animals, Figure 3.2D). Additionally, there was a second channel active on the membrane surface alongside the ~39 pS-channel (Figure 3.2A), with a calculated channel conductance of  $20.23 \pm 0.78$  pS ( $n=10$  and  $n>3$  animals, Figure 3.2C). This was consistent with the  $K_{ir}2.1$  channel that underlies the  $I_{k1}$  current.

To measure the conductance of the  $K_{ir}6.2/SUR2A$  channel, the protonophore 2,4-dinitrophenol (DNP) was applied to stimulate its activation by reducing intracellular ATP. The conductance of the conventional cardiac  $K_{ATP}$  ( $K_{ir}6.2/SUR2A$ ;  $78.53 \pm 1.60$  pS,  $n>10$  cells and  $n>3$  animals) was approximately double the conductance of the ~39 pS-conductance channel.

These results show that the conductance recorded for the  $K_{ir}6.2/SUR2A$  channel was consistent with previous papers (van Bever *et al.*, 2004) on native cardiomyocytes. The  $K_{ir}6.2/SUR2A$  channel did not show activity in normal physiological conditions but was activated in MI due to its ATP sensitivity (Zhang *et al.*, 2010; Wang *et al.*, 2003). These results also show a second, ~39 pS-conductance expressed on native cardiomyocyte membranes that is constitutively open in resting conditions. It was hypothesised that this ~39 pS channel a  $K_{ATP}$  channel (Yamada *et al.*, 1997).

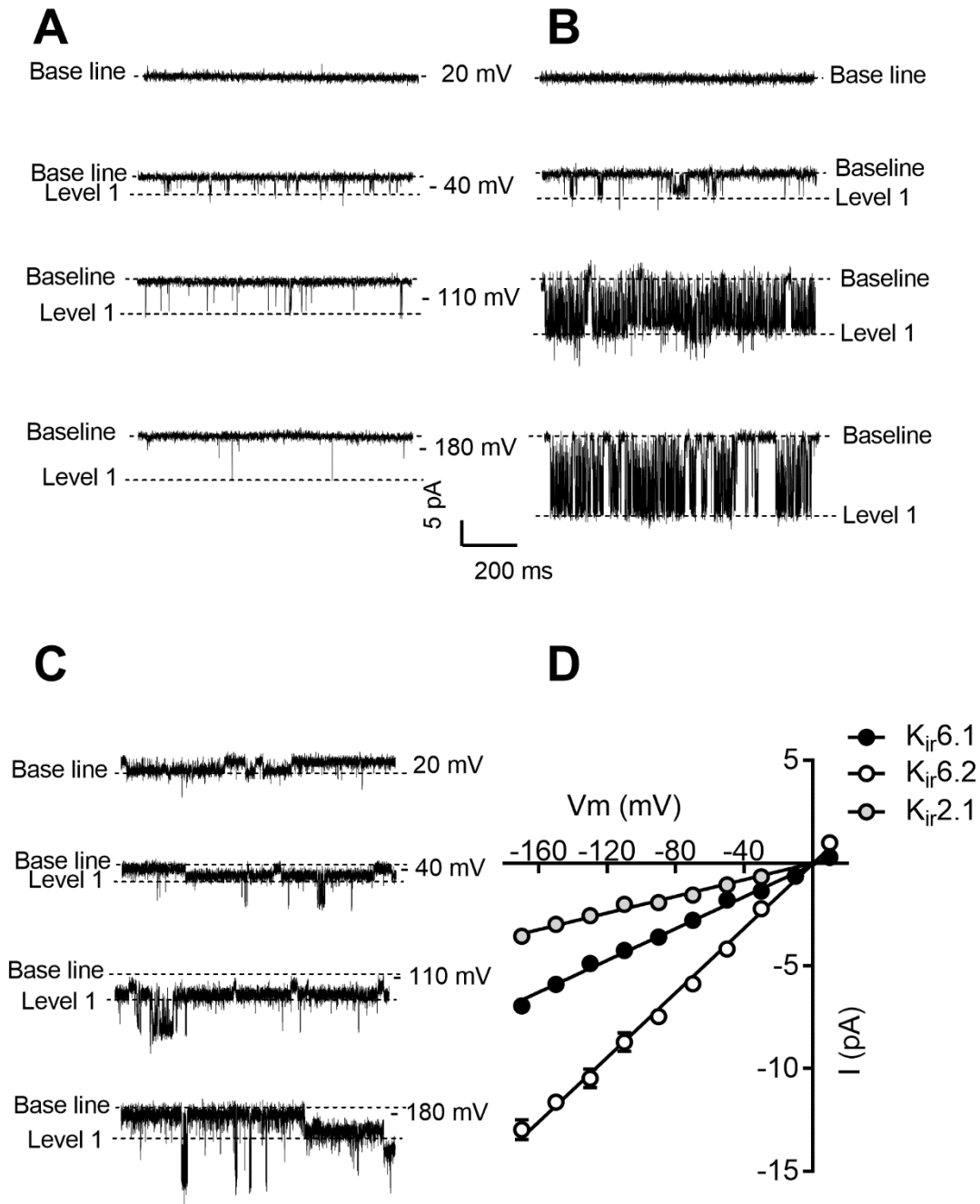


**Figure 3.2: A ~39 pS current is active in rat cardiomyocytes in normal Tyrode's solution and metabolic inhibition activates a ~78 pS  $K_{ir}6.2$  channel.** Voltage steps were applied, in the cell-attached configuration, from equivalent membrane potential steps of -180 mV to 10 mV for 4 s in 10 mV increments. A, Example recordings of the  $K_{ir}6.1$ -like conductance (A) and  $K_{ir}6.2$ /SUR2A channel conductance (B), activated by metabolic uncoupling with 2,4-dinitrophenol (DNP) at 10, -40, -110 and -180 mV. Example recordings of  $K_{ir}2.1$  channel (C), with smaller channel conductance compared with  $K_{ir}6.1$ -like channel. D, Single channel IV for the small and  $K_{ir}6.2$ /SUR2A conductance. The slope of regression lines were used to calculate the conductance for each channel, with  $38.71 \pm 0.92$  pS (small conductance channel) and  $78.53 \pm 1.60$  pS ( $K_{ir}6.2$ ). An additional small current expressing with the ~39 pS conductance currents (A), with calculated channel conductance of  $20.23 \pm 0.78$  pS. Data was presented in mean  $\pm$  SEM from  $n > 6$  cells and  $n > 3$  animals.

### 3.2.3 The effect of glibenclamide, a non-selective $K_{ATP}$ inhibitor, on the ~39 pS-conductance channel

In the vasculature,  $K_{ir}6.1/SUR2B$  currents have been shown to be inhibited by low nanomolar concentrations of glibenclamide (Yamada *et al.*, 1997). In this experiment, 10  $\mu$ M glibenclamide treatment was used to assess the block as this is a standard concentration used in the wider literature (Light *et al.*, 2000; Suzuki *et al.*, 2001; Pountney *et al.*, 2001). Figure 3.3A (i) shows an example trace in NT solution followed by 10  $\mu$ M glibenclamide treatment, where the open probability for this ~39 pS-channel was reduced (Figure 3.3A (iii)) compared with NT perfusion (Figure 3.3A (ii)). The calculated open probability (NPo) (Figure 3.3B) for this ~39 pS-conductance channel reduced from  $0.094 \pm 0.015$  (n=4) to  $0.004 \pm 0.003$  (n=4, \*  $p < 0.05$ ; Student paired t-test). These data suggest that the ~39 pS-conductance currents expressed on the cardiac sarcolemmal membrane are likely to be  $K_{ATP}$  currents separate to  $K_{ir}6.2$ -containing channels which are only opened with low ATP, however further investigation was required.

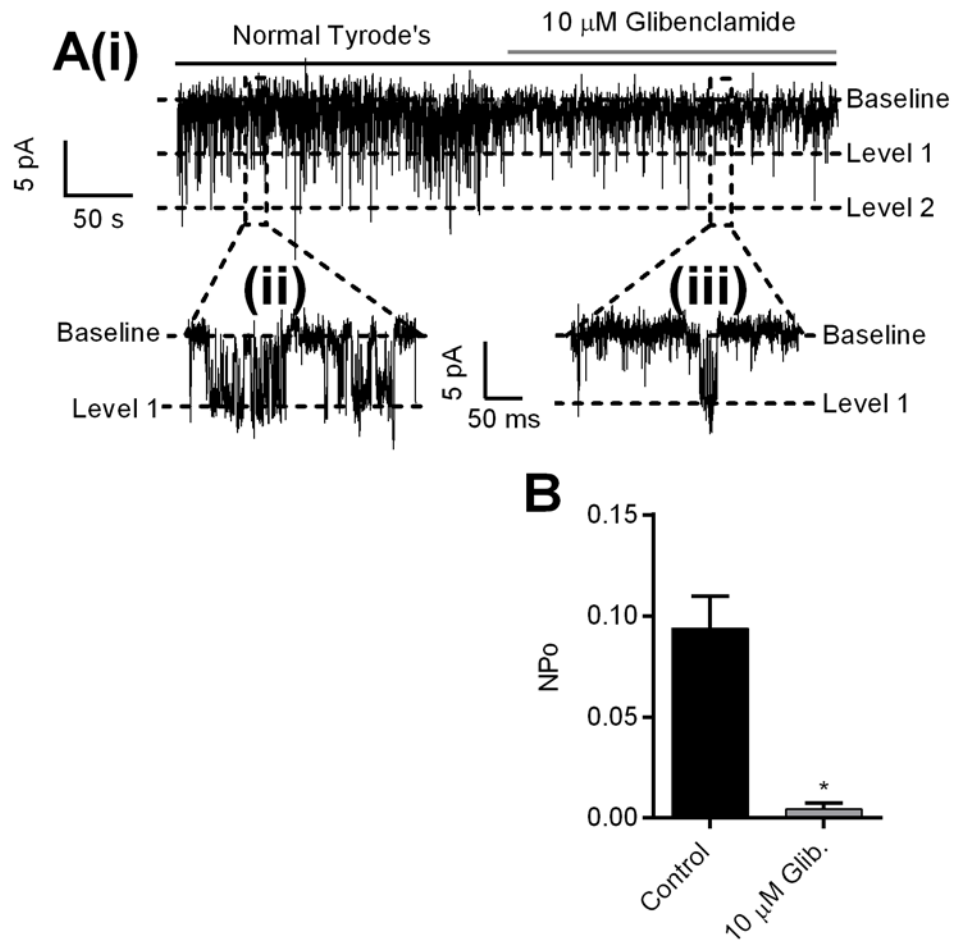


**Figure 3.3: 10 μM Glibenclamide treatment suppresses the small-conductance current at the cardiac sarcolemmal membrane.** A(i), Representative trace recorded from a cell-attached patch at the equivalent of  $\sim -110$  mV. Expanded traces showing the activity of the small conductance channel in control conditions (ii) and following perfusion with 10 μM glibenclamide in normal Tyrode's solution (iii). B, Histogram showing the NPo for the channel in control ( $0.094 \pm 0.015$ ,  $n=4$ ) and following 10 μM Glibenclamide treatment ( $0.004 \pm 0.003$  ( $n=4$ )) (\*  $p < 0.05$ ; Student paired t-test).

### 3.2.4 The effect of PNU37883A (a $K_{ir}6.1$ specific blocker) on the $\sim 39$ pS-current

PNU37883A (PNU) is a  $K_{ATP}$  channel inhibitor that specifically blocks  $K_{ir}6.1$  currents at low concentrations. As a pore blocker, PNU is not an SUR-dependent inhibitor and acts from the cytoplasmic side of membrane. In a previous study (Kovalev *et al.*, 2004),  $10 \mu\text{M}$  PNU was able to suppress about 70% of  $K_{ir}6.1/\text{SUR2B}$  currents but only 7% of  $K_{ir}6.2/\text{SUR2B}$  currents in *xenopus* oocytes. These findings suggest it has selectivity for  $K_{ir}6.1$ -containing channels at low concentrations.

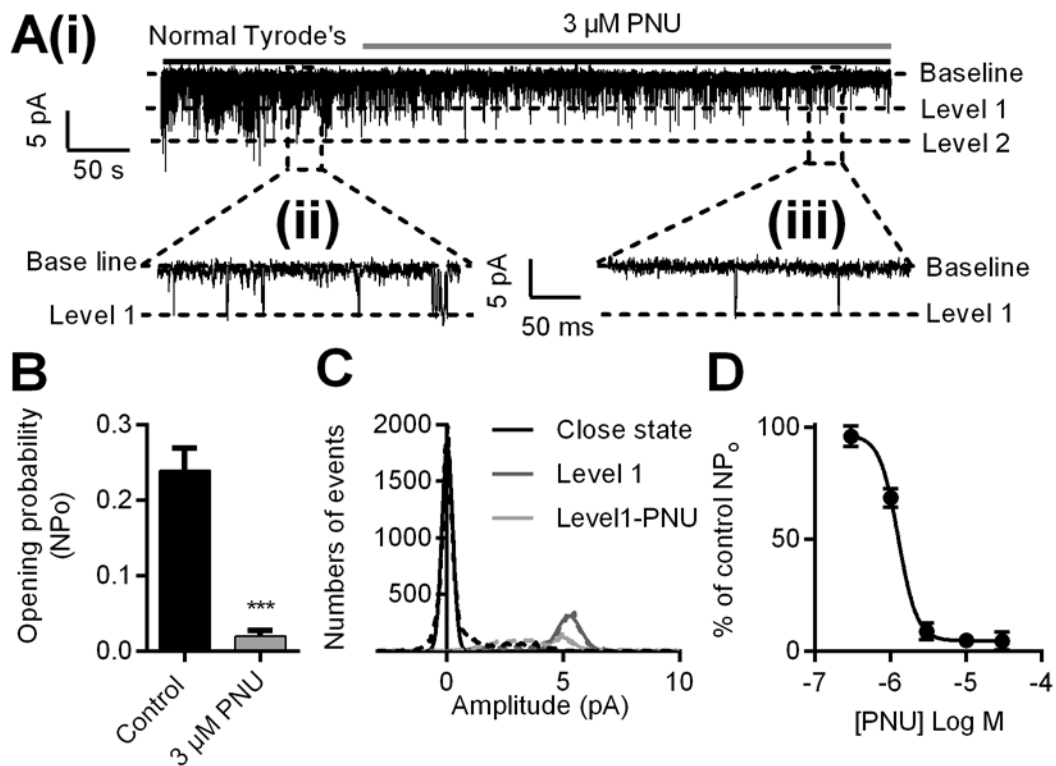


**Figure 3.4: PNU37883A, a  $K_{ir}6.1$  specific channel blocker, suppresses the small conductance current at the cardiac sarcolemmal membrane.** A(i), representative trace recorded from a cell-attached patch at the equivalent of  $\sim -110$  mV. Expanded traces showing the small conductance channel in control conditions (ii) and following perfusion with  $3 \mu\text{M}$  PNU in normal Tyrode's solution. B, Histogram showing the  $\text{NP}_o$  for the channel in control ( $0.23 \pm 0.03$  ( $n=8$ )) and following PNU treatment ( $0.02 \pm 0.01$  ( $n=8$ )) (\*\*\*) ( $p < 0.001$ ; Student paired t-test). C, Amplitude histogram showed no change in single-channel amplitude before or after  $3 \mu\text{M}$  PNU treatment. Data was presented in mean  $\pm$  SEM from  $n > 6$  cells and  $n > 3$  animals. D, Concentration response relation was drawn to illustrate the percentage inhibition on the  $\sim 39$  pS currents by PNU treatment in cell-attached configuration. Each data point was represented in mean  $\pm$  SEM ( $n > 3$ ). The fitted line correspond to least squares fit of Hill equation, with calculated  $\text{IC}_{50} = 1.26 \pm 0.15$ .

To assess the effects of PNU on the  $\sim 39$  pS-current, a concentration of  $3 \mu\text{M}$  was used to ensure that  $\text{K}_{\text{ir}6.2}$  channels were unaffected but enough to block  $\text{K}_{\text{ir}6.1}$ -containing channels (Kovalev *et al.*, 2004). Figure 3.4A shows an example of a cell-attached recording of  $\text{K}_{\text{ATP}}$  channel from freshly isolated rat cardiomyocyte. Following perfusion with  $3 \mu\text{M}$  PNU, the  $\sim 39$  pS-conductance channel currents showed a decrease in  $\text{NP}_0$ , from  $0.23 \pm 0.03$  (control,  $n=8$ ) to  $0.02 \pm 0.01$  (PNU treatment,  $n=8$ , \*\*\*  $p < 0.001$ ; Student paired t-test). The amplitude histogram showed no change in channel amplitude between control and PNU treatment group (Figure 3.4C). Figure 3.4D shows the concentration-response curve for PNU inhibition on the  $\sim 39$  pS-channel open probability in the cell-attached configuration, with an  $\text{IC}_{50}$  of  $1.26 \pm 0.15 \mu\text{M}$ , which demonstrates that the PNU concentration used in these experiments was sufficient to suppress the  $\sim 39$  pS-currents.

A PNU concentration-response curve was constructed from pinacidil-activated sarcolemmal  $\text{K}_{\text{ATP}}$  currents in acutely isolated cardiomyocytes to determine the relative contribution of the small conductance channel to the whole cell  $\text{K}_{\text{ATP}}$  current. Figure 3.5A shows a typical concentration curve experiment where data was acquired from whole-cell recording and holding membrane potential at  $0 \text{ mV}$ .  $100 \mu\text{M}$  pinacidil was used to activate  $\text{K}_{\text{ATP}}$  currents, and continuously perfused throughout the experiment. Two concentrations of PNU were perfused on each cardiomyocyte, with a 10-fold gap in concentration (eg.  $0.3 \mu\text{M}$  to  $3 \mu\text{M}$  and  $1 \mu\text{M}$  to  $10 \mu\text{M}$ ). At the end of the experiment,  $10 \mu\text{M}$  glibenclamide was added to inhibit all remaining  $\text{K}_{\text{ATP}}$  currents, so allowing the inhibition by PNU to be normalized to glibenclamide-sensitive  $\text{K}_{\text{ATP}}$  currents. Data was fitted with the Hill equation. Figure 3.5B shows the concentration-response profile for glibenclamide-sensitive  $\text{K}_{\text{ATP}}$  current inhibition by PNU where the  $\text{IC}_{50}$  was calculated to be  $\sim 4 \mu\text{M}$ . The  $\text{IC}_{50}$  calculated for glibenclamide-sensitive current in cardiomyocytes was similar to that for  $\text{K}_{\text{ir}6.1}$ -containing channels in *xenopus* oocytes (Kovalev *et al.*, 2004). These data suggest that part of the glibenclamide-sensitive current may be attributed to a native cardiac sarcolemmal  $\text{K}_{\text{ir}6.1}$   $\text{K}_{\text{ATP}}$  current. Furthermore, PNU was only able to inhibit around 30% of the glibenclamide-sensitive current (at concentrations of  $100 \mu\text{M}$ ). In this experiment, it was hypothesised that pinacidil activated two different currents, one of which was sensitive to PNU inhibition but the other current relatively insensitive to PNU; however, both currents were sensitive to Glibenclamide.

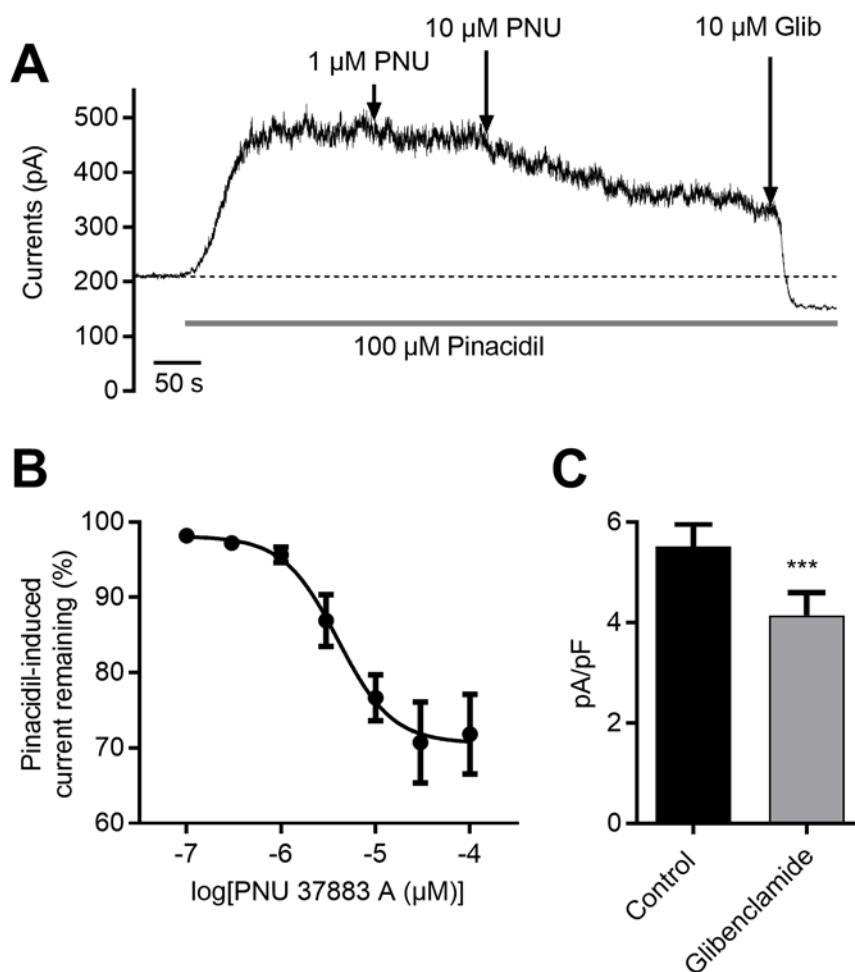


**Figure 3.5: The  $K_{ir}6.1$  specific blocker PNU37883A (PNU) partially inhibits the glibenclamide sensitive current activated by pinacidil.** A, Representative whole-cell current trace recorded at 0 mV from a freshly isolated rat cardiomyocyte. Each cell was exposed to two concentrations of PNU with 10  $\mu$ M glibenclamide at the end to determine glibenclamide-sensitive  $K_{ATP}$  current. B, Concentration response data showing the percentage of pinacidil-activated current blocked by PNU treatment. Each data point was represented in mean  $\pm$  SEM ( $n > 6$ , from  $> 3$  animals). The fitted line corresponds to least squares fit of Hill equation, with a calculated  $IC_{50} = 3.99 \pm 0.15$ . C, Histogram showing the mean post glibenclamide leak current compared to that at the start of the recording. The remaining leak current in glibenclamide was significantly smaller than the basal leak prior to pinacidil ( $5.51 \pm 0.45$  pA/pF (base line) and  $4.15 \pm 0.45$  pA/pF (glibenclamide) (\*\*\*)  $p < 0.0001$ ; Student t-test). Data was presented in mean  $\pm$  SEM from  $n > 6$  cells and  $n > 3$  animals.

Figure 3.5C demonstrates that the residual leak current after the glibenclamide inhibition was significantly reduced compared with the background currents before the application of pinacidil, from  $5.51 \pm 0.45$  pA/pF (baseline) to  $4.15 \pm 0.45$  pA/pF (glibenclamide). These data suggest there is native cardiac sarcolemmal  $K_{ATP}$  activity, or at least a glibenclamide-sensitive current that is active, in basal resting conditions.

In the previous experiments, pinacidil was used to evoke currents, however it was suggested that there was a basal level of glibenclamide-sensitive current prior to pinacidil-induced activation. To further investigate this, 3  $\mu$ M PNU was applied to the cell which was held at 0 mV in the absence of any pharmacological sulphonylurea activators. As in the previous experiment, 10  $\mu$ M glibenclamide was used to block all  $K_{ATP}$  currents at the end of the recording and leak currents were normalised to cell capacitance (Figure 3.6A (i)). Figure 3.6A (ii) shows there is a significant reduction in leak current from control ( $5.15 \pm 0.47$  pA/pF, n=9) in the presence of 3  $\mu$ M PNU ( $4.25 \pm 0.49$  pA/pF, n=9, \*\* p<0.005), but there was no further decrease in leak current following application of 10  $\mu$ M glibenclamide ( $4.27 \pm 0.47$  pA/pF, n=9; Repeated measures one-way ANOVA with Holm-Sidak post-test).

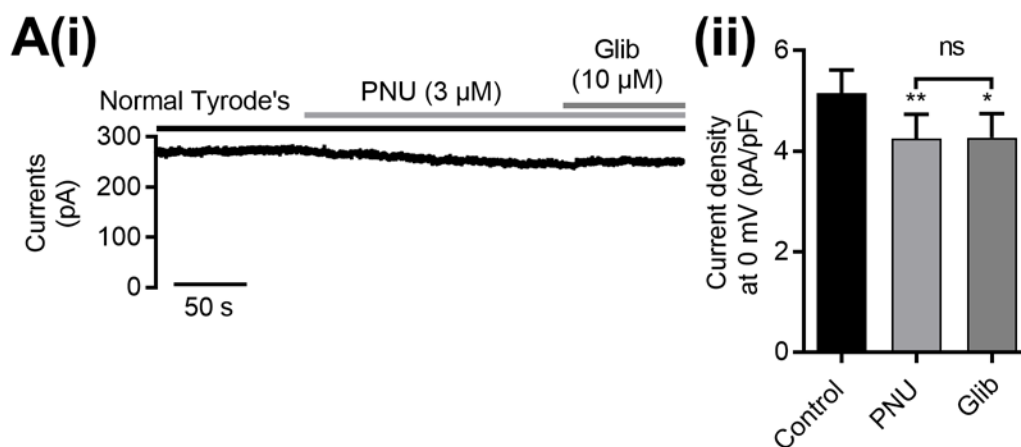


**Figure 3.6: 3  $\mu$ M PNU37883A blocks glibenclamide sensitive leak current.** A, Example trace recorded in the whole-cell configuration at a holding membrane potential at 0 mV in control, 3  $\mu$ M PNU and 10  $\mu$ M glibenclamide. (ii), histogram showing the mean data for cardiomyocyte background current from baseline ( $5.2 \pm 0.5$ , n=9) and following 3  $\mu$ M PNU treatment ( $4.2 \pm 0.5$ , n=9, \*\* p<0.005) and 10  $\mu$ M glibenclamide treatment ( $4.3 \pm 0.5$ , n=9, \* p<0.05; Repeated measures one-way ANOVA with Holm-Sidak post-test). Data was presented in mean (pA/pF)  $\pm$  SEM from n>3 animals.

To investigate whether this PNU and glibenclamide-sensitive current plays a physiological regulatory role in cardiomyocyte function, action potentials (AP) were recorded in the whole-cell configuration. APD<sub>90</sub> and RMP for each condition was measured, calculated and analysed as section 2.7.

Cells were first perfused in NT then switched to 3  $\mu$ M PNU and finally 10  $\mu$ M glibenclamide at the end of the recording. Figure 3.7A shows that 3  $\mu$ M PNU caused a prolongation of the action potential duration (APD), with no further prolongation seen with 10  $\mu$ M glibenclamide. The APD<sub>90</sub> showed that 3  $\mu$ M PNU caused a significant prolongation of the APD<sub>90</sub> in cardiomyocytes (Figure 3.7B), from 71.1 $\pm$ 2.8 ms (control, n=9) to 93.3 $\pm$ 6.1 ms (3  $\mu$ M PNU, n=9, \*p<0.05). 10  $\mu$ M glibenclamide caused no further APD<sub>90</sub> prolongation (95.6 $\pm$ 5.2 ms, n=9, ns; Repeated measures one-way ANOVA with Holm-Sidak post-test). Further investigation of the resting membrane potential was carried out measuring the initial membrane potential prior to triggering each action potential. Figure 3.7C revealed that 3  $\mu$ M PNU depolarised membrane potential from -67.4 $\pm$ 1.3 mV (control, n=8) to -61.8 $\pm$ 2.4 mV (3  $\mu$ M PNU, n=9, \*p<0.05; Repeated measures one-way ANOVA with Holm-Sidak post-test), however there was no further depolarization following treatment with 10  $\mu$ M glibenclamide (-64.4 $\pm$ 2.7 mV, n=8).

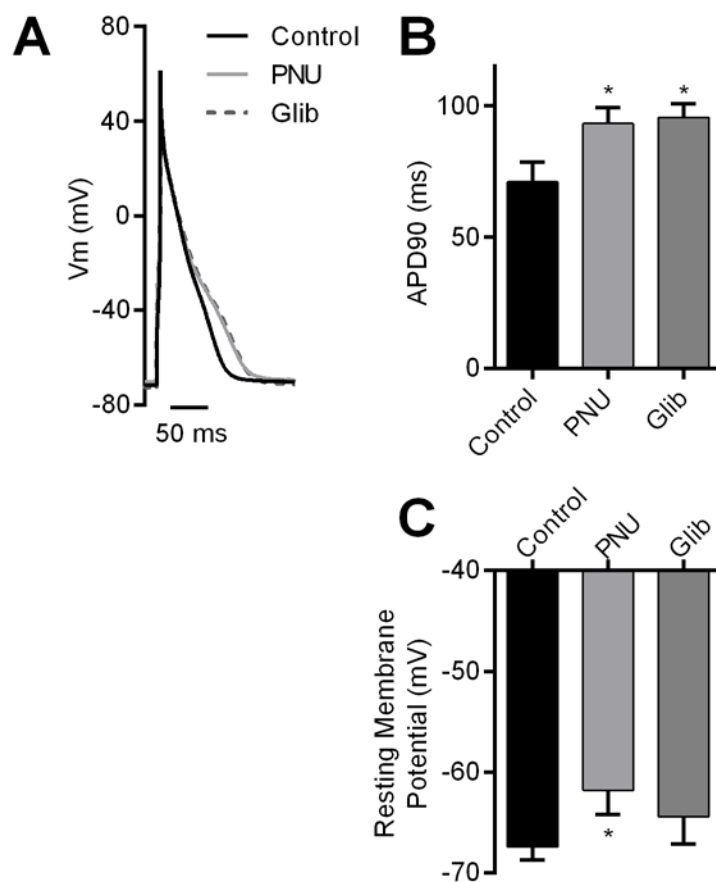


**Figure 3.7: 3  $\mu$ M PNU37883A prolonged action potential duration as well as depolarize resting membrane potential.** A, Example traces for rat cardiomyocyte AP, in control, 3  $\mu$ M PNU and 10  $\mu$ M glibenclamide group. B, Histogram showing 3  $\mu$ M prolonged the mean  $APD_{90}$  from  $71.1 \pm 2.8$  ms (control,  $n=9$ ) to  $93.3 \pm 6.1$  ms (3  $\mu$ M PNU,  $n=9$ ), further treatment with 10  $\mu$ M glibenclamide ( $95.6 \pm 5.2$  ms,  $n=9$ ) did not further prolong  $APD_{90}$  compare with PNU treatment. C, Mean data showing that 3  $\mu$ M PNU treatment depolarized membrane potential compared to resting condition, from  $-67.4 \pm 1.3$  mV (control,  $n=8$ ) to  $-61.8 \pm 2.4$  mV ( $n=8$ ,  $*p < 0.05$ ). Further treatment with 10  $\mu$ M glibenclamide not shown further depolarization on membrane potential ( $-64.4 \pm 2.7$  mV,  $n=8$ ), compare with 3  $\mu$ M PNU treatments. Repeated measures one-way ANOVA with Holm-Sidak post-test was used in analysis, statistical significance has been shown as  $*P < 0.05$ ,  $**P < 0.01$ , and  $***P < 0.001$  vs control.

Taken together, using pharmacological methods, these data demonstrate that the glibenclamide-sensitive component of basal currents at 0 mV may be due to a  $K_{ir}6.1$ -containing  $K_{ATP}$  channel expressed on the cardiac sarcolemmal membrane. This channel may also have a significant role in regulating the APD in cardiomyocytes in basal conditions, separate and in addition to the known role of  $K_{ir}6.2/SUR2A$  channels in shortening APD during times of ATP depletion. Finally, the putative  $K_{ir}6.1$  channel may have an important physiological role in regulating the resting membrane potential in cardiomyocytes.

### 3.2.5 Calcium transients in cardiomyocyte are prolonged by PNU37883A treatment.

The results above suggest the pharmacological blockade of the putative cardiac  $SarcoK_{ir}6.1$  prolongs cardiac APD. Given the link between the duration of the AP and intracellular  $Ca^{2+}$  release, a further question posed was whether the  $Ca^{2+}$  transients could be regulated by suppressing the cardiac  $SarcoK_{ir}6.1$  currents. To ensure the camera was running fast enough to capture the  $Ca^{2+}$  transients, Fluo-4, a single wavelength  $Ca^{2+}$  binding dye that excited at 480 nm and emits at 520 nm, was used. In this experiment, cardiomyocytes were perfused with NT for 3 min, followed by 5 min with 3  $\mu$ M PNU and finally 10  $\mu$ M glibenclamide. 0.5 Hz field stimulation was used to trigger the action potential durations throughout each experiment. The  $Ca^{2+}$  change was recorded at the end of each treatment for 30 s. Figure 3.8A (i), (ii) and (iii) shows example traces of  $Ca^{2+}$  transients in NT solution, 3  $\mu$ M PNU and 10  $\mu$ M glibenclamide respectively. The 50% and 90% to resting level in  $Ca^{2+}$  transients were measured in the experiments. Figure 3.8C demonstrates the 50% to resting level in  $Ca^{2+}$  transient in all NT (control), PNU and glibenclamide treatments, with  $323.6 \pm 10.5$  ms (control, n=8),  $399.3 \pm 18.3$  ms (PNU, n=8, \*\*\*p<0.001) and  $402.4 \pm 20.6$  ms (Glib, n=8, \*\*p<0.005; Repeated measures one-way ANOVA with Holm-Sidak post-test) respectively. Further investigation in 90% to resting level in  $Ca^{2+}$  transient demonstrated the same trend, Figure 3.8D show  $Ca^{2+}$  transient in PNU and glibenclamide was prolonged, with  $905.8 \pm 49.5$  ms (n=8, \*\*p<0.005) and  $928.4 \pm 53.8$  ms (n=8, \*\*p<0.005; Repeat measures one-way ANOVA with Holm-Sidak post-test) respectively compared to control condition ( $751.8 \pm 35.2$  ms, n=8).

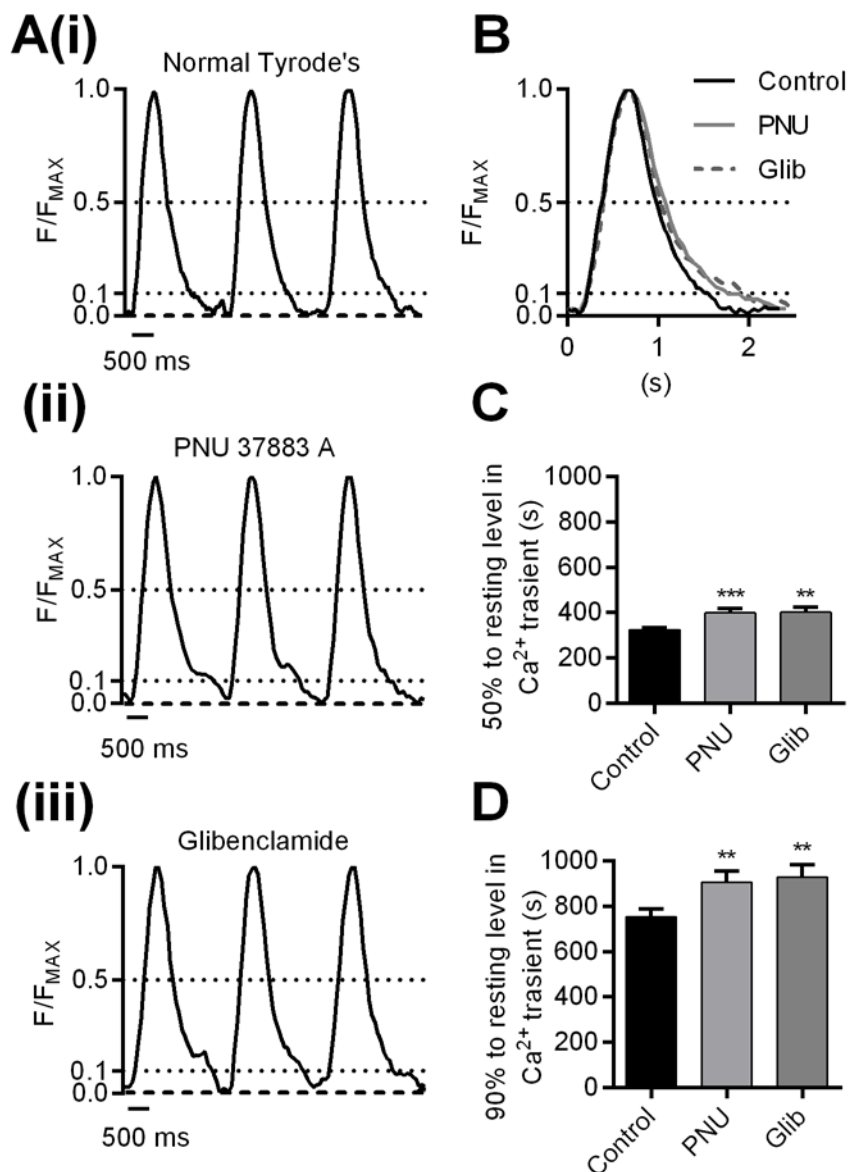


**Figure 3.8: Measuring rat cardiomyocyte  $\text{Ca}^{2+}$  transient in action potential duration using the single wavelength  $\text{Ca}^{2+}$  indicator, Fluo-4.** A(i), (ii) & (iii) Example traces showing the  $\text{Ca}^{2+}$  transients triggered by 0.5 Hz field stimulating, in NT, 3  $\mu\text{M}$  PNU and 10  $\mu\text{M}$  Glib respectively. B, Side-by-side comparison of both PNU and Glib treatments showing a prolonged  $\text{Ca}^{2+}$  transient, compared with control conditions. C, Mean data showed the time from maximum fluorescence intensity to 50% of resting level in  $\text{Ca}^{2+}$  transients in each control, PNU and Glib conditions, with  $323.6 \pm 10.5$  ms (control,  $n=8$ ),  $399.3 \pm 18.3$  ms (PNU,  $n=8$ ,  $***p < 0.001$ ) and  $402.4 \pm 20.6$  ms (Glib,  $n=8$ ,  $**p < 0.005$ ; Repeated measures one-way ANOVA Holm-Sidak post-test) respectively. D, Mean data showed the time from maximum fluorescence intensity to 90% of resting level  $\text{Ca}^{2+}$  transients in control, PNU and Glib conditions, with  $751.8 \pm 35.2$  ms (control,  $n=8$ ),  $905.8 \pm 49.5$  ms (PNU,  $n=8$ ,  $**p < 0.005$ ) and  $928.4 \pm 53.8$  ms (Glib,  $n=8$ ,  $**p < 0.005$ ; Repeated measures one-way ANOVA Holm-Sidak post-test) respectively.

These data suggests the putative SarcoK<sub>ir</sub>6.1-containing channel can play a role in regulating both AP and Ca<sup>2+</sup> transient duration.

### **3.2.6 Effect of rosiglitazone on the ~39 pS-conductance channel in rat cardiomyocytes**

Rosiglitazone has been used as an anti-diabetic drug which is known to act via PPAR- $\gamma$  receptors however it has been withdrawn from the European market due to its cardiovascular risk, which includes cardiac infarction, heart failure and increased mortality (Chen *et al.*, 2012). A recent study (Yu *et al.*, 2012) has shown that rosiglitazone inhibits the major vascular isoform of the K<sub>ATP</sub> channel, K<sub>ir</sub>6.1/SUR2B, with some degree of selectivity between K<sub>ir</sub>6.1 and K<sub>ir</sub>6.2 containing channels, IC<sub>50</sub> ~10  $\mu$ M on K<sub>ir</sub>6.1/SUR2B channel and IC<sub>50</sub> ~37  $\mu$ M on K<sub>ir</sub>6.2/SUR2A channel.

In the cell-attached configuration, with an increasing rosiglitazone concentration, a concentration-dependent block of the ~39 pS-conductance current was observed (Figure 3.9A (i)). The inhibition of the ~5 pA-current was expressed as a fraction of NPo in control solution and data used to form a concentration response curve. Using the Hill equation, the IC<sub>50</sub> of rosiglitazone for the small-conductance current was 14.5  $\mu$ M (Figure 3.9B, n>4). These data indicate that the ~39 pS-conductance channel can be inhibited by rosiglitazone with a similar IC<sub>50</sub> to the block of K<sub>ir</sub>6.1/SUR2B channels expressed in recombinant channel in HEK 293 cells (Yu *et al.*, 2012).

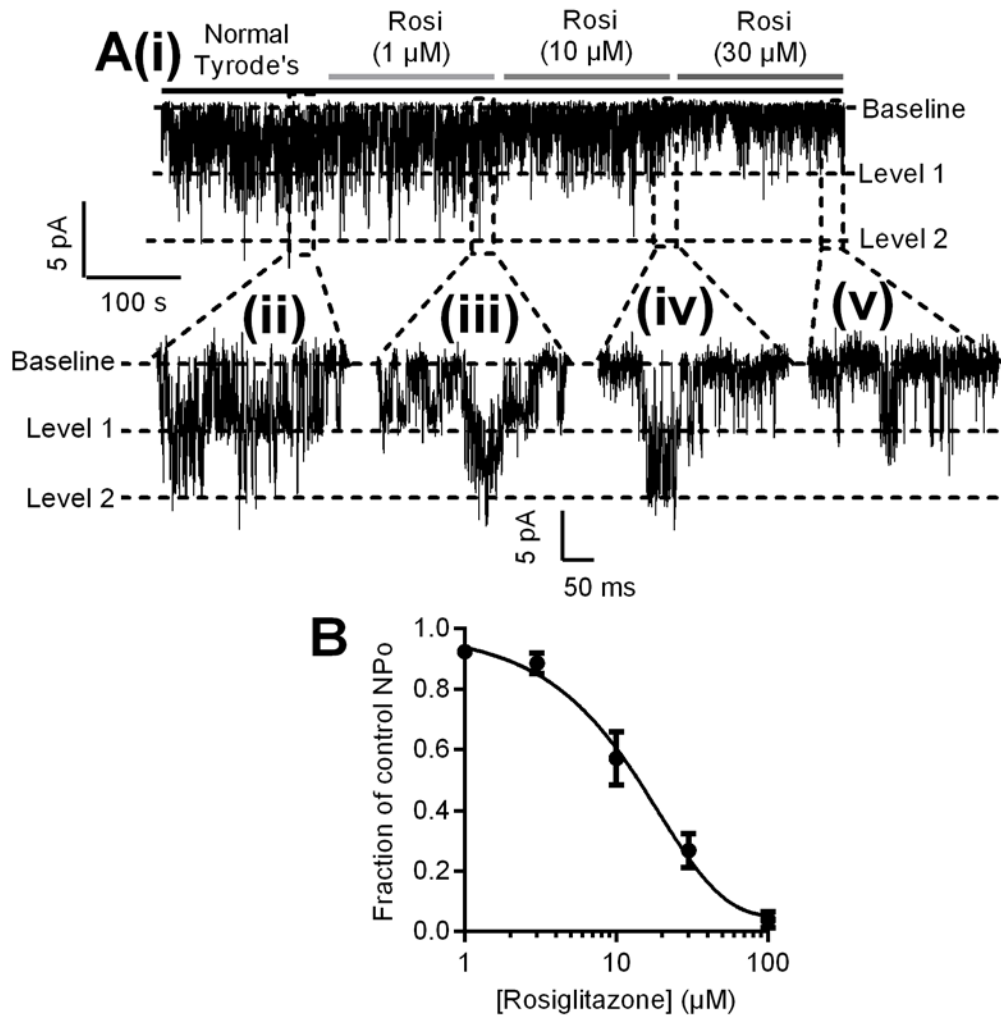
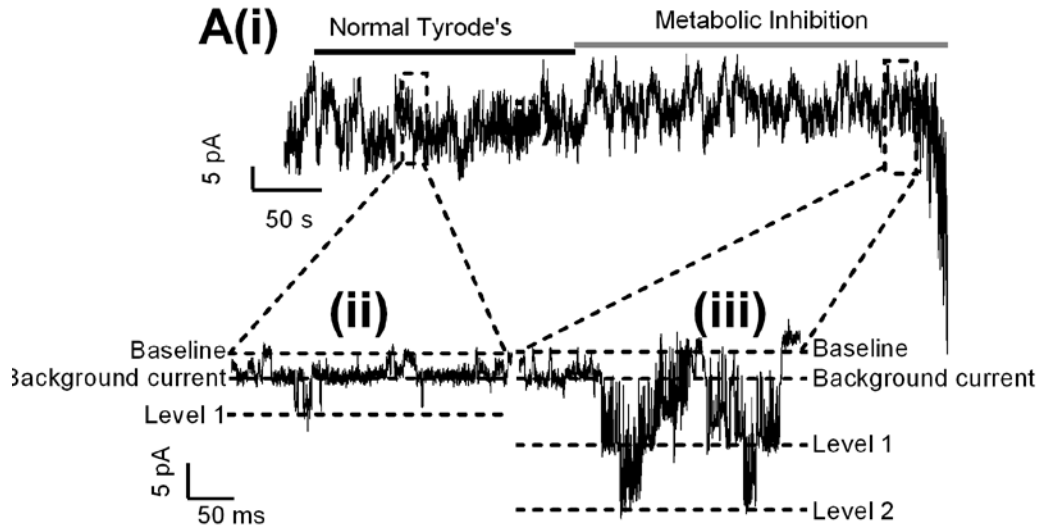


**Figure 3.9: Rosiglitazone suppressed the ~39 pS-conductance currents on cardiac sarcolemmal membrane.** A(i), Example recording of the effects of rosiglitazone on the ~39 pS conductance channel in the cell attached configuration. Channel activity was measured in NT (ii), 1  $\mu\text{M}$  (iii), 10  $\mu\text{M}$  (iv) and 30  $\mu\text{M}$  (v) rosiglitazone. B, Concentration response curve showing the NPo for each concentration expressed as a fraction of the NPo in control solution. By fit in the Hill equation, the  $\text{IC}_{50}$  of rosiglitazone for the small-conductance current was 14.50  $\mu\text{M}$  ( $n > 4$  cells for each data point from 4 animals).

### 3.2.7 Identification of the ~39 pS-conductance channel in cardiomyocytes of other species

It has been shown in this chapter that the ~39 pS-conductance current in Wistar rat cardiomyocytes can be inhibited by a  $K_{ir}6.1$  channel inhibitor and shares a similar conductance and apparent ATP-insensitivity identified in  $K_{ir}6.1$  channels. In addition, using the cell-attached configuration, this ~39 pS-conductance channel was found at both guinea pig and rabbit cardiomyocyte sarcolemmal membrane. Figure 3.10 shows an example recording of cell-attached patch recording from guinea pig cardiomyocytes with additional background currents. The ~39 pS-conductance current was resolved in resting conditions when there was a stable period with limited openings of other ionic currents (Figure 3.10A (ii)). Significant background currents can be seen in guinea pigs recordings, which were suggested to be  $K_{ir}2.1$  channel, as indicated by the channel amplitudes (Figure 3.2). The NPo of ~39 pS channel in guinea pig cardiomyocyte were later measured and analysed in Figure 6.7. Furthermore, metabolic inhibition was able to activate the well characterised cardiac ( $K_{ir}6.2/SUR2A$ )  $K_{ATP}$  channel (Figure 3.10A (iii)). Figure 3.10B (i) also shows this ~39 pS-conductance channel on the rabbit cardiomyocyte sarcolemmal membrane in addition to the metabolically-sensitive  $K_{ir}6.2/SUR2A$  channels (Figure 3.10B (ii)). No mean data was shown on rabbit recordings as only 2 recordings were done for the species.

## Guinea pig:



## Rabbit:

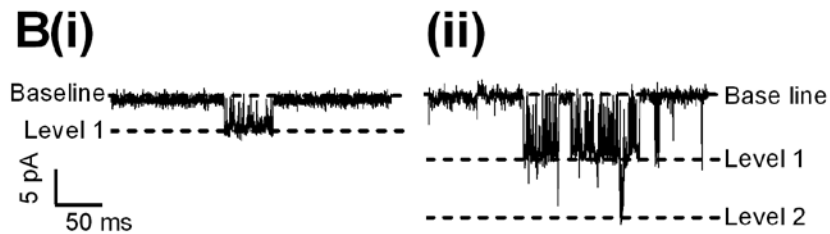


**Figure 3.10: The 39 pS-conductance channel current recorded from other species cardiomyocytes.** A(i), Representative trace recorded from guinea pig acute isolation cardiomyocyte, in cell-attached configuration at the equivalent of  $\sim -110$  mV. Expanded traces showing the  $\sim 39$  pS channel in control conditions (ii) with a background current that possibly  $I_{K1}$  current. (iii), Sample trace showing the sarcolemmal  $K_{ATP}$  channel ( $K_{ir}6.2/SUR2A$ ) current ( $\sim 10$  pA in amplitude) in cell-attached recording activated by metabolic inhibition. B(i), Same as Wistar rat and guinea pig, the  $\sim 39$  pS channel was recorded in control conditions in rabbit cardiomyocyte in cell-attached configuration, as well as the conventional cardiac sarcolemmal  $K_{ATP}$  channel ( $K_{ir}6.2/SUR2A$ ) current (ii).

### **3.2.8 Calcium transients in guinea pig cardiomyocyte can be prolonged by PNU37883A treatment in calcium fluorescence imaging.**

Our results above suggested the  $K_{ir}6.1$ -containing channel also plays an important role in regulating the cardiac APD in guinea pig cardiomyocyte. Given the link between the duration of the AP and the intracellular  $Ca^{2+}$  release, and the similar experiments done in Figure 3.8 in rat cardiomyocyte, the intracellular  $Ca^{2+}$  transients were measured in guinea pig cardiomyocytes (as outlined in Figure 3.8). In this experiment, cardiomyocytes were perfused with NT for 3 mins, followed by 5 mins with 3  $\mu$ M PNU and finally 10  $\mu$ M glibenclamide. 0.5 Hz field stimulation was used to trigger the AP throughout each experiment. The  $Ca^{2+}$  transients were recorded at the end of each treatment for 30 s. Figure 3.11A (i), (ii) and (iii) shows example traces of  $Ca^{2+}$  transients in NT solution, 3  $\mu$ M PNU and 10  $\mu$ M glibenclamide respectively. The 50% and 90% recovery to resting level in  $Ca^{2+}$  transients were measured in the experiments. Figure 3.11C demonstrates the 50% to resting level in  $Ca^{2+}$  transient in all NT (control), PNU and glibenclamide treatments, with 275.1 $\pm$ 11.3 ms (control, n=6), 317.1 $\pm$ 9.9 ms (PNU, n=6, \*\*\*p<0.001) and 306.2 $\pm$ 11.3 ms (Glib, n=6, \*\*\*p<0.001; Repeated measures one-way ANOVA with Holm-Sidak post-test) respectively. Further investigation in 90% to resting level in  $Ca^{2+}$  transient demonstrated the same trend, Figure 3.11D show  $Ca^{2+}$  transient in PNU and glibenclamide was prolonged, with 970.4 $\pm$ 40.0 ms (n=6, \*\*p<0.005) and 903.2 $\pm$ 37.5 ms (n=6, \*\*\*p<0.001) respectively compared to control condition (699.4 $\pm$ 33.3 ms, n=6; Repeated measures one-way ANOVA with Holm-Sidak post-test).

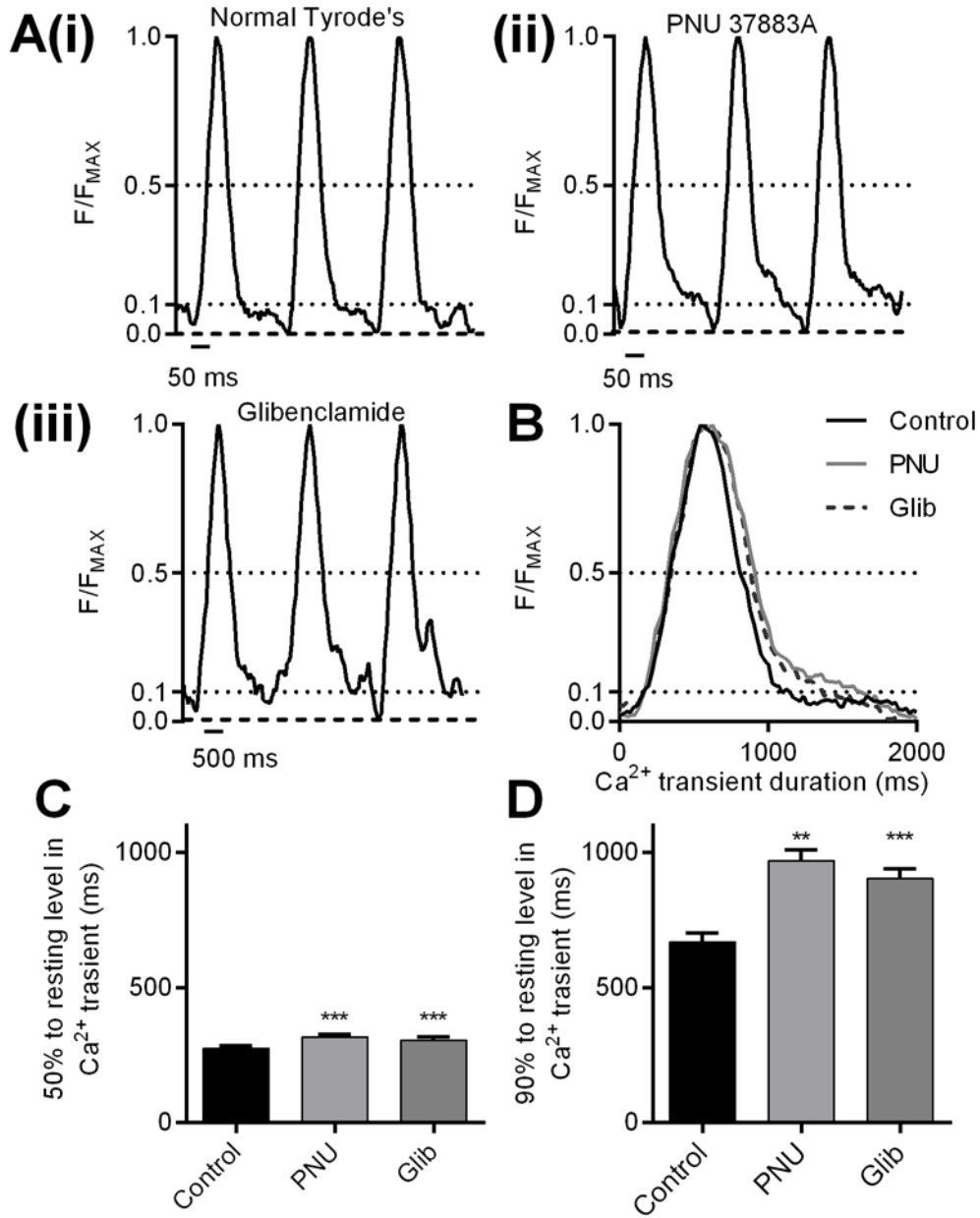


**Figure 3.11: Measuring guinea pig cardiomyocyte  $Ca^{2+}$  transient in action potential duration by single wavelength  $Ca^{2+}$  indicator, Fluo-4.** A(i), (ii) & (iii), Example traces showing the  $Ca^{2+}$  transients triggered by 0.5 Hz field stimulation, in NT, 3  $\mu$ M PNU and 10  $\mu$ M Glib respectively. B, Side-by-side comparison illustrates both PNU and Glib treatment prolonged  $Ca^{2+}$  transient duration compared with control conditions. C, Mean data showed the time from maximum fluorescence intensity to 50% to resting level in  $Ca^{2+}$  transients in each control, PNU and Glib conditions, with  $275.1 \pm 11.3$  s (control,  $n=6$ ),  $317.1 \pm 9.9$  (PNU,  $n=6$ , \*\*\* $p < 0.001$ ) and  $306.2 \pm 11.3$  (Glib,  $n=8$ , \*\*\* $p < 0.001$ ; Repeated measures one-way ANOVA Holm-Sidak post-test) respectively. D, Mean data showed the time from maximum fluorescence intensity to 90% to resting level in  $Ca^{2+}$  transients in each control, PNU and Glib conditions, with  $669.4 \pm 33.3$  s (control,  $n=6$ ),  $970.4 \pm 40.0$  (PNU,  $n=8$ , \*\* $p < 0.005$ ) and  $903.2 \pm 37.5$  (Glib,  $n=8$ , \*\*\* $p < 0.001$ ; Repeated measures one-way ANOVA Holm-Sidak post-test) respectively.

### 3.3 Discussion

In this chapter, data has been presented identifying a putative  $K_{ir}6.1$  subunit-containing channel at the rat, guinea pig and rabbit ventricular myocyte sarcolemmal membrane. Using electrophysiological and pharmacological tools, the features and properties of this channel have been investigated. Firstly, by using patch clamp, the electrophysiological properties have been studied and compared with the known  $K_{ir}6.1$ -containing channel properties documented in the literature. Using the data from the electrophysiological studies, and using specific pharmacological inhibition, the  $K_{ir}6.1$  subunit has been suggested to form the pore of this  $\sim 39$  pS-current in the ventricular myocytes.

In cardiomyocytes,  $K_{ir}6.2/SUR2A$  is widely accepted as the  $SarcoK_{ATP}$ , however loop-mutated  $K_{ir}6.1$  DNA significantly reduces  $K_{ATP}$  currents suggesting not only  $K_{ir}6.2/SUR2A$  but also  $K_{ir}6.1$  and  $SUR2B$  subunits are expressed at the cardiomyocyte surface (van Bever *et al.*, 2004). In addition, a number of studies have identified the protein or mRNA for the  $K_{ir}6.1$  and  $SUR2B$  subunits in cardiomyocytes (Lawrence *et al.*, 2002; Singh *et al.*, 2003; Morrissey *et al.*, 2005b). Furthermore, although up/down-regulation in  $K_{ir}6.1$  subunits usually attributed to a vascular defect (Wang *et al.*, 2003; Kane *et al.*, 2006; Tajada *et al.*, 2012), previous reports illustrate that the heart can also suffer multiple syndromes, such as Prinzmetal angina (Miki *et al.*, 2002b), J-wave syndrome and sudden infant death (Nichols *et al.*, 2013), from lacking or losing function of  $K_{ir}6.1$  subunits. In cardiomyocytes treated with urocotin to induce cardioprotection, both  $K_{ir}6.1$  protein and mRNA was increased (Lawrence *et al.*, 2002). Finally, 24 h following ischemia/reperfusion, the  $K_{ir}6.1$  protein and mRNA also shows a significant increase (Akao *et al.*, 1997), suggesting there is a  $K_{ir}6.1$ -containing channel expressed and that this potentially may have a role in cardioprotection.

It has been shown that  $K_{ir}6.1$  mRNA is expressed in cardiomyocyte (Akao *et al.*, 1997; Erginel-Unaltuna *et al.*, 1998; Lawrence *et al.*, 2002; Elrod *et al.*, 2008), as well as its protein (Singh *et al.*, 2003), although to date very few papers have shown a functional effect of this channel. Additionally, by using immunolocalization, the  $K_{ir}6.1$  subunits was found on cardiac sarcolemmal membrane (Morrissey *et al.*, 2005b). Until now, there is no cell-attached recording evidence directly showing the  $K_{ir}6.1$ -containing complex expressing

on the surface membrane. However, previous literature shows that pore loop-mutated  $K_{ir}6.1$  significantly suppress the maximum  $K_{ATP}$  current which activated by diazoxide and pinacidil in whole-cell recording (van Bever *et al.*, 2004). Moreover, in the border area of infarct, both  $K_{ir}6.1$  and SUR2B subunit mRNA and protein were up-regulated in post-infarct rat cardiomyocytes without a change in  $K_{ir}6.2$  subunits, which suggested the over expression of  $K_{ir}6.1$  subunits may also related to cardiac physiology (Isidoro Tavares *et al.*, 2007).

In this project, a current was identified with a conductance of  $\sim 39$  pS-expressed on the sarcolemmal surface, which we hypothesised was a  $K_{ir}6.1$ -containing channel. The  $K_{ir}6.1$ -containing channel amplitude and conductance were investigated. As metabolic sensors,  $K_{ATP}$  channels open in response to the depletion of ATP and the rise of ADP, which shortens the action potential duration (APD) so sparing intracellular ATP during metabolic inhibition (MI). To achieve the metabolic stress and induce the opening of  $K_{ATP}$  on the sarcolemmal cardiomyocyte membrane, cyanide and iodoacetate acid (CN & IAA) or 2, 4-dinitrophenol (DNP) were used in experiments. However, using the cell-attached configuration in patch clamp recording, the  $K_{ir}6.1$ -containing channel was found to be active even in resting condition, with an opening probability around  $\sim 0.1$ - $0.2$  (NPo). In comparison, the conventional cardiac sarcolemmal  $K_{ATP}$  (Sarco $K_{ATP}$ ,  $K_{ir}6.2$ /SUR2A) only opened in response to metabolic inhibition (Figure 3.1A (i)). This finding suggests that, unlike  $K_{ir}6.2$ /SUR2A channel, the  $K_{ir}6.1$ -containing channel could be relatively ATP insensitive as previously suggested in the literature (Farzaneh & Tinker, 2008; Yamada *et al.*, 2011). Additionally, previous evidence from our lab illustrated that the early opening of the conventional  $K_{ATP}$  channel was not the factor that leads to cardioprotection (Brennan *et al.*, 2015); the newly identified  $K_{ir}6.1$ -containing channel becomes a strong candidate to investigate to understand the apparent role of sulphonylurea drug-sensitivity in cardioprotection. In the data presented here, the  $K_{ir}6.1$ -containing channel is constitutively active in resting conditions, but the  $K_{ir}6.2$ /SUR2A is only activated following MI, so its constitutive activity can be used to distinguish and study the  $K_{ir}6.1$ -containing channels in native cardiomyocytes.

To characterise the newly identified  $K_{ir}6.1$ -containing channel on cardiac sarcolemma, voltage-step measurements were used to calculate the channel conductance of both the putative  $K_{ir}6.1$ -containing channel and  $K_{ir}6.2/SUR2A$  channel. In previous reports, the  $K_{ir}6.x$  subunits have been determined to be the key element defining the unitary channel conductance in  $K_{ATP}$  channel (Bao *et al.*, 2011), with SUR proteins having a modulatory role. Channels containing  $K_{ir}6.1$  have a channel conductance around  $\sim 35$  pS (Repunte *et al.*, 1999; Liss & Roeper, 2001), whilst this is  $\sim 80$  pS in  $K_{ir}6.2$ -containing channels (Isomoto *et al.*, 1996; Repunte *et al.*, 1999). Although there is evidence to suggest that the  $K_{ir}6.1$  and  $K_{ir}6.2$  can co-assemble to form functional ion channels (Kono *et al.*, 2000) in a recombinant system expressed in HEK 293 cells, no evidence suggests this  $K_{ir}6.1$ - $K_{ir}6.2$  heteromultimer expresses as native channel (Seharaseyon *et al.*, 2000b). Furthermore, the  $K_{ir}6.1$ - $K_{ir}6.2$  tandem channel conductance is always intermediate (Kono *et al.*, 2000; Babenko & Bryan, 2001; Cui *et al.*, 2001), which can be used to distinguish in experiments. The  $K_{ir}6.1$ -containing channel had a unitary conductance of  $38.71 \pm 0.92$  pS whilst the  $K_{ir}6.2/SUR2A$  channel had a unitary conductance of  $78.53 \pm 1.60$  pS, with no discernible intermediate conductances. Both calculated conductances are in agreement with literature on  $K_{ir}6.1$  expressed in other tissues and for the conventional cardiac  $K_{ir}6.2$ -containing  $K_{ATP}$  channel (Inagaki *et al.*, 1996; Yamada *et al.*, 1997; Aguilar-Bryan *et al.*, 1998; Repunte *et al.*, 1999; Suzuki *et al.*, 2001; Insuk *et al.*, 2003; Wang *et al.*, 2003; Shi *et al.*, 2007). Additionally, the channel conductance sometimes can be altered due to the change of experimental conditions, however, there was a consistent 2-fold difference when comparing  $K_{ir}6.1$ - and  $K_{ir}6.2$ -containing channels (Takano *et al.*, 1998; Repunte *et al.*, 1999; Kono *et al.*, 2000; Babenko & Bryan, 2001).

Holding the pipette potential at 40 mV, or an equivalent membrane potential of  $\sim -110$  mV, the  $K_{ir}6.1$ -containing channel passed a current of  $\sim 5$  pA in amplitude compared with  $K_{ir}6.2/SUR2A$  of  $\sim 10$  pA. The difference in single channel current amplitude between these two channels is clear therefore allowing them to be readily distinguished (Figure 3.1A (ii) & (iii)). Glibenclamide is a well-characterised sulphonylurea  $K_{ATP}$  channel blocker that does not select between pore-forming subunits, which has an inhibitory binding site on the  $\beta$ -subunits, SURs (Shi *et al.*, 2010). It was reported that the  $IC_{50}$  for  $K_{ir}6.1/SUR2A$  and  $K_{ir}6.2/SUR2A$  are  $\sim 5$  nM and  $\sim 3$  nM respectively (Lodwick *et al.*, 2014). In this study, the

~39 pS-conductance channel currents activity was significantly reduced by 10  $\mu\text{M}$  glibenclamide suggested this ~39 pS-currents is potentially a  $\text{K}_{\text{ATP}}$  current that has not been previously described at the cardiac cell membrane. From previous literature, application of glibenclamide abolished cardioprotection, increased infarct size and prolonged cardiac action potential duration (Tomai *et al.*, 1994; Bernardo *et al.*, 1999; Toyoda *et al.*, 2000; Budas *et al.*, 2004; Stoller *et al.*, 2010). The finding of this small conductance  $\text{K}_{\text{ATP}}$  channel leads to an interesting question of whether this channel plays an important role in normal cardiac cell physiological function or even as an effector of cardioprotection.

It was observed that this newly discovered  $\text{K}_{\text{ATP}}$  channel has a major difference from the conventional  $\text{K}_{\text{ATP}}$  channel; constitutive activity in resting conditions. This feature suggests that the channel is relatively ATP insensitive. The vascular  $\text{K}_{\text{ATP}}$  channel, thought to comprise of mainly  $\text{K}_{\text{ir}}6.1/\text{SUR2B}$  heterooctamers (Yamada *et al.*, 1997; Shi *et al.*, 2010), shows a similar property of constitutive activity (Yamada *et al.*, 1997). In contrast to the  $\text{K}_{\text{ir}}6.2/\text{SUR2A}$  channel, the vascular  $\text{K}_{\text{ATP}}$  channel is open in resting conditions to promote vasorelaxation (Shi *et al.*, 2010) and causes vasoconstriction when it is blocked (Miki *et al.*, 2002b). These properties suggest that this vascular isoform is perhaps less ATP-sensitive than the conventional cardiac isoform. In the reconstituted channel expressed in HEK 293 cells, the  $\text{K}_{\text{ir}}6.1/\text{SUR2B}$  complex was found to be not only insensitive to ATP inhibition but also activated by both ATP and ADP (Yamada *et al.*, 1997; Shi *et al.*, 2007). To identify whether the newly discovered ~39 pS-channel is a  $\text{K}_{\text{ir}}6.1$ -containing channel, a  $\text{K}_{\text{ir}}6.1$  pore blocker was used. PNU has been shown to inhibit  $\text{K}_{\text{ir}}6.1$ -containing channels (Kovalev *et al.*, 2004), with a selectivity for  $\text{K}_{\text{ir}}6.1$  over  $\text{K}_{\text{ir}}6.2$  at low concentrations, however PNU does have an inhibitory effect on  $\text{K}_{\text{ir}}6.2$  at higher concentrations. Data presented here shows that the NPo of  $\text{K}_{\text{ir}}6.1$ -containing channels were significantly inhibited by 3  $\mu\text{M}$  PNU, with an  $\text{IC}_{50}$  of  $1.26 \pm 0.15$ . These results further suggest the ~39 pS-conductance current is a  $\text{K}_{\text{ir}}6.1$ -containing current. In whole-cell recording, PNU-induced block of pinacidil-activated currents had an  $\text{EC}_{50}$  of ~4  $\mu\text{M}$ , close to the value (~5  $\mu\text{M}$ ) which was reported in previous literature (Kovalev *et al.*, 2004). Additionally, current remaining following treatment with glibenclamide was always smaller than the leak current prior to perfusion with pinacidil, suggests there is a basal  $\text{K}_{\text{ATP}}$  current active in resting conditions (Figure 3.5C), consistent with the hypothesis that the  $\text{K}_{\text{ir}}6.1$ -like current is constitutively active.

To further investigate this effect on leak current, PNU was applied to the cell in the absence of pinacidil to assess whether the basal  $K_{ATP}$  current was due to this potentially  $K_{ir}6.1$ -containing channel. This was followed by perfusion with glibenclamide to suppress all  $K_{ATP}$  currents. 3  $\mu$ M PNU significantly reduced the leak currents suggesting  $K_{ir}6.1$  activity in resting conditions similar to findings in cell-attached recording. No further reduction of leak current was seen following 10  $\mu$ M glibenclamide treatment, suggesting that  $K_{ir}6.1$ -containing channels are the only  $K_{ATP}$  currents active at the cardiomyocyte membrane surface at rest.

In a previous paper, application of PNU to the heart caused a decreased heart rate as well as ST-segment and J-point elevation (Hsu *et al.*, 2012), similar to the  $K_{ir}6.1$  missense mutation diseases and knockdown (Miki *et al.*, 2002b; Tester *et al.*, 2011). Moreover, it well documented that the cardiac action potential duration can be significantly shortened by using  $K_{ATP}$  channel openers and reversed by  $K_{ATP}$  channel blockers (McPherson *et al.*, 1993; Grover & Garlid, 2000; Suzuki *et al.*, 2001, 2002; Zhang *et al.*, 2010; Muntean *et al.*, 2014). Finally, the conventional  $K_{ATP}$  channel is indeed activated during metabolic inhibition, made the  $K_{ir}6.2/SUR2A$  currents can be excluded from regulating cardiac physiology in resting conditions (Brennan *et al.*, 2015). Given this potential regulatory role, the relationship between this  $K_{ir}6.1$ -containing current and action potential duration was investigated. In whole-cell recording configuration, 3  $\mu$ M PNU caused a prolongation of rat ventricular myocyte  $APD_{90}$ , with no further prolongation with 10  $\mu$ M glibenclamide treatment. The membrane potential was depolarized following PNU treatment, however there was no further depolarisation following glibenclamide treatment. The data presented suggests that the native cardiac basal  $K_{ATP}$  currents can be blocked, the  $APD_{90}$  prolonged and the membrane potential depolarised by 3  $\mu$ M PNU. In each case glibenclamide had shown no further effect. Linking the data from cell-attached recording together, the  $K_{ir}6.1$  containing channel is active in resting conditions and blocked by 3  $\mu$ M PNU. The data presented here suggest the hypothesis that  $K_{ir}6.1$  containing channels that the  $K_{ir}6.1$ -containing channel plays an important role in cardiomyocytes resting conditions by regulating APD and membrane potential.

It was documented that the cardiac sarcolemmal  $K_{ATP}$  channel has the ability to mediate the  $Ca^{2+}$  transients via modulation of the action potential duration. During hypoxia, the activation of Sarco $K_{ATP}$  leads to cardiac action potential shortening, a decline of  $Ca^{2+}$  influx via  $Ca^{2+}$  channels and NCX (Suzuki *et al.*, 2001). Here, the intracellular  $Ca^{2+}$  transients during each APD, in NT, 3  $\mu$ M PNU treatments and 10  $\mu$ M glibenclamide treatments were measured. In both 50% and 90% recovered to resting level in  $Ca^{2+}$  transient, PNU treatments significant prolonged the  $Ca^{2+}$  transient but no further prolongation effect in the follow treatment with glibenclamide. The similar trend to action potential duration suggests that the  $K_{ir}6.1$ -containing channel regulates the  $Ca^{2+}$  transient via action potential duration. This finding is important in cardiac  $K_{ATP}$  research, as it has been widely reported that the sarcolemmal  $K_{ATP}$  channel is closed under resting conditions, however opened in response of MI or preconditioning (Woodcock *et al.*, 2009; Zhang *et al.*, 2010). Interestingly, 10  $\mu$ M pinacidil has been shown to cause a shortening of the action potential duration as well as preserve intracellular ATP (McPherson *et al.*, 1993; Grover & Garlid, 2000), although this concentration of pinacidil is insufficient to activate the  $K_{ir}6.2/SUR2A$  channel (Lodwick *et al.*, 2014) but enough for activate the vasculature  $K_{ATP}$  channel (Suzuki *et al.*, 2001). Given these findings, it is possible that the newly identified  $K_{ir}6.1$ -containing channel not only plays an important role in regulating the cardiac APD in resting conditions but also could be involved in cardioprotection.

In addition to PNU37883A, rosiglitazone, a  $PPAR\gamma$  activator which was used to treat type-2 diabetes, has been shown to have an inhibitory effect on  $K_{ir}6.1$  (Yu *et al.*, 2012; Muntean *et al.*, 2014). Recent studies have shown that rosiglitazone can block  $K_{ir}6.1/SUR2B$  currents (Yu *et al.*, 2012; Wang *et al.*, 2013). Rosiglitazone has, however, been withdrawn from the European market due to potential risk of myocardial infarction (Kaul *et al.*, 2010) and cardiac fibrillation (Lu *et al.*, 2008). Data presented in this report, using cell-attached patch recording, shows that rosiglitazone suppressed cardiac native  $K_{ir}6.1$ -containing channels on the sarcolemmal membrane (Figure 3.9A). Additional, by fitting the percentage inhibition of  $K_{ir}6.1$  channel NPo using the Hill equation, gave an  $IC_{50}$  of 14.5  $\mu$ M, close to previous reports (Yu *et al.*, 2011, 2012; Wang *et al.*, 2013). Findings presented here may suggest that inhibition of this channel by rosiglitazone may underlie the increased the risk of cardiac infarction and fibrillation due to changes in action potential

duration and  $\text{Ca}^{2+}$  handling. It is hypothesised that the inhibition of native cardiac  $\text{K}_{\text{ir}}6.1$ -containing channels causes a prolongation of the APD and depolarisation of the membrane potential, so leading to  $[\text{Ca}^{2+}]_{\text{i}}$  overload. This hypothesis also fits previous reports (Kavak *et al.*, 2008) suggesting that rosiglitazone can significantly prolonged APD in rat cardiomyocyte as well as cause depolarisation of the membrane potential.

In conclusion, an ion channel that is hypothesised to contain  $\text{K}_{\text{ir}}6.1$  has been identified on cardiac sarcolemmal membrane surface, with a conductance of  $\sim 39$  pS. This potential cardiac  $\text{K}_{\text{ir}}6.1$  containing channel can be blocked by the selective  $\text{K}_{\text{ir}}6.1$  pore blocker PNU, with a similar  $\text{IC}_{50}$  to previous literature using transfected HEK 293 cells or *xenopus* oocyte expression systems. Data presented here suggests that this channel is active even in normal resting conditions with physiological ATP. Using pharmacological inhibitors, the  $\text{K}_{\text{ir}}6.1$  containing channel appears to be the only  $\text{K}_{\text{ATP}}$  channel active at the membrane surface in resting conditions. These findings were confirmed with an additional  $\text{K}_{\text{ir}}6.1$  blocker, rosiglitazone, which inhibited the putative  $\text{K}_{\text{ir}}6.1$ -containing sarcolemmal  $\text{K}_{\text{ATP}}$  current with a similar  $\text{IC}_{50}$  to the  $\text{K}_{\text{ir}}6.1/\text{SUR2B}$  channel reported in the literature. This newly identified native  $\text{K}_{\text{ir}}6.1$  containing currents appears to play a crucial role in regulating APD and membrane potential, supported by other reports using rosiglitazone. Finally, activity of a  $\text{K}_{\text{ir}}6.1$ -like sarcolemmal  $\text{K}_{\text{ATP}}$  channel was not limited to rat cardiomyocytes, but also found in guinea pig and rabbit cardiomyocytes, which's action potential electrically identical to human. The additional evidence from the  $\text{K}_{\text{ir}}6.1$  pharmacological inhibition and  $\text{K}_{\text{ir}}6.1$  specific knockdown prolonged the action potential duration and  $\text{Ca}^{2+}$  transient in guinea pig cardiomyocyte indicates that the  $\text{K}_{\text{ir}}6.1$ -containing channel modulating cardiac resting physiology in not an exception case in rat. These data also suggest that  $\text{K}_{\text{ir}}6.1$  may be expressed in ventricular myocytes in many species and plays an important, and to date poorly characterised role, in the regulation of cardiac function.

## **Chapter 4**

**Identification of the molecular nature of the ~39  
pS-current expressed at the cardiomyocyte  
membrane using shRNA**

## 4.1 Introduction

In the previous results chapter, a sarcolemmal  $K^+$  current with a conductance of  $\sim 39$  pS was identified using cell-attached patch recording. Using pharmacological tools and its electrophysiological properties, it was hypothesised that this was a  $K_{ATP}$  current with a  $K_{ir}6.1$  pore-forming subunit. It is well documented that  $K_{ir}6.1$  channel subunits are expressed in vascular smooth muscle cells (Wang *et al.*, 2003; Yamada *et al.*, 2011), however increasing evidence also shows  $K_{ir}6.1$  subunits are expressed in cardiomyocytes (Singh *et al.*, 2003; van Bever *et al.*, 2004; Pu *et al.*, 2008). Moreover, there is increasing evidence showing that  $K_{ir}6.1$  pore-forming subunits play an important role in normal cardiac physiology, where mutations or knockout can lead to sudden infant death syndrome, J-wave syndrome and angina (Miki *et al.*, 2002*b*; Tester *et al.*, 2011; Nichols *et al.*, 2013). Despite this, the distribution of  $K_{ir}6.1$  subunits in cardiomyocyte remains unclear. Although some evidence indirectly suggests  $K_{ir}6.1$  subunits form functional channels in myocardial mitochondria (mito $K_{ATP}$ ), such as measurement of mitochondrial oxidation (Liu *et al.*, 1998; Sato *et al.*, 1998), no evidence directly shows the  $K_{ir}6.1$  currents on mitochondrial membrane surface. Additionally, when measuring mitochondrial oxidation, there was no difference in redox state between  $K_{ir}6.1$  wild-type and  $K_{ir}6.1$  dominant-negative, suggesting the  $K^+$  channel in mitochondrial is unlikely a  $K_{ir}6.1$ -containing structure (Seharaseyon *et al.*, 2000*a*).

$K_{ir}6$  subunits cannot express at the cell surface without the  $\beta$ -subunit (Zerangue *et al.*, 1999), however the identity of this accessory subunit is currently unknown. Previous recordings in this study using the cell-attached configuration demonstrate that this sarcolemmal  $K_{ir}6.1$ -containing channel is open even in normal physiological conditions, different from the “conventional” cardiac sarcolemmal  $K_{ir}6.2/SUR2A$   $K_{ATP}$  channel, suggesting that it is relatively ATP-insensitive. In addition, the channel conductance fits with previous reports regarding the channel conductance of the vasculature  $K_{ATP}$  channel,  $K_{ir}6.1/SUR2B$  (Wang *et al.*, 2003; Yamada *et al.*, 2011). The sulphonylurea receptor subtype most often associated with vascular smooth muscle, SUR2B, has also been found to be expressed in cardiomyocytes (Singh *et al.*, 2003; Morrissey *et al.*, 2005*a*; Jovanović *et al.*, 2016). The SUR isoform expressed with the  $K_{ir}6.1$  tetramer is of importance as the

accessory subunit confers ADP and sulphonylurea drug sensitivity to the channel in addition to enhancing ATP-sensitivity. To understand the cellular, and pharmacological, control of this ionic current it is important to understand the channels molecular identity.

In this study, and given the relatively poor selectivity of most pharmacological agents against the different  $K_{ATP}$  subunits, an RNAi approach was used to confirm the identity of the pore.  $K_{ir}6.1$  specific shRNA sequences were used to demonstrate that the newly identified channel contained this pore-forming subunit. In addition, an RNAi approach was used to knockdown the SUR2 splice variants individually and assess the function of the  $K_{ir}6.1$  using electrophysiology. Cardiomyocytes are extremely difficult to transfect using lipid-based transfection reagents and so an adenoviral approach was used.

## 4.2 Results

### 4.2.1 The $K_{ir}6.1$ -like channel remains functional in cardiomyocytes following 24 h culture

Prior to using the shRNA-adenoviral constructs, a series of control experiments were carried out to ensure that, the ~39 pS-conductance channel activity remained following 24 h in culture. Control recordings of the ~39 pS-conductance channels NPo were also carried out with all subsequent recordings to determine the level of knockdown with each shRNA tested.

Figure 4.1A shows an example trace of the ~39 pS-conductance channel activity from a cardiomyocyte cultured for 24 h using cell-attached recording. The ~39 pS-conductance channel continues to be functionally expressed at the cardiomyocyte sarcolemmal surface. Similar to the freshly isolated myocyte, the  $K_{ir}6.2$ -containing  $K_{ATP}$  channels opened in response to ATP depletion during metabolic inhibition (cyanide & IAA, see chapter 2). In Figure 4.1B, the measured channel opening probability in 24 h cultured group is significantly higher compared to freshly isolated, from  $0.19 \pm 0.03$  (n=12) to  $0.64 \pm 0.16$  (n=16, \*p<0.05, Student unpaired t-test), compared to the freshly isolated cardiomyocyte. Figure 4.1C&D shows the amplitude histograms for both the ~39 pS-conductance and  $K_{ir}6.2$ -containing channels, with both channels having similar single channel currents

compare with freshly isolated cells, ( $\sim 5$  pA and  $\sim 10$  pA for  $\sim 39$  pS and  $K_{ir}6.2$ -containing channels respectively).

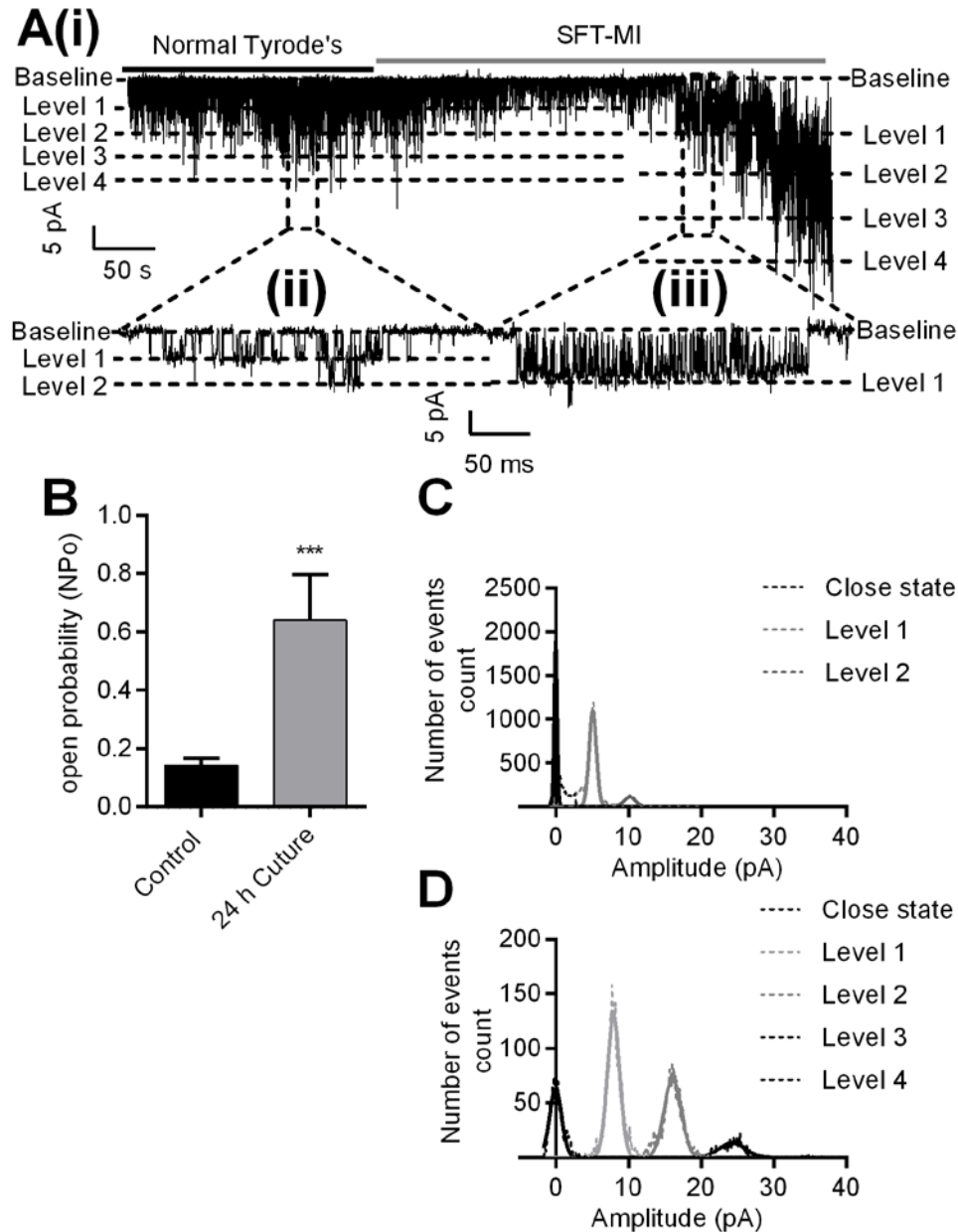


**Figure 4.1: Both small-conductance ( $K_{ir}6.1$ -like) and known sarcolemmal  $K_{ATP}$  channel ( $K_{ir}6.2$ ) are expressed in cardiomyocytes after 24 h in culture.** A(i), Sample trace using cell-attached patch recording following 24 h in culture at an equivalent membrane potential  $\sim 110$  mV as described previously. (ii), expanded trace showing the  $\sim 39$  pS-conductance channel open on the surface membrane after 24 h incubation, with an increasing channel activity ( $0.64 \pm 0.16$ ,  $n=16$ , B), compare with freshly isolated myocytes ( $0.19 \pm 0.03$ ,  $n=12$ ,  $*p < 0.05$ , Student unpaired t-test, B). (iii), expanded trace showing Sarc $K_{ATP}$ - $K_{ir}6.2$  channel current in metabolic inhibition (SFT-MI). Amplitude histograms show the number of events at each amplitude for  $K_{ir}6.1$ -like channel (C) and Sarc $K_{ATP}$ - $K_{ir}6.2$  (D).

In addition, in each cell-attached patch recordings that involved metabolic inhibition, a noticeable reduction was seen in  $K_{ir}6.1$  channel activity during the metabolic inhibition (Figure 3.1, Figure 4.1, Figure 4.2, Figure 4.3, Figure 4.4, Figure 4.7, Figure 4.8, Figure 6.2, Figure 6.3, Figure 6.6, Figure 6.9 and Figure 6.10). This phenomenon may possibly be due to the decreasing intracellular ATP level, which was described by Yamada *et al* (1997) that unlike the  $K_{ir}6.2$   $K_{ATP}$  channel, the  $K_{ir}6.1/SUR2B$  channel is ATP-insensitive and actually required ATP to maintain its activity. Satoh *et al* (1998) showed that 1 mM ATP in  $Mg^{2+}$ -free solution was sufficient to cause a noticeable increase in activity (NPo), from 0.95 to 6.02. In addition,  $K_{ir}6.1/SUR2B$  has a unique bell shape concentration-response curve, with ATP activating the channel in low concentrations and turning into an inhibitory effect in high concentrations (Yamada *et al.*, 1997; Satoh *et al.*, 1998). The  $EC_{50}/IC_{50}$  for the major  $K_{ATP}$  channel activity that is mediated by ATP and ADP is listed in table 1.3.

#### **4.2.2 The open probability of the ~39 pS-conductance channel was reduced following adenoviral infection with a $K_{ir}6.1$ -specific targeting shRNA**

To investigate whether the ~39 pS-current is indeed Kir6.1, two different specific  $K_{ir}6.1$  targeting shRNA,  $K_{ir}6.1A$  and  $K_{ir}6.1B$ , were adenovirally infected into cardiomyocytes. The targeted sequences for  $K_{ir}6.1A$  and for  $K_{ir}6.1B$  are shown in Table 2.9. shRNA  $K_{ir}6.1A$  and  $K_{ir}6.1B$  were prepared by Dr David Lodwick in an adenoviral package to overcome the difficulties of using conventional transfection in primary cells. The data presented in this study show both viruses reduced the activity of the  $K_{ir}6.1$ -like channel without altering the current amplitude. Each shRNA contained a mCherry fluorescence reporter gene, so that the infected cells fluoresce with 520 nm illumination (Figure 4.2B), and was used to identify infected cells for experimentation. Following infection with the  $K_{ir}6.1-A$  shRNA for 24 h, both ~39 pS-conductance channel and  $K_{ir}6.2$  channels could be resolved (Figure 4.2A (ii) & (iii)), however the ~39 pS-conductance channel activity on sarcolemma surface was significant reduced compared with cultured control cells ( $0.74 \pm 0.07$ ,  $n=8$ ) in control vs  $K_{ir}6.1-A$  infection ( $0.02 \pm 0.01$ ,  $n=13$ , \*\*\*  $p < 0.001$ ; Student unpaired t-test).

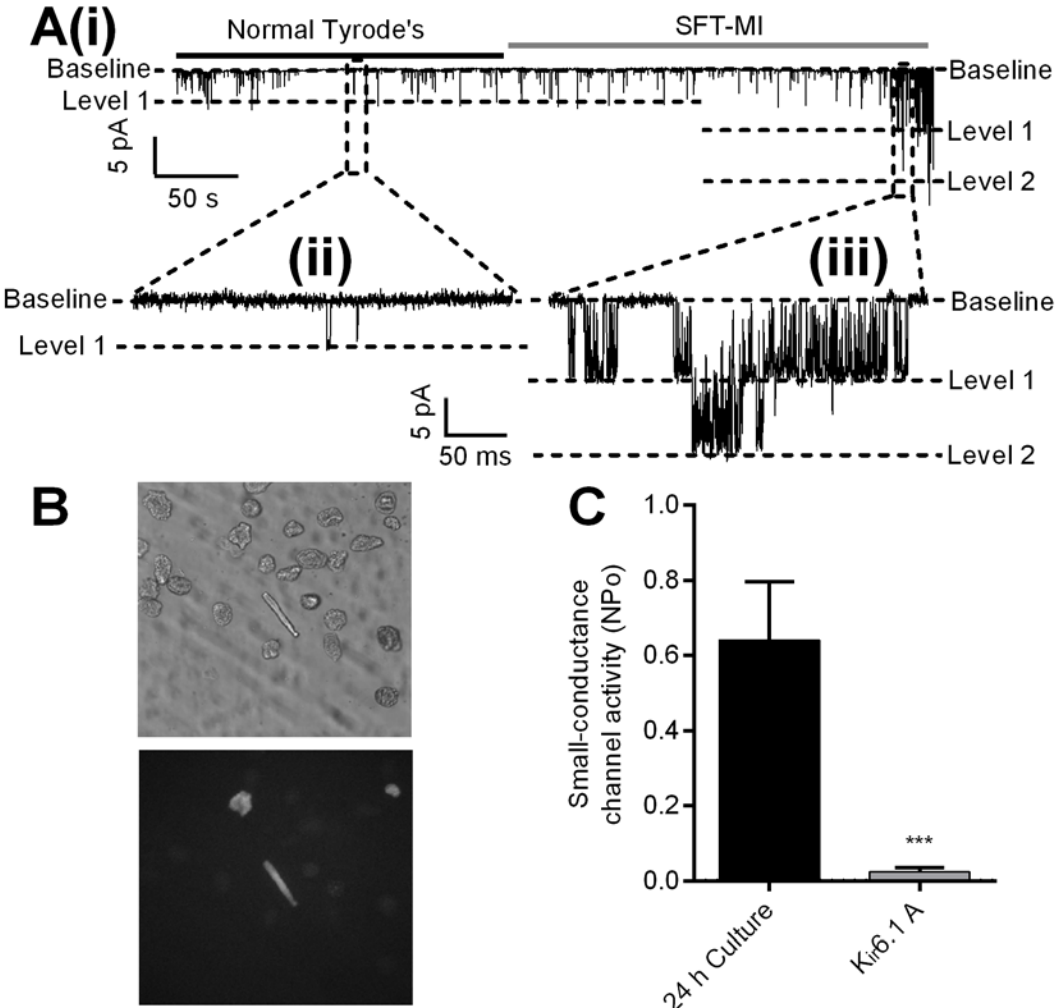


**Figure 4.2: K<sub>ir</sub>6.1 specific targeting shRNA (K<sub>ir</sub>6.1A) reduces the small-conductance channel activity following 24 h adenoviral infection.** A(i), Recording was acquired from cell-attached patches, as described previously. SFT-MI was used to activate K<sub>ir</sub>6.2 currents. Expanded traces show the small conductance, K<sub>ir</sub>6.1-like, channel activity (~5 pA) (ii) and the activity of SarcoK<sub>ATP</sub>-K<sub>ir</sub>6.2 following metabolic inhibition (~10 pA) (iii). Infected cardiomyocytes were identified by their mCherry fluorescence when illuminated with 520 nm light. C, Histogram showing the small-conductance channel activity (NPo) following 24 hour culture in control (0.64 ± 0.16 (n=16)) and in shRNA (K<sub>ir</sub>6.1A) infected (0.02 ± 0.01 (n=13)) cardiomyocytes. (\*\*\*) p < 0.001; Student unpaired t-test).



shRNA infection (Figure 4.2C), the ~39 pS-conductance channel NPo was reduced from 24 h control at  $0.74 \pm 0.07$  (n=8) to  $0.03 \pm 0.01$  (n=6, \*\*\*p<0.001; Student unpaired t-test), with no change in current amplitude (Figure 4.4A).

In these experiments, there was a significant reduction in the ~39 pS-conductance activity at the cardiomyocyte sarcolemmal surface. These data, together with the pharmacological and electrophysiological data, suggest that the pore forming subunit is  $K_{ir}6.1$ . The reduction of this  $K_{ir}6.1$  channels activity occurred rapidly, changing from an NPo of 0.74 to 0.03 in just 24 h time. These findings suggest that the turnover rate of this channel in the membrane is rapid.

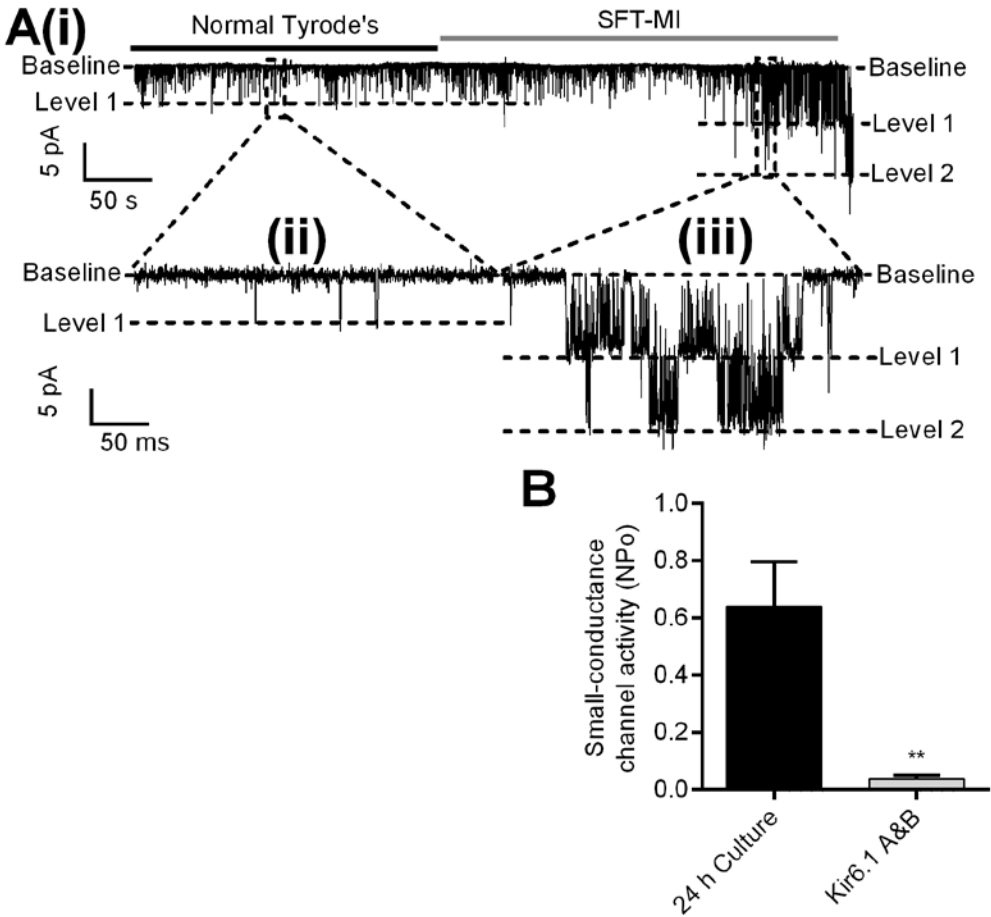


**Figure 4.4:  $K_{ir}6.1$  specific targeting shRNA  $K_{ir}6.1$  A&B reduced the small-conductance channel activity.** A(i) & (ii), Expanded traces shown down regulation of the small-conductance channel activity in resting condition.  $K_{ir}6.2$  channel currents activated in metabolic inhibition of ~10 pA. B, Expanded traces showing the ~39 pS-conductance channel activity (NPo) with both  $K_{ir}6.1$ -A & B shRNA, ( $0.64 \pm 0.16$  (n=16) to  $K_{ir}6.1$ -A&B infection ( $0.03 \pm 0.01$  (n=6)) (\*\*\*) p<0.001; Student unpaired t-test).

A further experiment was carried out to investigate whether adenoviral infection itself can alter the  $\sim 39$  pS-conductance open probability on cardiac sarcolemmal. Figure 4.5A (i) & (ii) demonstrated that there is no statistically significant change following infection of cardiomyocytes with a negative control, non-targeting, virus ( $0.18 \pm 0.04$ ,  $n=6$ ), compared with 24 h cultured group ( $0.64 \pm 0.16$ ,  $n=16$ ). Additionally, a  $K_{ir}6.2$  targeting virus (Storey *et al.*, 2013) also did not alter the  $\sim 39$  pS-conductance channel open probability, with  $0.45 \pm 2.0$  ( $n=6$ ; one-way ANOVA with Holm-Sidak post-test). A noticeable relatively large standard error, indicating a high level of data variability was shown on the 24 h culture group, which will be discussed in section 4.3. These data together suggest that both adenovirus infection and  $K_{ir}6.2$  knockdown virus infection did not alter the  $\sim 39$  pS-conductance channel properties. Taken together, there is a significant decrease in channel activity 24 h following shRNA  $K_{ir}6.1A/B$  adenoviral infection when compared to cultured control, or negative-control cardiomyocytes.

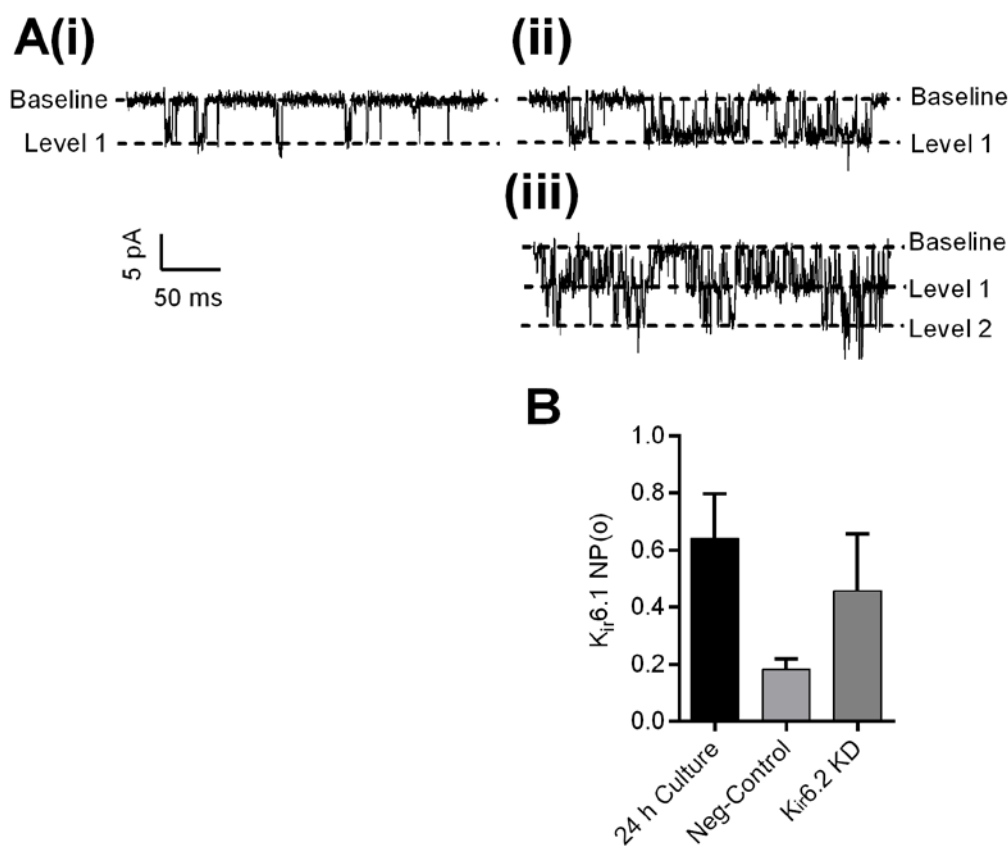
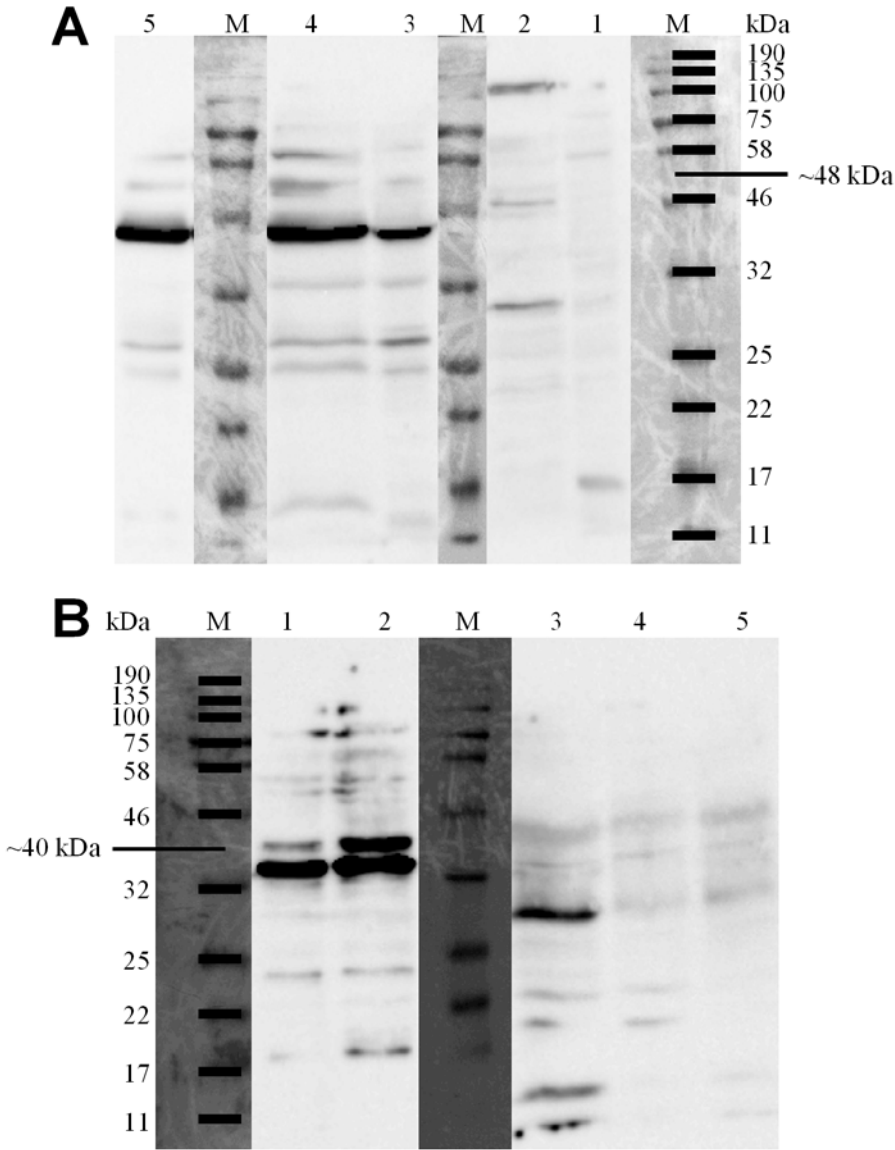


**Figure 4.5:  $K_{ir}6.1$  current is unaltered in both negative control virus and  $K_{ir}6.2$  knockdown, compared with 24 h culture cardiomyocyte.** A(i), (ii) & (iii), Example traces of  $K_{ir}6.1/SU2B$  channel activity in all 24 h culture, negative control and  $K_{ir}6.2$  gene knockdown cardiomyocytes. B, Mean data illustrating both negative control and  $K_{ir}6.2$  knockdown did not affect Sarco $K_{ir}6.1/SUR2B$  channel activity, with NP<sub>o</sub> values of  $0.18 \pm 0.04$  (ns,  $p=0.2032$ ,  $n=7$ ) and  $0.45 \pm 0.20$  (ns,  $p=0.5924$ ,  $n=6$ ; one-way ANOVA with Holm-Sidak post-test) respectively, compared with 24 h cultured group ( $0.64 \pm 0.16$ ,  $n=16$ ) 22

#### 4.2.3 Western blot analysis in fresh isolated, 24 h cultured and $K_{ir}6.1$ knockdown cardiomyocyte.

Using western blotting, the  $K_{ir}6.1$  and  $K_{ir}6.2$  subunits were detected in all freshly isolated, 24 h cultured and  $K_{ir}6.1$  knockdown cardiomyocytes. In Figure 4.6A and B, all lanes were loaded with 10  $\mu$ g protein. Lane 1 and lane 2 were loaded with non-transfected HEK 293 cells protein and HEK 293 transfected with  $K_{ir}6.1/SUR2B$  respectively showing a positive band around 48 kDa in lane 2, confirming data from a previous publication using the same antisera (Singh *et al.*, 2003). Lane 3, 4 and 5 were loaded with freshly isolated, 24 h cultured and  $K_{ir}6.1$  knockdown cardiomyocyte lysates respectively, which also shown bands around 48 kDa. Compared with freshly isolated cardiomyocyte (Figure 4.6A, lane 3), the band intensity shows an increase in 24 h cultured cardiomyocyte (Figure 4.6A, lane 4,) but a noticeable decrease in the  $K_{ir}6.1$  knockdown group (Figure 4.6A, lane 5). In Figure 4.6B, an anti- $K_{ir}6.2$  antibody was used to detect the  $K_{ir}6.2$  subunit. In lane 2 (HEK 293 transfection with  $K_{ir}6.2/SUR2A$ ), there is a positive band in the position near 40 kDa, compared with the non-transfection HEK 293 cells (lane 1). Lane 3, 4 and 5 were loaded with fresh isolated, 24 h cultured and  $K_{ir}6.1$  knockdown cardiomyocyte respectively, all 3 lanes show bands in the same position near 40 kDa with a similar intensity. Taken together, data suggests that the  $K_{ir}6.1$  knockdown did not alter the expression in  $K_{ir}6.2$  in cardiomyocyte. Furthermore, the decreasing intensity band in  $K_{ir}6.1$  KD cardiomyocyte in Figure 4.6A with comparable with the electrophysiology data demonstrating a functional  $K_{ir}6.1$  knockdown following shRNA infection. Unfortunately, the lack of high quality specific antibodies for both  $K_{ir}6.1$  and  $K_{ir}6.2$  make the blotting less convincing in terms of the knockdown effect. It can be seen that multiple bands appeared in non-HEK samples. Unlike HEK cells, cardiomyocyte are more complex and contain more varied proteins in the sample. The weak selective antibodies cannot efficiently work on these samples, even though they may work well on recombinant channels in HEK cells. In addition, although the functional data from patch clamp support the channel knockdown the absence of a control protein in this figure significantly reduces the strength of the knockdown validation.



Lane 1	Lane 2	Lane 3	Lane 4	Lane 5
HEK 293 non-transfection	HEK 293 transfected with Kir <sub>ir</sub> 6.1/SUR2B	Fresh isolated	24 h Culture	Kir <sub>ir</sub> 6.1 KD

**Figure 4.6: Analysis of Kir<sub>ir</sub>6.1 protein expression in freshly isolated, 24 h cultured and Kir<sub>ir</sub>6.1 KD cardiomyocyte by western blot.** Protein was extracted from enzymatically isolated cardiomyocyte and HEK 293 cells. A, An anti-Kir<sub>ir</sub>6.1 antisera was used in characterize Kir<sub>ir</sub>6.1 protein in western blot, a positive band shown near 48 kDa in lane 2. Lane 3, 4 and 5. Each lane was loaded 10 µg protein. B, An anti-Kir<sub>ir</sub>6.2 antibody (Alomone lab) was used in characterize Kir<sub>ir</sub>6.2 protein in western blot, a positive band shown near 40 kDa in lane 2. Lane 3, 4 and 5. Each lane was loaded with 10 µg protein.

#### 4.2.4 The open probability of the $K_{ir}6.1$ channel was reduced following adenoviral infection with a specific SUR2B, but not SUR2A, targeting shRNA

Both  $K_{ir}6.1$ - and  $K_{ir}6.2$ -containing channels remain functionally expressed in cardiomyocytes following 24 h culture (Figure 4.1). To investigate which SUR subunits co-express with  $K_{ir}6.1$  as functional channel on sarcolemmal surface, 2 different SUR specific targeting shRNA, SUR2A and SUR2B, were adenovirally infected into cardiomyocyte. In SUR2 family, there are two major splice variants, SUR2A and SUR2B, which comprised of 71% identical amino acids, only differing in their C-terminal 42 amino acids between each other due to the alternate use of exon 38 (Inagaki *et al.*, 1996; Isomoto *et al.*, 1996; Matsuo *et al.*, 2000). The SUR2A and SUR2B shRNA-adenoviral constructs were designed by Dr David Lodwick, the targeted sequences for SUR2A and for SUR2B are shown in Table 2.9. Each shRNA contained a mCherry fluorescence reporter gene so that infected cells emit fluorescence with 520 nm illumination.

Adenoviral infection with SUR2B specific targeting shRNA significantly reduced the  $K_{ir}6.1$  channel activity (Figure 4.7A), from  $0.64 \pm 0.16$  ( $n=16$ ) in 24 h culture control myocyte to  $0.08 \pm 0.03$  ( $n=9$ ,  $***p < 0.001$ ; Student unpaired t-test) in SUR2B infection myocyte (Figure 4.7B). The  $K_{ir}6.2$  channel was activated during metabolic inhibition (Figure 4.7A (iii)).

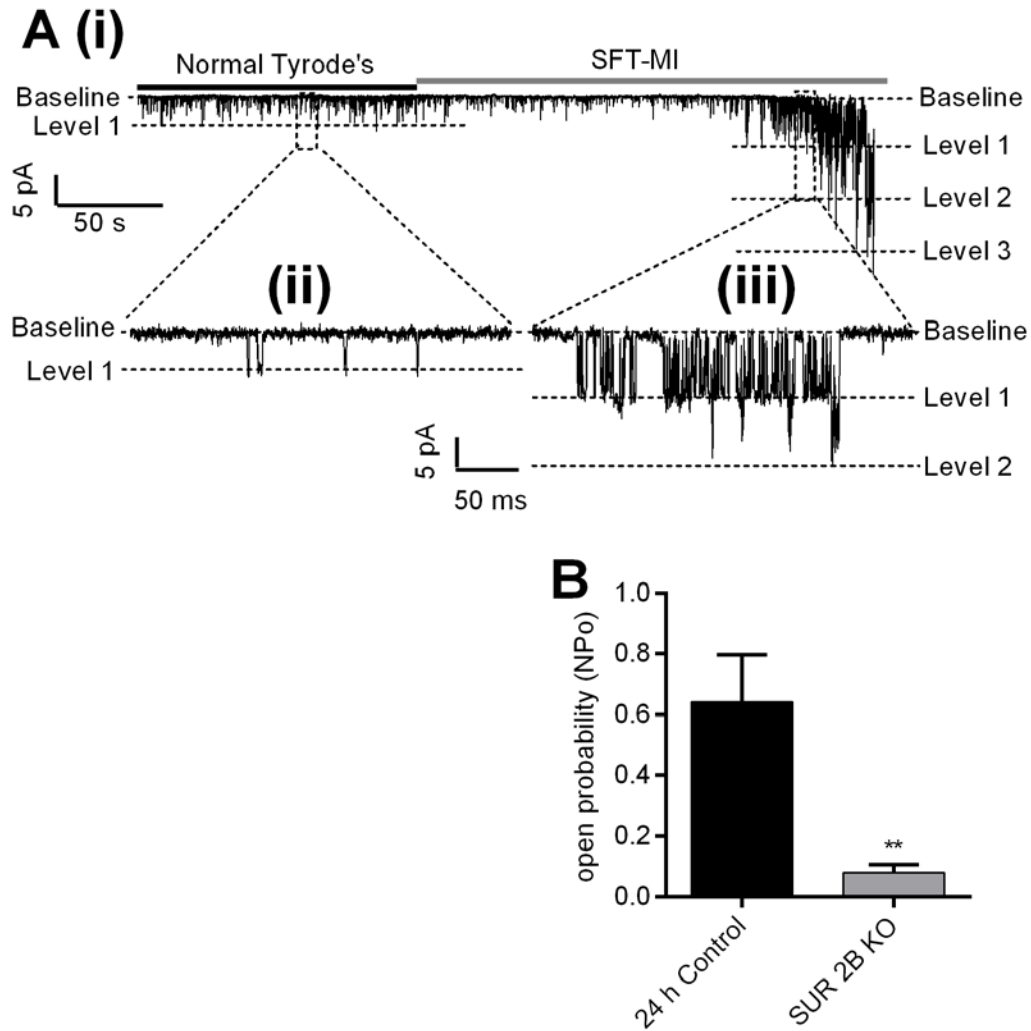


**Figure 4.7: SUR2B specific targeting shRNA reduced the  $K_{ir}6.1$ -containing channel activity following 24 h adenoviral infection.** A(i), Recording was acquired from cell-attached patches, with SFT-MI used to activate  $K_{ir}6.2$  currents. Expanded traces show the activity of the  $K_{ir}6.1$ -containing channel (ii) and Sarco $K_{ATP}$ - $K_{ir}6.2$  activates at  $\sim 5$  and  $\sim 10$  pA respectively. B, Histogram showing the  $K_{ir}6.1$ -containing channel activity (NPo) in 24 h culture control ( $0.64 \pm 0.16$ ,  $n=16$ ) and 24 h shRNA (SUR2B) infected ( $0.08 \pm 0.03$ ,  $n=9$ ) cardiomyocytes (\*\* $p < 0.005$ ; Student unpaired t-test).

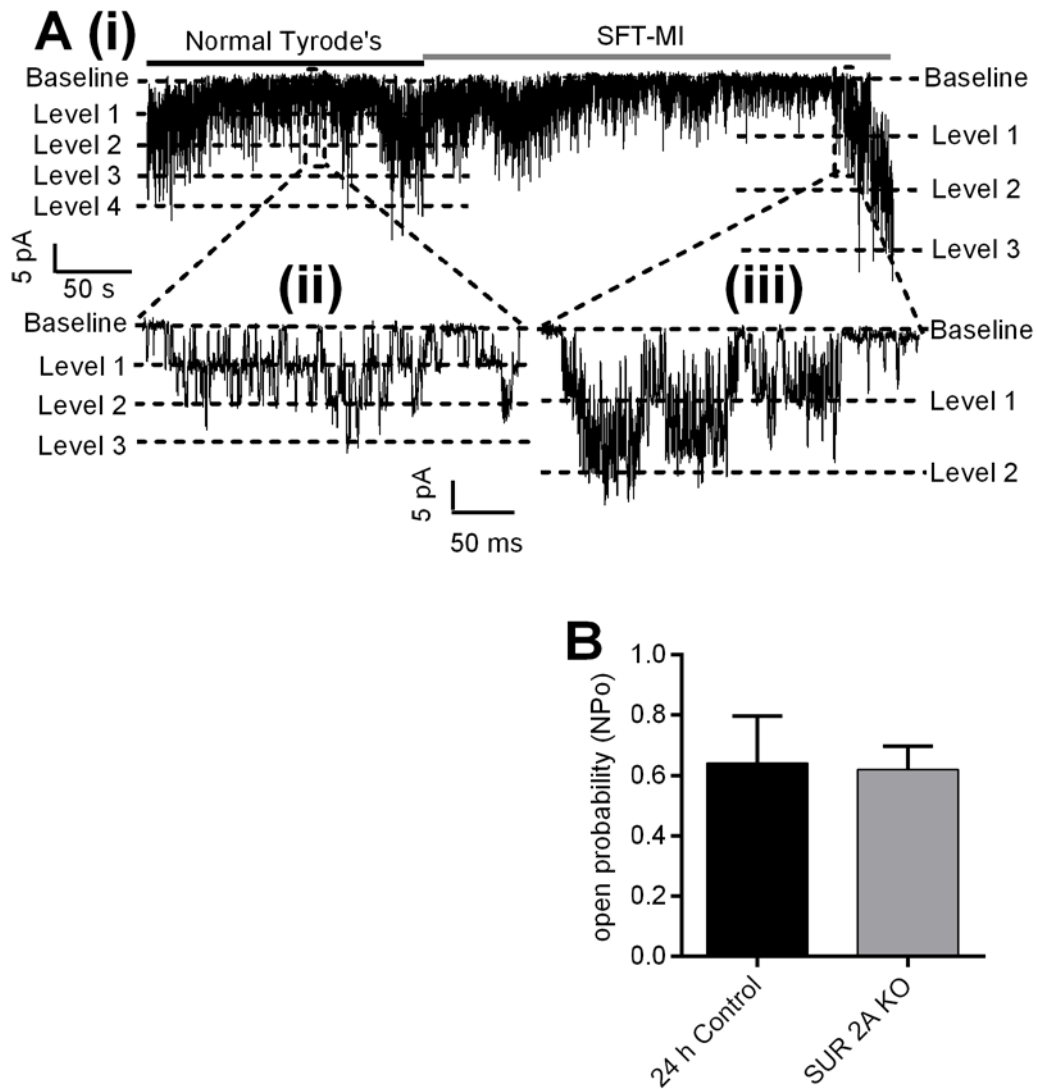


**Figure 4.8: SUR2A specific targeting shRNA has no reduction effect on the  $K_{ir}6.1$ -containing channel activity following 24 h adenoviral infection.** A(i), Recording was acquired from cell-attached patches, with SFT-MI used to activate  $K_{ir}6.2$  currents. Expanded traces show the activity of the  $K_{ir}6.1$ -containing (ii) and SarcK<sub>ATP</sub>- $K_{ir}6.2$  activates at after MI (iii), at ~5 and ~10 pA respectively. B, Histogram showing there is no different between  $K_{ir}6.1$ -containing channel activity (NPo) in 24 h culture control ( $0.64 \pm 0.16$ ,  $n=16$ ) and 24 h shRNA (SUR2A) infected ( $0.62 \pm 0.08$ ,  $n=6$ ) cardiomyocytes (ns,  $p > 0.05$ ; Student unpaired t-test).

Following 24 h infection with SUR2A shRNA (Figure 4.8A), the  $K_{ir}6.1$  channel activity (NPo) at the sarcolemmal surface was unaffected, compared with control ( $0.64 \pm 0.16$ ,  $n=16$ ) with SUR2A infection ( $0.62 \pm 0.08$ ,  $n=6$ , ns; Student unpaired t-test). The  $K_{ir}6.2$ -containing channel was unaffected after metabolic inhibition (Figure 4.8A (iii)).

In these experiments, there was a significant reduction in the  $K_{ir}6.1$  channel activity on the cardiac sarcolemmal surface following 24 h with SUR2B specific knockdown, but showed no reduction following 24 h infection with SUR2A-specific shRNA. These data suggest that SUR2B is co-expressed with the pore forming subunits  $K_{ir}6.1$ , which cardiac sarcolemmal surface channel could be the same subunit combination as the primary vasculature  $K_{ATP}$  complex,  $K_{ir}6.1/SUR2B$ .

#### **4.2.5 Infection with a shRNA against the $K_{ir}6.2$ subunit causes a reduction in the MI-activated currents measured using whole-cell recording.**

As described previously,  $K_{ir}6.2/SUR2A$  is often referred to as the cardiac  $K_{ATP}$  isoform and its activity is only really seen in cardiomyocytes during metabolic inhibition (Brennan *et al.*, 2015). It has been suggested in a small number of publications that  $K_{ir}6.1$  and  $K_{ir}6.2$  can co-assemble to form functional heteromeric channels, and there has been reports of dominant negative pore-forming subunits inhibiting the opposite  $K_{ir}6$  channel. To confirm that the shRNA approach was selective for each isoform as believed, the knockdown of  $K_{ir}6.2$  currents were investigated using whole cell recording, along with investigation of the leak current attributed to  $K_{ir}6.1$  activity. Holding the membrane potential at 0 mV, Figure 4.9A (i), (ii) and (iii) demonstrate the example traces in all 24 h cultured, negative-control virus infection and  $K_{ir}6.2$  knockdown respectively. The leak currents in resting condition were acquired prior to the perfusion of SFT-MI solution. Figure 4.9B illustrates there are no significant different in leak currents in all control, negative-control and  $K_{ir}6.2$ -knockdown conditions, with  $1.77 \pm 0.31$  pA/pF ( $n=5$ ),  $1.60 \pm 0.25$  pA/pF ( $n=6$ ) and  $1.35 \pm 0.29$  pA/pF ( $n=7$ ) respectively. Measuring the peak currents during SFT-MI perfusion, Figure 4.7C shows that there is a significant reduction in  $K_{ir}6.2$  knockdown group, with  $52.19 \pm 2.78$  ( $n=5$ , \*  $p < 0.05$ ; one-way ANOVA with Holm-Sidak post-test), compared with that in 24 h cultured group ( $74.01 \pm 6.06$ ,  $n=7$ ). No significant change between 24 h culture cardiomyocyte and negative-control virus infection myocyte, with  $74.01 \pm 6.06$  ( $n=7$ ) and

$67.79 \pm 5.64$  (n=7) respectively. Therefore, measuring the peak current during MI, the  $K_{ir}6.2$  knockdown was demonstrated to be of similar magnitude compared with previously published data (Storey *et al.*, 2013). Moreover, data suggests that neither negative-control virus infection nor  $K_{ir}6.2$  knockdown affected the cardiac basal currents in resting condition, supported the results found in the cell-attached configuration (Figure 4.5).

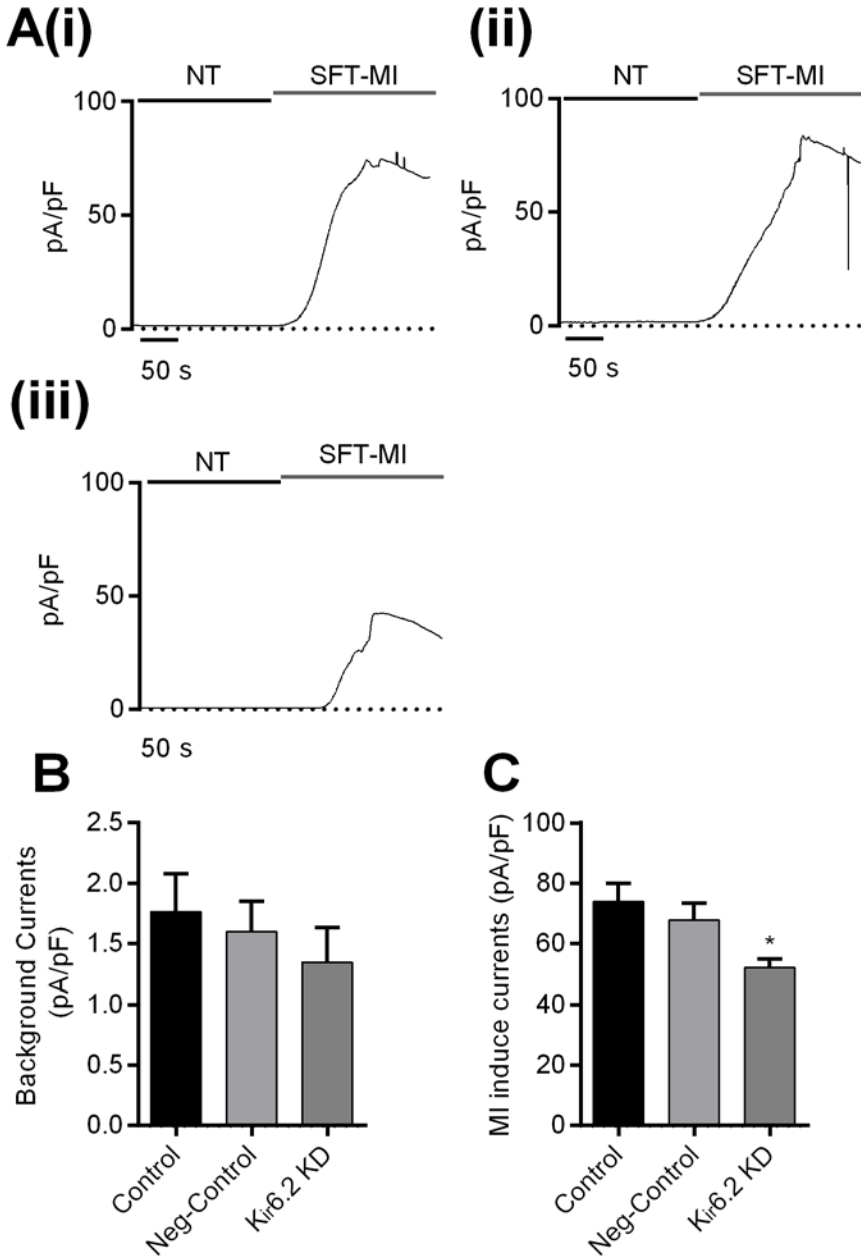


**Figure 4.9: Measuring both whole cell leak currents and MI induce currents in whole-cell recording configuration in all 24 h culture, negative control and Kir6.2 knockdown.** A(i), (ii) & (iii), Example traces illustrated the whole cell leak current in control condition and MI activation, in all 24 h cultured, negative control and Kir6.2 knockdown group. B, Mean data show there is no differences in whole cell leak currents in resting condition in both negative control and Kir6.2 knockdown group, with  $1.60 \pm 0.25$  pA/pF (n=6) and  $1.35 \pm 0.29$  pA/pF (n=7) respectively, compared with 24 h culture group ( $1.77 \pm 0.31$  pA/pF, n=5). C, Mean data illustrated the peak value of MI induced currents, with no differences between 24 h cultured myocyte ( $74.01 \pm 6.06$  pA/pF, n=7) and negative control virus infection ( $67.79 \pm 5.64$  pA/pF, n=7); significant reduction can be seen in Kir6.2 knockdown myocyte, with  $52.19 \pm 2.78$  pA/pF (n=5, \* p<0.05; one-way ANOVA with Holm-Sidak post-test).

#### 4.2.6 Knocking down $K_{ir}6.1$ prolongs the cardiac action potential in rat and guinea pig cultured cardiomyocytes

To assess the functional role of  $K_{ir}6.1$  in cardiomyocytes, cells were infected with  $K_{ir}6.1A$ -shRNA for 24 h. Action potentials were measured (as outlined in section 3.2.4, Chapter 3) in cultured control and  $K_{ir}6.1$  knockdown cells (Figure 4.10A). The  $APD_{90}$  was measured as well as the resting membrane potential. Figure 4.10A shows an example trace of APD in cultured control cardiomyocyte and  $K_{ir}6.1A$ -shRNA treated cardiomyocyte showing a prolongation in  $APD_{90}$ . Figure 4.10B also indicates that following 24 h infection with  $K_{ir}6.1$ -shRNA, the resting membrane was significantly depolarized, from  $-62.4 \pm 0.8$  mV ( $n=10$ , 24 h cultured) to  $-52.8 \pm 2.2$  mV ( $n=6$ ,  $K_{ir}6.1$  KD, \*\*\*  $p < 0.001$ ; unpaired Student t-test). Furthermore,  $APD_{90}$  was significantly prolonged following incubation with  $K_{ir}6.1$  targeting shRNA, (Figure 4.10C), with  $134.10 \pm 31.33$  ms ( $n=6$ , \*  $p < 0.05$ ; two-way ANOVA Holm-Sidak post-test), compared with 24 h cultured control myocyte ( $50.5 \pm 7.0$  ms,  $n=10$ ). Further evidence for successful knock down of  $K_{ir}6.1$  was the effectiveness of pharmacological inhibition using 3  $\mu$ M PNU, where a significant prolongation of  $APD_{90}$  was seen in 24 h cultured control cells from  $50.5 \pm 7.0$  ms ( $n=10$ ) to  $117.9 \pm 10.5$  ms, ( $n=10$ , \*  $p < 0.05$ ; two-way ANOVA Holm-Sidak post-test). In comparison, there was no significant prolongation of  $APD_{90}$  ( $158.8 \pm 3.3$  ms  $n=6$ ; two-way ANOVA Holm-Sidak post-test) in  $APD_{90}$  after 3  $\mu$ M PNU treatment in the  $K_{ir}6.1$ -shRNA treated group.

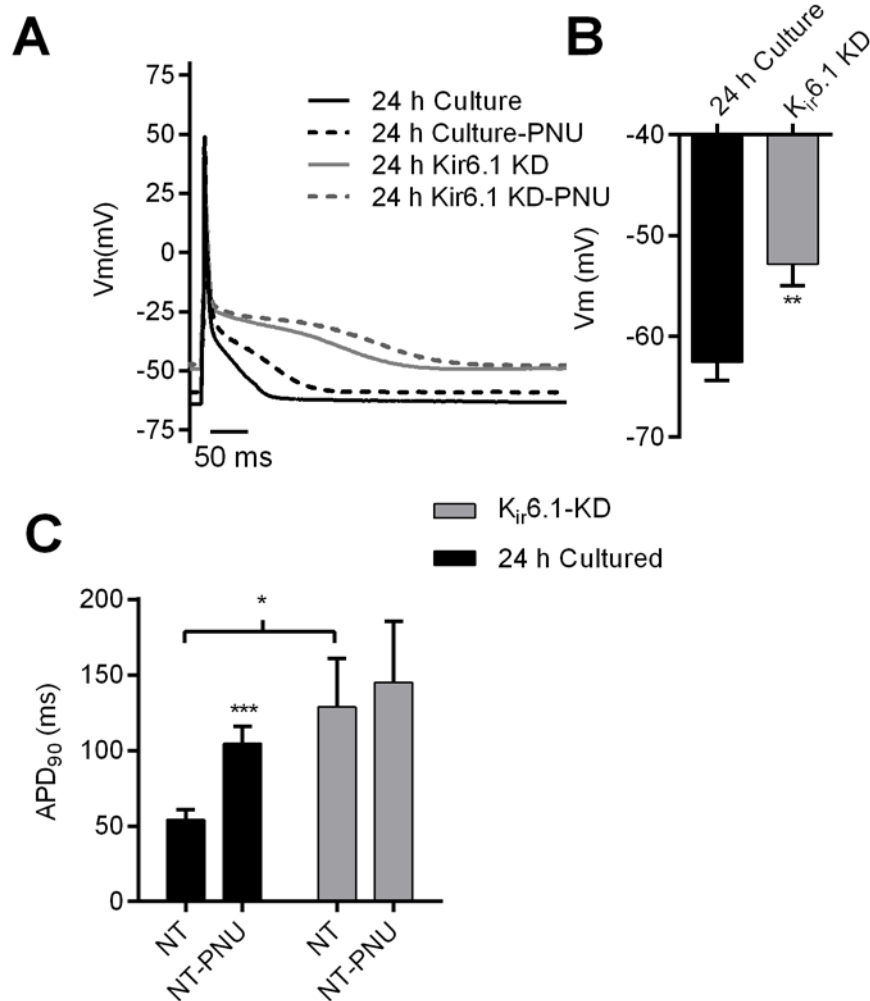


**Figure 4.10: Kir<sub>ir</sub>6.1 knockdown & PNU mediate to change action potential duration in 24 h culture rat cardiomyocyte.** A, Recording was acquired from 24 h culture/Kir<sub>ir</sub>6.1 KD cardiomyocyte in whole cell recordings. Action potential duration was recorded as well as resting membrane potential. B, Membrane potential was recorded from both 24 h culture group and Kir<sub>ir</sub>6.1 KD group shown significant depolarization after Kir<sub>ir</sub>6.1 knockdown, from  $-62.4 \pm 0.8$  mV (n=10, 24 h Culture) to  $-52.8 \pm 2.2$  mV (n=6, Kir<sub>ir</sub>6.1 KD, \*\*\*p<0.001, unpaired Student t-test). C, APD<sub>90</sub> was prolonged, from  $50.5 \pm 7.0$  ms (n=10) in 24 h culture to  $117.9 \pm 10.5$  ms (n=10, \*p<0.05, two-way ANOVA Holm-Sidak post-test) in 24 h culture-PNU treatment cells; and 24 h Kir<sub>ir</sub>6.1 KD cells ( $134.10 \pm 31.33$  ms, n=6, \*p<0.05, two-way ANOVA Holm-Sidak post-test), compared with 24 h culture group. No significant prolongation in APD<sub>90</sub> can be seen in Kir<sub>ir</sub>6.1 KD myocyte with 3  $\mu$ M PNU treatment ( $158.80 \pm 31.31$  ms, n=6, two-way ANOVA Holm-Sidak post-test).

Additionally, the  $APD_{90}$  and resting membrane potential was investigated in negative-control virus and  $K_{ir}6.2$ -shRNA treated cardiomyocytes (Figure 4.11A). Figure 4.11B demonstrates that there were no differences between 24 h cultured, negative-control virus and  $K_{ir}6.2$  knockdown cardiomyocytes, with  $47.3 \pm 7.0$  ms ( $n=9$ ),  $37.7 \pm 4.1$  ms ( $n=6$ ) and  $32.9 \pm 6.1$  ms ( $n=5$ ; two-way ANOVA Holm-Sidak post-test). Same with resting membrane potential, no significant difference can be same after negative-control virus infection ( $-67.1 \pm 2.2$  mV,  $n=6$ ) and  $K_{ir}6.2$  KD ( $-67.7 \pm 2.1$  mV,  $n=5$ ; two-way ANOVA Holm-Sidak post-test), compared with 24 h cultured cardiomyocyte ( $-62.4 \pm 0.8$  mV,  $n=10$ )

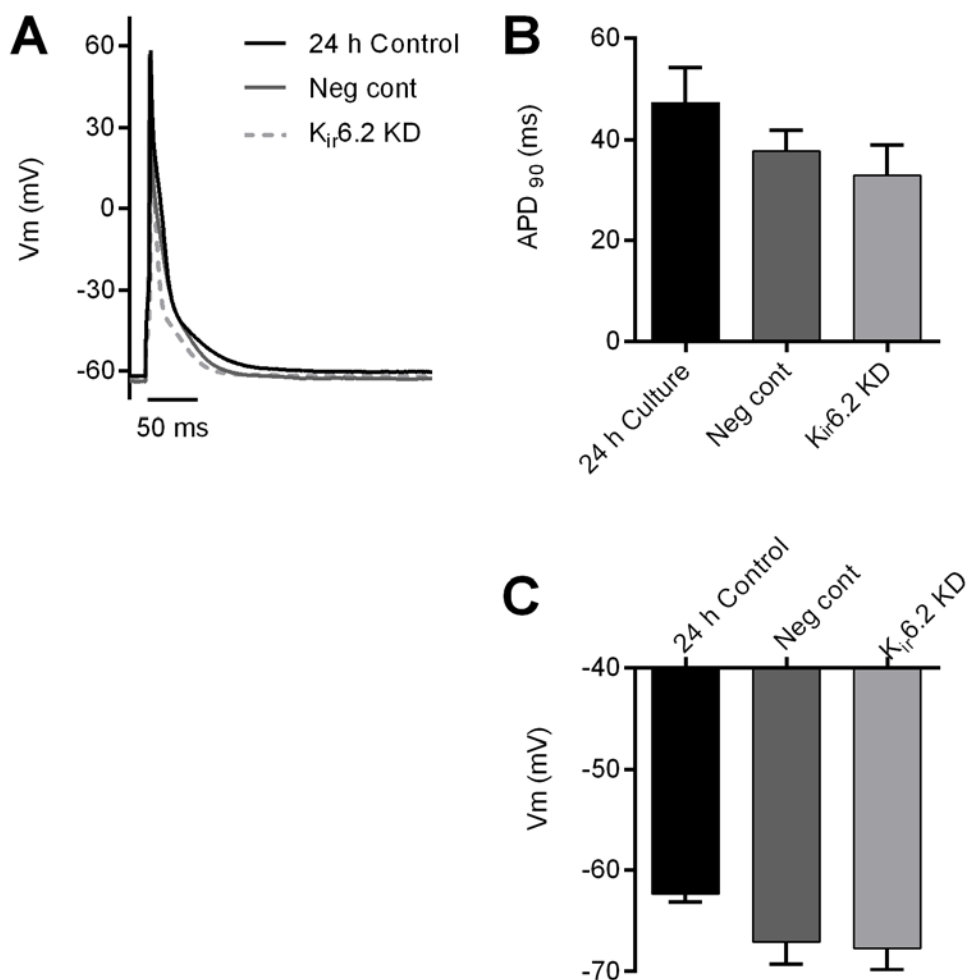


**Figure 4.11:  $K_{ir}6.2$  knockdown & negative control infection does not change the action potential duration in 24 h culture rat cardiomyocyte.** A, Recordings were acquired from 24 h culture,  $K_{ir}6.2$  KD and negative control virus infection cardiomyocyte in whole cell recordings. Action potential duration was recorded as well as resting membrane potential. B, No significant change in  $APD_{90}$  after negative control virus infection ( $37.7 \pm 4.1$  ms,  $n=6$ ) and  $K_{ir}6.2$  KD ( $32.9 \pm 6.1$  ms,  $n=5$ ; two-way ANOVA Holm-Sidak post-test), compared with 24 h culture control ( $47.3 \pm 7.0$  ms,  $n=9$ ). C, No significant differences in resting membrane potential between 24 h culture control ( $-62.4 \pm 0.8$  mV,  $n=10$ ), negative control ( $-67.1 \pm 2.2$  mV,  $n=6$ ) and  $K_{ir}6.2$  KD ( $-67.7 \pm 2.1$  mV,  $n=5$ ; two-way ANOVA Holm-Sidak post-test).

To confirm that  $K_{ir}6.1$  activity was not just a feature of rat cardiomyocytes, the effect of knockdown of  $K_{ir}6.1$  was investigated in GP cardiomyocytes. The shRNA sequences used in this study also had homology with guinea pig  $K_{ir}6.1$  RNA and so were used to knockdown the GP current. Both  $K_{ir}6.1$  targeting shRNA constructs ( $K_{ir}6.1$  A/B) were used in combination to infect GP cardiomyocytes. In these  $K_{ir}6.1$  KD experiments in GP cardiomyocytes, a similar phenomenon was observed with  $APD_{90}$  and resting membrane potential. Figure 4.12A (i) shows 3 representative AP recordings from a 24 h cultured GP cardiomyocyte, (i) a control traces, (ii) following addition of 3  $\mu$ M PNU treatments and (iii) with the addition of 10  $\mu$ M glibenclamide treatment. Like rat cardiomyocytes, the  $APD_{90}$  was significantly prolonged on treatment with 3  $\mu$ M PNU but no further prolongation was seen with 10  $\mu$ M glibenclamide. The mean  $APD_{90}$  in Figure 4.12B showed a PNU-induced prolongation of  $APD_{90}$  from  $197.4 \pm 45.6$  ms ( $n=4$ , 24 h culture) to  $292.4 \pm 43.0$  ms ( $n=4$ , 3  $\mu$ M PNU treatments,  $**p < 0.005$ ; one-way ANOVA with Holm-Sidak post-test). There was no further prolongation of  $APD_{90}$  following treatment with 10  $\mu$ M glibenclamide ( $298.6 \pm 40.0$  ms,  $n=4$ ). In terms of resting membrane potential, 3  $\mu$ M PNU treatment also showed a significant depolarisation, from  $-67.1 \pm 1.2$  mV ( $n=4$ ) in 24 h culture control to  $-61.0 \pm 2.6$  mV ( $n=4$ ,  $**p < 0.001$ ; Repeated measures one-way ANOVA with Holm-Sidak post-test) after PNU treatment. Addition of 10  $\mu$ M glibenclamide caused no significant depolarization in resting membrane potential ( $-61.8 \pm 2.8$  mV,  $n=4$ ).

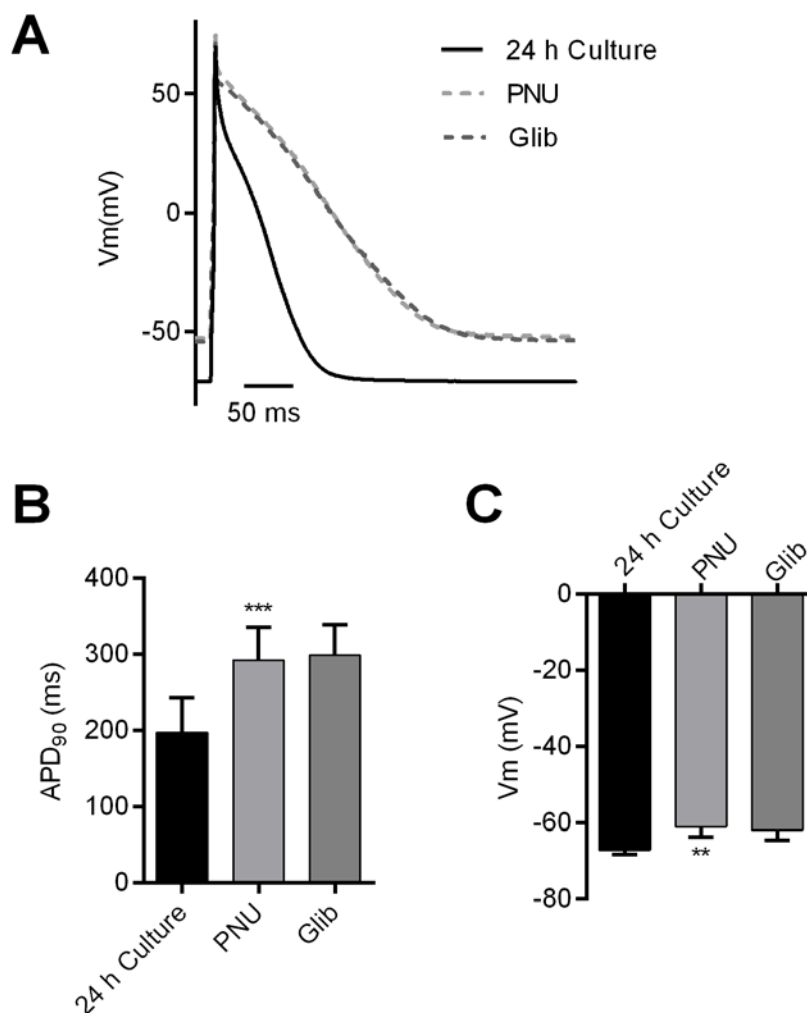


**Figure 4.12: PNU37883A prolonged the action potential duration in 24 h cultured guinea pig cardiomyocytes.** A, Recording was acquired from isolated cardiomyocytes in the whole-cell recording configuration. Example trace shows action potentials recorded from cultured control guinea pig cardiomyocytes, following perfusion with 3  $\mu$ M PNU and followed by 10  $\mu$ M glibenclamide. B, The histogram shows mean data in cultured guinea pig cardiomyocytes, 3  $\mu$ M PNU can significantly prolong APD<sub>90</sub>, from 197.4 $\pm$ 45.6 ms (n=4, 24 h culture) to 292.4 $\pm$ 43.0 ms (n=4, 3  $\mu$ M PNU treatments, \*\*p<0.005; one-way ANOVA with Holm-Sidak post-test) with no further prolongation following 10  $\mu$ M glibenclamide treatment (298.6 $\pm$ 40.0 ms, n=4). C, 3  $\mu$ M PNU treatment also showed a significant depolarisation on resting membrane potential, from -67.1 $\pm$ 1.2 mV (n=4) in 24 h culture control to -61.0 $\pm$ 2.6 mV (n=4, \*\*p<0.001,) after PNU treatment. Addition of 10  $\mu$ M glibenclamide caused no significant depolarization in resting membrane potential (-61.8 $\pm$ 2.8 mV, n=4).

Figure 4.13A shows that following  $K_{ir}6.1$ -shRNA infection, the  $APD_{90}$  was prolonged, from  $197.4 \pm 45.6$  ms ( $n=4$ , 24 h culture group) to  $328.1 \pm 16.9$  ms ( $K_{ir}6.1$  KD,  $n=4$ ,  $*p < 0.05$ , Student unpaired t-test). Coupled to the  $APD_{90}$  prolongation, there was a marked depolarisation of the resting membrane potential seen in  $K_{ir}6.1$  KD ( $-53.5 \pm 1.7$  mV,  $n=4$ ,  $*p < 0.05$ ; one-way ANOVA with Holm-Sidak post-test), compared with 24 h control group ( $-66.9 \pm 1.3$  mV,  $n=4$ , Figure 4.13C). Finally, in  $K_{ir}6.1$ -knockdown cardiomyocytes, there was no  $APD_{90}$  prolongation with 3  $\mu$ M PNU treatment ( $-56.1 \pm 5.4$  mV,  $n=4$ ).

These  $K_{ir}6.1$  specific targeting shRNA infection data suggests a role for the  $K_{ir}6.1$  subunits in modulation of the action potential duration. As a result, knockdown of  $K_{ir}6.1$  subunits prolonged the APD and depolarised the resting membrane potential in both guinea pig and rat. Finally, following PNU treatment, there was no additional APD prolongation by PNU in  $K_{ir}6.1$  KD cells, suggesting a key role for Kir6.1 in modulation of the APD.

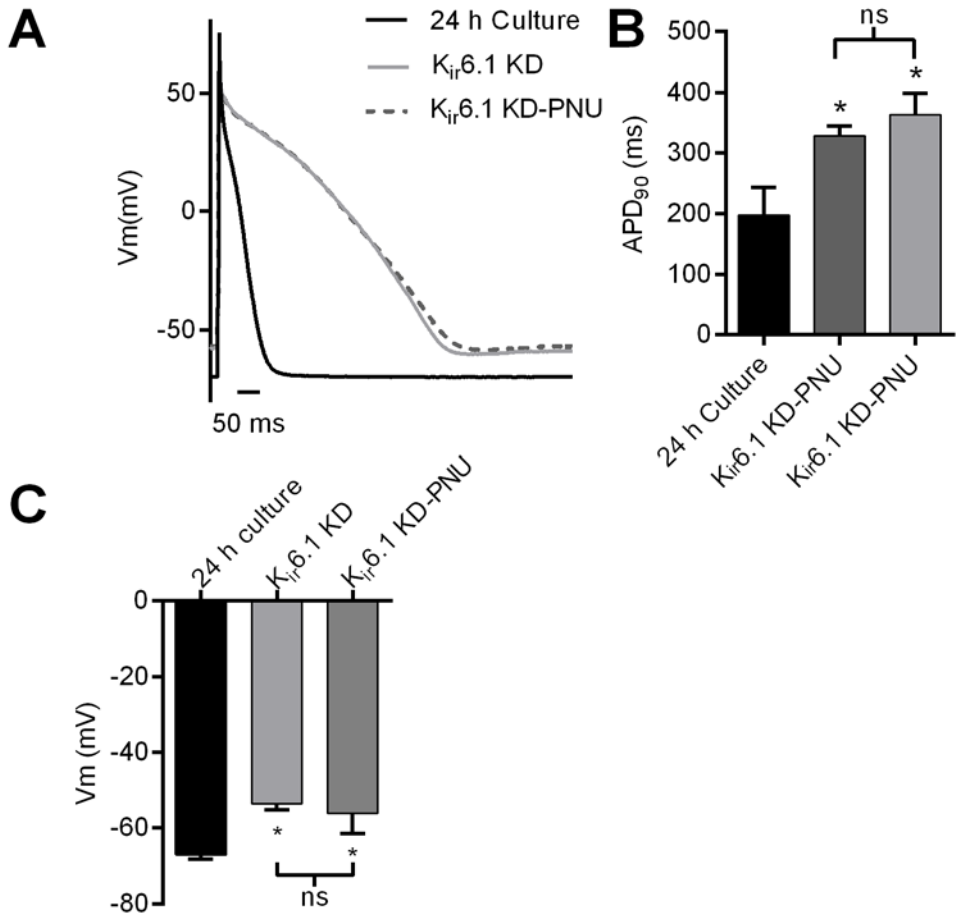


**Figure 4.13: Kir<sub>ir</sub>6.1 targeting shRNA (Kir<sub>ir</sub>6.1 A&B) prolonged the action potential duration in 24 h cultured guinea pig cardiomyocytes.** A, Recording was acquired from isolated cardiomyocytes in the whole-cell recording configuration. Example trace shows action potentials recorded from cultured GP cardiomyocytes, Kir<sub>ir</sub>6.1 knockdown myocyte and followed by 3  $\mu$ M PNU treatment. B, The histogram shows mean data in 24 h culture/Kir<sub>ir</sub>6.1 knockdown GP cardiomyocytes, Kir<sub>ir</sub>6.1 knockdown can significantly prolong APD<sub>90</sub>, from 197.4 $\pm$ 45.6 ms (n=4, 24 h culture) to 328.1 $\pm$ 16.9 ms (n=4, Kir<sub>ir</sub>6.1 knockdown, \*p<0.05, one-way ANOVA with Holm-Sidak post-test) with no further prolongation following 3  $\mu$ M PNU treatment (363.3 $\pm$ 35.6 ms, n=4). C, Kir<sub>ir</sub>6.1-knockdown cardiomyocytes also showed a significant depolarization from -66.9 $\pm$ 1.3 mV (n=4) in 24 h culture control to -53.5 $\pm$ 1.7 mV (n=4, Kir<sub>ir</sub>6.1 KD, \*p<0.05, one-way ANOVA with Holm-Sidak post-test) in Kir<sub>ir</sub>6.1 knockdown group. Addition of 3  $\mu$ M PNU to Kir<sub>ir</sub>6.1 knockdown cardiomyocytes caused no significant depolarization in resting membrane potential (-56.1 $\pm$  5.4 mV, n=4).

#### 4.2.7 Functional effects of SUR knockdown on cardiac action potential duration and resting membrane potential in rat cultured cardiomyocytes

To further confirm a role for distinct SUR subunits in the two identified  $K_{ATP}$  currents, each SUR was knocked down individually to assess their effect on the AP. Action potentials were measured in cultured control and SUR2A knock down cells (Figure 4.14A). The  $APD_{90}$  was measured as well as the resting membrane potential. Figure 4.14A shows an example trace of APD cultured control cardiomyocyte, SUR2A-shRNA infected cardiomyocyte and SUR2B-shRNA infected cardiomyocyte, showing a prolongation in  $APD_{90}$  in SUR2B knockdown cell, but no prolongation was seen in SUR2A knockdown cells.

Given the cell-attached data, and similar data using  $K_{ir}6.1$  knockdown, it was hypothesised that knockdown of SUR2B would cause a prolongation of the APD. Following SUR2B knockdown,  $APD_{90}$  was significantly prolonged (Figure 4.14B,  $APD_{90}$   $149.3 \pm 35.4$  ms,  $n=6$ ,  $**p < 0.005$ ), compared with 24 h culture myocyte ( $54.2 \pm 6.6$  ms,  $n=11$ ). No significant prolongation of  $APD_{90}$  was seen following 24 h culture with SUR2A knockdown ( $46.4 \pm 8.2$  ms,  $n=7$ , ns; one-way ANOVA with Holm-Sidak post-test), compared with 24 h culture control ( $54.2 \pm 6.6$  ms,  $n=11$ ). This finding gives further evidence against the involvement of the SUR2A subunit co-assembling with  $K_{ir}6.1$  in cardiomyocytes. In comparison,  $K_{ir}6.1$ -knockdown group ( $128.7 \pm 32.2$  ms,  $n=6$ , Figure 4.14) and SUR2B knockdown group ( $149.3 \pm 35.4$  ms,  $n=6$ ) showed no significant difference in  $APD_{90}$  suggesting SUR2B and  $K_{ir}6.1$  are key components of this complex. In terms of resting membrane potential, SUR2A-shRNA infection did not alter the resting membrane potential, with  $-62.6 \pm 1.8$  mV ( $n=6$ ) compared with 24 h culture myocyte ( $-62.5 \pm 1.8$  mV,  $n=11$ ). Similar trend to the  $K_{ir}6.1$ -knockdown (Figure 4.10), resting membrane potential in SUR2B-knockdown myocytes was depolarized, from  $-62.5 \pm 1.8$  mV ( $n=11$ ) to  $-49.2 \pm 2.7$  mV ( $n=6$ ,  $***p < 0.001$ ; one-way ANOVA with Holm-Sidak post-test).

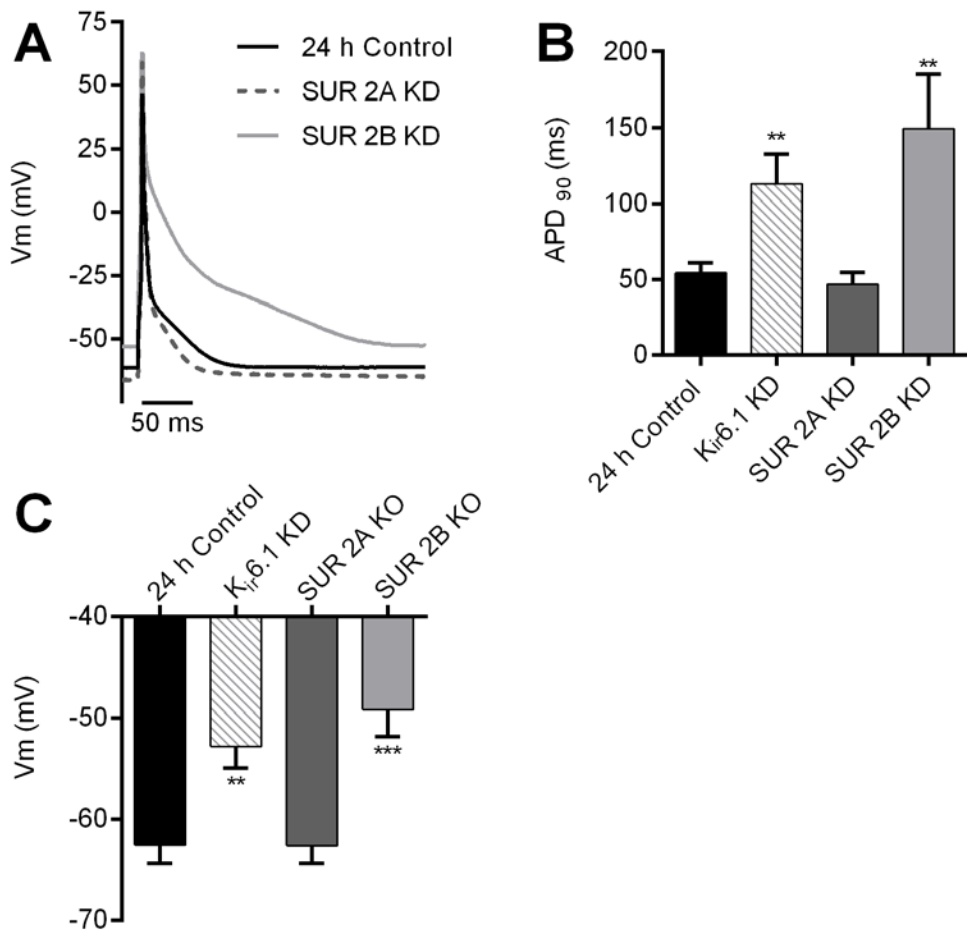


**Figure 4.14: Effect of infect both of SUR specific targeting shRNA (SUR2A/SUR2B) on action potential duration in 24 h culture cardiomyocyte.** A, Recording was acquired from 24 h culture or infection cardiomyocyte in whole-cell recording configuration. Example trace shows action potentials recorded from cultured control cardiomyocyte, SUR2A-KD cardiomyocyte and SUR2B-KD cardiomyocyte. B, The histogram shows mean data in cultured cardiomyocyte, SUR2B shRNA infection can significant prolong APD<sub>90</sub>, from 54.2±6.6 ms (n=11, 24 h culture) to 149.3±35.4 ms (n=6, SUR2B-knockdown, \*\*p<0.005; one-way ANOVA with Holm-Sidak post-test) but no prolongation can be seen in SUR2A-knockdown myocyte (46.4±8.2 ms, n=7). C, SUR2B-knockdown also showed a significant depolarization on resting membrane potential, from -62.5±1.8 mV (n=11) in 24 h culture myocyte to -49.2±2.7 mV (n=6, \*\*\*p<0.001; one-way ANOVA with Holm-Sidak post-test) in SUR2B-knockdown myocyte. No change in resting membrane potential in SUR2A knockdown myocyte (-62.6±1.8 mV, n=6).

Figure 4.15A&B shows example traces of action potential duration using 3  $\mu\text{M}$  PNU to pharmacologically block  $\text{K}_{\text{ir}}6.1$  channels and followed by 10  $\mu\text{M}$  glibenclamide treatments, in SUR2A and SUR2B knockdown groups respectively. In SUR2A-knockdown myocytes, similar to 24 h control (Figure 4.10), 3  $\mu\text{M}$  PNU prolonged  $\text{APD}_{90}$  ( $118.3 \pm 22.8$  ms,  $n=7$ ,  $**p < 0.005$ ) compared with NT perfusion ( $46.4 \pm 8.2$  ms,  $n=7$ ); with no further  $\text{APD}_{90}$  prolongation in the end perfusion with 10  $\mu\text{M}$  glibenclamide ( $103.3 \pm 16.6$  ms,  $n=7$ ; Repeated measures two-way ANOVA with Holm-Sidak's post-test). In the SUR2B-knockdown group, similar to  $\text{K}_{\text{ir}}6.1$ -knockdown (Figure 4.10), the  $\text{APD}_{90}$  was not altered by PNU and subsequent glibenclamide treatments, with  $152.9 \pm 31.2$  ms ( $n=6$ , ns) and  $159.1 \pm 35.5$  ms ( $n=6$ , ns; Repeated measures two-way ANOVA with Holm-Sidak's post-test) compared with 24 h culture control condition ( $149.3 \pm 35.4$  ms,  $n=6$ ).

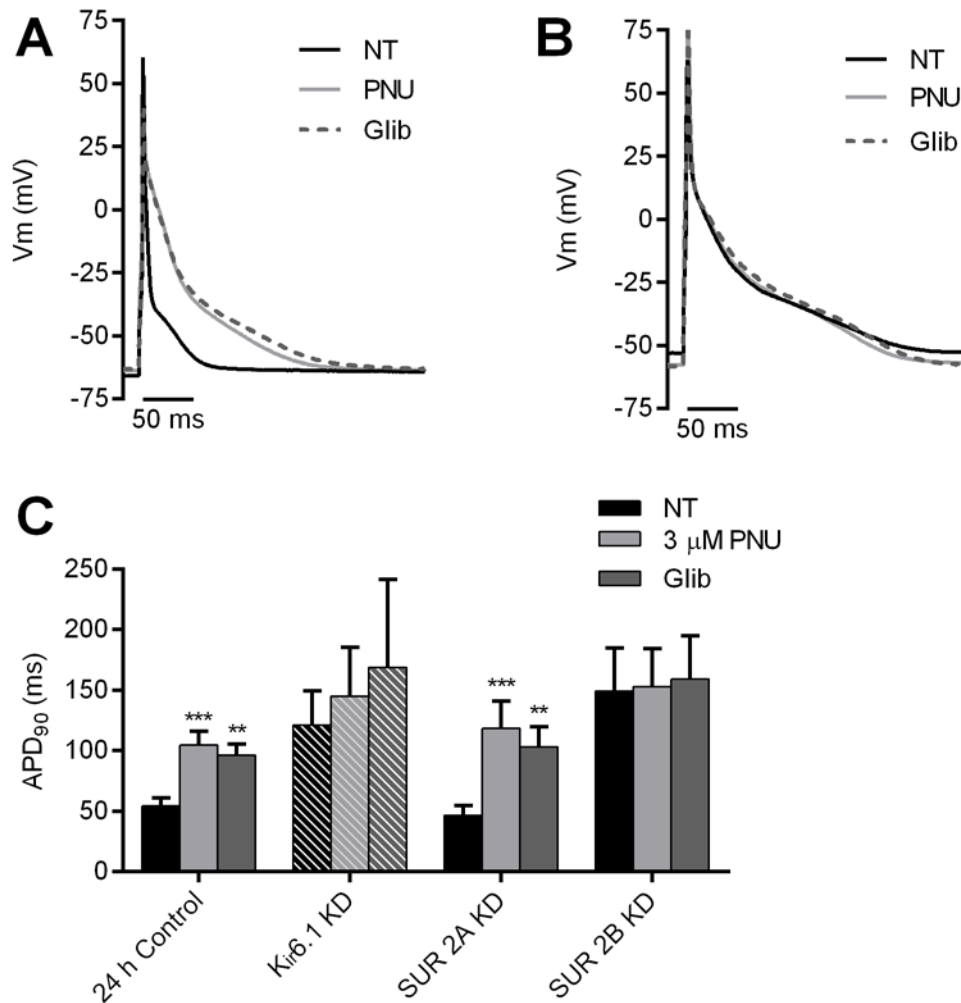


**Figure 4.15: PNU and Glibenclamide treatments alter the action potential duration in both 24 h cultured and SUR2A knockdown cardiomyocyte but not SUR2B knockdown.** A&B, Recording was acquired from either SUR2A-targeting or SUR2B-targeting shRNA infection cardiomyocyte in whole-cell recording configuration respectively. Example trace shows action potentials recorded from NT, 3  $\mu$ M PNU and 10  $\mu$ M glibenclamide treatments. C, The histogram shows mean data that 3  $\mu$ M PNU treatments significantly prolonged APD<sub>90</sub> in 24 h cultured and SUR2A knockdown myocyte from 54.2 $\pm$ 6.6 ms (n=11, 24 h culture) to 104.5 $\pm$ 11.5 ms (n=11, 24 h culture-PNU, \*\*\*p<0.001) and 46.4 $\pm$ 8.2 ms (n=7, SUR2A-knockdown) to 118.3 $\pm$ 22.8 ms (n=7, SUR2A-knockdown-PNU, \*\*p<0.005). No further prolongation can be seen in the follow glibenclamide treatments, with 96.1 $\pm$ 9.1 ms (n=11) in 24 h culture myocyte and 103.3 $\pm$ 16.6 ms (n=7) in SUR2A-knockdown group. Myocytes after SUR2B-knockdown do not shown prolongation in APD<sub>90</sub> after PNU and glibenclamide treatments, with 152.9 $\pm$ 31.2 ms (n=6) and 159.1 $\pm$ 35.5 ms (n=6) respectively compared with NT perfusion (149.3 $\pm$ 35.4 ms, n=6; Repeated measures two-way ANOVA with Holm-Sidak's post-test).

### 4.3 Discussion

In the literature, the  $K_{ir}6.1/SUR2B$  is often described as the vasculature  $K_{ATP}$  channel complex (Insuk *et al.*, 2003; Wang *et al.*, 2003; Yoshida *et al.*, 2004a), which causes vasodilation during strong activation (Wang *et al.*, 2003). This complex, unlike the classic cardiac/skeletal muscle  $K_{ir}6.2/SUR2A$  complex, is relatively ATP-insensitive (Yamada *et al.*, 1997) demonstrating constitutive activity modulated by protein kinases activated by vasoconstrictors or dilators (Burke *et al.*, 2008). The findings presented here suggest that the newly identified  $\sim 39$  pS- $K_{ATP}$  channel at the cardiac sarcolemmal membrane surface is comprised of  $K_{ir}6.1$  and SUR2B, and has a constitutive activity consistent with that of the known vascular isoform.

The data presented in this chapter gives supporting evidence that the  $\sim 39$  pS-conductance identified on the cardiomyocyte sarcolemmal membrane is a  $K_{ir}6.1$  subunit-containing channel. By using specific  $K_{ir}6.1$  targeting shRNA, the function and expression of this channel was investigated by using electrophysiology, pharmacological tools and western blotting. Using patch clamp recording it has been shown that the activity of the  $\sim 39$  pS-conductance channel was markedly reduced in cell-attached recording following adenoviral infection with  $K_{ir}6.1$ -targeting shRNA. Furthermore, in both GP and rat, there were significant differences in the cardiac APD as well as  $Ca^{2+}$  transients, following  $K_{ir}6.1$  knockdown or pharmacological inhibition. These data provide more evidence that this  $K_{ir}6.1$ -containing channel plays an important role in modulating cardiac physiology in resting conditions in cardiomyocyte of 2 different species.

In the first results chapter, by using pharmacological inhibition, a  $\sim 39$  pS-conductance channel in cardiac sarcolemmal surface was suggested as a  $K_{ir}6.1$ -containing channel. To obtain more evidence that this was indeed a  $K_{ir}6.1$ -containing channel, specific gene knockdown was adopted in this chapter. Following 24 h culture, cell-attached recording not only revealed that the  $K_{ir}6.1$ -channel was still active, but that its activity was significantly increased. This up-regulation of  $K_{ir}6.1$ -containing currents could have occurred due to a number of reasons including the change of pH (Baukowitz *et al.*, 1999), hypoxia stress during incubation (Akao *et al.*, 1997; Budas *et al.*, 2004) or compound stimulation in culture media. This increase in  $K_{ir}6.1$  activity in culture was beneficial in this study as the

successful knockdown was easier to observe. However, a pronounced standard error bar is shown in the NPo in 24 h culture group in Figure 4.5. There is no statistical significance according to the analysis, however, the negative-control virus still has a trend of reducing the  $K_{ir}6.1$  channel activity. The apparently knockdown of sarcolemmal  $K_{ir}6.1$  channel activity by the negative-control virus may be caused by an off-target effect through RNAi. To confirm this, a control virus would be needed for these knockdown experiments. Secondly, the distribution of  $K_{ATP}$  channel in the cardiac sarcolemmal membrane may be a factor. Singh *et al* (2003) showed that the  $K_{ir}6.1$  and SUR2B subunits closely associated with the t-tubule network. This may mean that the distribution of  $K_{ir}6.1$  at the cell surface may be variable and the majority is located within the membrane that it largely inaccessible to the patch pipette in the t-tubule. Two different  $K_{ir}6.1$  targeting shRNA,  $K_{ir}6.1A$  and  $K_{ir}6.1B$ , were used to knockdown  $K_{ir}6.1$ . Following 24 h infection with either  $K_{ir}6.1$  shRNA, the ~39 pS-conductance currents were significantly reduced. The reduction of the intensity of the  $K_{ir}6.1$  band in knockdown cardiomyocytes also supports the electrophysiology data suggesting a functional  $K_{ir}6.1$  knockdown. To further distinguish between  $K_{ir}6.1$  and  $K_{ir}6.2$  containing channels at the cardiomyocyte membrane, the  $K_{ir}6.2$  subunits expression level was investigated in western blotting. The  $K_{ir}6.2$  subunits expression level remains the same in all freshly isolation, 24 h cultured and  $K_{ir}6.1$  knockdown lysates, suggesting that the  $K_{ir}6.2$  expression was not altered by  $K_{ir}6.1$  knockdown. Although gels were equally loaded in each sample in terms of the calculated protein, and the results fit with the electrophysiology data, the absence of an internal control is a confounding issue for these western blots due to the potential inaccuracy in protein concentration.

$K_{ir}6.1$  knockdown data presented here gives more evidence that the ~39 pS-current expressed on the cardiomyocyte membrane surface is indeed a  $K_{ir}6.1$ -containing channel. The relatively rapid knockdown effect suggests that this channel is turned over rapidly at the membrane surface, and that subunit trafficking from the endoplasmic reticulum (ER) to the membrane surface takes less than 24 h. These findings agree with previous literature suggesting both  $K_{ir}6.1$  mRNA and protein is up-regulated 24 h following ischemia/reperfusion or urocortin-induced cardioprotection (Akao *et al.*, 1997; Lawrence *et al.*, 2002).

K<sub>ir</sub>6 proteins contain a C-terminal endoplasmic reticulum retention sequence (RXR) that, unless masked by co-assembly with a sulphonylurea receptor, prevents the channels being transported to the membrane surface (Zerangue *et al.*, 1999; Ng *et al.*, 2010). To fully understand the properties of the cardiac sarcolemmal K<sub>ir</sub>6.1-pore channel it is important to know which  $\beta$ -subunit co-expresses on the cell surface.

Although not a pore forming subunit, SUR subunits are involved in modulation of the K<sub>ATP</sub> opening state, as SUR contains two NBFs that carry multiple binding sites for both drugs and nucleotide (Reimann *et al.*, 2001). Previous literature suggest the difference in amino acids between SUR2A and SUR2B causes opposing behaviour when co-expressed with K<sub>ir</sub>6 as SUR2B-containing channels require intracellular ATP or nucleotides to open but intracellular ATP has a marked inhibitory effect in SUR2A-comprising K<sub>ATP</sub> channel complexes (Satoh *et al.*, 1998). In terms of pharmacology, the SUR2B-containing channel can be activated by diazoxide in the presence of Mg-ATP whilst SUR2A-containing channel requires Mg-ADP (Reimann *et al.*, 2000). Therefore, it is important to investigate which SUR subunits are expressed with this cardiac K<sub>ir</sub>6.1-containing channel to fully understand its regulation.

In the first results chapters, a K<sub>ir</sub>6.1-containing channel expressed in cardiomyocyte membrane was shown that shares electrophysiological and pharmacological properties with the known features of the vascular type K<sub>ATP</sub> isoform from experimental studies. This, taken together with the knockdown data, led to the hypothesis that the  $\beta$ -subunit in this K<sub>ir</sub>6.1 comprising complex is SUR2B. Further supporting evidence for SUR2B playing a role in the K<sub>ir</sub>6.1 channel complex stems from the identification of the expression of this isoform in cardiomyocytes. Previous studies demonstrated not only the SUR2B mRNA expressed in ventricular myocyte alone with K<sub>ir</sub>6.1 (van Bever *et al.*, 2004) but also SUR2B protein which immunofluorescence analysis illustrated their localization is in sarcolemmal surface (Singh *et al.*, 2003).

These data presented above is strong evidence that the newly identified K<sub>ir</sub>6.1-containing channel co-expresses with SUR2B  $\beta$ -subunits in the cardiomyocyte sarcolemmal membrane. By using specific SUR2A and SUR2B specific targeting shRNA, the  $\beta$ -subunits co-expressing with each K<sub>ir</sub>6  $\alpha$ -subunit was identified by using electrophysiology and

pharmacological tools. The SUR specific targeting shRNA infection data suggest that the SUR subunits co-express with  $K_{ir}6.1$  subunits on cardiomyocyte membrane is SUR2B. Using patch clamp, it was shown that the  $K_{ir}6.1$ -containing channel activity was significantly decreased in cell-attached recording following 24 h adenoviral infection with SUR2B targeting shRNA but there was no significant reduction in  $K_{ir}6.1$ -containing channel activity following infection with SUR2A targeting shRNA. Furthermore, similar to  $K_{ir}6.1$ -knockdown (Figure 4.10), SUR2B knockdown also prolonged the cardiac action potential duration as well as causing depolarisation in the resting membrane potential. There was no alteration of the  $APD_{90}$  or the resting membrane potential in SUR2A knockdown cardiomyocytes. Finally, PNU treatment on SUR2B knockdown cardiomyocyte shows no further action potential prolongation, suggesting that SUR2B-knockdown abolished the expression of  $K_{ir}6.1$ -containing channel in sarcolemmal membrane further proved that SUR2B indeed the  $\beta$ -subunits and co-express with  $K_{ir}6.1$ -containing channel on cardiomyocyte sarcolemmal surface.

#### **4.3.1 The functional role of $K_{ir}6.1$ /SUR2B in cardiomyocytes**

Having identified that the  $K_{ir}6.1$ /SUR2B complex is expressed in the cardiomyocyte membrane, it is important to understand the physiological role of the channel.  $K_{ir}6.1$ -containing channels display a weak inward rectification displaying a near linear current voltage relationship. This suggests that its activity would affect electrical signalling across the range of membrane potentials seen during cardiomyocyte normal function. Given that the  $K_{ir}6.1$ /SUR2B complex appears to have constitutive activity in freshly isolated cardiomyocytes, it suggests that there is a role for this channel in the modulation of the action potential duration and the resting membrane potential which fit the experiment results from the first results chapter.

Using current clamp recording, the action potential and resting membrane potentials of cardiomyocytes were investigated in cultured control and  $K_{ir}6.1$ -knockdown conditions. Comparison between 24 h cultured control myocytes and  $K_{ir}6.1$  knockdown myocytes revealed marked differences in both the resting membrane potential and APD. The resting membrane potential was markedly depolarized and the  $APD_{90}$  significantly prolonged following  $K_{ir}6.1$  knockdown. In the literature, the cardiac sarcolemmal  $K_{ATP}$  complex has

been shown to modulate the cardiac APD using pharmacological inhibition or activation (Billman *et al.*, 1998). Although the cardiac  $K_{ATP}$  was considered to be a complex of  $K_{ir}6.2/SUR2A$  subunits (Inagaki *et al.*, 1996), and functional as a protective factor in ischemia by mediating APD (Suzuki *et al.*, 2002), increasing evidence suggests that this  $K_{ir}6.2/SUR2A$  complex is not the complete story in ischaemic protection. Furthermore, the  $K_{ir}6.2/SUR2A$  channel opened by ATP depletion, such as during ischaemia, is known to shorten APD leading to electrical failure of the action potential and so contractile failure (Brennan *et al.*, 2015). A study has demonstrated that there is a decreased heart rate following  $K_{ir}6.1$  specific inhibition with PNU which suggests  $K_{ir}6.1$  could be a factor in mediating APD (Hsu *et al.*, 2012). Additionally,  $K_{ir}6.1$  KO mice show a prolonged APD in cardiomyocytes, giving additional supporting evidence of a role for the  $K_{ir}6.1$  channel in mediating APD in cardiomyocytes (Tong *et al.*, 2006). In the presented data, shRNA knockdown  $K_{ir}6.1$  did prolong the cardiomyocyte APD as well as cause a significant depolarisation of the resting membrane potential. Moreover, addition of 3  $\mu$ M PNU causes a significant APD prolongation and resting membrane potential depolarisation in 24 h cultured myocytes yet has no further effect following  $K_{ir}6.1$  knockdown. These findings add more evidence that the  $K_{ir}6.1$ -containing channel plays a functional role in modulating the cardiac action potential and the resting membrane potential. In addition, the results from whole-cell recording configuration indicates the  $K_{ir}6.2$  did not play a role in resting condition, which shows no difference in whole cell leak currents but a significant reduces the peak currents in MI. This finding fits well with the previous study in our lab (Brennan *et al.*, 2015) in which the accepted cardiac  $K_{ATP}$  ( $K_{ir}6.2/SUR2A$ ) channel opening is in response to the depletion of ATP (or rise of ADP) and results in cardiac contractile failure to preserve the remaining ATP to maintain  $Ca^{2+}$  homeostasis. Finally, APD recordings from  $K_{ir}6.2$  knockdown myocyte further suggest the  $K_{ir}6.2$ -containing channel was not involved in modulating cardiac action potential duration in resting conditions, with no change in resting membrane potential or action potential duration compared with 24 h culture or negative-control virus infection. This result agreed with previous report that no differences can be seen in action potential duration between control or  $K_{ir}6.2$ -knockout mice, in terms of resting membrane potential or APD (Suzuki *et al.*, 2001, 2002).

In summary, the data in this chapter presents evidence that the sarcolemmal  $\sim 39$  pS-conductance channel identified on the cardiomyocyte surface membrane contains a  $K_{ir}6.1$ -pore forming subunit. This has been demonstrated using shRNA knockdown with 2 different  $K_{ir}6.1$  specific targeting shRNA. In addition, the data demonstrates a functional role for the  $K_{ir}6.1$ -containing channel in modulating the cardiac action potential and  $Ca^{2+}$  transient. The ability of this current to modulate the action potential and resting membrane potential leads to the question that whether  $K_{ir}6.1$  plays a role in cardioprotection? Previous publication from our group show that opening of the “conventional” sarcolemmal  $K_{ATP}$  channel ( $K_{ir}6.2/SUR2A$ ) is actually delayed in metabolic stress following cardioprotective stimuli (Brennan *et al.*, 2015). Given the pharmacological evidence that  $K_{ATP}$  channels are involved in cardioprotection, and the evidence that  $K_{ir}6.1$  activity is markedly increased in culture affecting action potential and membrane potential, makes a  $K_{ir}6.1$  sarcolemmal channel an interesting candidate for further investigation.

## **Chapter 5**

**The physiological role of  $K_{ir}6.1$ /SUR2B channel at  
the cardiomyocyte cell surface.**

## 5.1 Introduction

In the previous results chapters, the  $K_{ir}6.1/SUR2B$  channel complex was demonstrated to be expressed at the cardiomyocyte membrane surface. It was shown that this  $K_{ir}6.1/SUR2B$  current was active in normal physiological conditions in cardiomyocytes of all species tested; however, the physiological relevance of this constitutive activity remained unclear. In this chapter, the significance of the function of the sarcolemmal  $K_{ir}6.1/SUR2B$  current was investigated, using pharmacological inhibition and genetic knockdown of both the pore forming and  $\beta$ -subunits.

In addition to patch clamp electrophysiological recording, phenotypic functional experiments investigating contractile function and fluorescence imaging was used. In the contractile function phenotypic screen, cardiomyocytes were perfused at a constant temperature of  $32\pm 2^\circ\text{C}$  and stimulated to contract using electric field stimulation (EFS) at 1 Hz. This protocol allowed assessment of the functional outcomes following simulated ischaemia and reperfusion using a metabolic inhibition and washout (reperfusion) (MI/R) protocol. By using pharmacological modulation, or genetic knockdown, the contribution of the  $K_{ir}6.1/SUR2B$  current could be investigated. The perfusion sequence of the MI/R protocol is shown in Figure 5.1A. Using this established protocol, the degree of cardioprotection of the cell preparation can be assessed where typically between 30 and 40% recover contractile function following 10 minutes of washout and ~70% of cells survive, as measured by Trypan blue exclusion. Any cell preparation with a contractile recovery greater than 40% was considered as cardioprotected and so was not used for experimentation. By measuring the percentage contractile recovery at the end of reperfusion, a cardioprotective or cardiotoxic effect of a treatment can be revealed in each condition. This protocol was also used for fluorescence imaging experiments, where the changes in intracellular accumulation of  $\text{Ca}^{2+}$  and  $\text{Mg}^{2+}$  are also established measures of a cardioprotected phenotype.

To investigate the role of  $K_{ir}6.1/SUR2B$  channels in cardiomyocytes, PNU37883A was used to inhibit the  $K_{ir}6.1/SUR2B$  complex to investigate whether there was a direct effect of its activity on cellular function in freshly isolated cardiomyocytes. Following on from this, it was further investigated in cultured cardiomyocytes following  $K_{ir}6$  and SUR isoform-specific knockdown.

It was hypothesised that, given the channels constitutive activity in resting physiological conditions, that this  $K_{ir}6.1/SUR2B$  current plays a role in regulating action potential duration and resting membrane potential. Furthermore, it was hypothesised that the inhibition of this channel would have a cardiotoxic effect when investigated using the MI/R protocol by its potentially depolarising effect on the membrane potential and a prolongation of the action potential.

## 5.2 Results

### 5.2.1 The effect of pharmacological inhibition of $K_{ir}6.1/SUR2B$ currents in freshly isolated cardiomyocytes in a metabolic inhibition and reperfusion (MI/R) protocol

Cardiomyocytes were perfused for 3 min with NT, 7 min SFT-MI and then washed out with 10 min NT as indicated in Figure 5.1A. The numbers of contractile cardiomyocytes were counted every 30 s throughout the protocol to construct time course data (Figure 5.1B (i)). Figure 5.1B (ii) shows the mean time to contractile failure in SFT-MI perfusion in both control and 3  $\mu$ M PNU-treated groups. With PNU present in all solutions, the time to contractile failure was significantly shortened, from  $154.0 \pm 1.9$  s (control, 6 experiments, 102 cells) to  $120.1 \pm 5.1$  s (PNU treatment, 6 experiments, 143 cells, \*\*\* $p < 0.001$ ; Student's unpaired t-test). Figure 5.1B (iii) shows the mean percentage of contractile recovery at the end of the protocol, showing  $32.0 \pm 1.2\%$  ( $n=6$ ) contractile recovery in the control group but with a lower recovery rate in the PNU-treated group  $23.8 \pm 3.4\%$  ( $n=6$ , \* $p < 0.05$ ; Student's unpaired t-test). Figure 5.1B (iv) shows the mean percentage of cell survival at the end of NT reperfusion. The percentage of cell survival in PNU treatment group significantly decreased, from  $76.2 \pm 3.4\%$  (control,  $n=6$ ) to  $68.0 \pm 1.2\%$  (PNU treatment,  $n=6$ , \*\*  $p < 0.01$ ; Student's unpaired t-test).

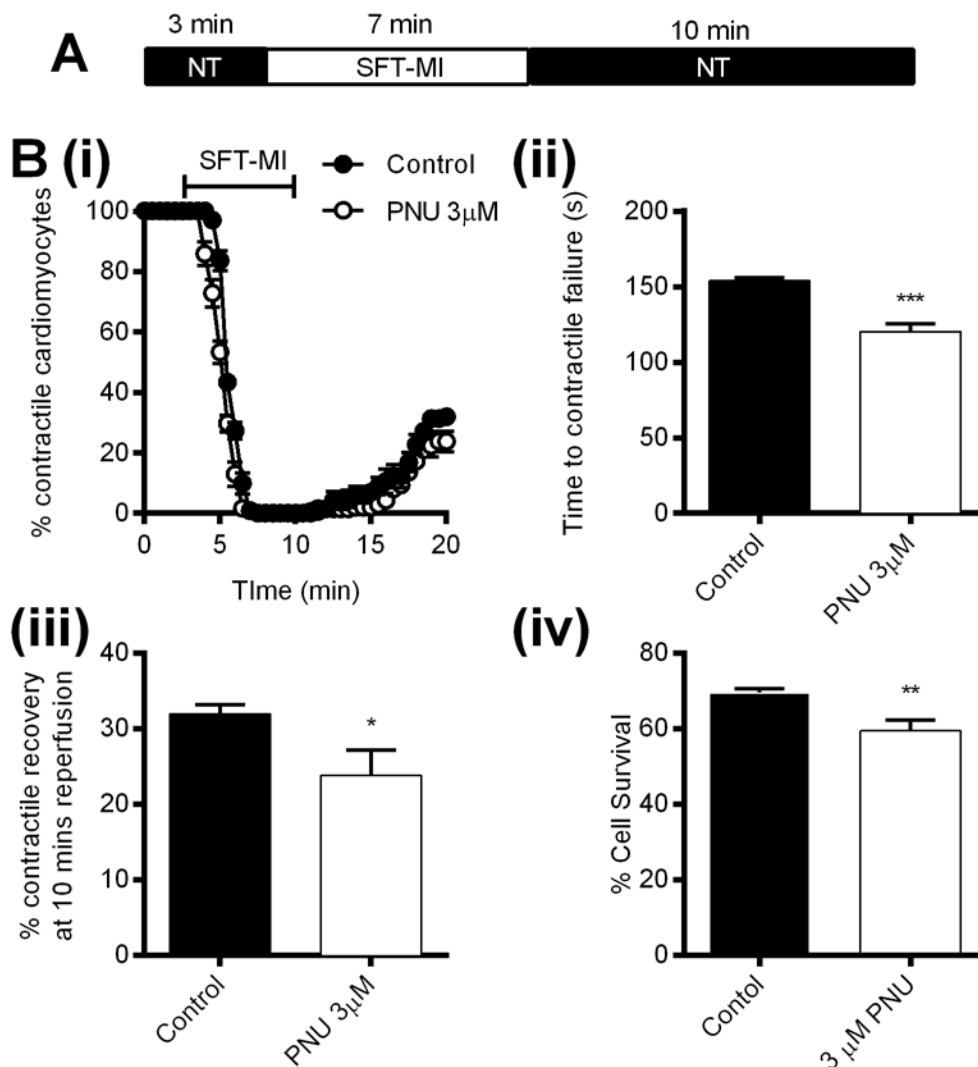


**Figure 5.1: 3  $\mu$ M PNU treatment leads to early contractile failure, decreased contractile recovery and decreased cell survival with a metabolic inhibition and reperfusion (MI/R) protocol.** A, An outline of the MI/R protocol where cardiomyocytes were perfused with NT solution (3 min) followed by SFT-MI (7 min), then re-perfused with NT for the final 10 min. The whole protocol was procced at  $34 \pm 2$   $^{\circ}$ C and contractions were triggered by 1 Hz EFS. B(i), Example time course traces showing the percentage of contractile cardiomyocytes throughout the MI/R protocol in control and PNU (3  $\mu$ M) treated cardiomyocytes. (ii), Bar chart showing the mean time to contractile failure in MI, ( $154.0 \pm 1.9$  s ( $n=6$ ) in control group and  $120.1 \pm 5.1$  s ( $n=6$ , \*\*\* $p < 0.001$ ; Student unpaired t-test)). (iii), Mean percentage of contractile recovery following MI/R for both control and PNU treatment group with  $32.0 \pm 1.2\%$  ( $n=6$ ) and  $23.8 \pm 3.4\%$  ( $n=6$ , \*  $p < 0.05$ ; Student unpaired t-test) regaining contractile function respectively. (iv), The mean percentage of cell survival at the end of reperfusion was shown on bar chats, with  $76.2 \pm 3.4\%$  ( $n=6$ ) in control and  $68.0 \pm 1.2\%$  ( $n=6$ , \*\* $p < 0.01$ ; Student unpaired t-test) in PNU treatment group.

Although there was a significant reduction in contractile recovery, suggesting a potentially cardiotoxic effect of PNU, the 7 min MI/R protocol is designed to look for improvements in protection rather than abolition. A protocol using a shorter duration of SFT-MI, 5 min, is used in the laboratory as a standard protocol for investigating treatments potentially cardiotoxic in control cells. Using this modified MI/R protocol, Figure 5.2B (iii) a larger difference in percentage of contractile recovery was seen, from  $68.1 \pm 2.1\%$  (6 experiment, 158 cells) in control group to  $36.8 \pm 2.7\%$  (6 experiment, 136 cells,  $***p < 0.001$ ; Student's unpaired t-test) in PNU-treated group. Moreover, there was a significant decrease in the percentage of cell survival, from  $89.2 \pm 2.1\%$  (n=6) in control and  $79.7 \pm 1.8\%$  (n=6,  $**p < 0.01$ ; Student unpaired t-test) in PNU treatment group.

These results show that the pharmacological inhibition of the  $K_{ir}6.1/SUR2B$  currents in freshly isolated cardiomyocytes leads to an early contractile failure during metabolic inhibition, as well as lower contractile recovery and fewer cells surviving following reperfusion.

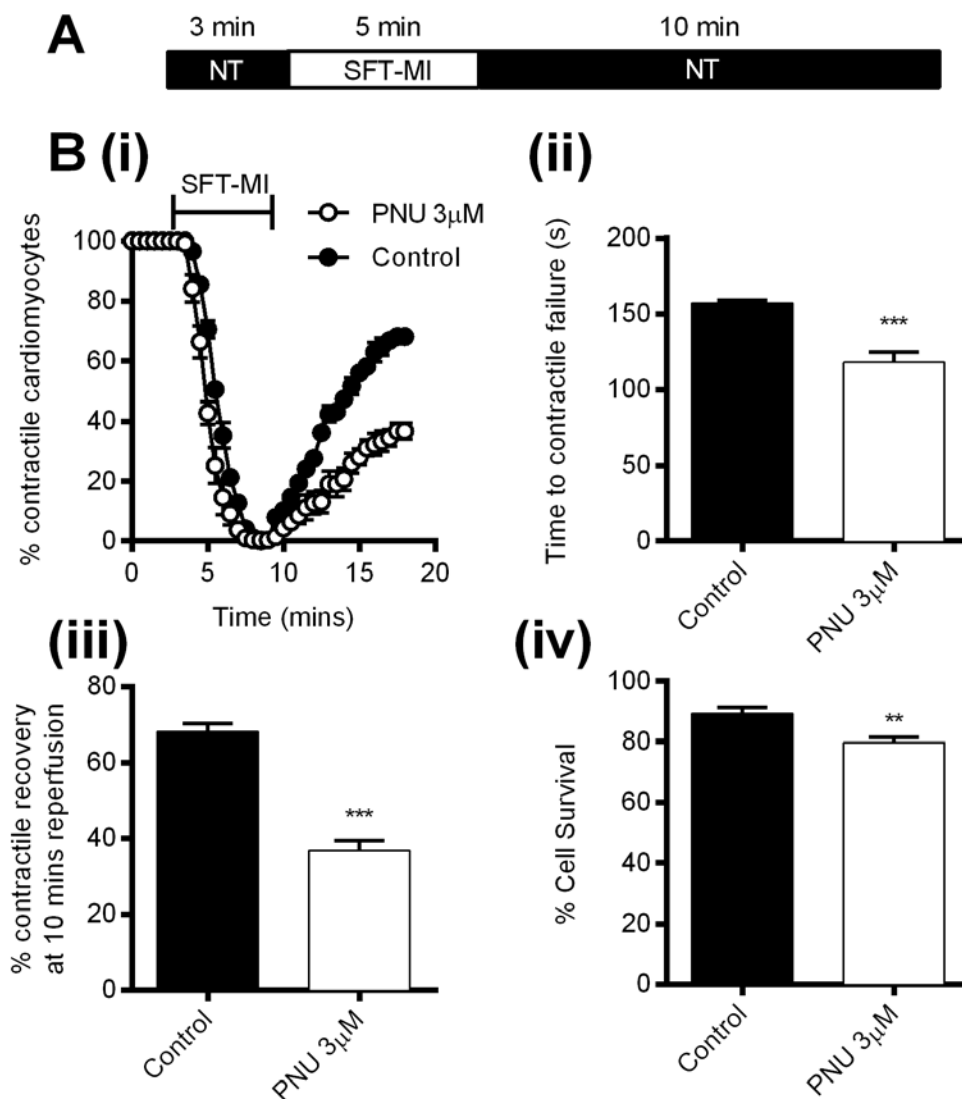


**Figure 5.2: The cardiotoxic effect of 3  $\mu$ M PNU treatments is more clearly revealed using a modified MI/R protocol.** A, A modified MI/R protocol was used in these experiments with a short period of SFT-MI perfusion (5 min) designed to reveal cardiotoxicity. B(i), Example time course traces showing the percentage of contractile cardiomyocytes throughout the MI/R protocol in control and PNU (3  $\mu$ M) treated cardiomyocytes. (ii), Bar chart showing the mean time to contractile failure in MI, with  $157.1 \pm 1.8$  s ( $n=6$ ) in control group and  $117.9 \pm 6.7$  s ( $n=6$ , \*\*\*  $p < 0.001$ ; Student unpaired t-test) in the PNU group. (iii), Mean percentage of contractile recovery after the modified MI/R for both control and PNU treatment group with  $68.1 \pm 2.1$ % ( $n=6$ ) and  $36.8 \pm 2.7$ % ( $n=6$ , \*\*\*  $p < 0.001$ ; Student unpaired t-test) respectively. (iv), The mean percentage of cell survival was shown on bar charts, with  $89.2 \pm 2.1$ % ( $n=6$ ) in control and  $79.7 \pm 1.8$ % ( $n=6$ , \*\*  $p < 0.01$ ; Student unpaired t-test) in PNU treatment group.

Experiments carried out by Dr Sean Brennan.

### 5.2.2 The effect of isoform-specific subunit knockdown on cardiomyocyte contractile recovery and survival in MI/R.

To investigate the effects of a loss of function of different  $K_{ATP}$  channel subunits in cardiomyocytes,  $K_{ir6.1}$  and  $K_{ir6.2}$  were selectively knocked down and their contractile recovery rate, as well as percentage cell survival, was measured following the MI/R protocol as outlined above. Figure 5.3 shows there was no difference in contractile recovery between negative control virus-infected group and the 24 h cultured control group in both percentages of contractile recovery and cell survival, however selective knockdown of  $K_{ir6.1}$  isoforms resulted in a significant reduction in contractile recovery following the MI/R protocol, from  $65.4 \pm 2.0\%$  (24 h control,  $n=27$ ) to  $39.7 \pm 3.1\%$  ( $K_{ir6.1}$  KD,  $n=14$ ,  $***p < 0.001$ ). Additionally,  $K_{ir6.2}$  KD also decreased the contractile recovery in MI/R protocol from  $65.4 \pm 2.0\%$  (24 h control,  $n=27$ ) to  $51.0 \pm 2.2\%$ ,  $n=9$ ,  $***p < 0.005$ ; one-way ANOVA with Holm-Sidak post-test) respectively. In terms of cell survival following simulated reperfusion,  $K_{ir6.1}$  KD significantly reduced the percentage cell survival compared with 24 h cultured control group, from  $92.4 \pm 1.4\%$  (24 h control,  $n=21$ ) to  $81.0 \pm 2.0\%$  ( $K_{ir6.1}$  KD,  $n=14$ ,  $***p < 0.001$ ; one-way ANOVA with Holm-Sidak post-test). Interestingly, no reduction was seen in  $K_{ir6.2}$  KD ( $88.6 \pm 1.8\%$ ,  $n=6$ ). The similar results in contractile recovery and cell survival in both 24 h culture control and virally infected negative control suggests that the process of infection does not adversely influence the cells functional recovery following the MI/R protocol.

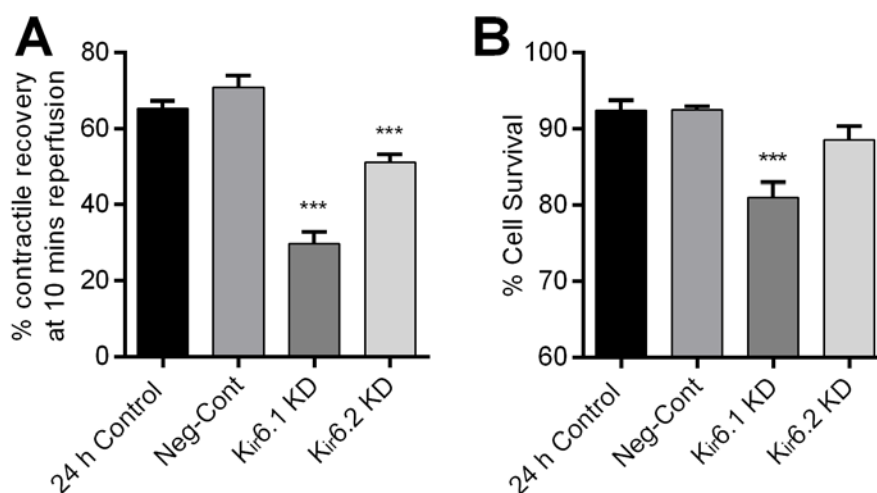


**Figure 5.3: Contractile recovery and percentage cell survival was reduced in  $K_{ir}6.1$  KD and  $K_{ir}6.2$  KD infected cells compared with 24 h cultured and negative control.** A, Bar chart showed the mean data of percentage contractile recovery in 24 h control, negative control,  $K_{ir}6.1$  KD and  $K_{ir}6.2$  KD. Both  $K_{ir}6.1$  KD and  $K_{ir}6.2$  KD reduce the percentage contractile recovery significantly, from  $65.4 \pm 2.0\%$  (24 h control,  $n=27$ ) to  $39.7 \pm 3.1\%$  ( $K_{ir}6.1$  KD,  $n=14$ , \*\*\*  $p < 0.001$ ); from  $65.4 \pm 2.0\%$  (24 h control,  $n=27$ ) to  $51.0 \pm 2.2\%$ ,  $n=9$ , \*\*\*  $p < 0.005$ ; one-way ANOVA with Holm-Sidak post-test). B, Mean data of percentage cell survival after reperfusion showed no difference between 24 h control, negative control and  $K_{ir}6.2$  KD; but significantly reduced in  $K_{ir}6.1$  KD myocyte, from  $92.4 \pm 1.4\%$  (24 h control,  $n=21$ ) to  $81.0 \pm 2.0\%$  ( $K_{ir}6.1$  KD,  $n=14$ , \*\*\*  $p < 0.001$ ; one-way ANOVA with Holm-Sidak post-test).

Further experiments were carried out on cardiomyocytes following  $\beta$ -subunit knockdown. Figure 5.4A demonstrates that the percentage contractile recovery was reduced following SUR2B knockdown, from  $65.4 \pm 2.0\%$  (24 h control,  $n=27$ ) to  $41.4 \pm 3.1\%$  (SUR2B KD,  $n=8$ , \*\*\* $p < 0.001$ ). However, no reduction was seen following SUR2A KD ( $71.0 \pm 5.2\%$ ,  $n=7$ ; one-way ANOVA with Holm-Sidak post-test). A similar trend was observed in percentage cell survival, where figure 5.4B illustrates SUR2B KD significantly reduced the percentage cell survival from  $92.4 \pm 1.4\%$  (24 h control,  $n=21$ ) to  $78.5 \pm 3.4\%$  (SUR2B KD,  $n=6$ , \*\*\* $p < 0.001$ ). Conversely, selective knockdown of SUR2A did not significantly affect the outcome ( $95.8 \pm 1.0\%$ ,  $n=7$ ; one-way ANOVA with Holm-Sidak post-test), compared with 24 h culture control/negative control virus-infected cells.

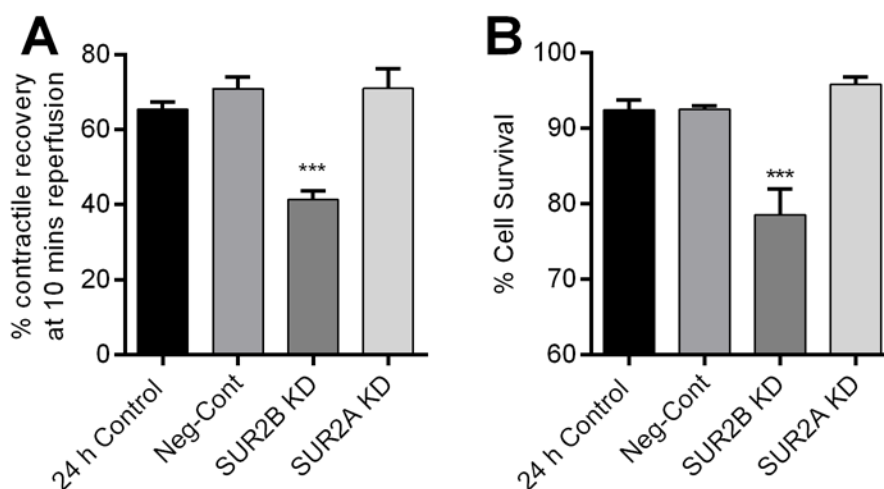


**Figure 5.4: Decreasing in contractile recovery rate and percentage cell survival after MI/R protocol on SUR2B KD myocytes compared with 24 h control and negative control.** A, Bar chart shown the mean data of percentage contractile recovery in 24 h control, negative control, SUR2B KD and SUR2A KD. SUR2B KD reduce the percentage contractile recovery significantly, from  $65.4 \pm 2.0\%$  (24 h control,  $n=27$ ) to  $41.4 \pm 3.1\%$  (SUR2B KD,  $n=8$ , \*\*\*  $p < 0.001$ ; one-way ANOVA with Holm-Sidak post-test); no reduction can be seen in SUR2A KD ( $71.0 \pm 5.2\%$ ,  $n=7$ ). B, Mean data of percentage cell survival after reperfusion showed no difference between 24 h control, negative control and SUR2A KD; but significantly reduced in SUR2B KD myocyte, from  $92.4 \pm 1.4\%$  (24 h control,  $n=21$ ) to  $78.5 \pm 3.4\%$  (SUR2B KD,  $n=6$ , \*\*\*  $p < 0.001$ ; one-way ANOVA with Holm-Sidak post-test).

When PNU treatment was used to pharmacologically inhibit the  $K_{ir}6.1$ -containing channel, all 24 h culture control, negative control and  $K_{ir}6.2$  KD groups showed a smaller contractile recovery and cell survival following the MI/R protocol. Figure 5.5A demonstrates that  $3 \mu\text{M}$  PNU treatment reduced the percentage of contractile recovery in 24 h control, negative control and  $K_{ir}6.2$  KD myocytes, from  $65.4 \pm 2.0\%$  (24 h control,  $n=27$ ) to  $46.0 \pm 2.2\%$  (24 h control-PNU,  $n=6$ ; \*\*\*  $p < 0.001$ ),  $70.9 \pm 3.1\%$  (negative control,  $n=8$ ) to  $44.3 \pm 2.2\%$  (negative control-PNU,  $n=8$ , \*\*\*  $p < 0.001$ ) and  $51.0 \pm 2.2\%$  ( $K_{ir}6.2$  KD,  $n=9$ ) to  $34.5 \pm 2.7\%$  ( $K_{ir}6.2$  KD,  $n=7$ , \*\*\*  $p < 0.001$ ; two-way ANOVA with Holm-Sidak post-test) respectively. The same trend is shown in Figure 5.5B, where the percentage cell survival after  $3 \mu\text{M}$  PNU treatments was also decreased, from  $92.4 \pm 1.4\%$  (24 h control,  $n=21$ ) to  $79.8 \pm 4.5\%$  (24 h control-PNU,  $n=4$ ; \*\*\*  $p < 0.001$ ),  $92.5 \pm 0.5\%$  (negative control,  $n=8$ ) to  $78.6 \pm 1.8\%$  (negative control-PNU,  $n=6$ , \*\*\*  $p < 0.001$ ) and  $88.6 \pm 1.8\%$  ( $K_{ir}6.2$  KD,  $n=8$ ) to  $73.1 \pm 4.2\%$  ( $K_{ir}6.2$  KD-PNU,  $n=7$ , \*\*\*  $p < 0.001$ ; two-way ANOVA with Holm-Sidak post-test).

Taken together, these data with isoform-specific knockdown suggests that the SarcoK<sub>ir</sub>6.1/SUR2B currents play a vital role in the normal physiological responses in cardiomyocytes where either K<sub>ir</sub>6.1 or SUR2B specific knockdown can significantly reduce both percentage contractile recovery and cell survival, following MI/R. K<sub>ir</sub>6.2 knockdown also reduces the percentage contractile recovery however, perhaps surprisingly, there is no worsening in the percentage of cell survival following reperfusion. The outcome may be due to the regulation of Ca<sup>2+</sup> transient by K<sub>ir</sub>6.1-containing channels that are still functional in K<sub>ir</sub>6.2 KD myocytes, so preventing the myocyte from overloading with Ca<sup>2+</sup> during metabolic stress so reducing Ca<sup>2+</sup> overload-induced damage on reperfusion.

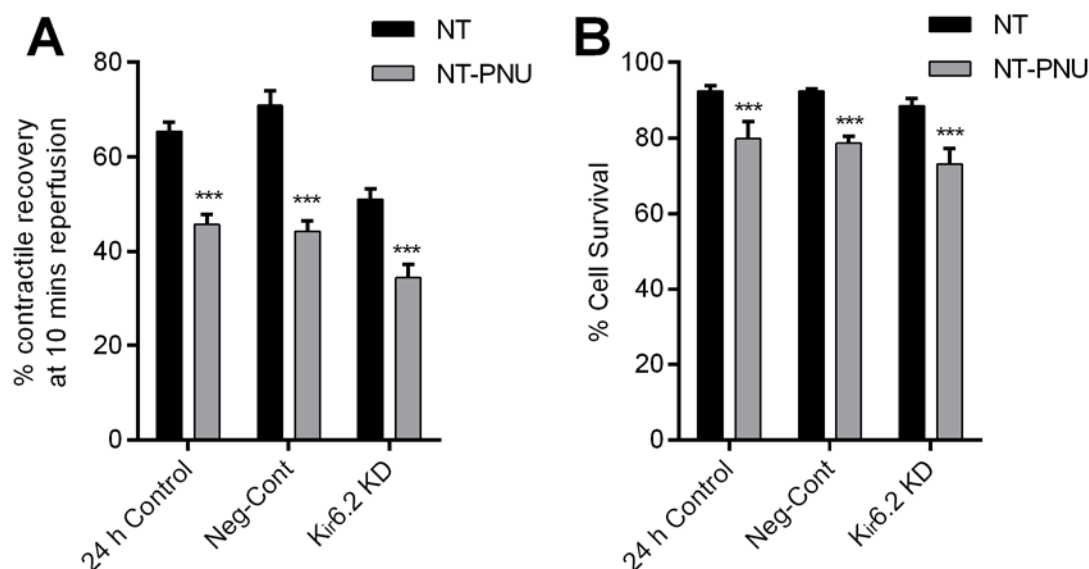


**Figure 5.5: 3  $\mu$ M PNU treatments reduce contractile recovery following a MI/R protocol as well as percentage cell survival in 24 h control, negative control and K<sub>ir</sub>6.2 KD.** A, Bar charts showing 3  $\mu$ M PNU treatment reduces contractile recovery percentage in 24 h control, negative control and K<sub>ir</sub>6.2 KD myocytes, from 65.4 $\pm$ 2.0% (24 h control, n=27) to 46.0 $\pm$ 2.2% (24 h control-PNU, n=6; \*\*\*p<0.001), 70.9 $\pm$ 3.1% (negative control, n=8) to 44.3 $\pm$ 2.2% (negative control-PNU, n=8, \*\*\*p<0.001) and 51.0 $\pm$ 2.2% (K<sub>ir</sub>6.2KD, n=9) to 34.5 $\pm$ 2.7% (K<sub>ir</sub>6.2 KD, n=7, \*\*\*p<0.001; two-way ANOVA with Holm-Sidak post-test) respectively. B, Mean data of percentage cell survival after reperfusion showed 3  $\mu$ M PNU significantly reduce the percentage cell survival in 24 h control, negative control and K<sub>ir</sub>6.2 KD myocytes, from 92.4 $\pm$ 1.4% (24 h control, n=21) to 79.8 $\pm$ 4.5% (24 h control-PNU, n=4; \*\*\*p<0.001), 92.5 $\pm$ 0.5% (negative control, n=8) to 78.6 $\pm$ 1.8% (negative control-PNU, n=6, \*\*\*p<0.001) and 88.6 $\pm$ 1.8% (K<sub>ir</sub>6.2KD, n=8) to 73.1 $\pm$ 4.2% (K<sub>ir</sub>6.2 KD-PNU, n=7, \*\*\*p<0.001; two-way ANOVA with Holm-Sidak post-test) respectively

### 5.2.3 $K_{ir}6.1$ knockdown causes early calcium and magnesium accumulation during metabolic inhibition.

Contractile function data suggests that  $K_{ir}6.1/SUR2B$  channels play a significant role in normal physiological conditions in cardiomyocytes. It was hypothesised that this occurred by modulating resting membrane potential and the APD (Figure 3.7) as well as  $Ca^{2+}$  transient (Figure 3.8). It was hypothesised that this would also affect intracellular  $Ca^{2+}$  homeostasis and the accumulation of  $Ca^{2+}$ , and depletion of ATP, during metabolic inhibition. Previously, data demonstrated that  $K_{ir}6.1$  knockdown could significantly prolong  $APD_{90}$ , compared with 24 h culture cells (Figure 4.10). It was hypothesised that prolongation of  $APD_{90}$  could increase entry of  $Ca^{2+}$  into cardiomyocytes, requiring an increased ATP consumption to remove the  $Ca^{2+}$ , so leading to more rapid depletion of ATP during metabolic inhibition. To further confirm this functional role for the cardiac sarcolemmal  $K_{ir}6.1/SUR2B$  channel, the  $K_{ir}6.1$  gene was knocked down and intracellular  $Ca^{2+}$  and  $Mg^{2+}$  (as a surrogate marker for ATP depletion) measured during the MI/R protocol.

Figure 5.6A (i) & (ii) shows the intracellular  $Ca^{2+}$  change during the MI/R protocol in both 24 h cultured and  $K_{ir}6.1$  knockdown conditions. Fura-2 was used in experiments as a fluorescent indicator for changing  $Ca^{2+}$ . This indicator is used the laboratory as it is a ratiometric indicator. These indicators are useful when investigating contractile cells as the ratio of emitted fluorescence (>520 nm) from the 340:380 excitation wavelengths (with  $Ca^{2+}$ -bound Fura-2 excited by 340 nm light, whilst 380 nm excites the free indicator). By plotting the ratio of fluorescence, rather than  $F/F_0$  as with single wavelength indicators, movement artefacts associated with contraction can be compensated for. In the experiments presented here, it was identified during analysis that only the 340 nm data had been captured due to a hardware failure. As these experiments were designed to investigate a “time to increase” of intracellular  $Ca^{2+}$  fluorescence, just the 340 nm wavelength was used. Each trace was averaged from fluorescence measurements from greater than 6 cells for each experiment, and normalized to maximum fluorescence ( $F_{max}$ ) intensity. Figure 5.6B shows the mean data of time to 50% of  $F_{max}$  intensity during metabolic inhibition. There was a significant difference between 24 h culture and  $K_{ir}6.1$  KD group, with  $350.0 \pm 11.6$  s ( $n=4$ ) to

247.3±31.4 s (n=4, \* p<0.05; Student unpaired t-test) in time to F<sub>50%</sub>. These data indicate that a reduced expression of K<sub>ir</sub>6.1/SUR2B current leads to a more rapid accumulation of Ca<sup>2+</sup> during metabolic inhibition compared with 24 h cultured cardiomyocytes.

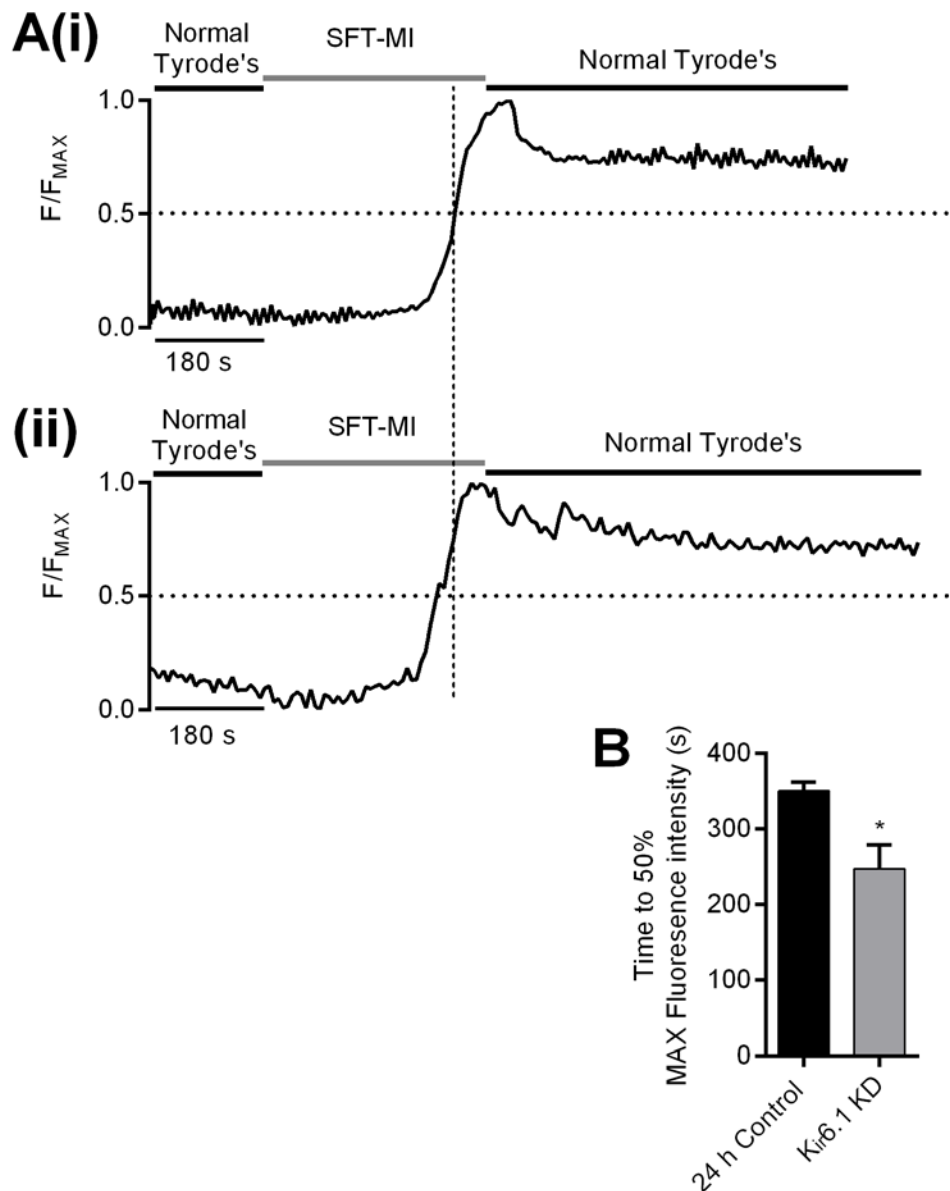


**Figure 5.6: The effect of K<sub>ir</sub>6.1 KD on Ca<sup>2+</sup> during metabolic inhibition.** A(i) & (ii), Example traces showing the calcium fluorescence intensity changing during MI/R protocol in 24 h cultured cardiomyocyte and 24 h K<sub>ir</sub>6.1 knockdown cardiomyocyte respectively. Fura-2 was used as Ca<sup>2+</sup> indicator the 340 nm wavelength channel was used to determine the intercellular Ca<sup>2+</sup> concentration. B, Time to 50% maximum fluorescence intensity was measured in both cultured and K<sub>ir</sub>6.1 KD group, with 350.0±11.6 s (n=4) and 247.3±31.4 s (n=4, \*p<0.05; Student unpaired t-test) respectively.

Magnesium Green (MgGreen) is a fluorescent indicator that binds to free intracellular  $Mg^{2+}$ . As most intracellular  $Mg^{2+}$  is normally bound to ATP, an increase in cytosolic  $Mg^{2+}$  is a surrogate marker of a decrease in intracellular ATP. To determine whether knockdown  $K_{ir}6.1/SUR2B$  increased the rate of ADP accumulation/ATP depletion, MgGreen fluorescence was measured in 24 h control,  $K_{ir}6.1$  knockdown and SUR2B knockdown cardiomyocytes. Figure 5.7A (i), (ii) and (iii) shows the  $Mg^{2+}$  fluorescence change during MI/R protocol. Similar to the  $Ca^{2+}$  fluorescence analysis, each trace was averaged from >6 cells from each experiment. All traces were normalized so the  $F_{max}=1$ . Example traces in Figure 5.7A shows the selective knockdown of  $K_{ir}6.1$  or SUR2B shortens the time to 50% maximal fluorescence of  $Mg^{2+}$  green during metabolic inhibition. Figure 5.7B shows the mean time to 50%  $F_{max}$  in selective knockdown on  $K_{ir}6.1$  and SUR2B, with  $243.2\pm 9.5$  s ( $K_{ir}6.1$  KD,  $n=6$  \* $p<0.05$ ) and  $256.3\pm 14.1$  s (SUR2B KD,  $n=6$ , \*\* $p<0.01$ ; one-way ANOVA with Holm-Sidak post-test), compared to  $307.3\pm 13.22$  s (24 h culture,  $n=9$ ).

These data are consistent with previous results with  $Ca^{2+}$  fluorescence measurements suggesting that an absence of  $K_{ir}6.1$  expression leads to more rapid  $Ca^{2+}$  overload during metabolic inhibition so increasing the rate of ATP consumption. This leads to a more substantial intracellular  $Ca^{2+}$  at reperfusion, and so a greater potential for reperfusion injury.

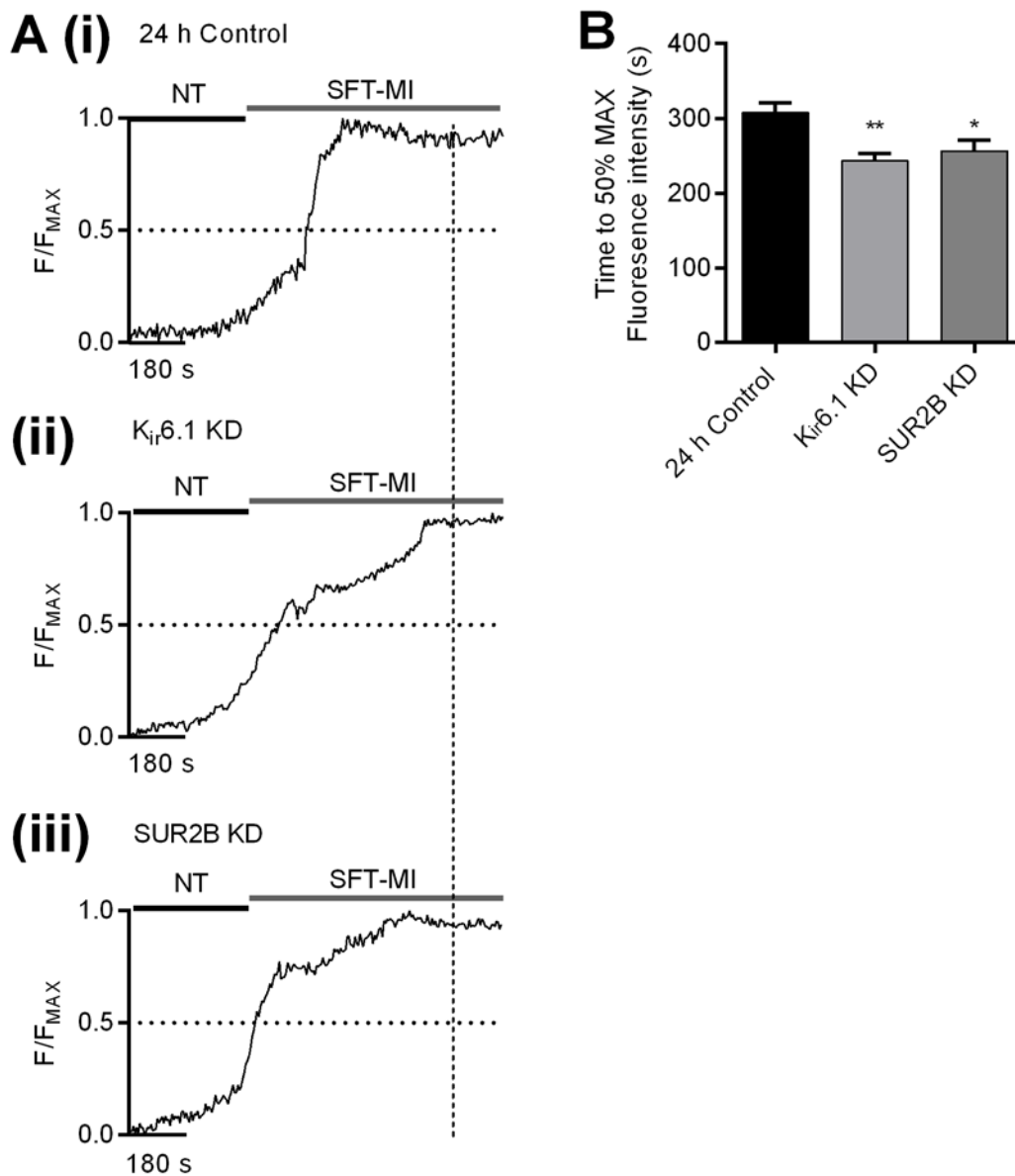


**Figure 5.7: The effects of subunit knockdown on the changes in Magnesium Green fluorescence intensity on 24 h cultured, Kir6.1 knockdown and SUR2B knockdown cardiomyocyte.** A(i), (ii) & (iii), Example traces showed the change of magnesium green intensity during MI/R protocol, in 24 h cultured, Kir6.1 KD and SUR2B KD respectively. B, Time to 50% maximum fluorescence intensity was measured in 24 h cultured, Kir6.1 KD and SUR2B KD group, with 307.3±13.22 s (n=9), 243.2±9.5 s (n=6\* p<0.05; one-way ANOVA Holm-Sidak post-test) and 256.3±14.1 s (n=6, \*\*p<0.01; one-way ANOVA with Holm-Sidak post-test) respectively.

### 5.3 Discussion

The data in this chapter illustrates the importance of the  $K_{ir}6.1/SUR2B$  channel complex on the cardiomyocyte sarcolemmal membrane. The data suggest that the channel is playing a significant role in regulating  $[Ca^{2+}]_i$  and the utilisation of intracellular ATP, during metabolic inhibition, by fine-tuning the resting membrane potential and action potential duration. By using specific pharmacological inhibitors of  $K_{ir}6.1$ , the function of this channel was investigated using MI/R protocol on freshly isolated cells. To study this in more detail, the effect of  $K_{ir}6.1$ ,  $K_{ir}6.2$ , SUR2A and SUR2B shRNA knockdown along with infection with a negative control virus was also illustrated during a MI/R protocol. Viewing the results in this phenotypic assay, both  $K_{ir}6.1$  and SUR2B knockdown have a significantly cardiotoxic effect, but knockdown of  $K_{ir}6.2$  or SUR2A did not, when compared to the negative-control adenoviral infection. Furthermore, the  $Ca^{2+}$  and  $Mg^{2+}$  fluorescence imaging gave additional supporting evidence that the absence of  $K_{ir}6.1$  channel leads to both more rapid depletion in ATP and accelerated accumulation in intracellular  $Ca^{2+}$  during metabolic inhibition. These data suggest that this  $K_{ir}6.1/SUR2B$  channel plays an important physiological role in the control of electrical activity in resting conditions.

It is well documented in the literature that the shortening of APD allows less  $Ca^{2+}$  entry into cardiomyocyte, reducing intracellular  $Ca^{2+}$  overload, so resulting in reduced ischemic injury (Fryer *et al.*, 1999; Bernardo *et al.*, 1999; Patel *et al.*, 2002). In much of the literature,  $K_{ir}6.2/SUR2A$  is considered as the conventional cardiac  $K_{ATP}$  isoform which demonstrates cardiotoxicity after  $K_{ir}6.2$  knockdown (Suzuki *et al.*, 2001; Du *et al.*, 2014), increasing infarct size *in vivo* in ischemia/injury model. The data presented in Figure 5.3A fit in with previous literature that cardiac sarcolemmal  $K_{ir}6.2$ -containing channel plays an important role in cardioprotection, which after knockdown  $K_{ir}6.2$  in cardiomyocyte the cell survival in reperfusion was significantly decreased after MI/R protocol.

Perhaps somewhat opposed to this hypothesis of  $K_{ir}6.2/SUR2A$  being involved in cardioprotection comes from previous research from the host laboratory (Brennan *et al.*, 2015). In this study, it was suggested that the conventional cardiac  $K_{ATP}$  ( $K_{ir}6.2/SUR2A$ ) channel complex shows a delayed opening during the metabolic inhibition, which coincides with the delayed time to contractile failure. This suggests the opening of this conventional

cardiac  $K_{ATP}$  is in fact responding to ATP depletion, limiting further ATP consumption via decreasing cell contraction and reducing the damage from  $Ca^{2+}$  overload following reperfusion after metabolic stress. The timing of the opening of the  $K_{ir}6.2/SUR2A$  complex was dependent on the ATP/ADP ratio of the cell and the rate at which it declined. However, the delayed opening of  $K_{ir}6.2/SUR2A$  in metabolic stress in cardioprotected cells suggest that there is another cardioprotective factor active in the preceding ischemia that limits the consumption of intracellular ATP, or maintains ATP synthesis for longer, and delayed the  $K_{ir}6.2/SUR2A$  opening time so delaying contractile failure. The newly discovered cardiac  $K_{ir}6.1/SUR2B$  becomes a potential candidate due to its relative ATP-insensitivity allowing it to be constitutively active.

In the literature, not only do  $K_{ir}6.1$ -null animals show a high mortality rate suffering cardiac syndromes such as Prinzmetal angina and sudden cardiac death, but also in the clinic the mutation of  $K_{ir}6.1$  is highly associated with sudden infant death syndrome and Brugada syndrome, all showing ST-elevation on ECG recordings (Miki *et al.*, 2002b; Tester *et al.*, 2011; Nakaya, 2014). In addition, previous literature shows that a vascular-specific knockout of  $K_{ir}6.1$  did not develop ST-segment elevation when measuring ECG (Aziz *et al.*, 2014), where in full knockout animals this ST-elevation suggested myocardial injury (Stoller *et al.*, 2010). Furthermore, use of ergonovine to induce vasoconstriction in the vascular-specific  $K_{ir}6.1$  knockdown can also cause heart block followed by sudden death, however only ST-depression was seen in ECG (Aziz *et al.*, 2014), which is associated with coronary damage rather than myocardial infarction in the clinic (Sclarovsky *et al.*, 1988; Diderholm, 2002). These papers suggest that  $K_{ir}6.1$  play an essential role in maintaining resting cardiac function by an effect either from the vasculature, or in the cardiomyocytes themselves.

The data presented in this chapter supports the hypothesis that these damaging effects may be due to effects in the cardiomyocytes. During the MI/R protocol, cell contractile function was recorded and the time to contractile failure in each cell during metabolic inhibition was noted, as was the percentage contractile recovery and cell survival at the end of reperfusion. On treatment with 3  $\mu$ M PNU to block the  $K_{ir}6.1$  channel, both the time to contractile failure and the rate of contractile recovery on reperfusion were significantly reduced with

increasing cell death, suggesting the pharmacological inhibition of this channel has a cardiotoxic effect. A similar trend was seen in knockdown cardiomyocytes, where either  $K_{ir}6.1$  or SUR2B subunits knockdown significantly decreased the percentage of cell recovery after reperfusion.

These data suggest the absence of  $K_{ir}6.1$  reduces cell survival following metabolic inhibition, suggesting that  $K_{ir}6.1/SUR2B$  plays a key role in normal physiological control of membrane potential and the cardiac action potential.

Furthermore, the earlier contractile failure time in PNU treatment group can be seen, compare to the control group, suggests that the  $K_{ir}6.1/SUR2B$  current plays an important protective role during the metabolic stress by limiting the consumption of intracellular ATP so that the heart remains functional. Given this modulation of cellular excitability, it is entirely plausible that this channel may provide a protective effect for cardiomyocyte during metabolic inhibition. In earlier results chapters, it was shown that either pharmacological inhibition or gene knockdown of the  $K_{ir}6.1$  channel, significantly prolonged the action potential duration and the associated  $Ca^{2+}$  transient duration. It was hypothesised that the prolonged APD leads to a greater  $Ca^{2+}$  influx into cells, increases  $Ca^{2+}$  accumulation so resulting in increasing consumption of ATP and infarct size in ischemia. Previous literature supports this hypothesis, where the cardioprotection imparted by ischaemic preconditioning can be blocked by using glibenclamide to suppress  $K_{ATP}$  currents (Gross & Auchampach, 1992), also showing an increased infarct size, as well as low blood glucose.

Interestingly, following  $K_{ir}6.2$  specific knockdown, Figure 5.3B, shows there was no decrease in cell survival after MI/R protocol. It is hypothesised that although the  $K_{ir}6.2$  subunits were knocked down in cardiomyocytes, the expression of  $K_{ir}6.1$  was still able to regulate action potential duration. This limited the entry of  $Ca^{2+}$  so preventing intracellular  $Ca^{2+}$  overload during hypoxia (or metabolic inhibition) and therefore reduced the number of cells that entered a state of hypercontracture on reperfusion. Therefore, the finding here is not against previous literature which well documented that the  $K_{ir}6.2$  is essential for cardioprotection (Suzuki *et al.*, 2001; Budas *et al.*, 2004; Wojtovich *et al.*, 2013; Du *et al.*, 2014). Figure 5.6 and Figure 5.7 support this hypothesis, where in the absence of  $K_{ir}6.1$  subunits, both  $Ca^{2+}$  and  $Mg^{2+}$  accumulation during MI occurs earlier compared with control

cardiomyocytes. Further investigation, using PNU to block the  $K_{ir}6.1$  channel in  $K_{ir}6.2$ -knockdown cardiomyocytes, support this hypothesis, where pharmacological inhibition of the  $K_{ir}6.1$  pore significantly reduced cell survival. These findings suggests the  $K_{ir}6.1/SUR2B$  channel plays an important role in  $Ca^{2+}$  transient regulation in physiological conditions and acts to prevent  $Ca^{2+}$  overload with metabolic stress.

The intracellular  $Ca^{2+}$  was measured during MI/R protocol using a fluorescence measurement system and Fura-2 as a fluorescent indicator. In Figure 5.6A (i) and (ii), a noticeable increase in intracellular  $Ca^{2+}$  concentration was seen during metabolic inhibition, which occurred earlier in cardiomyocytes where  $K_{ir}6.1$  was knockdown (Figure 5.6B). Furthermore,  $Mg^{2+}$  green fluorescence imaging also indicated that knockdown of  $K_{ir}6.1$  channel expression in cardiomyocyte lead to earlier ATP depletion during metabolic inhibition (Figure 5.7). These data support the hypothesis that the cardiac sarcolemmal  $K_{ir}6.1$  channel plays a role in the modulation of the action potential duration and the resting potential, so regulating  $Ca^{2+}$  influx during metabolic inhibition, slowing the rate of ATP depletion and so limiting the potential damage by  $Ca^{2+}$  overload. Such a mechanism would be similar in cardioprotection if the activities of the  $K_{ir}6.1/SUR2B$  current was increased, which will slow down the influx of  $Ca^{2+}$ , protecting the myocyte from  $Ca^{2+}$  overloading and even hypercontractile in reperfusion. Taken together, both results in the fluorescence imaging experiments suggest that the cardiac sarcolemmal  $K_{ir}6.1$  channel has a role in the regulation of intracellular  $Ca^{2+}$  and ATP via modulation of the cardiac action potential duration and the resting membrane potential. However, the absence of  $K_{ir}6.1$  expression in cardiomyocyte caused by any reason had a cardiotoxic effect on the cells.

In conclusion, the results presented in this chapter suggest a key role for the cardiac sarcolemmal  $K_{ir}6.1/SUR2B$  channel complex in modulating membrane potential in normal physiological conditions. A key role for this channel in the response to ischaemia has also be demonstrated using cardiomyocytes perfused with a metabolic inhibition/reperfusion protocol, where both pharmacological or shRNA knockdown of cardiac  $K_{ir}6.1/SUR2B$  reduce recovery following metabolic inhibition. These findings suggest that the newly discovered  $K_{ir}6.1/SUR2B$  channel in cardiomyocytes acts in a regulatory fashion controlling cell membrane potential and action potential duration. In contrast,  $K_{ir}6.2/SUR2A$  acts as a

metabolic sensor when opens in times of severe ATP depletion, leading contractile failure to try and preserve the last remaining intracellular ATP.

With this key regulatory role established, it is hypothesised that an increased  $K_{ir}6.1/SUR2B$  in cardiomyocytes may be cardioprotective via its role in regulating membrane and action potentials, and may link the protective effects of sulphonylurea activators and  $K_{ATP}$  in the heart. This hypothesis will be investigated in the final results chapter.

## **Chapter 6**

**A role for cardiomyocyte sarcolemmal**

**$K_{ir}6.1/SUR2B$  in cardioprotection**

## 6.1 Introduction

In the previous results chapters, the experimental evidence presented suggests that the cardiac sarcolemmal  $K_{ir}6.1/SUR2B$  channel complex plays a significant role in regulating cardiomyocyte function in physiological resting conditions. It was demonstrated that the constitutive activity of this small conductance current could modulate the resting membrane potential and the action potential duration in cardiomyocytes. Furthermore, it was shown that disruption of the  $K_{ir}6.1/SUR2B$  complex either pharmacologically, or using shRNA knockdown, was sufficient to cause a distinct damaging change where  $Ca^{2+}$  overload was worsened in a MI/R protocol.

Given that knockdown or pharmacological inhibition of this small conductance  $K_{ATP}$  current would worsen the damage caused by MI/R, it was hypothesised that an increase in the channel activity could be a putative protective mechanism. In a previous publication from our laboratory (Brennan *et al.*, 2015), it was demonstrated that the  $K_{ir}6.2/SUR2A$  channel is only activated on severe ATP depletion, further demonstrated by a delayed opening following a cardioprotective stimuli, such as ischaemic preconditioning (IPC). This finding is at odds with the literature that demonstrates a connection between sulphonylurea and cardioprotection. Compounds known to activate  $K_{ATP}$  currents, such as diazoxide and pinacidil, have a profoundly cardioprotective effect, whilst compounds such as glibenclamide worsen the outcome following ischaemia. The evidence from our laboratories previous publication is at odds with this finding as sarcolemmal  $K_{ATP}$  ( $K_{ir}6.2/SUR2A$ ) activity is *delayed* after cardioprotection rather than activating early to protect the cells. This finding suggests that there is another cardioprotective factor that is modulated by  $K_{ATP}$  channel openers, which preserves ATP during a metabolic challenge to maintain myocyte function and so cause a delayed opening of  $K_{ir}6.2/SUR2A$ .

Given the data presented in the previous results chapters of a small conductance, relatively ATP-insensitive and constitutively active  $K_{ATP}$  current in cardiomyocytes, it was hypothesised that this newly discovered  $K_{ir}6.1/SUR2B$  may be an important candidate to investigate as a potential effector of cardioprotection.

## 6.2 Results

### 6.2.1 3 $\mu$ M PNU37883A reduces the protection imparted by ischaemic preconditioning.

Ischemic preconditioning (IPC) is a well described cardioprotective mechanism triggered by several brief periods of ischaemia or hypoxia prior to the main ischaemic insult that enhances the tolerance of the myocardium to metabolic stress. To prepare IPC cardiomyocytes, hearts were perfused on a Langendorff canula where, to simulate short periods of ischaemia, perfusion was halted for three 5-min periods, with 5-min of normal perfusion between each break. This halted perfusion mimicked the brief ischaemia/hypoxia that can trigger the IPC phenotype and the resulting isolated cells were then cardioprotected (Figure 6.1A) (Rodrigo & Samani, 2007; Brennan *et al.*, 2015). Previous publications from the laboratory have identified a number of cellular phenotypic responses to metabolic stress that can be used to distinguish cardioprotected and non-cardioprotected cells. This includes; a delay in the time to activation of  $K_{ir}6.2/SUR2A$  current, delayed time to contractile and action potential failure, increased percentage of contractile recovery and an increased percentage of cell survival following metabolic inhibition (Sims *et al.*, 2014; Brennan *et al.*, 2015). Figure 6.1B (i) demonstrates representative traces of the percentage contractile cardiomyocytes during a MI/R protocol, in both IPC control group and treatment with 3  $\mu$ M PNU (IPC-PNU). Mean data demonstrates that in the IPC group, the time to contractile failure in MI was prolonged from  $154.0 \pm 1.9$  s (control, n=6) to  $210.5 \pm 5.3$  s (IPC, n=6, \*\*\* $p < 0.0001$ ). The percentage contractile recovery and cell survival were also increased, from  $32.0 \pm 1.2\%$  (control, n=6) to  $82.9 \pm 3.2\%$  (IPC, n=6); from  $69.6 \pm 1.0\%$  (n=6) in control to  $91.8 \pm 2.3\%$  in IPC group (n=6) respectively. These data demonstrate that IPC cells were cardioprotected as evident from the prolonged time to contractile failure, increased contractile recovery and increased cell survival at the end of the protocol. In the presence of 3  $\mu$ M PNU, there was a reduced time to contractile failure MI ( $168.4 \pm 5.7$  s, n=6) and decreased percentage of contractile recovery ( $45.2 \pm 2.1\%$ , n=6) and cell survival ( $91.8 \pm 2.3\%$ , n=6).

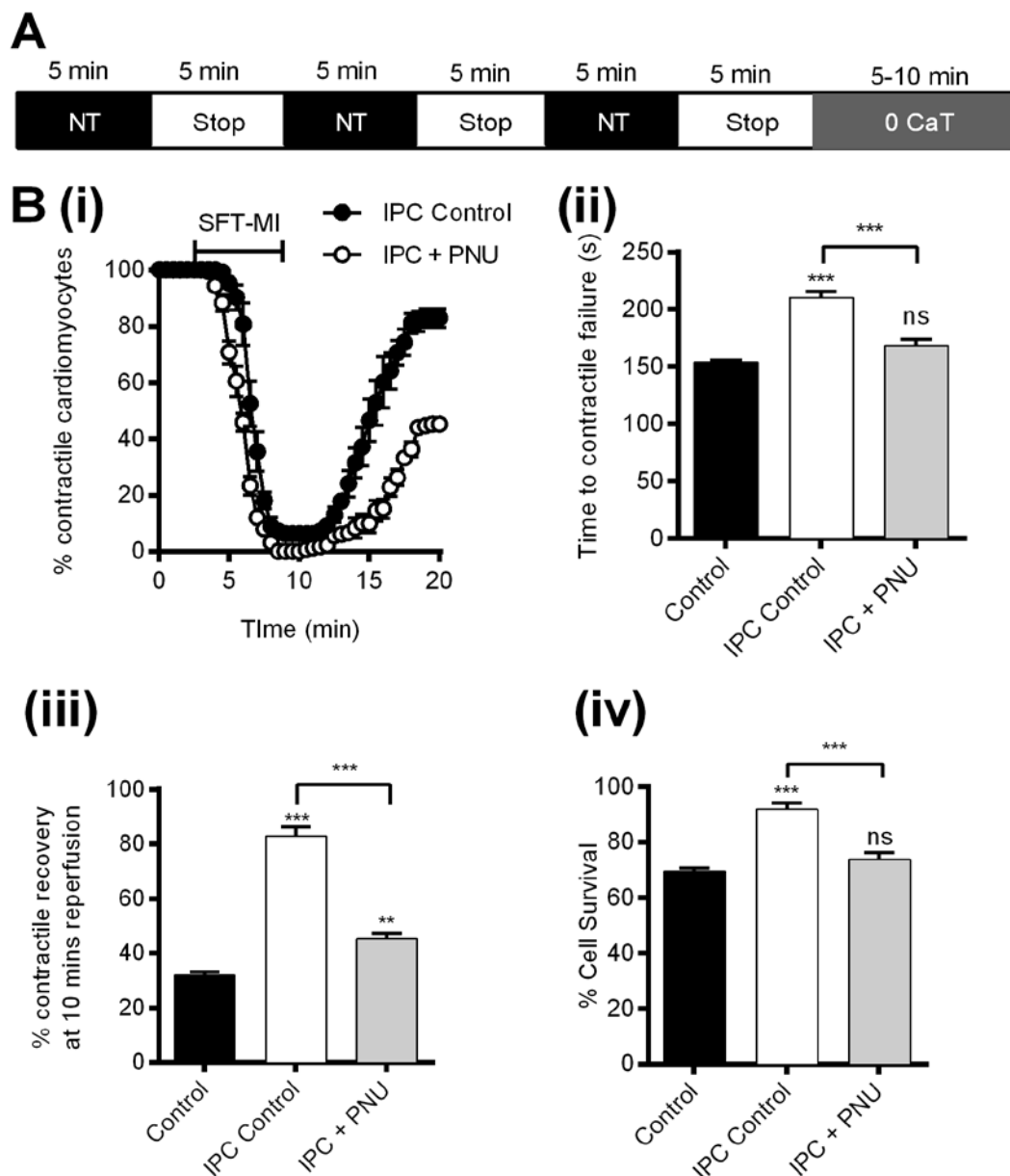


**Figure 6.1: 3  $\mu$ M treatments attenuate the cardioprotective effect in ischemia preconditioning cardiomyocyte.** A, A protocol for imparting IPC in cardiomyocytes. B(i), Example traces shown the time course of contractile percentage during the MI/R protocol in IPC and IPC with 3  $\mu$ M treatment cardiomyocyte. (ii), Bar chat shown the mean contractile failure time in MI, with 154.0 $\pm$ 1.9 s (n=6) in control group and 210.5 $\pm$ 5.3 s in IPC group (n=6, \*\*\*p<0.001). 3  $\mu$ M PNU treatments shortened the time to contractile failure in MI, with 168.4 $\pm$ 5.7 s (n=6, \*\*\*p<0.001; one-way ANOVA Holm-Sidak post-test), compare with IPC group; no significant differences can be seen compared with control group. (iii), Mean percentage of contractile recovery after MI/R for all control, IPC and IPC-PNU treatment group was illustrated, with 32.0 $\pm$ 1.2% (n=6), 82.9 $\pm$ 3.2% (n=6, \*\*\*p<0.001) and 45.2 $\pm$ 2.1% (n=6, \*\*p<0.01; one-way ANOVA Holm-Sidak post-test) respectively. (iv), The mean percentage of cell survival at the end of reperfusion was shown on bar chat, with 69.6 $\pm$ 1.0% (n=6) in control, 91.8 $\pm$ 2.3% in IPC group (n=6, \*\*\*p<0.001; one-way ANOVA Holm-Sidak post-test) and 73.8 $\pm$ 2.6% in IPC-PNU treatment group.

Some experiments carried out by Dr Sean Brennan and Dr Richard Rainbow

The findings suggest that selective inhibition of  $K_{ir}6.1/SUR2B$  current was substantially reversing the protection afforded by IPC, leading to the hypothesis that IPC caused an increase in activity of the  $K_{ir}6.1/SUR2B$  current. To investigate this, cell attached patch recording was used to record cardiac sarcolemmal  $K_{ir}6.1/SUR2B$  activity in IPC cardiomyocytes. Figure 6.2A is representative of the  $K_{ir}6.1/SUR2B$  channel activity on the sarcolemmal membrane of IPC cardiomyocytes, illustrating a significant increase in open probability (NPo), from  $0.13 \pm 0.02$  (n=34) in control to  $0.64 \pm 0.12$  (n=9, \*\*\*p<0.001) in IPC cells (Figure 6.2B). It also shows a noticeable increase in numbers of open levels on membrane surface, from ~2 levels in control myocyte to ~6 levels in IPC cells. These data suggest that either the activity of the  $K_{ir}6.1/SUR2B$  channel has been up-regulated in IPC cardiomyocytes or the numbers of channels inserted in the membrane surface was increased. Furthermore, after metabolic inhibition was applied, the time to  $K_{ir}6.2/SUR2A$  channel activation was significantly delayed, from  $162.0 \pm 7.9$  s (control, n=6) to  $328.4 \pm 18.1$  s (IPC, n=15, \*\*\* p<0.0001). These findings of a delayed opening of  $K_{ir}6.2/SUR2A$  is similar to that reported previously by the group (Brennan *et al.*, 2015).

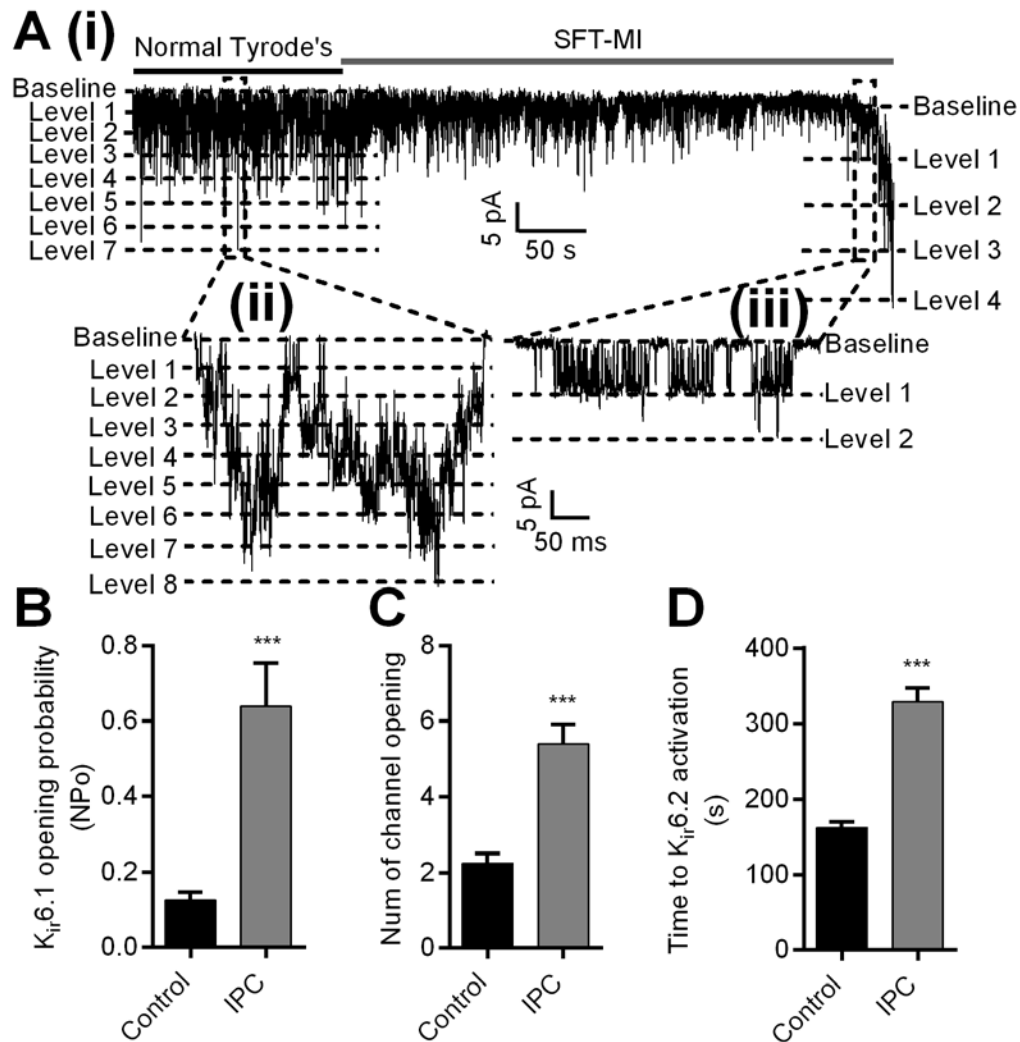


**Figure 6.2: An increased open probability of cardiac sarcolemmal  $K_{ir.6.1}$  channels following IPC.** A(i), Representative trace recorded from cell-attached patch at the equivalent of  $\sim$ -110 mV, from IPC cardiomyocytes. Expanded traces showing a massive opening of  $K_{ir.6.1}$  channel in resting condition in IPC myocyte (ii) and  $K_{ir.6.2}$  currents appears after applied metabolic inhibition (iii). B, Histogram showing mean NPo for the  $K_{ir.6.1}$  channel in control ( $0.13 \pm 0.02$ ,  $n=34$ ) and IPC ( $0.64 \pm 0.12$ ,  $n=9$ , \*\*\*  $p < 0.001$ ; Student unpaired t-test). C, Considering the maximum opening levels are the numbers of channel opening in one patch, a significant increasing in channel numbers can be seen in IPC cells ( $5.40 \pm 0.52$ ,  $n=10$ , \*\*\*  $p < 0.001$ ; Student unpaired t-test), compare with control group ( $2.25 \pm 0.26$  ( $n=24$ )). D. Mean data presented the delayed activation in  $K_{ir.6.2}$  during MI, from  $162.0 \pm 7.9$  s (control,  $n=34$ ) to  $328.4 \pm 18.1$  s (IPC,  $n=15$ , \*\*\*  $p < 0.0001$ ; Student unpaired t-test).

To further confirm that it was a  $K_{ir}6.1$  current that was upregulated following cardioprotection, the  $K_{ir}6.1$  specific inhibitor, 3  $\mu\text{M}$  PNU, was used. In PNU, the  $K_{ir}6.1/\text{SUR2B}$  channel open probability was significantly reduced in IPC cardiomyocytes as demonstrated in the example trace (Figure 6.3A). Mean data, shown in Figure 6.3B, illustrates that there was a significant reduction in NPo in IPC-PNU group, with  $0.04 \pm 0.02$  (IPC-PNU,  $n=6$ ,  $***p < 0.001$ ) compared with IPC control group ( $0.64 \pm 0.12$ ,  $n=9$ ,  $***p < 0.001$ ; Student unpaired t-test). Furthermore, the time to MI-induced  $K_{ir}6.2/\text{SUR2A}$  current activation in IPC was shortened by 3  $\mu\text{M}$  PNU treatments ( $130.6 \pm 18.7$  s, IPC-PNU,  $n=6$ ,  $***p < 0.0001$ ; Student unpaired t-test) compared with that in the IPC group ( $328.4 \pm 18.1$  s,  $n=15$ ). The time to  $K_{ir}6.2/\text{SUR2A}$  opening, and the NPo of  $K_{ir}6.1/\text{SUR2B}$ , following PNU treatment in IPC cells was similar to that in control (non-IPC) cells. Taken together, plotting the  $K_{ir}6.1/\text{SUR2B}$  activity against time to the time to  $K_{ir}6.2/\text{SUR2A}$  current activation, the data presented in Figure 6.3D suggests the increase in activity of  $K_{ir}6.1/\text{SUR2B}$  can delay the  $K_{ir}6.2/\text{SUR2A}$  opening in metabolic inhibition.

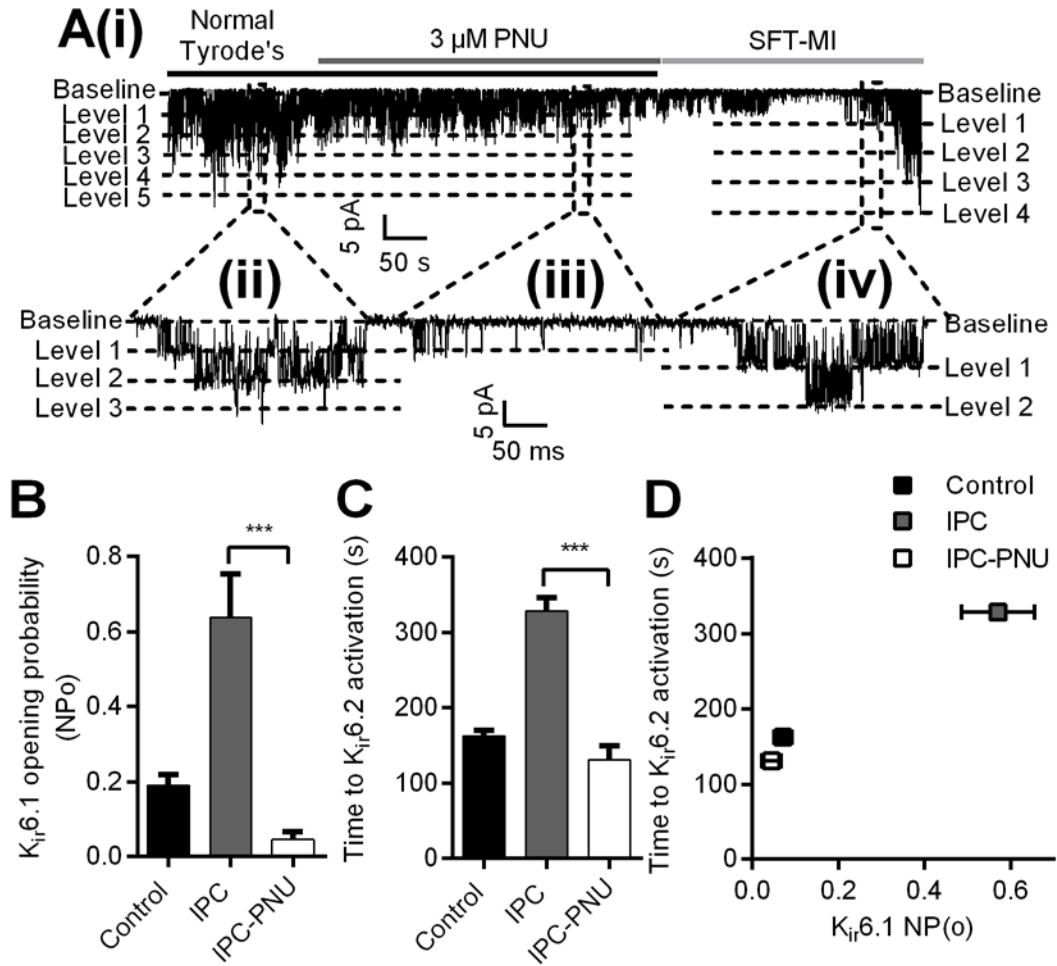


**Figure 6.3: PNU37883A inhibits the up-regulated Kir<sub>v</sub>6.1 activity in IPC cells, as well as shortening the time to Kir<sub>v</sub>6.2 activation during MI.** A(i), Recording was acquired from cell-attached patches, as described in Fig6.1, Kir<sub>v</sub>6.1 up-regulated in resting condition (ii), but can be inhibited by 3  $\mu$ M PNU (iii). Finally, Kir<sub>v</sub>6.2 was activated by metabolic inhibition (iv). B, Mean data shows 3  $\mu$ M PNU treatment can suppress the up-regulated Kir<sub>v</sub>6.1 currents, from  $0.64 \pm 0.12$  (IPC, n=9) to  $0.04 \pm 0.02$  (IPC-PNU, n=6, \*\*\* p<0.001; Student unpaired t-test). C, Histogram illustrated 3  $\mu$ M PNU treatment bring the time to Kir<sub>v</sub>6.2 activation forward in MI in IPC cardiomyocyte, from  $328.4 \pm 18.1$  s (IPC, n=15) to  $130.6 \pm 18.7$  s (IPC-PNU, n=6, \*\*\* p<0.0001; Student unpaired t-test). D, Graph showing the Kir<sub>v</sub>6.1 NP<sub>o</sub> against time to MI activation Kir<sub>v</sub>6.2, suggest a direct correlation between them.

### **6.2.2 The increasing whole-cell residual leak current and APD shortening in IPC myocyte can be reversed by 3 $\mu$ M PNU treatment.**

In Figure 6.2, the data using cell-attached recording suggests there is a substantial up-regulation in sarcolemmal  $K_{ir}6.1/SUR2B$  current. To further investigate the potential impact of this on the cardiomyocyte function the whole-cell recording configuration was used to record the leak current seen at 0 mV, similar to experiments in Figure 3.6. Data in Figure 6.4A show that 3  $\mu$ M PNU suppressed the leak currents in IPC cardiomyocytes but no further inhibition was seen with 10  $\mu$ M glibenclamide treatment. Mean data in Figure 6.4B demonstrate the basal leak currents in IPC cardiomyocyte is increased compared with freshly isolated cells, from  $5.2 \pm 0.5$  pA/pF (control, n=9, from Figure 3.6) to  $7.8 \pm 1.5$  pA/pF (IPC, n=6, \*\*\*  $p < 0.001$ ; Student unpaired t-test). Figure 6.4C shows there is a significant reduction in glibenclamide sensitive current between IPC ( $1.3 \pm 0.2$  pA/pF, n=6) and in the presence of 3  $\mu$ M PNU ( $0.4 \pm 2.3$  pA/pF, n=6, \*\*  $p < 0.005$ ; Student paired t-test).

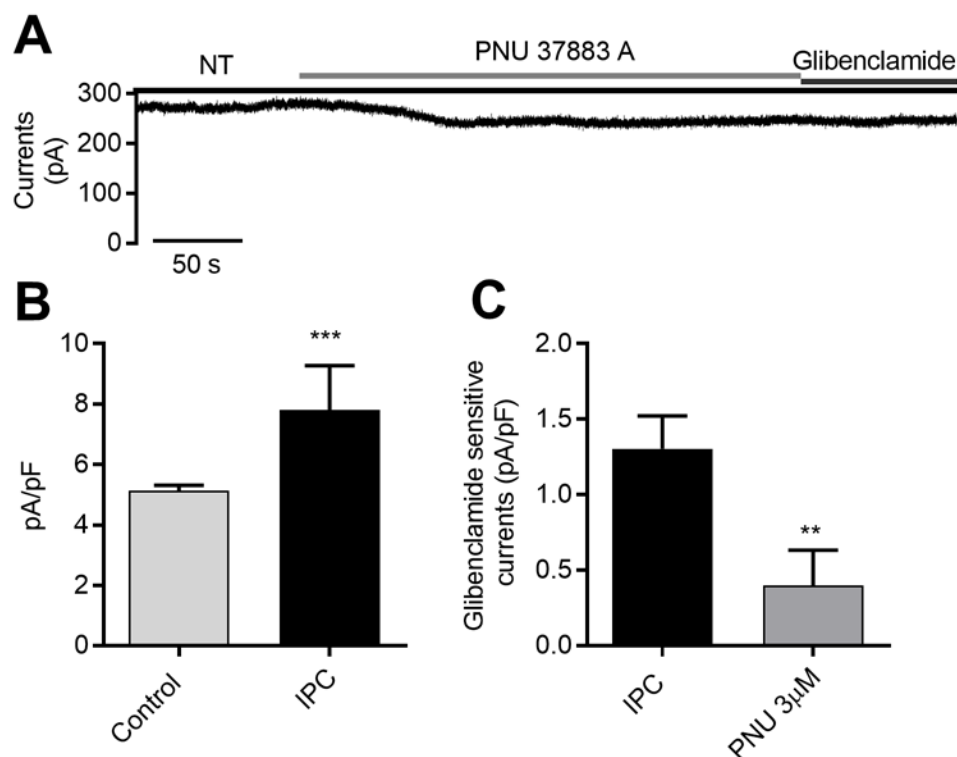


**Figure 6.4: Glibenclamide sensitive leak current was also sensitive to 3  $\mu$ M PNU37883 A in IPC cardiomyocyte.** A, Example trace recorded in whole-cell configuration at a holding membrane potential at 0 mV in resting condition (both control and IPC control), 3  $\mu$ M PNU and 10  $\mu$ M glibenclamide treatments. B, histogram showing the mean data for cardiomyocyte background current was significantly increased from control myocyte ( $5.2 \pm 0.5$  pA/pF,  $n=9$ ) to IPC myocyte ( $7.8 \pm 1.5$  pA/pF,  $n=6$ , \*\*\*  $p < 0.001$ ; Student unpaired t-test). Subtracting the background current by applied 10  $\mu$ M glibenclamide, huge reduction shown in glibenclamide sensitive currents by the 3  $\mu$ M PNU treatment, with  $0.4 \pm 2.3$  pA/pF, ( $n=6$ , \*\*  $p < 0.005$ ; Student paired t-test) compared with IPC cardiomyocyte ( $1.3 \pm 0.2$  pA/pF,  $n=6$ ) in IPC cardiomyocyte. Data was presented in mean  $\pm$  SEM from  $n > 3$  animals.

In Figure 6.1, the pharmacological inhibition of  $K_{ir}6.1/SUR2B$  currents by PNU reverses the cardioprotection imparted by IPC. In addition, data in Figure 3.7 show that PNU treatment prolonged cardiomyocyte action potential duration. Using the same method as in Figure 3.7, cells were first perfused in NT then switched to 3  $\mu$ M PNU and finally 10  $\mu$ M glibenclamide at the end of the recording. Figure 6.5A shows that PNU prolonged the cardiac action potential duration; however, as with non-protected cells in Figure 3.7, there was no further prolongation with glibenclamide treatment. Mean data in Figure 6.5B shows in IPC cardiomyocytes, the  $APD_{90}$  is significantly shortened compared with non-cardioprotected, freshly isolated cells, from  $71.1 \pm 2.8$  ms (control,  $n=9$ ) to  $46.9 \pm 6.4$  ms (IPC

control, n=7, \*\*\*p<0.001; Student unpaired t-test). In Figure 6.5C, the bar chart shows that treatment with 3  $\mu$ M PNU is sufficient to prolong the APD<sub>90</sub> in IPC cardiomyocytes, from 53.6 $\pm$ 11.5 ms (IPC control, n=5) to 78.7 $\pm$ 11.4 ms (PNU, n=5, \*\*p<0.01); perfusion with 10  $\mu$ M glibenclamide did not further prolong APD<sub>90</sub> (75.3  $\pm$ 12.3 ms (n=5)) compared with PNU treatment. Further investigation of the resting membrane potential was carried out measuring the initial membrane potential prior to triggering each action potential. Figure 6.5D revealed that 3  $\mu$ M PNU depolarised membrane potential from -70.2 $\pm$ 0.6 mV (IPC control, n=5) to -66.4 $\pm$ 1.0 mV (PNU, n=5, \*p<0.05; Repeated measures one-way ANOVA with Holm-Sidak post-test), however there was no further depolarization following treatment with 10  $\mu$ M glibenclamide (-67.6 $\pm$ 1.3 mV, n=5).

The results presented here fit with the hypothesis that the activity of K<sub>ir</sub>6.1/SUR2B is upregulated following ischaemic preconditioning. The increased NPo seen in Figure 6.2, the shorter APD and the slightly hyperpolarised membrane potential all support the hypothesis that increased K<sub>ir</sub>6.1/SUR2B currents may be cardioprotective due to altering the electrical activity.

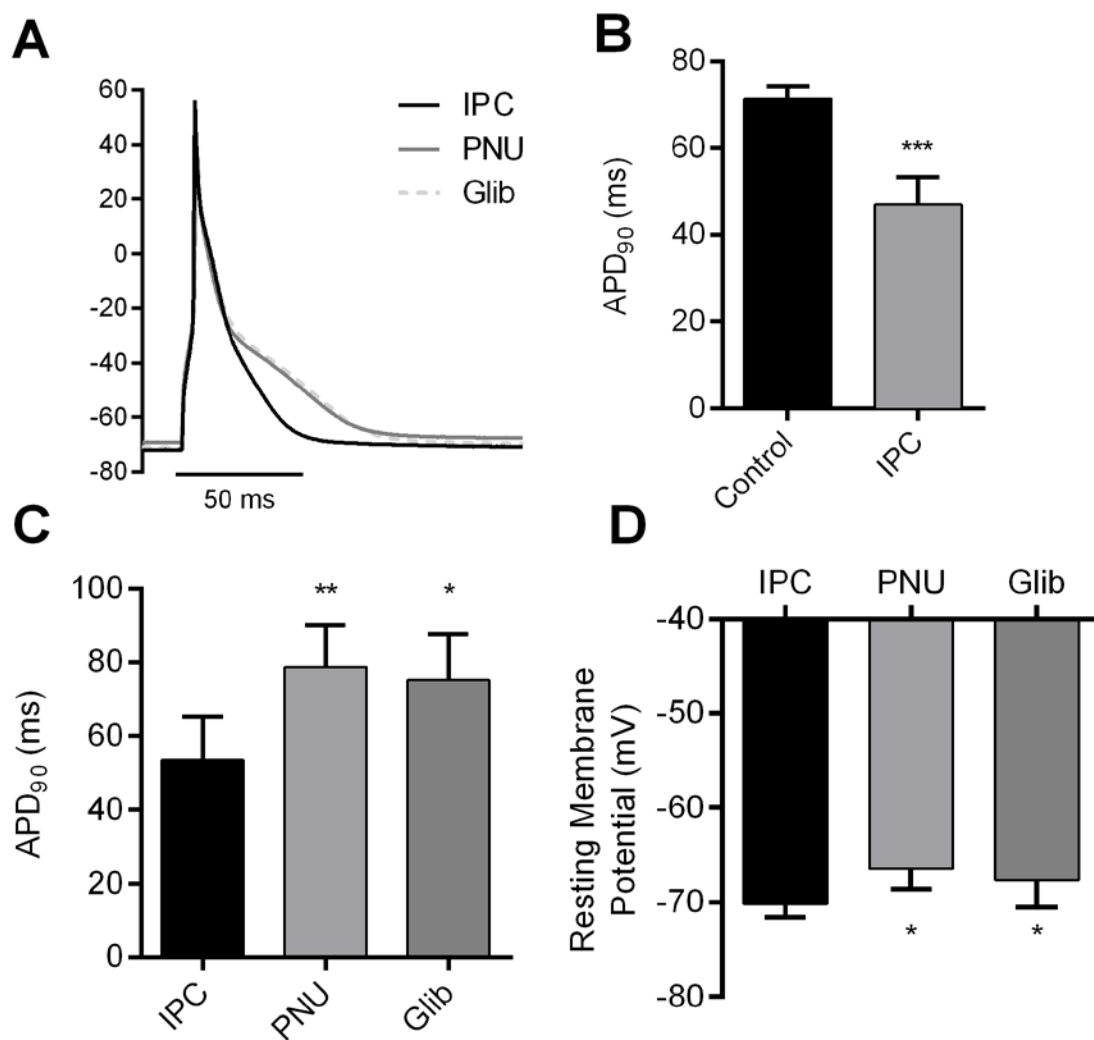
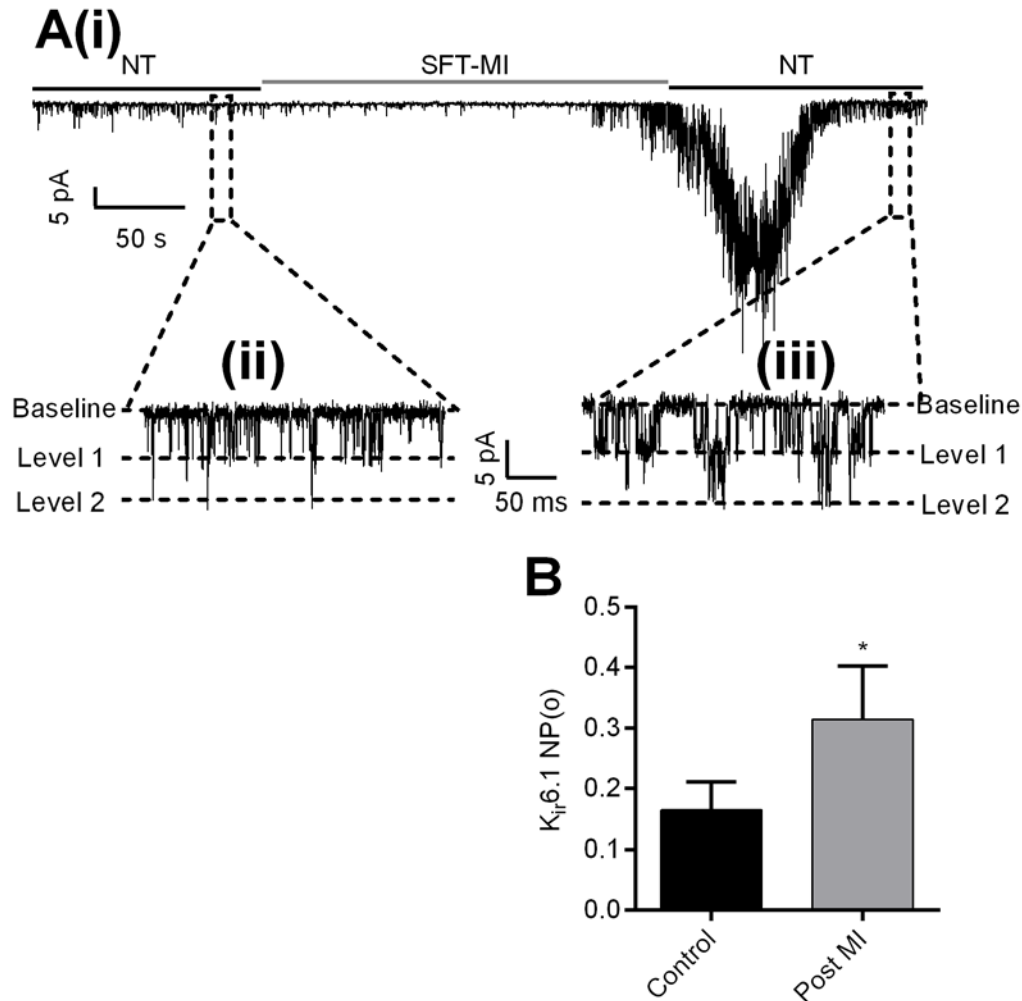


**Figure 6.5: 3  $\mu$ M PNU treatment reverses the shortening of the APD seen following IPC.** A. Recording acquired from IPC cardiomyocyte in whole cell configuration. Example traces of rat cardiomyocyte action potentials in IPC control, 3  $\mu$ M PNU and 10  $\mu$ M glibenclamide treatments. B. histogram shown the mean APD<sub>90</sub> in IPC cardiomyocyte was shortened compared with control myocyte, from 71.1 $\pm$ 2.8 ms (control, n=9) to 46.9 $\pm$ 6.4 ms (IPC control, n=7, \*\*\*p<0.001; Student unpaired t-test). C. Statistical mean value shown 3  $\mu$ M prolonged the APD<sub>90</sub> from 53.6 $\pm$ 11.5 ms (IPC control, n=5) to 78.7 $\pm$ 11.4 ms (PNU, n=5, \*\*p<0.01), further treatment with 10  $\mu$ M glibenclamide (75.3  $\pm$ 12.3 ms, n=5, \*P<0.05; pared one-way ANOVA Holm-Sidak post-test) did not prolonged APD<sub>90</sub> compare with PNU treatment. D. Mean data shown 3  $\mu$ M PNU treatment depolarized membrane potential compare with resting condition, from -70.2 $\pm$ 0.6 mV (IPC control, n=5) to -66.4 $\pm$ 1.0 mV (PNU, n=5, \*p<0.05). Further treatment with 10  $\mu$ M glibenclamide not shown further depolarization on membrane potential (Glibenclamide, -67.6 $\pm$ 1.3 mV, n=5), compare with 3  $\mu$ M PNU treatments.

### 6.2.3 Increasing in SarcoK<sub>ir</sub>6.1/SUR2B channel activity following a metabolic stress/reperfusion cycle in cell-attached recording, in both rat and guinea pig cardiomyocytes.

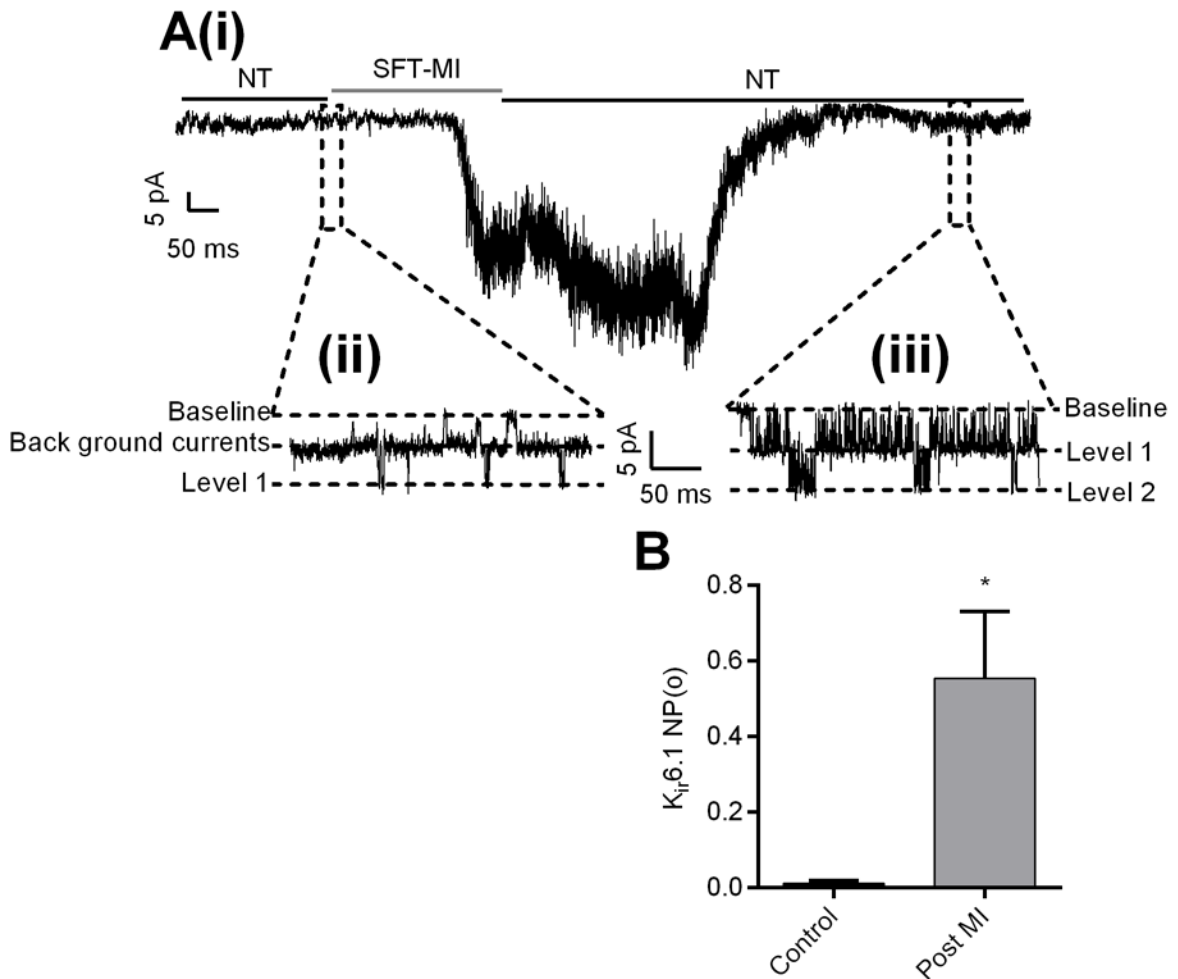
Given that the ischaemic preconditioning protocol used in the whole heart prior to cell isolation involves short periods of ischaemia and reperfusion, it was hypothesised that short periods of metabolic inhibition may increase the activity of the K<sub>ir</sub>6.2/SUR2B complex. The data in IPC cardiomyocytes shows that there is a marked increase in K<sub>ir</sub>6.1/SUR2B activity in IPC cardiomyocytes (Figure 6.2), so to investigate whether this increase in activity occurs in non-cardioprotected cardiomyocytes a short metabolic inhibition and reperfusion protocol was used. An experiment was designed that mimics short periods of ischaemia. In cell-attached patch recordings, perfusion was switched to SFT-MI solution. The appearance of the ~10 pA K<sub>ir</sub>6.2/SUR2A channel activity was a marker of ATP depletion, and so cells were then immediately reperfused with normal Tyrode's solution to restore ATP and inhibit Kir6.2/SUR2A. The K<sub>ir</sub>6.1/SUR2B channel activity was measured before metabolic inhibition and after K<sub>ir</sub>6.2 activity was inhibited by the restoration of ATP on reperfusion with Normal Tyrode's solution.

Figure 6.6A (i) shows an example trace of cell-attached recording throughout a metabolic stress/reperfusion cycle, showing an increased K<sub>ir</sub>6.1/SUR2B activity following the metabolic inhibition (Figure 6.6A (iii)) compared with that before MI (Figure 6.6A (ii)). The mean data presented in Figure 6.6B demonstrates the K<sub>ir</sub>6.1/SUR2B NP<sub>o</sub> was significantly increased following metabolic stress ( $0.31 \pm 0.09$ ,  $n=7$ ,  $*p < 0.05$ ; Student paired t-test), compared with control NP<sub>o</sub> prior to metabolic stress ( $0.16 \pm 0.05$ ,  $n=7$ ).



**Figure 6.6: Increasing SarcoK<sub>ir</sub>.6.1/SUR2B channel activity after a metabolic stress/reperfusion cycle in cell-attached recording from rat cardiomyocytes.** A(i), Example recording of cardiac sarcolemmal currents recorded by cell-attached patch from acutely isolation cardiomyocytes, with equivalent membrane potential of ~-110 mV. (ii), Example trace showing K<sub>ir</sub>.6.1/SUR2B currents expression in resting condition. (iii), The expression of K<sub>ir</sub>.6.1/SUR2B currents increased after a cycle of metabolic stress. B, Mean data showing the K<sub>ir</sub>.6.1/SUR2B channel opening probability significantly increased after MI, with  $0.16 \pm 0.05$  (n=7) in control and  $0.31 \pm 0.09$  (n=7, \* p<0.05; Student paired t-test) in post MI condition.

To investigate whether this also occurred in other species, guinea pig cardiomyocytes were subjected to a metabolic stress/reperfusion cycle. Figure 6.7A (i) shows a typical trace using cell-attached recording in a guinea pig myocyte, with a low activity prior to (Figure 6.7A (ii)) and a significant increase following metabolic stress (Figure 6.7A (iii)). Mean data in Figure 6.7B shows that the  $K_{ir}6.1/SUR2B$  channel NPo significantly increased following MI, with  $0.01 \pm 0.01$  (n=6) in control and  $0.55 \pm 0.18$  (n=6, \*  $p < 0.05$ ; Student paired t-test) in post MI condition.



**Figure 6.7: Increasing expression of Sarco $K_{ir}6.1/SUR2B$  current after a metabolic stress/reperfusion cycle in cell-attached recording from guinea pig (GP) cardiomyocytes.** A(i), Example recording of cardiac sarcolemmal currents recorded by cell-attached patch from acutely isolated GP cardiomyocytes, with equivalent membrane potential of  $\sim -110$  mV. (ii), Example trace showing  $K_{ir}6.1/SUR2B$  currents expression in resting condition. (iii), The expression of  $K_{ir}6.1/SUR2B$  currents increased after a cycle of metabolic stress. B, Mean data showing the  $K_{ir}6.1/SUR2B$  channel opening probability significantly increased after MI, with  $0.01 \pm 0.01$  (n=6) in control and  $0.55 \pm 0.18$  (n=6, \*  $p < 0.05$ ; Student paired t-test) in post MI condition.

These results demonstrate that, in both GP and rat cardiomyocytes, one cycle of hypoxia/reperfusion is sufficient to trigger the up-regulation of sarcolemmal  $K_{ir}6.1/SUR2B$  currents. The mechanism behind this increase in activity are unclear, however it is possible that an increased ADP, or AMP, caused by the metabolic inhibition may have caused an increased activity of the  $K_{ir}6.1/SUR2B$  channel.

#### **6.2.4 Cardioprotection imparted by a 5 min pre-treatment with adenosine is abolished by 3 $\mu$ M PNU37883A.**

Adenosine is a known cardioprotective factor which has been shown to attenuate cardiac hypertrophy, is anti-fibrotic (Puhl *et al.*, 2016), and is a component of the cascade that triggers ischaemic preconditioning (Liu *et al.*, 1991; Grover *et al.*, 1992; Cohen *et al.*, 2000; Toyoda *et al.*, 2000). Using the phenotypic screen outlined in Figure 6.1, cells were pre-treated for 5 min with 100  $\mu$ M adenosine prior to the MI/R protocol as indicated in Figure 6.8A. The numbers of contractile myocytes were counted every 30 s during the whole MI/R protocol to build up a time course (Figure 6.8B (i)). Figure 6.8B (ii) shows the mean data for the time to contractile failure in SFT-MI perfusion, compared with control ( $154.0 \pm 9$  s,  $n=6$ ), adenosine pre-treatment group ( $217.0 \pm 11.8$  s,  $n=6$ ,  $***p < 0.0001$ ), where there was a significantly delay in the time to contractile failure. However, co-treatment with 3  $\mu$ M PNU in both the adenosine pre-treatment and during the MI/R period, reversed the delay in contractile failure seen with adenosine pre-treatment (adenosine-PNU,  $169.9 \pm 6.8$  s,  $n=6$ , ns). Figure 6.8B (iii) shows that the mean percentage of contractile recovery at the end of the protocol was increased by adenosine pre-treatment ( $66.4 \pm 4.5\%$ ,  $n=6$ ,  $***p < 0.001$ ), compared with control group ( $32.0 \pm 1.2\%$ ,  $n=6$ ) however, PNU treatment reversed the increased contractile recovery seen with adenosine ( $38.8 \pm 4.9\%$ ,  $n=6$ ). The percentage of cell survival, Figure 6.8B (iv), was also increased by adenosine pre-treatment from  $69.6 \pm 1.0\%$  (control,  $n=6$ ) to  $87.4 \pm 1.7\%$  (adenosine pre-treatment,  $n=6$ ,  $*** p < 0.001$ ). PNU treatment also reversed the enhanced cell survival by adenosine pre-treatment, with  $75.8 \pm 1.9\%$  ( $n=6$ ,  $*p < 0.05$ ) in adenosine-PNU group.

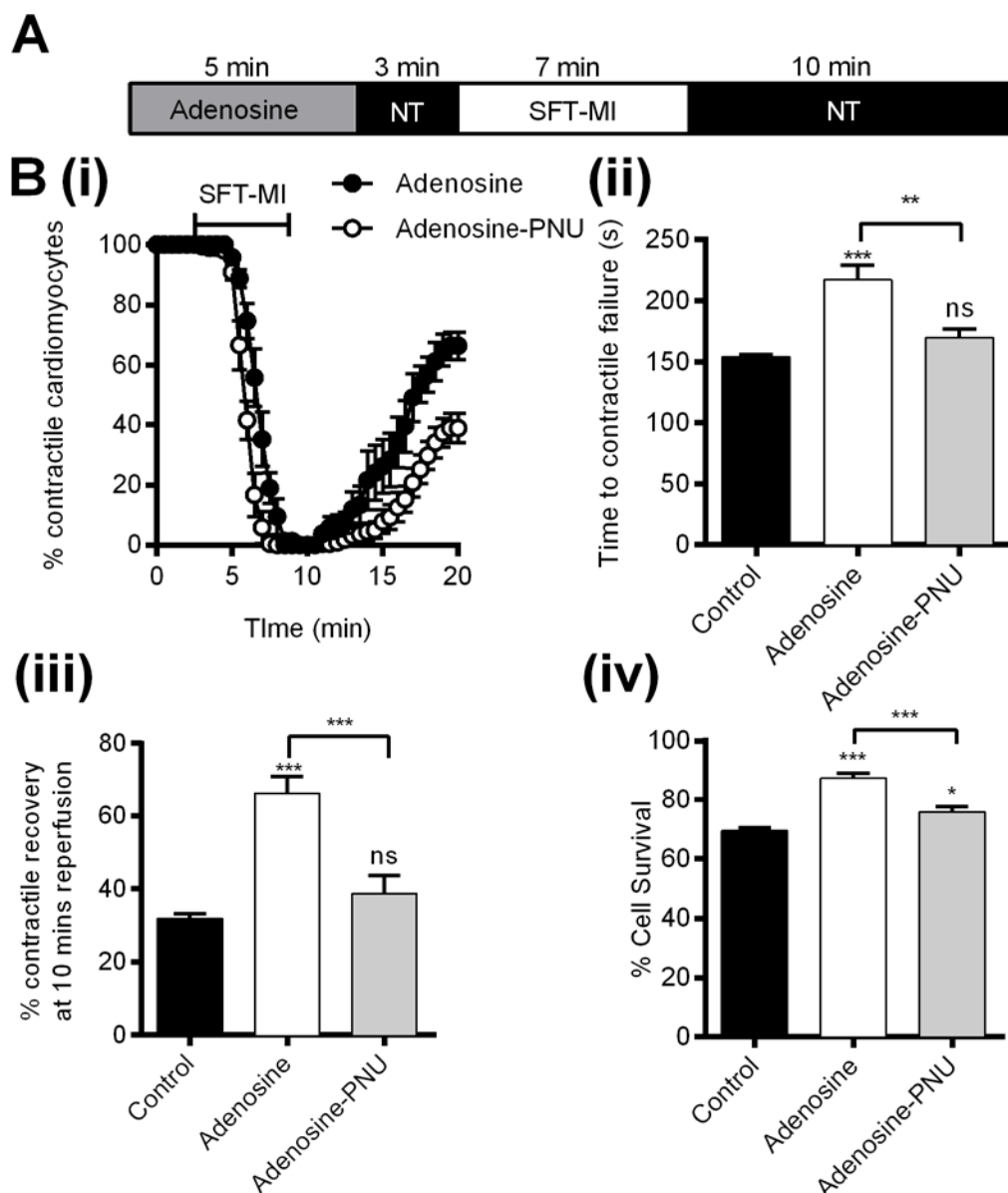


**Figure 6.8: 3  $\mu$ M PNU treatment attenuates the enhanced cell survival following adenosine pre-treatment.** A, Representative of MI/R protocol, with 5 min pre-treatment in 100  $\mu$ M adenosine in initial. B(i), Example traces shown the time course of contractile percentage during MI/R protocol in adenosine and adenosine-PNU group which with 3  $\mu$ M PNU in the whole MI/R protocol after 5 min adenosine pre-treatment. (ii), Bar chart shows the mean contractile failure time in MI was significantly delayed by adenosine pre-treatment, from 154.0 $\pm$ 9 s (control, n=6) to 217.0 $\pm$ 11.8 s (adenosine, n=6, \*\*\*p<0.0001; one-way ANOVA Holm-Sidak post-test); 3  $\mu$ M PNU treatment cancel the delayed contractile failure by adenosine pre-treatment, with 169.9 $\pm$ 6.8 s (adenosine-PNU, n=6). (iii), Mean percentage of contractile recovery after MI/R for all control, adenosine and adenosine-PNU treatment group was illustrated, with 32.0 $\pm$ 1.2% (n=6), 66.4 $\pm$ 4.5% (n=6, \*\*\*p<0.001; one-way ANOVA Holm-Sidak post-test) and 38.8 $\pm$ 4.9% (n=6) respectively. (iv), The mean percentage of cell survival at the end of reperfusion was shown on bar charts, with 69.6 $\pm$ 1.0% (n=6) in control, 87.4 $\pm$ 1.7% (n=6, \*\*\*p<0.001) in adenosine pre-treatment group and 75.8 $\pm$ 1.9% (n=6, \*p<0.05; one-way ANOVA Holm-Sidak post-test).

Some experiments carried out by Dr Sean Brennan and Dr Richard Rainbow

Data presented here suggests that the cardioprotective phenotype imparted by pre-treatment with adenosine can be inhibited by PNU. To investigate whether cardiac  $K_{ir}6.1/SUR2B$  currents play a role in adenosine-triggered cardioprotection, patch clamp (cell-attach configuration) was performed to illustrate channel activity on cardiac membrane surface. Figure 6.9A (i) demonstrates a representative recording in the cell-attached configuration following 5 min adenosine pre-treatment, showing cardiac  $K_{ir}6.1/SUR2B$  current activity in control conditions (Figure 6.9A (ii)) and  $K_{ir}6.2/SUR2A$  currents stimulated by MI (Figure 6.9A (iii)). Mean data shows the cardiac sarcolemmal  $K_{ir}6.1/SUR2B$  currents were up-regulated by 5 min adenosine pre-treatment, from  $0.13 \pm 0.02$  (n=34) in control to  $0.31 \pm 0.07$  (n=23, \*\*p<0.01; Student unpaired t-test) in adenosine pre-treated cells. In addition, Figure 6.9C shows that the activation of  $K_{ir}6.2/SUR2A$  currents were significantly delayed, from  $162.0 \pm 7.9$  s (control, n=34) to  $315.9 \pm 12.3$  s (adenosine, n=23, \*\*\*p<0.001; Student unpaired t-test). Figure 6.9D shows that adenosine pre-treatment upregulated  $K_{ir}6.1/SUR2B$  channel NPo as well as delayed the activation of  $K_{ir}6.2/SUR2B$  current during MI.

Adenosine, and by implication adenosine receptors, are an important component of the signalling cascade that leads to cardioprotection and may increase Sarco $K_{ATP}$  channel opening. Evidence presented here suggests the cardiac Sarco $K_{ir}6.1/SUR2B$  currents are upregulated by adenosine treatment, as well as the activation of conventional  $K_{ir}6.2/SUR2A$  channel in metabolic inhibition.

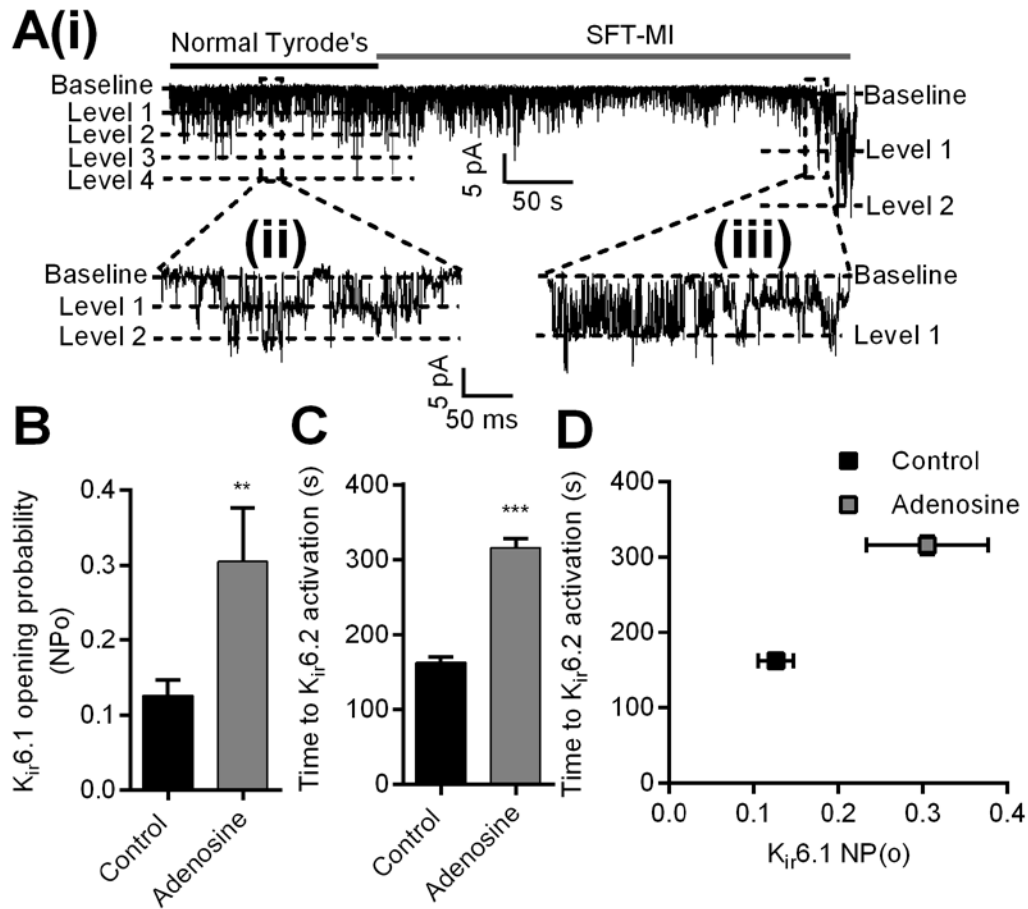


**Figure 6.9: Adenosine pre-treatment up-regulates cardiac sarcolemmal  $K_{ir6.1}$  currents and delays the activation of  $K_{ir6.2}$  currents during MI.** A(i), Recording was acquired from cell-attached patches. Cardiomyocytes were pre-treated with 100  $\mu$ M adenosine for 5 min before patching. SFT-MI was used to activate  $K_{ir6.2}$  currents. Expanded traces show the  $K_{ir6.1}$  currents activity after adenosine pre-treatment (ii) and the activation of  $K_{ir6.2}$  currents after MI (iii). B, Histogram shows adenosine pre-treatment significantly up-regulate  $K_{ir6.1}$  opening probability, from  $0.13 \pm 0.02$  (control,  $n=34$ ) to  $0.31 \pm 0.07$  (adenosine,  $n=23$ ,  $*p < 0.05$ ; Student unpaired t-test). C, Bar chart shows adenosine mediates a delayed activation in  $K_{ir6.2}$  during MI, from  $162.0 \pm 7.9$  s (control,  $n=34$ ) to  $315.9 \pm 12.3$  s (adenosine,  $n=23$ ,  $***p < 0.001$ ; Student unpaired t-test). D, Graph shows the  $K_{ir6.1}$  opening probability against time to MI induces  $K_{ir6.2}$  activation; suggest a direct correlation between them.

### 6.2.5 Differences in SarcoK<sub>ir</sub>6.1/SUR2B open probability on cardiomyocytes between male and female littermates.

Up to the point of menopause, females are less likely to suffer a severe heart attack compared to age matched males. Data in the literature suggests that the female heart is protected from ischaemic injury via an oestrogen-dependent mechanism that may involve steroid oestrogen intracellular receptors, or non-genomic effects via a surface GPCR (GPER30) (Deschamps *et al.*, 2011; Fukumoto *et al.*, 2013; Colareda *et al.*, 2016). In unpublished data from the laboratory, female-derived cardiomyocytes showed a much higher contractile recovery rate and survival rate ( $65.6 \pm 8.4\%$  in contractile recovery,  $89.5 \pm 2.7\%$  in cell survival,  $n = 8$  exp, 4 rats), compared to male littermates ( $24.3 \pm 3.6\%$  in contractile recovery,  $76.1 \pm 2.1\%$  in cell survival,  $n = 8$  exp, 4 rats). It was hypothesised that this increased contractile recovery may well be indicative of an increase K<sub>ir</sub>6.1/SUR2B activity in the female rat-derived cardiomyocytes. To investigate whether SarcoK<sub>ir</sub>6.1/SUR2B currents play a role in the differences in the inherent cardioprotection between the two sexes, patch clamp (cell-attach configuration) was used.

Figure 6.10A (i) shows a representative trace of cell-attached recording from a female heart-derived cardiomyocyte showing an up-regulated K<sub>ir</sub>6.1/SUR2B current in control conditions (Figure 6.10A (ii)) and delayed activation of K<sub>ir</sub>6.2/SUR2A currents during MI (Figure 6.10A (iii)). Mean data shows the open probability was significantly increased in female cardiomyocytes, from  $0.13 \pm 0.02$  ( $n = 34$ ) in male heart-derived group to  $0.48 \pm 0.07$  ( $n = 6$ , \*\*\*  $p < 0.001$ ) in cells from a female heart. With increasing K<sub>ir</sub>6.1/SUR2B currents, similar to previous protective interventions, the activation of K<sub>ir</sub>6.2/SUR2A was delayed, from  $157.7 \pm 12.0$  s (Male,  $n = 15$ ) to  $336.5 \pm 14.2$  s (Female,  $n = 6$ , \*\*\*  $p < 0.001$ ). These data suggest that in female heart-derived cells, similar to other cardioprotected phenotypes, K<sub>ir</sub>6.1/SUR2B activity is markedly increased at the cell membrane surface.

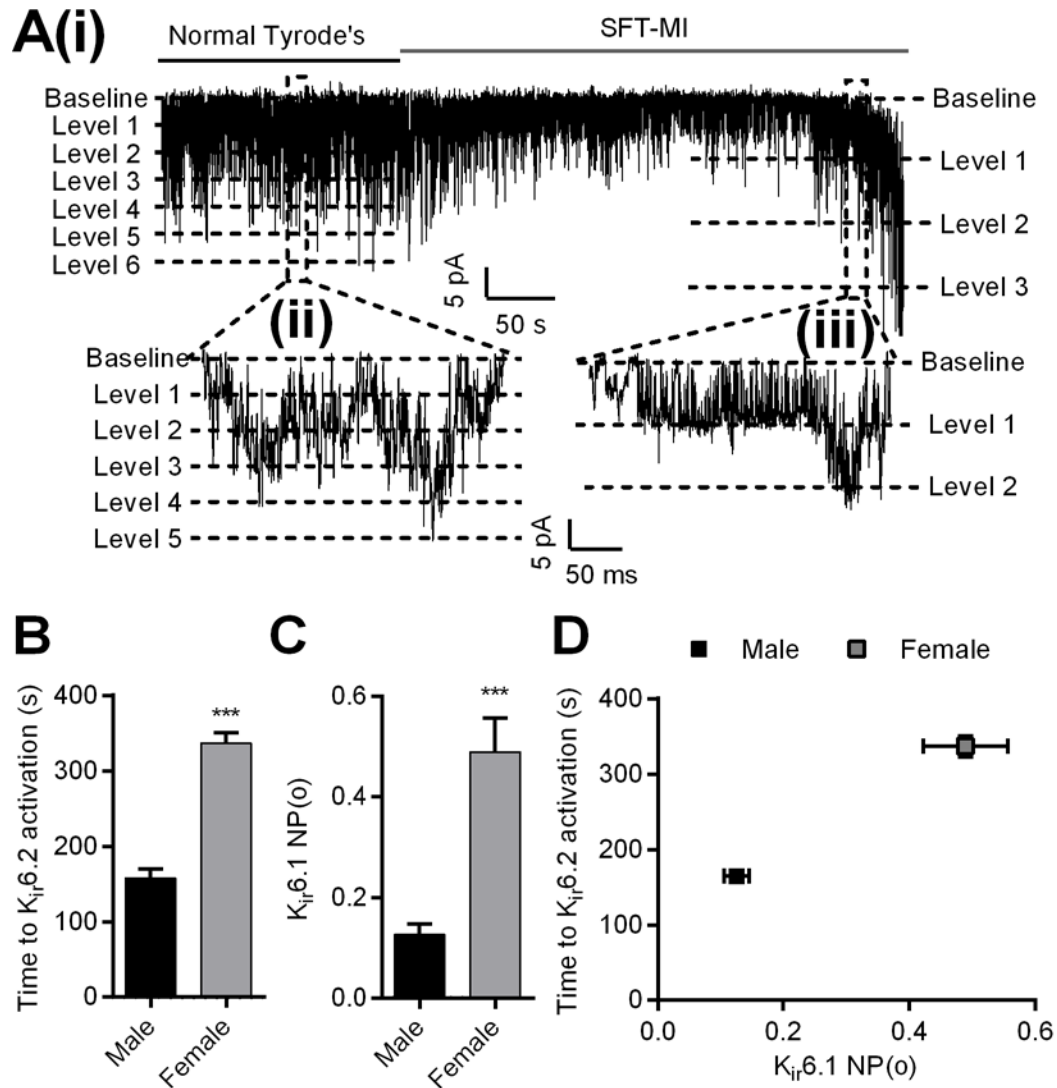


**Figure 6.10: Up-regulation of cardiac sarcolemmal  $K_{ir6.1}$  currents in female Wister rat, with delayed activation of  $K_{ir6.2}$  currents during MI.** A(i), Recording was acquired from female Wister rat in cell-attached configuration. SFT-MI was used to activate  $K_{ir6.2}$  currents. Expanded traces show the  $K_{ir6.1}$  currents activity after in female rat cardiomyocyte (ii) and the activation of  $K_{ir6.2}$  currents after MI (iii). B, Histogram shows significantly up-regulation of  $K_{ir6.1}$  opening probability in female group, from  $0.13 \pm 0.02$  (Male,  $n=34$ ) to  $0.48 \pm 0.07$  (Female,  $n=6$ ,  $***p < 0.001$ ; Student unpaired t-test). C, Bar chart shows a delayed activation in  $K_{ir6.2}$  during MI in female myocyte, from  $157.7 \pm 12.0$  s (Male,  $n=15$ ) to  $336.5 \pm 14.2$  s (Female,  $n=6$ ,  $***p < 0.001$ ; Student unpaired t-test). D, Graph shows the  $K_{ir6.1}$  opening probability against time to MI induces  $K_{ir6.2}$  activation; suggest a direct correlation relationship.

### 6.3 Discussion

In this chapter, the relationship between the SarcoK<sub>ir</sub>6.1/SUR2B channel activity and cardioprotection was investigated. The data suggests the SarcoK<sub>ir</sub>6.1/SUR2B activity plays an important role in cardioprotection from different stimuli, however it is not currently known whether the activity of this channel imparts protection, or is a marker, or consequence, of activation of cardioprotective pathways. In non-cardioprotected conditions, we hypothesised that the absence of K<sub>ir</sub>6.1/SUR2B activity, or expression, in cardiomyocytes causes a cardiotoxic effect, leading to metabolic inhibition intolerance. Moreover, in cardioprotected myocytes, such as following ischaemic preconditioning (IPC) we hypothesise that the SarcoK<sub>ir</sub>6.1/SUR2B channels increases activity/expression to hyperpolarise resting membrane potential and shorten action potential duration, so limiting Ca<sup>2+</sup> influx and preserving intracellular ATP. By using both a phenotypic screen (MI/R protocol) and patch clamp, the strength of the protection was measured following different stimuli, as well as the SarcoK<sub>ir</sub>6.1/SUR2B channel activity. Furthermore, by using a K<sub>ir</sub>6.1 specific pharmacological inhibitor, the effect of SarcoK<sub>ir</sub>6.1/SUR2B currents in cardioprotection was investigated. These data suggest that in IPC, adenosine treatment and female-derived cells, SarcoK<sub>ir</sub>6.1/SUR2B current is a key component of the protection in cardiomyocytes.

Ischaemic preconditioning is a cardioprotective mechanism that has been widely reported, which is stimulated by a series of brief ischaemic events in the heart that results in protection against a major ischemic event (Murry *et al.*, 1986). The opening of SarcoK<sub>ATP</sub> channels on the cardiomyocyte sarcolemmal membrane was hypothesised to be one of the protective factor in IPC (Bernardo *et al.*, 1999; Budas *et al.*, 2004). Previous research suggests that activation of the sarcolemmal K<sub>ATP</sub> channel could impart a cardioprotective effect via shortening of APD, so preserving intracellular ATP and limiting Ca<sup>2+</sup> influx to prevent Ca<sup>2+</sup> overload (Bernardo *et al.*, 1999). The phenotypic screen experiments (Figure 6.1) suggest a similar interpretation of the results is possible. Given several perfusion interruptions prior to cardiac cell isolation, the acutely isolated cells show cardioprotection, measured as a delayed contractile failure time in MI and increased contractile recovery and cell survival following reperfusion. To date, the SarcoK<sub>ir</sub>6.2/SUR2A channel is considered

as the functional SarcK<sub>ATP</sub> channel in cardiomyocytes and has been suggested to play a role in K<sub>ATP</sub>-induced protection as well as IPC (Suzuki *et al.*, 2002; Wojtovich *et al.*, 2013). In these studies, there was an increased infarct size when investigating ischemia/reperfusion in K<sub>ir</sub>6.2 KO animal. However, in a previous paper from our group, the K<sub>ir</sub>6.2/SUR2A channel displayed a delayed opening in IPC, or other cardioprotected conditions, and appeared to activate only in metabolic inhibition with no activity in control conditions (Brennan *et al.*, 2015). Together with the results from last chapter, it was hypothesised that in IPC myocytes, the SarcK<sub>ir</sub>6.1/SUR2B channel activity was increased in normal physiological conditions and so mediates cardioprotection via a shortened APD and hyperpolarised membrane potential. With application of PNU37883A, a K<sub>ir</sub>6.1-specific blocker, the protective effect seen in IPC myocyte was reversed (Figure 6.1). To further investigate the electrophysiological activity on IPC cardiomyocytes sarcolemmal membrane, cell-attached patch recording was used in IPC cardiomyocytes. The data supported the hypothesis; the SarcK<sub>ir</sub>6.1/SUR2B channel activity was significantly increased, including both the NPo and the number of channels opening (Figure 6.2). Whole-cell recording in IPC cells provided more evidence to this hypothesis, the whole-cell leak currents was significantly increased (Figure 6.4) in resting condition in IPC cells. Furthermore, by measuring action potential duration, it was identified that APD<sub>90</sub> in IPC cells was significantly shortened compared with freshly isolated myocytes, which was reversed by PNU treatment (Figure 6.5). It was first hypothesised by Noma (1983) that the K<sub>ATP</sub> channel may serve as a protective factor due to its able to shorten the action potential duration by opening, so limiting the time for Ca<sup>2+</sup> entry via L-type Ca<sup>2+</sup> channel as well as extending the time for outward Ca<sup>2+</sup> flux via the NCX. It is hypothesised that this would lead to two cardioprotective outcomes, firstly to preserve intracellular ATP due to less Ca<sup>2+</sup> influx so reducing the energy demand on the cells; and the second is to limit intracellular Ca<sup>2+</sup> overload during hypoxia, which also benefit the cell survival during reperfusion (Inserre *et al.*, 2002). On application of metabolic inhibition, as it was suggested in the groups previous publication (Brennan *et al.*, 2015), the K<sub>ir</sub>6.2/SUR2A channel was activated later, indicated it is only activated in response to a substantial depletion in ATP. These findings provide supporting evidence to our hypothesis and suggest that K<sub>ir</sub>6.2/SUR2A acts as a crude response to severe ATP depletion and not as an effector of

cardioprotection in sustaining intracellular ATP levels. Further evidences can be seen in  $K_{ir}6.2$ -null mice cardiomyocyte (Suzuki *et al.*, 2001), which the action potential duration and the whole cell leak currents were not altered by  $K_{ir}6.2$  knockout, suggesting the  $K_{ir}6.2$ -containing channel did not tend to open and regulate action potential duration in resting conditions.

In any group of cardiomyocytes that exhibited a cardioprotected phenotype, the activation of  $K_{ir}6.2/SUR2A$  was delayed in MI significantly longer than the control cells, suggesting there is another protective factor in IPC cells other than  $K_{ir}6.2/SUR2A$  (Brennan *et al.*, 2015). PNU37883A reversed the increased open probability of the upregulated  $K_{ir}6.1/SUR2B$  complex, but also shortened the time to  $K_{ir}6.2/SUR2A$  current activation in MI, suggesting the cardioprotection was reversed (at least in part) in IPC cardiomyocytes by blocking Sarco $K_{ir}6.1/SUR2B$  currents. It is interesting to plot the  $K_{ir}6.1/SUR2B$  open probability against time to  $K_{ir}6.2/SUR2A$  activation in MI in one graph (Figure 6.3D), which suggests there is a direct correlation between these two parameters.

During ischaemia, intracellular ATP in the hypoxic myocyte can be quickly degraded into adenosine (Cohen *et al.*, 2000). Adenosine plays a central role in cardiac preconditioning, and ischaemic preconditioning can be mimicked by perfusion of adenosine into the ischaemic area (Cohen *et al.*, 2000; Toyoda *et al.*, 2000). Further evidence for a role for adenosine in cardioprotection is that adenosine receptor antagonists can abolish the cardioprotection afforded by adenosine (Liu *et al.*, 1991). In the cellular investigations presented here, adenosine was used to trigger cardioprotection. A 5 min pre-treatment with adenosine (Figure 6.8) triggered a cardioprotected phenotype in acutely isolated cells, with extended time to contractile failure and increased contractile recovery and cell survival. By using cell attached recording, similar to IPC cells, it was shown that the Sarco $K_{ir}6.1/SUR2B$  open probability was significantly increased. In addition, there was a prolonged time to activation of Sarco $K_{ir}6.2/SUR2A$  currents in MI. Perfusion with 3  $\mu$ M PNU37883A reversed the cardioprotective effect in the MI/R protocol where treated cells showed no differences in time to contractile failure or contractile recovery compared with control myocyte. Previous papers reported that the adenosine A1 receptor is a mediator of cardioprotection in the preconditioned heart (Liu *et al.*, 1991; Grover *et al.*, 1992; Puhl *et*

*al.*, 2016), which upregulates SarcoK<sub>ATP</sub> channels in whole cell currents (Kirsch *et al.*, 1990). The signalling pathway involved remains unclear, however previous reports suggests PKC is involved in this cardioprotection mechanism as inhibition of PKC can abolish the adenosine-induced cardioprotection (Cohen *et al.*, 2000). Our previous data suggests that specifically the PKC $\epsilon$  isoform may be involved in this protection; however, there was not enough time in this project to investigate a role for PKC $\epsilon$  in the modulation of the K<sub>ir</sub>6.1/SUR2B channel.

Our data supports the hypothesis that there is a signalling event triggered by a number of different cardioprotective stimuli, which causes an increase in SarcoK<sub>ir</sub>6.1/SUR2B activity. It is hypothesised that the increased activity of the K<sub>ir</sub>6.1/SUR2B channel mediates cardioprotection via a shortening of the cardiac action potential duration, which reduces the influx and release of Ca<sup>2+</sup> so preserves intracellular ATP for longer during ischaemia so reducing Ca<sup>2+</sup> overload and cell death.

An intrinsic cardioprotective mechanism occurs in pre-menopausal female hearts where this group are significantly less likely to have a severe heart attack than age-matched males. It is believed that this fundamental difference may be due to regulation by sex hormones as this intrinsic protection only lasts until menopause. Previous studies have demonstrated that there is a difference in cardiac function between sexes, and in animal models the female heart is more tolerant to cardiac stress and reperfusion injury (Tsai, 2002; Lagranha *et al.*, 2010). Additionally, ECG recording have illustrated that the ST-segment in female ECG is usually lower in amplitude compared with males (Surawicz & Parikh, 2003). ST-segment elevation, usually indicative of infarction, is common and led to premature death in K<sub>ir</sub>6.1 channel knockout animals (Miki *et al.*, 2002*b*). In addition, PKC activation was suggested by previous reports to be involved in hormonal cardioprotection (Edwards *et al.*, 2009), with seemingly common pathways involved in IPC (Downey *et al.*, 2007) as well as SarcoK<sub>ATP</sub> trafficking (Budasz *et al.*, 2004). The data presented here demonstrates a significant up-regulation of SarcoK<sub>ir</sub>6.1/SUR2B activity in female Wistar myocytes (Figure 6.10), coupled with a significant prolongation in K<sub>ir</sub>6.2 activation in MI. We hypothesis that oestrogen may upregulate SarcoK<sub>ir</sub>6.1/SUR2B currents therefore protects the heart from ischaemia/reperfusion injury in female myocardium.

In this chapter, the open probability of cardiac SarcoK<sub>ir</sub>6.1/SUR2B in several cardioprotective mechanisms was investigated. In each case, there was common evidence of an increased activity of the K<sub>ir</sub>6.1/SUR2B current and a delay in the time to the opening of the K<sub>ir</sub>6.2/SUR2A complex. These results suggest the K<sub>ir</sub>6.1/SUR2B channel on cardiomyocyte sarcolemmal membrane may play an important role in cardioprotection. Furthermore, using SFT-MI to mimic the brief hypoxia before MI shows not only the rat but also in guinea pig cardiomyocyte, the K<sub>ir</sub>6.1/SUR2B currents significantly increased, suggest the up-regulation after hypoxia in preconditioning cells may not be a feature limited to one species. Currently, it is not clear whether K<sub>ir</sub>6.1/SUR2B activity increased to cause cardioprotection, or whether its activity upregulation because of cardioprotection, however it is hypothesised that it plays a key effector role by reducing electrical excitability. In the previous results chapter it was determined that the SarcoK<sub>ir</sub>6.1/SUR2B modulated action potential duration which could regulate intracellular ATP and Ca<sup>2+</sup> influx. Therefore, it is hypothesised that the upregulation in K<sub>ir</sub>6.1/SUR2B currents in cardioprotection in fact shorten the action potential duration as well as limits Ca<sup>2+</sup> influx leading cardioprotection which reduce the ischemia/ischemia reperfusion injury. The data presented his support this hypothesis, with K<sub>ir</sub>6.1/SUR2B activity increased and the time to K<sub>ir</sub>6.2/SUR2A activation significantly delayed in metabolic inhibition. It is hypothesised that this “classic” cardiac sarcolemmal K<sub>ATP</sub> current (K<sub>ir</sub>6.2/SUR2A) is only activated by a substantial ATP depletion. In experiments with PNU37883A, the time to K<sub>ir</sub>6.2 activation in MI was significant shortened compared to IPC, which indicated the ATP depletion was faster when the inhibition of SarcoK<sub>ir</sub>6.1/SUR2B current. Furthermore, it was shown in the MI/R contractile function experiments that blocking the SarcoK<sub>ir</sub>6.1/SUR2B channel with PNU markedly reduced cardioprotection and lead to early contractile failure (caused by substantial activation of K<sub>ir</sub>6.2/SUR2A on ATP depletion), reduced contractile recovery and reduced cell survival.

The data presented here suggests that K<sub>ir</sub>6.1/SUR2B may provide a missing link between the pharmacological evidence suggesting a role for K<sub>ATP</sub> channels in cardioprotection and the lack of direct evidence supporting an increased channel activity or earlier activation. These findings may also explain the disconnection between the literature regarding the pharmacology and the evidence that the “classic” cardiac sarcolemmal K<sub>ATP</sub> complex is

opened later in cardioprotected cells. These findings require further investigation to clarify the mechanism of regulation and whether the  $K_{ir}6.1/SUR2B$  complex could be a viable therapeutic target for pharmacological cardioprotection.

## **Chapter 7**

### **General Discussion**

## 7.1 $K_{ir}6.1/SUR2B$ : an unexpected finding at the cardiac sarcolemmal membrane surface

Since the initial discovery of  $K_{ATP}$  channels in guinea pig cardiomyocytes by Noma (1983),  $K_{ATP}$  channels have been found to be ubiquitously expressed. Its activity has been found to be of key importance in organs such as the pancreas in islet alpha- and beta-cells, neurones, skeletal muscle and smooth muscle cells. In each cell type, the  $K_{ATP}$  channel plays an important role in regulating cellular physiology. Furthermore,  $K_{ATP}$  has been suggested to be expressed inside cells on organelle membranes, such as mitochondrial and nuclear membrane (Bajgar *et al.*, 2001; Singh *et al.*, 2003; van Bever *et al.*, 2004; Zhang *et al.*, 2010).  $K_{ATP}$  complex have been identified that regulated by the metabolic state of the cell and so play an important role in linking metabolism with electrical excitability.  $K_{ATP}$  complexes, which have a  $K_{ir}6.2$  pore with a larger conductance ( $\sim 80$  pS), are mainly distributed in pancreatic islet cells, skeletal muscle, cardiomyocytes and some neurons.  $K_{ATP}$  channel containing a  $K_{ir}6.1$  pore, which has a smaller conductance of  $\sim 39$  pS, are normally found in other brain tissue (e.g. the hippocampus) and vascular smooth muscle cells.

On the cardiac sarcolemmal membrane, it has long been established that the  $K_{ATP}$  current that can be activated by metabolic inhibition is formed from  $K_{ir}6.2$ -pore forming subunits which coupled to SUR2A accessory subunits and is often referred to as the cardiac Sarco $K_{ATP}$  channel complex (Singh *et al.*, 2003; Budas *et al.*, 2004; Edwards *et al.*, 2009; Garg *et al.*, 2009; Li *et al.*, 2010a). The ‘dogma’ regarding this  $K_{ir}6.2/SUR2A$  complex as the Sarco $K_{ATP}$  complex in the heart has been supported by data from several hundred publications, where this explanation satisfies most experimental findings. In this project, it is suggested that the “ $I_{K_{ATP}}$ ” current in cardiomyocytes may actually be formed of more than one  $K_{ATP}$  complex.

In this study, using cell-attached patch recording, the functional expression of 2 types of  $K_{ATP}$  channel was identified with different conductances that closely matched published data for both  $K_{ir}6.1$  and  $K_{ir}6.2$  subunits. By using the protonophore 2,4-dinitrophenol (DNP)  $K_{ir}6.2$  channel currents were activated with a single channel current amplitude of  $\sim 9.8 \pm 0.2$  pA at  $-110$  mV (conductance  $\sim 79$  pS), which was in contrast to the putative  $K_{ir}6.1$  complex,

that was constitutively active with a single channel current of  $\sim 5.4 \pm 0.4$  pA (conductance;  $\sim 39$  pS) (Figure 3.2C). Thus, both the accepted and newly identified  $K_{ir}6.1$ -Sarco $K_{ATP}$  channel conductance fits with published data relating to  $K_{ir}6.1$  and  $K_{ir}6.2$  (Repunte *et al.*, 1999; Kono *et al.*, 2000; Li *et al.*, 2003; Wang *et al.*, 2003; Yu *et al.*, 2012).

### 7.1.1 Evidence for a $K_{ir}6.1$ /SUR2B at the sarcolemmal membrane

In addition to the channel conductance, further evidence supporting this channel being a  $K_{ir}6.1$ -containing channel came from the use of pharmacological tools. Glibenclamide, a sulfonylurea blocker, was the first used to inhibit the  $K_{ATP}$  current as it well documented as being a non-selective  $K_{ATP}$  channel blocker (Fujita *et al.*, 2006; Lodwick *et al.*, 2014). Glibenclamide has been used to block  $K_{ATP}$  as a treatment in type-II diabetes as a mechanism to increase insulin secretion (Bryan & Aguilar-Bryan, 1999). When using glibenclamide to block the cardiac type  $K_{ATP}$ , in the whole-cell recording configuration, the  $IC_{50}$  of  $K_{ir}6.2$ /SUR2A channel was reported as  $\sim 6$  nM (Lodwick *et al.*, 2014). Glibenclamide also demonstrates a substantial block of  $K_{ir}6.1$ /SUR2B channels, with an  $IC_{50}$  between 6 to 60 nM (Hambrock *et al.*, 2001; Lawrence *et al.*, 2001). Thus, the glibenclamide has been shown to effectively inhibit both  $K_{ir}6.1$  and  $K_{ir}6.2$  currents at nM concentrations. In cell attached patch recording, 10  $\mu$ M glibenclamide significantly reduced the activity of the  $\sim 39$  pS-conductance (Figure 3.3), as did the  $K_{ir}6.1$  pore-blocking compound, PNU (Kovalev *et al.*, 2004; Teramoto, 2006*b*). The block by PNU is unaffected by the SUR subunit type co-expressed with the  $K_{ir}6.1$  pore as PNU is a pore blocker of the  $K_{ir}6.1$  channel. PNU has been demonstrated to be effective at inhibiting  $K_{ir}6.1$ /SUR2B channels in vascular smooth muscle (Cui *et al.*, 2003; Tan *et al.*, 2007; Aziz *et al.*, 2010). In the data presented in this study, there was a delay in the inhibition of the  $K_{ir}6.1$  channel on application of 3  $\mu$ M PNU suggesting the action site of PNU was located on cytoplasmic side of membrane. A previous study suggested the same that the delay in PNU inhibitory effect is because the drug needs to cross the sarcolemmal membrane and act on the cytoplasmic side of pore (Aziz *et al.*, 2010). In addition, drug given to treat type 2 diabetes, rosiglitazone, a PPAR- $\gamma$  agonist (Yu *et al.*, 2011), was shown to suppress  $K_{ir}6.1$  currents (Yu *et al.*, 2012). Rosiglitazone has been reported to endanger patients by increasing the risk of myocardial infarction (Gliomas, 2015) and cardiac fibrillation by a currently unknown

mechanism (Lu *et al.*, 2008), and was withdrawn from European market (Kaul *et al.*, 2010). The cardiac action potential duration was also prolonged by the rosiglitazone treatment in the isolated ventricular myocyte from canine or rat heart (Kavak *et al.*, 2008; Szentandrassy *et al.*, 2011). In this study, the putative cardiac SarcoK<sub>ir</sub>6.1 current was inhibited by rosiglitazone with an IC<sub>50</sub> of 14.5  $\mu$ M, concurring with the literature on the effect of rosiglitazone on K<sub>ir</sub>6.1 (Yu *et al.*, 2011, 2012; Wang *et al.*, 2013).

Data in this study demonstrates that knockdown of K<sub>ir</sub>6.2 subunits reduced the metabolic stress-induced K<sub>ATP</sub> current (attributed to K<sub>ir</sub>6.2/SUR2A in cardiac cells) but there was no alteration in the activity of the putative SarcoK<sub>ir</sub>6.1 channel. This phenomenon strongly supports the existence of a second, K<sub>ir</sub>6.1-containing, non-K<sub>ir</sub>6.2, K<sub>ATP</sub> current expressed on the sarcolemmal surface that is active in resting conditions. Furthermore, knockdown K<sub>ir</sub>6.1 gene by using 2 different K<sub>ir</sub>6.1-targeting shRNA sequences significantly reduced the SarcoK<sub>ir</sub>6.1 currents, which was validated by western blotting. Furthermore, using selective shRNA against SUR2A and SUR2B, a significant reduction in SarcoK<sub>ir</sub>6.1 currents in SUR2B knockdown not SUR2A knockdown was seen, suggesting that the  $\beta$ -subunits for the SarcoK<sub>ir</sub>6.1 channel is SUR2B. The evidence presented in this project suggests that the  $\sim$ 39 pS-current expressed at the cardiac sarcolemmal membrane is K<sub>ir</sub>6.1/SUR2B; a subunit combination normally associated with vasculature type K<sub>ATP</sub> channels.

These findings suggest that there are two components, rather than one, to the cardiac sarcolemmal K<sub>ATP</sub> current (I<sub>KATP</sub>); a large conductance (I<sub>KATP-LC</sub>) that is comprised of the conventionally regarded cardiac K<sub>ATP</sub> subunits, K<sub>ir</sub>6.2/SUR2A, and a smaller conductance (I<sub>KATP-SC</sub>) that is comprised of K<sub>ir</sub>6.1/SUR2B.

### **7.1.2 Evidence in the literature that K<sub>ir</sub>6.1/SUR2B is expressed in cardiomyocytes**

It has been previously reported that both K<sub>ir</sub>6.1 and K<sub>ir</sub>6.2, and SUR2A and SUR2B, are expressed in ventricular cardiomyocytes (Singh *et al.*, 2003; van Bever *et al.*, 2004; Morrissey *et al.*, 2005b; Isidoro Tavares *et al.*, 2007; Zhang *et al.*, 2010). Using western blotting and immunofluorescence, the localization of the K<sub>ir</sub>6.1 protein expression was suggested to be both at the sarcolemmal membrane (Morrissey *et al.*, 2005b; Isidoro Tavares *et al.*, 2007) and in the mitochondria (Suzuki *et al.*, 1997; Singh *et al.*, 2003; Lacza, 2003). By purifying the putative mitochondrial K<sub>ir</sub>6.1 and identify the protein by mass

spectrometry, Foster (2008) proposed that two widely used commercial antibodies were actually detecting two different proteins, NADH-dehydrogenase flavoprotein 1 and mitochondrial isocitrate dehydrogenase, rather than the  $K_{ir}6.1$  protein in mitochondria. Furthermore, the presence of  $K_{ir}6.1$  mRNA in cardiomyocytes has also been reported in several publications (Akao *et al.*, 1997; Lu & Halvorsen, 1997; Erginel-Unaltuna *et al.*, 1998; Lawrence *et al.*, 2002; Elrod *et al.*, 2008). As previously discussed,  $K_{ir}6.1$  knockout animals often suffer from sudden cardiac death attributed to the loss of  $K_{ir}6.1$  function. It was hypothesised that the lack of  $K_{ir}6.1$  in the vasculature of these animals was causing a predisposition to spontaneous ischaemia and cardiac dysfunction (Miki *et al.*, 2002b). Evidence from this study showed that the coronary arteries were prone to vasospasm, with a phenotype much like Prinzmetal angina, so being the putative cause of the ischaemia that was evidence from a marked ST-elevation in the ECG. Although the study by Miki (2002) did not show a prolongation in cardiac APD in  $K_{ir}6.1$ -null mice, transgenic mice that expressed a dominant negative  $K_{ir}6.1$  channel did demonstrate a prolonged cardiac APD compared with the WT mice (Tong *et al.*, 2006), suggesting a compensatory mechanism exists in the  $K_{ir}6.1$ -null mice. Taken together with the data presented in this study, these findings strongly suggest that  $K_{ir}6.1$  plays a role in the regulation of normal cardiac physiological function. Perhaps more compelling evidence comes from a vascular-specific  $K_{ir}6.1$  knockout animal, where a Prinzmetal angina-like phenotype was still present, however there was no apparent ST-segment elevation and reduced sudden cardiac death in these animals (Aziz *et al.*, 2014). These data suggest that the heart is able to express  $K_{ir}6.1$ , which exerts protective effect during ischaemic insults and so provide compelling evidence for a role for  $K_{ir}6.1$  in the heart.

There is a marked controversy in the literature on the location of  $K_{ir}6.1$  within the intercellular compartments. Some research suggests that the  $K_{ir}6.1$  protein expression can be found within the mitochondria of cells (Suzuki *et al.*, 1997; Lacza, 2003; Van Cuong *et al.*, 2005), suggesting  $K_{ir}6.1$  was a functional component of a mitochondrial  $K_{ATP}$  channel. Moreover, a number of studies implicated the opening of the mito $K_{ATP}$  channel with the activation of a series of downstream signalling events that have been proposed to be crucial in cardioprotection (Cohen *et al.*, 2001; Nakazawa *et al.*, 2001; Costa *et al.*, 2005). However, there is equally compelling evidence against the localisation of  $K_{ir}6.1$

mitochondria. Using immunolocalization, Morrissey *et al* (2005a) suggested that the  $K_{ir}6.1$  protein was expressed at the cardiac sarcolemmal surface, rather than in the mitochondria. In addition, immunoblot experiments detected no  $K_{ir}6.1$  subunits in the mitochondria, only at the cell surface (Kuniyasu *et al.*, 2003). Furthermore, transfection of dominant-negative  $K_{ir}6.1$  subunits into cardiomyocytes caused the sarcolemmal  $K_{ATP}$  currents to be suppressed (Pountney *et al.*, 2001). This was suggested to be due to cross-reactivity between  $K_{ir}6.1$  and  $K_{ir}6.2$  subunits. To date, there has been no definitive evidence linking  $K_{ir}6.1$  expression to either the mitochondrial or the sarcolemmal membrane in cardiomyocytes.

## 7.2 A role for $K_{ir}6.1$ in cardiac function?

The role that  $K_{ir}6.1$  is hypothesised to play in cardiac function in physiological conditions, from data presented in this study, is highly associated with its apparent constitutive activity.  $I_{K_{ATP-SC}}$ , unlike the “classical” cardiac  $K_{ATP}$ ,  $K_{ir}6.2/SUR2B$ , is constitutively active so behaving more like the most commonly described vasculature  $K_{ATP}$  channel,  $K_{ir}6.1/SUR2B$ , which also demonstrates constitutive activity (Yamada *et al.*, 1997). This is considered to be key to the vascular isoforms role in promoting vasorelaxation (Shi *et al.*, 2010) and contributing to vasoconstriction when it is blocked (Miki *et al.*, 2002b). The cardiac  $I_{K_{ATP-SC}}$  channel illustrates a similar trend in activity, unlike the “classical”  $K_{ir}6.2/SUR2A$  complex, with constitutive activity in normal physiological conditions without a stimulus of metabolic stress.

In vascular smooth muscle,  $K_{ir}6.1/SUR2B$  channel is relatively ATP-insensitive (Yamada *et al.*, 1997), and can be activated by both ATP and ADP (Yamada *et al.*, 1997; Shi *et al.*, 2007b). Results from Figure 3.7 illustrate that specific blockade of the  $K_{ir}6.1$  currents by PNU prolonged the APD in acute isolated myocyte as well as causing depolarization of the resting membrane potential. It was suggested, in previous literature, that  $K_{ATP}$  may play a role in the action potential repolarization as well as resting membrane potential (Schmitt *et al.*, 2014); a suggestion at odds with the known activity of the  $K_{ir}6.2$  current in normal physiological conditions, where the channel would be blocked by ATP. By using pharmacological  $K_{ATP}$  channel openers, such as 10  $\mu$ M pinacidil, there was a noticeable shortening of the cardiac APD; a concentration was not sufficient to induce the opening of

$K_{ir}6.2$  (McPherson *et al.*, 1993; Grover & Garlid, 2000). The pinacidil  $EC_{50}$  is  $\sim 0.2 \mu\text{M}$  for  $K_{ir}6.1/SUR2B$  (Suzuki *et al.*, 2001) and  $\sim 40 \mu\text{M}$  for  $K_{ir}6.2/SUR2A$  channel (Lodwick *et al.*, 2014), which suggests  $10 \mu\text{M}$  pinacidil would have little effect on the  $K_{ir}6.2/SUR2A$  currents. Data presented in this study agrees with this finding that the  $K_{ir}6.1$  channel activity is involved in APD regulation. These data demonstrates that by either pharmacological blockade or genetic knockdown of  $K_{ir}6.1/SUR2B$  subunits causes a significant prolongation of the  $APD_{90}$  and caused membrane potential depolarisation (Figure 3.7, Figure 4.10). Similar results were also shown in guinea pig cardiomyocytes following pharmacological inhibition or gene knockdown (Figure 4.12 and 4.13).

As the  $SarcoK_{ir}6.1$  current potentially regulates the action potential duration, it was hypothesised that the channel regulates the  $Ca^{2+}$  transients as well as intracellular  $Ca^{2+}$  homeostasis and ATP. The data gathered in this study confirmed this hypothesis, where a prolongation of the  $Ca^{2+}$  transients was seen after application of the  $K_{ir}6.1$ -specific blocker, PNU (Figure 3.8). Furthermore, under metabolic stress, the loss-of-function in  $K_{ir}6.1$  channel in cardiomyocyte caused a more rapid intracellular  $Ca^{2+}$  and  $Mg^{2+}$  accumulation, supporting the hypothesis that  $K_{ir}6.1$  regulates intracellular ATP and  $Ca^{2+}$  concentration via APD (Figure 5.6, Figure 5.7). Thus, the role that  $K_{ir}6.1$  channel plays can be suggested as: a) The  $K_{ir}6.1/SUR2B$  channel constitutive activity in normal physiological conditions plays a significant role in APD regulation, in repolarization and resting membrane potential. b) During metabolic inhibition, the activity of  $K_{ir}6.1$  channel regulates  $Ca^{2+}$  influx so that slowing the rate of ATP depletion and reducing the risk of potential damage by  $Ca^{2+}$  overload. If ATP depletion continues, then the  $K_{ir}6.2/SUR2A$  channel opens, acting as a metabolic sensor that is activated by severe ATP-depletion. These findings add further weight to our hypothesis of there being a small conductance (SC) and large conductance (LC) component to  $I_{KATP}$  in cardiomyocytes.

### 7.2.1 The differences in function and activity of $K_{ir}6.1/SUR2B$ and $K_{ir}6.2/SUR2A$

In all experiments carried out in this investigation, the  $K_{ir}6.2/SUR2A$  channel was not active in normal physiological conditions and was only activated following several minutes of perfusion with a metabolic inhibition solution (Figure 3.1, Figure 4.1-4.4, Figure 4.7-4.8, Figure 6.2-6.3 and Figure 6.9-6.10). These data confirmed previous findings from the

laboratory where it was shown that the opening of  $K_{ir}6.2/SUR2A$  occurred only after ATP depletion (Brennan *et al.*, 2015). The reason for this delayed opening of  $K_{ir}6.2$  channel in metabolic stress is due to its ATP-sensitivity, where 1 mM intracellular ATP is sufficient to inhibit the channel opening (Inagaki *et al.*, 1995; Ammälä *et al.*, 1996; Isomoto *et al.*, 1996; Suzuki *et al.*, 2001), with an  $IC_{50}$  of  $\sim 20 \mu M$  in the presence of  $Mg^{2+}$  (Kono *et al.*, 2000; Lodwick *et al.*, 2014). In physiological concentrations of ATP, which rounds 4.3 mM, the  $K_{ir}6.2$  channels are strongly inhibited (Pelzmann *et al.*, 2003). If not induced by a pharmacological activator, the  $K_{ir}6.2$  will be blocked by ATP in physiological condition, thus, the role that  $K_{ir}6.2$  plays is limited to during metabolic stress. Data from this study suggests that the knockdown of  $K_{ir}6.2$  subunits has no effect on the cardiac action potential duration (Figure 4.11), but there was a marked reduction in the metabolic inhibition-induced whole cell currents (Figure 4.9). A similar phenomenon was seen in a previous study in the knock out mouse, with no alteration in cardiac action potential in  $K_{ir}6.2$ -null mouse (Suzuki *et al.*, 2001). McPherson *et al* (1993) suggested that the opening of  $K_{ir}6.2$  causes contractile failure and preserves ATP, which was supported by the findings of Suzuki (2002) using a  $K_{ir}6.2$ -null mouse where the contraction was indeed prolonged. Moreover, In a study by Brennan *et al* (2015), by investigating 3 parameters during metabolic inhibition, 1) the time to  $K_{ir}6.2$  activation, 2) the time to contractile failure and 3) the time to action potential failure, all 3 parameters were identical in each condition, strongly suggesting the delayed opening of  $K_{ir}6.2$  channel is actually causing the delay in the time to contractile failure and thus linking  $K_{ir}6.2/SUR2A$  activity to contractile function. Thus, this study suggests alternative functions for the two components of  $I_{KATP}$ , with the  $K_{ATP-LC}$  current being the final protection for the heart against complete ATP depletion during metabolic stress, so acting as an energy sensor. In contrast,  $I_{KATP-SC}$  has a regulatory role in modulating the resting potential and the APD in normal physiological conditions.

### 7.2.2 Pharmacological and electrophysiological function

It has been shown that glibenclamide can abolish cardioprotection and demonstrates an increased infarct size as well as prolong action potential duration (Tomai *et al.*, 1994; Bernardo *et al.*, 1999; Toyoda *et al.*, 2000; Rainbow *et al.*, 2004; Budas *et al.*, 2004; Stoller *et al.*, 2010; Brennan *et al.*, 2015). In experiments presented in this study using cell-

attached patch recording, the SarcoK<sub>ir</sub>6.1/SUR2B currents was suppressed by the application of 10  $\mu$ M glibenclamide in the perfusion. In this study, 3  $\mu$ M PNU has a cardiotoxic effect on cells, worsening the outcome for cardiomyocytes following a metabolic inhibition/reperfusion protocol, demonstrating an increasing cell death and reduced contractile recovery. In addition to PNU, rosiglitazone was used as K<sub>ir</sub>6.1/SUR2B specific channel blocker, which act on the K<sub>ir</sub>6.1 intracellular domains (Yu *et al.*, 2012; Muntean *et al.*, 2014). From data presented in this study, in the cell attached configuration, the cardiac sarcolemmal surface K<sub>ir</sub>6.1 channel activity was significantly inhibited (Kavak *et al.*, 2008; Szentandrassy *et al.*, 2011). HMR 1883 or HMR 1098 (sodium salt of HMR 1883) specifically inhibits membrane K<sub>ATP</sub>, K<sub>ir</sub>6.2/SUR2A, which demonstrates a prolongation effect in rilmakalim or hypoxia induced APD shortening (Billman *et al.*, 1998). The usefulness of HMR 1098 in dissecting the relative roles of K<sub>ir</sub>6.2 and K<sub>ir</sub>6.1 is limited as HMR 1098 is no longer effective at blocking the K<sub>ir</sub>6.2/SUR2A complex when intracellular ADP levels are elevated, as would happen during ischaemia (Rainbow *et al.*, 2005).

### 7.2.3 Does K<sub>ir</sub>6.1/SUR2B explain the disconnection between K<sub>ATP</sub> function and observable pharmacological modulation of the heart?

Pharmacological evidence shows that I<sub>KATP</sub> plays a role in both the normal physiological role and in cardioprotection (McPherson *et al.*, 1993; Billman *et al.*, 1998; Grover & Garlid, 2000). Glibenclamide causes a significant prolongation of the cardiac action potential and potentiators of I<sub>KATP</sub> impart cardioprotection to the heart (Ripoll *et al.*, 1993; Tomai *et al.*, 1994; Kristiansen *et al.*, 2005; Kim *et al.*, 2012; Novakovic *et al.*, 2013) The finding that glibenclamide prolongs the cardiac action potential is at odds with the functional properties of the K<sub>ir</sub>6.2/SUR2A complex which, as outlined in section 1.2.1, will be completely blocked by normal physiological concentrations of ATP. Such disconnect in the channel activity and the functional effect of sulphonylureas has been attributed to several different hypotheses, including that there are local depletion of ATP in microdomains around the K<sub>ATP</sub> complex, so causing an activation of the current. The existence of a second component to I<sub>KATP</sub> provides a compelling hypothesis as to how glibenclamide is able to prolong the APD despite the fact that all currently accepted, sarcolemmal K<sub>ATP</sub> channels should be blocked by physiological ATP.

### 7.3 Is cardiac sarcolemmal $K_{ir}6.1/SUR2B$ a key effector of cardioprotection?

The existence of a second component of  $I_{K_{ATP}}$  also brings an exciting new hypothesis as to how  $K_{ATP}$  channel activation may be linked to cardioprotection. Pharmacological activation of  $I_{K_{ATP}}$  has been suggested to be cardioprotective, and glibenclamide (and other blockers) are able to abolish protection afforded by most protective stimuli (Gross & Auchampach, 1992; Gross & Fryer, 1999; Toyoda *et al.*, 2000; Brennan *et al.*, 2015). The presence of  $I_{K_{ATP-SC}}$  provides the basis of a new hypothesis for  $K_{ATP}$ -induced cardioprotection.

#### 7.3.1 Hypothesis for a role of $K_{ir}6.1/SUR2B$ and not $K_{ir}6.2/SUR2A$ in cardioprotection

Previous studies suggest that the  $K_{ATP}$  channel not only exists on cardiomyocyte membranes, but also in intracellular structures, such as mitochondrial membrane and sarcoplasmic reticulum membrane. Since Suzuki *et al* (1997) first discovered a  $K_{ir}6.1$ -like protein expressed in mitochondria by immunoblot analysis of the mitochondrial fraction, there has been controversy regarding the locations of functional  $K_{ir}6.1$  channel in cardiomyocytes and their role in cardioprotection. Seharaseyon *et al* (2000) found that only surface  $K_{ATP}$  channel function was disrupted following transfection of a dominant negative  $K_{ir}6.2$  into rabbit cardiomyocytes, whereas the  $K_{ATP}$  channel in the mitochondria remained functional. Findings from Suzuki *et al* (2002) supported the idea that mito $K_{ATP}$  function was preserved even in isolated cardiac cells from  $K_{ir}6.2$ -knockout mice, which indicated that the  $K_{ir}6.2$   $K_{ATP}$  channel may not form part of the mito $K_{ATP}$ . Therefore, it continued to raise the possibility that  $K_{ir}6.1$  was part of the putative mito $K_{ATP}$  and functional during IPC. The potential connections between mito $K_{ATP}$  and IPC were described by Wang *et al* (2001), where IPC was hypothesised to induce the mito $K_{ATP}$  opening by causing uptake of  $Ca^{2+}$  into the mitochondria as well as causing the generation of ROS. By measuring the ROS level with MitoTracker Red, Oldenburg (2004) suggested that the NO caused a significant increase in fluorescence intensity which can be reversed by the putative mito $K_{ATP}$  blocker 5-HD. These findings suggest that NO activates the chain reaction of kinase that cause the opening of mito $K_{ATP}$ . As a result, the mitochondrial membrane permeability transition pore (mPTP) opens and the  $Ca^{2+}$  diffuses from the mitochondria matrix to cytoplasm due to the depolarization of mitochondria membrane potential (Halestrap *et al.*, 2007; Kinnally *et al.*,

2011).

Evidence for a mitochondrial  $K_{ir}6.1$  channel is controversial, with many publications suggesting that it is not part of a  $mitoK_{ATP}$  complex. Seharaseyon *et al* (2000a) used dominant negative  $K_{ir}6.1$  subunits in cardiomyocytes and suggested that there was no  $K_{ir}6.1$  channel in the mitochondria as the effect of diazoxide on the mitochondria was the same in control cells. Furthermore, there was no difference in flavoprotein autofluorescence in cardiomyocytes from  $K_{ir}6.1$  knockout animals compared to WT.

In  $K_{ir}6.1$ -null mice, Miki *et al* (2002b) showed a sudden death with an ST-segment elevation in ECG, suggesting myocardial damage. From previously published data from our group, the “conventional” cardiac  $K_{ATP}$ ,  $K_{ir}6.2/SUR2A$  channel, activity is actually delayed after IPC, or any other cardioprotection stimuli (Brennan *et al.*, 2015) rather than activated by it. This raised the hypothesis that there was another cardioprotective factor involved in the preservation of intracellular ATP, which resulted in a delayed opening of the  $K_{ir}6.2$  channel. Evidence from this project suggests that  $K_{ir}6.1$  may well be a candidate channel for this role; as the  $SarcoK_{ir}6.1$  currents show a substantial increase in protected cardiomyocytes where the protection has been induced by different stimuli, such as IPC, adenosine and gender differences (Chapter 6). Using PNU37883A, the cardioprotection was partially blocked, in addition, the time to  $K_{ir}6.2$  activation was earlier during metabolic inhibition. In cardioprotected myocytes treated with 3  $\mu$ M PNU showed a marked reduction in their protection, manifesting as a lower contractile recovery and cell survival. It was hypothesised, therefore, that the enhanced activity of  $K_{ir}6.1$ -containing channels was a key component in cardioprotection. It was of note to see that even in the normal physiological conditions, contractile recovery was reduced when the  $K_{ir}6.1$  channel was inhibited with 3  $\mu$ M PNU. Besides IPC, adenosine pre-treatment induced protection and gender-dependent protection was also associated with a significant increase in  $SarcoK_{ir}6.1$  currents (Figure 6.9, Figure 6.10). In addition, by using MI/R protocol, adenosine-induced cardioprotection was also been blocked by PNU, demonstrating a reduction in cell contractile recovery and survival rate (Figure 6.8).

It was hypothesised that the  $K_{ATP}$  channel opens as a cardioprotective effector in IPC, which imparts the protective effect by shortening the APD so preserving intracellular ATP and limiting  $Ca^{2+}$  influx to prevent  $Ca^{2+}$  overload (Bernardo *et al.*, 1999). As we have already demonstrated that the conventional cardiac channel,  $K_{ir}6.2/SUR2A$ , showed a delayed activation following protective stimuli, the  $K_{ir}6.1/SUR2B$  component becomes a compelling candidate to play a key role in cardioprotection. It was hypothesised that cardioprotective stimuli caused an up-regulation in  $K_{ir}6.1$  channel activity to cause a shortened APD and more hyperpolarised membrane potential. The data presented in this thesis confirms this hypothesis, and that treatment with PNU abolishes these cardioprotection-induced changes (Figure 6.5). Both  $Ca^{2+}$  and  $Mg^{2+}$  imaging suggested that the increased activity of the  $K_{ir}6.1$  channel has a role in regulating both intracellular  $Ca^{2+}$ , ATP/ADP as well as the action potential and membrane potential. Conversely, loss-of-function on the  $K_{ir}6.1$  channel resulted in prolonged  $Ca^{2+}$  transients in normal physiological conditions as well as rapid  $Ca^{2+}$  and ADP accumulation during metabolic stress (Figure 3.11, Figure 5.6 and Figure 5.7).

Although previous literature demonstrates a delayed opening of  $K_{ir}6.2/SUR2A$  in metabolic stress in protected cells, this does not exclude  $K_{ir}6.2$  from playing a role in cardioprotection; however, not necessarily as an effector as previously suggested. An increased infarct size has already been reported in several studies following ischemia/reperfusion in  $K_{ir}6.2$  KO animals suggesting that this channel is important in limiting infarct size (Suzuki *et al.*, 2002; Wojtovich *et al.*, 2013). Data presented in this study does not disagree with these findings as  $K_{ir}6.2$  knockdown cells demonstrated less contractile recovery following an MI/R protocol in phenotypic screen experiments (Figure 5.3). In normal physiological conditions, the action potential duration and resting membrane potential were normal in  $K_{ir}6.2$ -knockdown cells. It was hypothesised that as  $K_{ir}6.1$  was not affected by  $K_{ir}6.2$  knockdown and so the action potential duration, as well as  $Ca^{2+}$  transients, were still regulated by  $K_{ir}6.1$ , therefore in the early stages of ischaemia the accumulation of  $Ca^{2+}$  was not as severe as seen in  $K_{ir}6.1$  knockdown. In  $K_{ir}6.1$ -knockdown cells, the levels of intracellular  $Ca^{2+}$  at the time of  $K_{ir}6.2/SUR2A$  opening, and at reperfusion, would be much higher than in WT cells and so the cell survival would be much

lower.

All of these findings suggest that the SarcoK<sub>ir</sub>6.1 channel may be an important factor in the cardioprotective process. Furthermore, the enhanced opening of SarcoK<sub>ir</sub>6.1 channel in the membrane seen following cardioprotective stimuli was not as substantial as that of the K<sub>ir</sub>6.2 channel, therefore the constitutive opening of this small conductance channel is not sufficient to cause contractile failure, unlike the K<sub>ir</sub>6.2 channel. The K<sub>ir</sub>6.1 current seems to be able to reduce APD and resting membrane potential to the point that it improves the efficiency of Ca<sup>2+</sup> handling and preserve intracellular ATP without causing potential disastrous complete action potential failure.

### 7.3.2 What mechanism might be modulating K<sub>ir</sub>6.1/SUR2B?

In this project, the signalling pathway that modulates K<sub>ir</sub>6.1/SUR2B was not investigated due to insufficient time. The signalling pathways in cardioprotection are varied, however many converge on the activation of protein kinase C (PKC), in particular the  $\epsilon$  and  $\delta$  isoforms.

In this study, 3 different cardioprotective stimuli were investigated; IPC, adenosine pre-treatment and gender-dependent protection. In each case, all three were associated with up-regulation of K<sub>ir</sub>6.1. In the “classic” cardioprotection, IPC, the signalling pathway has been suggesting by several previous studies to involve the accumulation of adenosine during the ischaemia. The accumulation of adenosine can therefore activates PKC $\epsilon$  so leading to an increase in SarcoK<sub>ATP</sub> currents (Liu *et al.*, 1996). Evidence for this is from the use of pharmacological antagonists for the adenosine receptors, where a none-selective adenosine antagonist 8-SPT reverses the cardioprotection (Bernardo *et al.*, 1999; Schoemaker & van Heijningen, 2000; Liem *et al.*, 2002; Gross & Peart, 2003; Hausenloy & Yellon, 2008). Light *et al* (2001) demonstrates a similar result that by using adenosine A<sub>1</sub> receptor agonist, the cardioprotective effect was mediated via activation of PKC and SarcoK<sub>ATP</sub>, where the effect was also blocked by an adenosine A<sub>1</sub> selective antagonist, DPCPX.

Females show an inherent cardioprotection from ischaemic insults, such as myocardial infarct, when compared with age-matched males up to the time of menopause. At this point,

the differences tend to equalize, and in later life can even be worse for females. This inherent female-specific cardioprotection has been suggested to involve PKC $\epsilon$  (Bae & Zhang, 2005). Moreover, Bae & Zhang (2005) identified that female hearts expressed a higher level of the active (phosphorylated) form of PKC $\epsilon$  compared that in the male as well as a significant increasing in phosphor-PKC $\epsilon$  following reperfusion in females over males. In addition, Edwards *et al* (2009) suggested that the PKC $\epsilon$  is the key factor in the enrichment of SarcoK<sub>ATP</sub> in female heart.

In terms of the specific K<sub>ir</sub>6.1/SUR2B channel, some literature suggests the activation of PKC inhibits the K<sub>ir</sub>6.1/SUR2B channel (Cole *et al.*, 2000; Suga *et al.*, 2001; Thorneloe *et al.*, 2002; Jiao *et al.*, 2008). In mesenteric smooth muscle cell, the activation of PKC by Angiotensin II was known to cause contraction via suppressing K<sub>ir</sub>6.1/SUR2B currents and potentiation of Ca<sup>2+</sup> currents (Cole *et al.*, 2000). Furthermore, following application of arginine vasopressin, a PKC activator, the K<sub>ir</sub>6.1/SUR2B currents were significantly inhibited, where the inhibitory effect was reversed by PKC antagonists such as calphostin-C or PKC inhibitor peptide (PKCi) (Shi *et al.*, 2007). Moreover, the inhibitory effect was achieved by internalisation of the K<sub>ir</sub>6.1/SUR2B channel (Jiao *et al.*, 2008). The channel kinetics analysis supports this idea, which demonstrates no alteration in single channel burst duration but prolonged interburst interval (Cole *et al.*, 2000).

Whereas PKC tends to inhibit the vascular K<sub>ATP</sub> isoform, PKA tends to show a stimulatory effect on the current. Using isoprenaline, which activates cyclic AMP-dependent protein kinase (PKA) via  $\beta$ -adrenoceptors, a robust K<sub>ATP</sub> current was elicited in smooth muscle cells as well as a hyperpolarisation of the membrane potential (Nelson *et al.*, 2011). Furthermore, the increased K<sub>ATP</sub> currents that were activated by isoprenaline were inhibited by PKA inhibitor KT5720 (Nelson *et al.*, 2011), suggesting the vasculature K<sub>ATP</sub> channel is PKA-dependent. In addition, Shi *et al* (2007) demonstrated the a similar results in K<sub>ir</sub>6.1/SUR2B recombinant channel in HEK cells, where isoprenaline activated the K<sub>ir</sub>6.1/SUR2B current but the increased current was blocked by PKA inhibitors such as RP-cAMP and RKI5-24. In K<sub>ir</sub>6.1/SUR2B recombinant channel investigations, a significant up-regulation of current was seen following application of vasoactive intestinal polypeptide, a PKA signalling pathway activator (Shi *et al.*, 2007; Yang *et al.*, 2008). Additionally,

directly perfused catalytic subunit of PKA to the  $K_{ir}6.1/SUR2B$  recombinant channel in HEK cells, in the inside-out configuration, caused a significant increase in the channel activity (Shi *et al.*, 2007).

In cardiac cells, PKA was activated by ischaemic preconditioning, and the cardioprotective effect was abolished by PKA inhibitors (Ye *et al.*, 2010). Furthermore, IPC triggers an increase in NO via eNOS phosphorylation, which requires the activation of PKA signalling pathway (Yang *et al.*, 2013). Additionally, Khaliulin *et al* (2010) suggested that the adenosine-induced cardioprotection did not act through a single effector of PKC but required both synergistic PKA and PKC actions.

Thus, the modulation of Sarco $K_{ir}6.1$  remains unclear. Further work is required on the Sarco $K_{ir}6.1$  signalling pathway. The identification of Sarco $K_{ir}6.1$  as a putative effector of at least part of the cardioprotective phenotype marks a big step forward in our understanding of the intrinsic protection that can be afforded to the myocardium.

#### **7.4 Future directions for research**

The work presented in this thesis presented a vasculature type  $K_{ATP}$  channel,  $K_{ir}6.1/SUR2B$ , expressed on the cardiac sarcolemmal membrane, which regulates cardiac physiology in resting conditions as well as potentially being a cardioprotective effector via shortening the APD. However, in order to further clarify the channels properties as well as its physiological role, there are still questions to answer.

Firstly, what signalling pathway regulates the  $K_{ir}6.1/SUR2B$  channel in cardiomyocytes? Although the activation of  $PKC\epsilon$  was suggested to increase the  $K_{ATP}$  currents, previous studies have already shown that the vasculature  $K_{ATP}$  channel is actually inhibited by the activation of PKC. It was suggested by the vasculature type  $K_{ATP}$  research that the  $K_{ir}6.1/SUR2B$  channel can be activated by PKA signalling which signal is also involved in cardioprotection, provided a strong candidate signalling in future research. Given that the pathways involved in cardioprotection are multifactorial, it is plausible that PKA activation may modulate the surface  $K_{ir}6.1/SUR2B$  currents whilst  $PKC\epsilon$ , which is known to be

translocated to the mitochondria, may have an alternative intracellular effect on preserving energy.

Secondly, the absence of a control protein in the western blotting experiments significantly reduces the strength of the knockdown data. Although the functional data using shRNA knockdown and pharmacological inhibition show similar results; in order to complete this story the effects on protein (western blotting) and mRNA (PCR) need to be completed.

Thirdly, all experiments in this project were carried out in isolated cardiomyocytes. It would be interesting to determine in whole-heart experiments whether a  $K_{ir}6.1$  specific blocker such as PNU37883A, can increase, or a specific activator reduce, the infarct size in coronary ligation experiments.

## 7.5 Conclusions

In this study, expression of functional  $K_{ir}6.1/SUR2B$  channels has been identified at the cell surface. The current was shown to be constitutively active, in keeping with current understanding of this subunit combination from other tissues, and was demonstrated to play a role in the modulation of the action potential and resting membrane potential. The current was identified in three different species and the functional effects of this current demonstrate in both rat and guinea pig cardiomyocytes. The current was increased following cardioprotective stimuli, and the cardioprotection was abolished by treatment with a selective  $K_{ir}6.1$  blocker.

This study shows that the  $I_{KATP}$  current in ventricular myocytes is comprised of two components. Firstly, the classically described  $K_{ir}6.2/SUR2A$  large conductance current ( $I_{KATP-LC}$ ).  $I_{KATP-LC}$  is a metabolically sensitive component that fulfils the original description of  $K_{ATP}$  in cardiac cells of a current that activates in conditions of severe ATP depletion to protect the remaining ATP reserves. Secondly, the newly identified  $K_{ir}6.1/SUR2B$  small conductance current ( $I_{KATP-SC}$ ).  $I_{KATP-SC}$  is constitutively active and modulates the resting membrane potential and the action potential duration. Additionally,  $I_{KATP-SC}$  is potentiated by cardioprotective stimuli that cause a shortening of the APD and a hyperpolarization. This reduces  $Ca^{2+}$ -influx during each contractile cycle, so reducing ATP

consumption, which further limits  $\text{Ca}^{2+}$  overload in ischaemic conditions. This has the effect of allowing cells to continue to function for longer during metabolic stress, helping to explain our previous findings (Brennan *et al.*, 2015), and reduces the incidence of reperfusion injury.

Should a selective activator of  $\text{I}_{\text{KATP-SC}}$  be identified, this compound could potentially be used to pharmacologically induce cardioprotection in hearts of people at risk of myocardial infarction. The identification of this  $\text{K}_{\text{ir}}6.1/\text{SUR2B}$  channel complex in the myocardium is a unique opportunity to develop a novel therapeutic, as a potential drug target, in the complex field of ischaemia and reperfusion injury.

## References

- Ackerman MJ & Clapham DE (1997). Ion Channels — Basic Science and Clinical Disease ed. Epstein FH. *N Engl J Med* **336**, 1575–1586.
- Aggarwal NT, Shi NQ & Makielski JC (2013). ATP-sensitive potassium currents from channels formed by Kir6 and a modified cardiac mitochondrial SUR2 variant. *Channels*; DOI: 10.4161/chan.26181.
- Aguilar-Bryan L, Clement JP, Gonzalez G, Kunjilwar K, Babenko A & Bryan J (1998). Toward understanding the assembly and structure of K(ATP) channels. *Physiol Rev* **78**, 227–245.
- Ahmad AMZ, Ali GSR & Tariq W (2014). Remote ischemic preconditioning is a safe adjuvant technique to myocardial protection but adds no clinical benefit after on-pump coronary artery bypass grafting. *Heart Surg Forum* **17**, E220–E223.
- Akao M, Otani H, Horie M, Takano M, Kuniyasu a, Nakayama H, Kouchi I, Murakami T & Sasayama S (1997). Myocardial ischemia induces differential regulation of KATP channel gene expression in rat hearts. *J Clin Invest* **100**, 3053–3059.
- Akrouh A, Halcomb SE, Nichols CG & Sala-Rabanal M (2011). Molecular biology of KATP and disease channels and implications for health. *IUBMB Life* **61**, 971–978.
- Aldakkak M, Stowe DF, Chen Q, Lesnefsky EJ & Camara AKS (2008). Inhibited mitochondrial respiration by amobarbital during cardiac ischaemia improves redox state and reduces matrix Ca<sup>2+</sup> overload and ROS release. *Cardiovasc Res* **77**, 406–415.
- Allen TGJ & Brown D a (2004). Modulation of the excitability of cholinergic basal forebrain neurones by KATP channels. *J Physiol* **554**, 353–370.
- Amin AS, Tan HL & Wilde AAM (2010). Cardiac ion channels in health and disease. *Heart Rhythm* **7**, 117–126.

- Ammälä C, Moorhouse A & Ashcroft FM (1996). The sulphonylurea receptor confers diazoxide sensitivity on the inwardly rectifying K<sup>+</sup> channel Kir6.1 expressed in human embryonic kidney cells. *J Physiol* **494** ( Pt 3, 709–714.
- An WF, Bowlby MR, Betty M, Cao J, Ling HP, Mendoza G, Hinson JW, Mattsson KI, Strassle BW, Trimmer JS & Rhodes KJ (2000). Modulation of A-type potassium channels by a family of calcium sensors. *Nature* **403**, 553–556.
- Antcliff JF, Haider S, Proks P, Sansom MS & Ashcroft FM (2005). Functional analysis of a structural model of the ATP-binding site of the KATP channel Kir6.2 subunit. *EMBO J* **24**, 229–239.
- Ashcroft FM (2005). ATP-sensitive potassium channelopathies: focus on insulin secretion. *J Clin Invest* **115**, 2047–2058.
- Ashfield R, Gribble FM, Ashcroft SJH & Ashcroft FM (2000). Identification of the high-affinity tolbutamide site on the SUR1 subunit of the K(ATP) channel. *Diabetes* **48**, 1341–1347.
- Avshalumov M V & Rice ME (2003). Activation of ATP-sensitive K<sup>+</sup> (K(ATP)) channels by H<sub>2</sub>O<sub>2</sub> underlies glutamate-dependent inhibition of striatal dopamine release. *Proc Natl Acad Sci U S A* **100**, 11729–11734.
- Aziz Q, Thomas A, Khambra T & Tinker A (2010). Phenformin has a direct inhibitory effect on the ATP-sensitive potassium channel. *Eur J Pharmacol* **634**, 26–32.
- Aziz Q, Thomas AM, Gomes J, Ang R, Sones WR, Li Y, Ng KE, Gee L & Tinker A (2014). The ATP-sensitive potassium channel subunit, Kir6.1, in vascular smooth muscle plays a major role in blood pressure control. *Hypertension* **64**, 523–529.
- Aziz Q, Thomas AM, Khambra T & Tinker A (2012). Regulation of the ATP-sensitive potassium channel subunit, Kir6.2, by a Ca<sup>2+</sup>-dependent protein kinase C. *J Biol Chem* **287**, 6196–6207.
- Babenko AP & Bryan J (2001). A Conserved Inhibitory and Differential Stimulatory Action of Nucleotides on KIR6.0/SUR Complexes Is Essential for Excitation-

- Metabolism Coupling by KATP Channels. *J Biol Chem* **276**, 49083–49092.
- Babenko AP, Gonzalez G, Aguilar-Bryan L & Bryan J (1998). Reconstituted human cardiac KATP channels: functional identity with the native channels from the sarcolemma of human ventricular cells. *Circ Res* **83**, 1132–1143.
- Babenko AP, Gonzalez G & Bryan J (1999). Two Regions of Sulfonylurea Receptor Specify the Spontaneous Bursting and ATP Inhibition of K ATP Channel Isoforms. *J Biol Chem* **274**, 11587–11592.
- Bae S & Zhang L (2005). Gender Differences in Cardioprotection against Ischemia / Reperfusion Injury in Adult Rat Hearts : Focus on Akt and Protein Kinase C Signaling. *Pharmacology* **315**, 1125–1135.
- Bajgar R, Seetharaman S, Kowaltowski AJ, Garlid KD & Paucek P (2001). Identification and Properties of a Novel Intracellular (Mitochondrial) ATP-sensitive Potassium Channel in Brain. *J Biol Chem* **276**, 33369–33374.
- Ballanyi K (2004). Protective role of neuronal KATP channels in brain hypoxia. *J Exp Biol* **207**, 3201–3212.
- Bao L, Kefaloyianni E, Lader J, Hong M, Morley G, Fishman GI, Sobie EA & Coetzee WA (2011). Unique properties of the ATP-sensitive K<sup>+</sup> channel in the mouse ventricular cardiac conduction system. *Circ Arrhythmia Electrophysiol* **4**, 926–935.
- Barajas-Martínez H, Hu D, Ferrer T, Onetti CG, Wu Y, Burashnikov E, Boyle M, Surman T, Urrutia J, Veltmann C, Schimpf R, Borggreffe M, Wolpert C, Ibrahim BB, Sánchez-Chapula JA, Winters S, Haïssaguerre M & Antzelevitch C (2012). Molecular genetic and functional association of Brugada and early repolarization syndromes with S422L missense mutation in KCNJ8. *Hear Rhythm* **9**, 548–555.
- Barhanin J, Lesage F, Guillemare E, Fink M, Lazdunski M & Romey G (1996). KvLQT1 and IsK (minK) proteins associate to form the IKS cardiac potassium current. *Nature* **384**, 78–80.
- Baruscotti M, Bucchi A & DiFrancesco D (2005). Physiology and pharmacology of the

- cardiac pacemaker (“funny”) current. *Pharmacol Ther* **107**, 59–79.
- Baukrowitz T, Tucker SJ, Schulte U, Benndorf K, Ruppersberg JP & Fakler B (1999). Inward rectification in K(ATP) channels: A pH switch in the pore. *EMBO J* **18**, 847–853.
- Bennett K, James C & Hussain K (2010). Pancreatic  $\beta$ -cell KATP channels: Hypoglycaemia and hyperglycaemia. *Rev Endocr Metab Disord* **11**, 157–163.
- Bennett PB, Yazawa K, Makita N & George AL (1995). Molecular mechanism for an inherited cardiac arrhythmia. *Nature* **376**, 683–685.
- Berg JM, Tymoczko JL & Stryer L (2002). Biochemistry. 5th edition. New York: W H Freeman; 2002. Section 13.6, Gap Junctions Allow Ions and Small Molecules to Flow between Communicating Cells.
- Bernardo NL, Okubo S, Maaieh MM, Wood MA & Kukreja RC (1999). Delayed preconditioning with adenosine is mediated by opening of ATP-sensitive K(+) channels in rabbit heart. *Am J Physiol* **277**, H128-35.
- Bernstein E, Caudy AA, Hammond SM & Hannon GJ (2001). Role for a bidentate ribonuclease in the initiation step of RNA interference. *Nature* **409**, 363–366.
- van Bever L, Poitry S, Faure C, Norman RI, Roatti A & Baertschi AJ (2004). Pore loop-mutated rat KIR6.1 and KIR6.2 suppress KATP current in rat cardiomyocytes. *Am J Physiol Heart Circ Physiol* **287**, H850-9.
- Beyder A, Rae JL, Bernard C, Strege PR, Sachs F & Farrugia G (2010). Mechanosensitivity of Nav1.5, a voltage-sensitive sodium channel. *J Physiol* **588**, 4969–4985.
- Bezannilla F & Perozo E (2003). The voltage sensor and the gate in ion channels. *Adv Protein Chem* **63**, 211–241.
- Bienengraeber M, Olson TM, Selivanov VA, Kathmann EC, O’Cochlain F, Gao F, Karger AB, Ballew JD, Hodgson DM, Zingman L V, Pang Y-P, Alekseev AE & Terzic A

- (2004). ABCC9 mutations identified in human dilated cardiomyopathy disrupt catalytic KATP channel gating. *Nat Genet* **36**, 382–387.
- Billman GE, Englert HC & Schölkens B a (1998). HMR 1883, a novel cardioselective inhibitor of the ATP-sensitive potassium channel. Part II: effects on susceptibility to ventricular fibrillation induced by myocardial ischemia in conscious dogs. *J Pharmacol Exp Ther* **286**, 1465–1473.
- Birnbaum Y, Hale SL & Kloner RA (1997). Ischemic preconditioning at a distance: reduction of myocardial infarct size by partial reduction of blood supply combined with rapid stimulation of the gastrocnemius muscle in the rabbit. *Circulation* **96**, 1641–1646.
- Bodi I (2005). The L-type calcium channel in the heart: the beat goes on. *J Clin Invest* **115**, 3306–3317.
- Bodi I (2012). *Cardiac Arrhythmias - New Considerations*. Breijo-Marquez FR. InTech. Available at: <http://www.intechopen.com/books/atherosclerotic-cardiovascular-disease>.
- Van Bon BWMM et al. (2012). Cantú Syndrome Is Caused by Mutations in ABCC9. *Am J Hum Genet* **90**, 1094–1101.
- Bond CT, Pessia M, Xia XM, Lagrutta A, Kavanaugh MP & Adelman JP (1994). Cloning and expression of a family of inward rectifier potassium channels. *Receptors Channels* **2**, 183–191.
- Bøtker HE, Kharbanda R, Schmidt MR, Bøttcher M, Kalltoft AK, Terkelsen CJ, Munk K & Andersen NH (2010). Remote ischaemic conditioning before hospital admission, as a complement to angioplasty, and effect on myocardial salvage in patients with acute myocardial infarction: a randomised trial. *Lancet* **375**, 727–734.
- Bourgonje VJA, Vos MA, Ozdemir S, Doisne N, Acsai K, Varro A, Sztojokov-Ivanov A, Zupko I, Rauch E, Kattner L, Bito V, Houtman M, Van Der Nagel R, Beekman JD, Van Veen TAB, Sipido KR & Antoons G (2013). Combined Na<sup>+</sup>/Ca<sup>2+</sup> exchanger and l-type calcium channel block as a potential strategy to suppress arrhythmias and

- maintain ventricular function. *Circ Arrhythmia Electrophysiol* **6**, 371–379.
- Boyden PA, Pu J, Pinto J & Keurs HE (2000). Ca(2+) transients and Ca(2+) waves in purkinje cells : role in action potential initiation. *Circ Res* **86**, 448–455.
- Boyett MR, Honjo H & Kodama I (2000). The sinoatrial node, a heterogeneous pacemaker structure. *Cardiovasc Res* **47**, 658–687.
- Braun GS, Veh RW, Segerer S, Horster MF & Huber SM (2002). Developmental expression and functional significance of Kir channel subunits in ureteric bud and nephron epithelia. *Pflugers Arch Eur J Physiol* **445**, 321–330.
- Bredt DS, Wang TL, Cohen NA, Guggino WB & Snyder SH (1995). Cloning and expression of two brain-specific inwardly rectifying potassium channels. *Proc Natl Acad Sci* **92**, 6753–6757.
- Brennan S, Jackson R, Patel M, Sims MW, Hudman D, Norman RI, Lodwick D & Rainbow RD (2015). Early opening of sarcolemmal ATP-sensitive potassium channels is not a key step in PKC-mediated cardioprotection. *J Mol Cell Cardiol* **79**, 42–53.
- Brette F & Orchard CH (2006). No apparent requirement for neuronal sodium channels in excitation-contraction coupling in rat ventricular myocytes. *Circ Res* **98**, 667–674.
- Bronson SK & Smithies O (1994). Altering mice by homologous recombination using embryonic stem cells. *J Biol Chem* **269**, 27155–27158.
- Brown AM (2004). Drugs, hERG and sudden death. *Cell Calcium* **35**, 543–547.
- Brunner F, Maier R, Andrew P, Wölkart G, Zechner R & Mayer B (2003). Attenuation of myocardial ischemia/reperfusion injury in mice with myocyte-specific overexpression of endothelial nitric oxide synthase. *Cardiovasc Res* **57**, 55–62.
- Bryan J & Aguilar-Bryan L (1999). Sulfonylurea receptors: ABC transporters that regulate ATP-sensitive K<sup>+</sup> channels. *Biochim Biophys Acta - Biomembr* **1461**, 285–303.
- Bryant SM, Wan X, Shipsey SJ & Hart G (1998). Regional differences in the delayed rectifier current (I(Kr) and I(Ks)) contribute to the differences in action potential

- duration in basal left ventricular myocytes in guinea-pig. *Cardiovasc Res* **40**, 322–331.
- Budas GR, Churchill EN & Mochly-Rosen D (2007). Cardioprotective mechanisms of PKC isozyme-selective activators and inhibitors in the treatment of ischemia-reperfusion injury. *Pharmacol Res* **55**, 523–536.
- Budas GR, Jovanovic S, Crawford RM & Jovanovic A (2004). Hypoxia-induced preconditioning in adult stimulated cardiomyocytes is mediated by the opening and trafficking of sarcolemmal KATP channels. *FASEB J* **18**, 1046–1048.
- Burashnikov A & Antzelevitch C (2011). Novel pharmacological targets for the rhythm control management of atrial fibrillation. *Pharmacol Ther* **132**, 300–313.
- Burke MA, Mutharasan RK & Ardehali H (2008). The sulfonylurea receptor, an atypical ATP-binding cassette protein, and its regulation of the KATP channel. *Circ Res* **102**, 164–176.
- Burton FL & Cobbe SM (2001). Dispersion of ventricular repolarization and refractory period. *Cardiovasc Res* **50**, 10–23.
- Calloe K, Cordeiro JM, Di Diego JM, Hansen RS, Grunnet M, Olesen SP & Antzelevitch C (2009). A transient outward potassium current activator recapitulates the electrocardiographic manifestations of Brugada syndrome. *Cardiovasc Res* **81**, 686–694.
- CALLOE K, NOF E, JESPERSEN T, DI DIEGO JM, CHLUS N, OLESEN S-P, ANTZELEVITCH C & CORDEIRO JM (2011). Comparison of the Effects of a Transient Outward Potassium Channel Activator on Currents Recorded from Atrial and Ventricular Cardiomyocytes. *J Cardiovasc Electrophysiol* **22**, 1057–1066.
- Campbell JD, Sansom MS & Ashcroft FM (2003). Potassium channel regulation. *EMBO Rep* **4**, 1038–1042.
- Carmeliet E (1987). Slow inactivation of the sodium current in rabbit cardiac Purkinje fibres. *Pflugers Arch Eur J Physiol* **408**, 18–26.

- Casademont J & Miró O (2002). Electron transport chain defects in heart failure. *Heart Fail Rev* **7**, 131–139.
- Chen M, Dong Y & Simard JM (2003). Functional coupling between sulfonylurea receptor type 1 and a nonselective cation channel in reactive astrocytes from adult rat brain. *J Neurosci* **23**, 8568–8577.
- Chen P-SS, Chen LS, Fishbein MC, Lin S-FF & Nattel S (2014). Role of the autonomic nervous system in atrial fibrillation: Pathophysiology and therapy. *Circ Res* **114**, 1500–1515.
- Chen X, Yang L & Zhai S Di (2012). Risk of cardiovascular disease and all-cause mortality among diabetic patients prescribed rosiglitazone or pioglitazone: A meta-analysis of retrospective cohort studies. *Chin Med J (Engl)* **125**, 4301–4306.
- Cheng J, Kamiya K, Liu W, Tsuji Y, Toyama J & Kodama I (1999). Heterogeneous distribution of the two components of delayed rectifier K<sup>+</sup> current: a potential mechanism of the proarrhythmic effects of methanesulfonanilide class III agents. *CardiovascRes* **43**, 135–147.
- Cheng J, Van Norstrand DW, Medeiros-Domingo A, Valdivia C, Tan BH, Ye B, Kroboth S, Vatta M, Tester DJ, January CT, Makielski JC & Ackerman MJ (2009). Alpha1-syntrophin mutations identified in sudden infant death syndrome cause an increase in late cardiac sodium current. *CircArrhythmElectrophysiol* **2**, 667–676.
- Cheung MMH, Kharbanda RK, Konstantinov IE, Shimizu M, Frndova H, Li J, Holtby HM, Cox PN, Smallhorn JF, Van Arsdell GS & Redington AN (2006). Randomized Controlled Trial of the Effects of Remote Ischemic Preconditioning on Children Undergoing Cardiac Surgery. *J Am Coll Cardiol* **47**, 2277–2282.
- Chutkow WA, Samuel V, Hansen PA, Pu J, Valdivia CR, Makielski JC & Burant CF (2001). Disruption of Sur2-containing KATP channels enhances insulin-stimulated glucose uptake in skeletal muscle. *Proc Natl Acad Sci U S A* **98**, 11760–11764.
- Clarke PA & Mathews MB (1995). Interactions between the double-stranded RNA binding

motif and RNA: definition of the binding site for the interferon-induced protein kinase DAI (PKR) on adenovirus VA RNA. *RNA* **1**, 7–20.

Cohen M V, Baines CP & Downey JM (2000). Ischemic preconditioning: from adenosine receptor to KATP channel. *Annu Rev Physiol* **62**, 79–109.

Cohen M V, Yang XM, Liu GS, Heusch G & Downey JM (2001). Acetylcholine, bradykinin, opioids, and phenylephrine, but not adenosine, trigger preconditioning by generating free radicals and opening mitochondrial K(ATP) channels. *Circ Res* **89**, 273–278.

Colareda GA, Ragone MI & Consolini AE (2016). Sex differences in the mechano-energetic effects of genistein on stunned rat and guinea pig hearts. *Clin Exp Pharmacol Physiol* **43**, 102–115.

Cole WC, Malcolm T, Walsh MP & Light PE (2000). Inhibition by protein kinase C of the K(NDP) subtype of vascular smooth muscle ATP-sensitive potassium channel. *Circ Res* **87**, 112–117.

Colquhoun D & Hawkes a G (1982). On the stochastic properties of bursts of single ion channel openings and of clusters of bursts. *Philos Trans R Soc Lond B Biol Sci* **300**, 1–59.

Costa ADT, Garlid KD, West IC, Lincoln TM, Downey JM, Cohen M V. & Critz SD (2005). Protein kinase G transmits the cardioprotective signal from cytosol to mitochondria. *Circ Res* **97**, 329–336.

Cui Y, Giblin JP, Clapp LH & Tinker a (2001). A mechanism for ATP-sensitive potassium channel diversity: Functional coassembly of two pore-forming subunits. *Proc Natl Acad Sci U S A* **98**, 729–734.

Cui Y, Tinker A & Clapp LH (2003). Different molecular sites of action for the KATP channel inhibitors, PNU-99963 and PNU-37883A. *Br J Pharmacol* **139**, 122–128.

Cullen BR (2006). Induction of stable RNA interference in mammalian cells. *Gene Ther* **13**, 503–508.

- Van Cuong D, Kim N, Joo H, Youm JB, Chung JY, Lee Y, Park WS, Kim E, Park YS & Han J (2005). Subunit composition of ATP-sensitive potassium channels in mitochondria of rat hearts. *Mitochondrion* **5**, 121–133.
- D'hahan N, Moreau C, Prost A-L, Jacquet H, Alekseev a E, Terzic A & Vivaudou M (1999). Pharmacological plasticity of cardiac ATP-sensitive potassium channels toward diazoxide revealed by ADP. *Proc Natl Acad Sci* **96**, 12162–12167.
- Dabrowski M, Trapp S & Ashcroft FM (2003). Pyridine nucleotide regulation of the K ATP channel Kir6 . 2 / SUR1 expressed in *Xenopus* oocytes. 357–363.
- Das M, Parker JE & Halestrap AP (2003). Matrix volume measurements challenge the existence of diazoxide/glibenclamide-sensitive KATP channels in rat mitochondria. *J Physiol* **547**, 893–902.
- Das S (2004). Pharmacological preconditioning with resveratrol: role of CREB-dependent Bcl-2 signaling via adenosine A3 receptor activation. *AJP Hear Circ Physiol* **288**, H328–H335.
- Davies LM, Purves GI, Barrett-Jolley R & Dart C (2010). Interaction with caveolin-1 modulates vascular ATP-sensitive potassium (KATP) channel activity. *J Physiol* **588**, 3255–3266.
- Delaney JT, Muhammad R, Blair MA, Kor K, Fish FA, Roden DM & Darbar D (2012). A KCNJ8 mutation associated with early repolarization and atrial fibrillation. *Europace* **14**, 1428–1432.
- Deschamps A, Murphy E & Sun J (2011). Estrogen receptor activation and cardioprotection in ischemia reperfusioninjury. *Trends Cardiovasc Med* **20**, 73–78.
- Deschênes I & Tomaselli GF (2002). Modulation of Kv4.3 current by accessory subunits. *FEBS Lett* **528**, 183–188.
- Diderholm E (2002). ST depression in ECG at entry indicates severe coronary lesions and large benefits of an early invasive treatment strategy in unstable coronary artery disease. The FRISC II ECG substudy. *Eur Heart J* **23**, 41–49.

- DiFrancesco D (1995). The onset and autonomic regulation of cardiac pacemaker activity: relevance of the f current. *Cardiovasc Res* **29**, 449–456.
- DiFrancesco D (2010). The Role of the Funny Current in Pacemaker Activity. *Circ Res* **106**, 434–446.
- Diness TG, Hansen RS, Olesen S-P & Grunnet M (2006). Frequency-dependent modulation of KCNQ1 and HERG1 potassium channels. *Biochem Biophys Res Commun* **343**, 1224–1233.
- Doerr T, Denger R & Trautwein W (1989). Calcium currents in single SA nodal cells of the rabbit heart studied with action potential clamp. *Pflügers Arch* **413**, 599–603.
- Dörschner H, Brekardin E, Uhde I, Schwanstecher C & Schwanstecher M (1999). Stoichiometry of sulfonylurea-induced ATP-sensitive potassium channel closure. *Mol Pharmacol* **55**, 1060–1066.
- Downey JM, Davis AM & Cohen M V. (2007). Signaling pathways in ischemic preconditioning. *Heart Fail Rev* **12**, 181–188.
- Dröse S, Brandt U & Hanley PJ (2006). K<sup>+</sup>-independent actions of diazoxide question the role of inner membrane KATP channels in mitochondrial cytoprotective signaling. *J Biol Chem* **281**, 23733–23739.
- Du R-H, Dai T, Cao W-J, Lu M, Ding J & Hu G (2014). Kir6.2-containing ATP-sensitive K(+) channel is required for cardioprotection of resveratrol in mice. *Cardiovasc Diabetol* **13**, 35.
- Eaton MJ, Skatchkov SN, Brune A, Biedermann B, Veh RW & Reichenbach A (2002). SUR1 and Kir6.1 subunits of K(ATP)-channels are co-localized in retinal glial (Müller) cells. *Neuroreport* **13**, 57–60.
- Edwards AG, Rees ML, Gioscia RA, Zachman DK, Lynch JM, Browder JC, Chicco AJ & Moore RL (2009). PKC-permitted elevation of sarcolemmal KATP concentration may explain female-specific resistance to myocardial infarction. *J Physiol* **587**, 5723–5737.

- Edwards H V., Scott JD & Baillie GS (2012). PKA phosphorylation of the small heat-shock protein Hsp20 enhances its cardioprotective effects. *Biochem Soc Trans* **40**, 210–214.
- Ekman M, Rippe C, Sadegh MK, Dabestani S, Mörgelin M, Uvelius B & Swärd K (2012). Association of muscarinic M3 receptors and Kir6.1 with caveolae in human detrusor muscle. *Eur J Pharmacol* **683**, 238–245.
- Elrod JW, Harrell M, Flagg TP, Gundewar S, Magnuson MA, Nichols CG, Coetzee WA & Lefler DJ (2008). Role of sulfonylurea receptor type 1 subunits of ATP-sensitive potassium channels in myocardial ischemia/reperfusion injury. *Circulation* **117**, 1405–1413.
- Erginel-Unaltuna N, Yang WP & Blamires M a (1998). Genomic organization and expression of KCNJ8/Kir6.1, a gene encoding a subunit of an ATP-sensitive potassium channel. *Gene* **211**, 71–78.
- Fabiato A (1985). Time and calcium dependence of activation and inactivation of calcium-induced release of calcium from the sarcoplasmic reticulum of a skinned canine cardiac Purkinje cell. *J Gen Physiol* **85**, 247–289.
- Faivre J-F & Findlay I (1990). Action potential duration and activation of ATP-sensitive potassium current in isolated guinea-pig ventricular myocytes. *Biochim Biophys Acta - Biomembr* **1029**, 167–172.
- Farzaneh T & Tinker A (2008). Differences in the mechanism of metabolic regulation of ATP-sensitive K<sup>+</sup> channels containing Kir6.1 and Kir6.2 subunits. *Cardiovasc Res* **79**, 621–631.
- Fedele F, Mancone M, Chilian WM, Severino P, Canali E, Logan S, De Marchis ML, Volterrani M, Palmirotta R & Guadagni F (2013). Role of genetic polymorphisms of ion channels in the pathophysiology of coronary microvascular dysfunction and ischemic heart disease. *Basic Res Cardiol* **108**, 387.
- Fedida D & Giles WR (1991). Regional variations in action potentials and transient outward current in myocytes isolated from rabbit left ventricle. *J Physiol* **442**, 191–

209.

- Feng J, Li H & Rosenkranz ER (2000). Bradykinin protects the rabbit heart after cardioplegic ischemia via NO-dependent pathways. *Ann Thorac Surg* **70**, 2119–2124.
- Fenwick EM, Marty A & Neher E (1982). Sodium and calcium channels in bovine chromaffin cells. *J Physiol* **331**, 599–635.
- Findlay I (1993). Sulphonylurea drugs no longer inhibit ATP-sensitive K<sup>+</sup> channels during metabolic stress in cardiac muscle. *J Pharmacol Exp Ther* **266**, 456–467.
- Fire A, Xu S, Montgomery MK, Kostas SA, Driver SE & Mello CC (1998). Potent and specific genetic interference by double-stranded RNA in *Caenorhabditis elegans*. *Nature* **391**, 806–811.
- Fischer-Lougheed J, Liu JH, Espinos E, Mordasini D, Bader CR, Belin D & Bernheim L (2001). Human myoblast fusion requires expression of functional inward rectifier Kir2.1 channels. *J Cell Biol* **153**, 677–685.
- Flagg TP, Enkvetchakul D, Koster JC & Nichols CG (2010). Muscle KATP Channels: Recent Insights to Energy Sensing and Myoprotection. *Physiol Rev* **90**, 799–829.
- Flagg TP, Kurata HT, Masia R, Caputa G, Magnuson MA, Lefer DJ, Coetzee WA & Nichols CG (2008). Differential structure of atrial and ventricular KATP: Atrial KATP channels require SUR1. *Circ Res* **103**, 1458–1465.
- Flagg TP & Nichols CG (2011). “Cardiac K ATP”: A family of ion channels. *Circ Arrhythmia Electrophysiol* **4**, 796–798.
- Foster DB, Ho AS, Rucker J, Garlid AO, Chen L, Sidor A, Garlid KD, Rourke BO & O’Rourke B (2012). Mitochondrial ROMK channel is a molecular component of mitoKATP. *Circ Res* **111**, 446–454.
- Foster DB, Rucker JJ & Marbán E (2008). Is Kir6.1 a subunit of mitoK(ATP)? *Biochem Biophys Res Commun* **366**, 649–656.
- Fryer RM, Hsu AK, Eells JT, Nagase H & Gross GJ (1999). Opioid-Induced Second

Window of Cardioprotection : Potential Role of Mitochondrial KATP Channels. *Circ Res* **84**, 846–851.

Fujita H, Ogura T, Tamagawa M, Uemura H, Sato T, Ishida a, Imamaki M, Kimura F, Miyazaki M & Nakaya H (2006). A key role for the subunit SUR2B in the preferential activation of vascular KATP channels by isoflurane. *Br J Pharmacol* **149**, 573–580.

Fujiwara T & Angus JA (1996). Analysis of relaxation and repolarization mechanisms of nicorandil in rat mesenteric artery. *Br J Pharmacol* **119**, 1549–1556.

Fukumoto T, Tawa M, Yamashita N, Ohkita M & Matsumura Y (2013). Protective effects of 17beta-estradiol on post-ischemic cardiac dysfunction and norepinephrine overflow through the non-genomic estrogen receptor/nitric oxide-mediated pathway in the rat heart. *Eur J Pharmacol* **699**, 74–80.

Fukuzaki K, Sato T, Miki T, Seino S & Nakaya H (2008). Role of sarcolemmal ATP-sensitive K<sup>+</sup> channels in the regulation of sinoatrial node automaticity: an evaluation using Kir6.2-deficient mice. *J Physiol* **586**, 2767–2778.

Garg V, Jiao J & Hu K (2009). Regulation of ATP-sensitive K<sup>+</sup> channels by caveolin-enriched microdomains in cardiac myocytes. *Cardiovasc Res* **82**, 51–58.

Garlid KD (2000). Opening mitochondrial K(ATP) in the heart - What happens, and what does not happen. *Basic Res Cardiol* **95**, 275–279.

Garlid KD, Paucek P, Yarov-Yarovoy V, Murray HN, Darbenzio RB, D'Alonzo AJ, Lodge NJ, Smith MA & Grover GJ (1997). Cardioprotective Effect of Diazoxide and Its Interaction With Mitochondrial ATP-Sensitive K<sup>+</sup> Channels Possible Mechanism of Cardioprotection. *Circ Res* **81**, 1072–1082.

Gho BCG, Eskildsen-Helmond YEG, De Zeeuw S, Lamers JMJ & Verdouw PD (1997). Does protein kinase C play a pivotal role in the mechanisms of ischemic preconditioning? *Cardiovasc Drugs Ther* **10**, 775–786.

Gho BCG, Schoemaker RG, van den Doel MA, Duncker DJ & Verdouw PD (1996). Myocardial protection by brief ischemia in noncardiac tissue. *Circulation* **94**, 2193–

2200.

- Ghovanloo MR, Abdelsayed M & Ruben PC (2016). Effects of amiodarone and N-desethylamiodarone on cardiac voltage-gated sodium channels. *Front Pharmacol* **7**, 1–11.
- Gliomas L (2015). Comprehensive, Integrative Genomic Analysis of Diffuse Lower-Grade Gliomas. *N Engl J Med* **248**:1–2498.
- Gopalakrishna R & Anderson WB (1989). Ca<sup>2+</sup>- and phospholipid-independent activation of protein kinase C by selective oxidative modification of the regulatory domain. *Proc Natl Acad Sci U S A* **86**, 6758–6762.
- Grange DK, Lorch SM, Cole PL & Singh GK (2006). Cantu syndrome in a woman and her two daughters: Further confirmation of autosomal dominant inheritance and review of the cardiac manifestations. *Am J Med Genet Part A* **140A**, 1673–1680.
- Gregory MM, Yoshioka C, Kandasamy B, DiMaio F & Shyng S-L (2017). Anti-diabetic drug binding site in K ATP channels revealed by Cryo-EM. *bioRxiv*172908.
- Gribble FM & Reimann F (2002). Pharmacological modulation of K(ATP) channels. *Biochem Soc Trans* **30**, 333–339.
- Gross GJ & Auchampach J a (1992). Blockade of ATP-sensitive potassium channels prevents myocardial preconditioning in dogs. *Circ Res* **70**, 223–233.
- Gross GJ & Fryer RM (1999). Sarcolemmal versus mitochondrial ATP-sensitive K<sup>+</sup> channels and myocardial preconditioning. *Circ Res* **84**, 973–979.
- Gross GJ & Peart JN (2003). KATP channels and myocardial preconditioning: an update. *Am J Physiol Heart Circ Physiol* **285**, H921–H930.
- Grover GJ & Garlid KD (2000). ATP-Sensitive potassium channels: a review of their cardioprotective pharmacology. *J Mol Cell Cardiol* **32**, 677–695.
- Grover GJ, Sleph PG & Dzwonczyk S (1992). Role of myocardial ATP-sensitive potassium channels in mediating preconditioning in the dog heart and their possible interaction

- with adenosine A1-receptors. *Circulation* **86**, 1310–1316.
- Gumina RJ, Pucar D, Bast P, Hodgson DM, Kurtz CE, Dzeja PP, Miki T, Seino S & Terzic A (2003). Knockout of Kir6.2 negates ischemic preconditioning-induced protection of myocardial energetics. *Am J Physiol - Hear Circ Physiol* **284**, H2106–H2113.
- Guo A, Zhang C, Wei S, Chen B & Song L-S (2013). Emerging mechanisms of T-tubule remodelling in heart failure. *Cardiovasc Res* **98**, 204–215.
- Györke I & Györke S (1998). Regulation of the cardiac ryanodine receptor channel by luminal Ca<sup>2+</sup> involves luminal Ca<sup>2+</sup> sensing sites. *Biophys J* **75**, 2801–2810.
- Györke S & Fill M (1993). Ryanodine receptor adaptation: control mechanism of Ca(2+)-induced Ca<sup>2+</sup> release in heart. *Science* **260**, 807–809.
- Hagiwara N, Irisawa H & Kameyama M (1988). Contribution of two types of calcium currents to the pacemaker potentials of rabbit sino-atrial node cells. *J Physiol* **395**, 233–253.
- HAÏSSAGUERRE M, CHATEL S, Sacher F, Weerasooriya R, Probst V, LOUSSOUARN G, HORLITZ M, Liersch R, Schulze-Bahr E, WILDE A, Käab S, Koster J, Rudy Y, Marec H LE & SCHOTT JJ (2009). Ventricular fibrillation with prominent early repolarization associated with a rare variant of KCNJ8/KATP channel. *J Cardiovasc Electrophysiol* **20**, 93–98.
- Halestrap AP, Clarke SJ & Khaliulin I (2007). The role of mitochondria in protection of the heart by preconditioning. *Biochim Biophys Acta* **1767**, 1007–1031.
- Hambrock A et al. (2001). Characterization of a mutant sulfonylurea receptor SUR2B with high affinity for sulfonylureas and openers: differences in the coupling to Kir6.x subtypes. *Mol Pharmacol* **60**, 190–199.
- Hammond SM, Bernstein E, Beach D & Hannon GJ (2000). An RNA-directed nuclease mediates post-transcriptional gene silencing in Drosophila cells. *Nature* **404**, 293–296.
- Hanley PJ, Mickel M, Löffler M, Brandt U & Daut J (2002). K ATP channel-independent

- targets of diazoxide and 5-hydroxydecanoate in the heart. *J Physiol* **542**, 735–741.
- Hanna ST, Cao K, Sun X & Wang R (2005). Mediation of the effect of nicotine on Kir6.1 channels by superoxide anion production. *J Cardiovasc Pharmacol* **45**, 447–455.
- Hattersley AT & Ashcroft FM (2005). Activating mutations in Kir6.2 and neonatal diabetes: New clinical syndromes, new scientific insights, and new therapy. *Diabetes* **54**, 2503–2513.
- Hausenloy DJ, Candilio L, Evans R, Ariti C, Jenkins DP, Kolvekar S, Knight R, Kunst G, Laing C, Nicholas J, Pepper J, Robertson S, Xenou M, Clayton T & Yellon DM (2015). Remote Ischemic Preconditioning and Outcomes of Cardiac Surgery. *N Engl J Med* **373**, 1408–1417.
- Hausenloy DJ & Yellon DM (2004). New directions for protecting the heart against ischaemia-reperfusion injury: Targeting the Reperfusion Injury Salvage Kinase (RISK)-pathway. *Cardiovasc Res* **61**, 448–460.
- Hausenloy DJ & Yellon DM (2008). Remote ischaemic preconditioning: Underlying mechanisms and clinical application. *Cardiovasc Res* **79**, 377–386.
- Heidland UE, Heintzen MP, Michel CJ & Strauer BE (2000). Effect of adjunctive intracoronary adenosine on myocardial ischemia, hemodynamic function and left ventricular performance during percutaneous transluminal coronary angioplasty: clinical access to ischemic preconditioning? *Coron Artery Dis* **11**, 421–428.
- Hennan JK, Swillo RE, Morgan GA, Rossman EI, Kantrowitz J, Butera J, Petersen JS, Gardell SJ & Vlasuk GP (2009). GAP-134 ([2S,4R]-1-[2-aminoacetyl]4-benzamidopyrrolidine-2-carboxylic acid) prevents spontaneous ventricular arrhythmias and reduces infarct size during myocardial ischemia/reperfusion injury in open-chest dogs. *J Cardiovasc Pharmacol Ther* **14**, 207–214.
- Heurteaux C, Lauritzen I, Widmann C & Lazdunski M (1995). Essential role of adenosine, adenosine A1 receptors, and ATP-sensitive K<sup>+</sup> channels in cerebral ischemic preconditioning. *Proc Natl Acad Sci USA* **92**, 4666–4670.

- Ho SY & Nihoyannopoulos P (2006). Anatomy, echocardiography, and normal right ventricular dimensions. *Heart* **92 Suppl 1**, i2-13.
- Hsieh GC, Kolasa T, Sullivan JP & Brioni JD (2001). Dual mechanism of action of nicorandil on rabbit corpus cavernosal smooth muscle tone. *Int J Impot Res* **13**, 240–246.
- Hsu C-Y, Fang S-Y, Chen Y-Z, Roan J-N, Chang S-W, Huang C-C, Liu Y-C, Lam C-F & Tsai Y-C (2012). Cardiovascular Protection of Activating KATP Channel During Ischemia-Reperfusion Acidosis. *Shock* **37**, 653–658.
- Hsu PD, Lander ES & Zhang F (2014). Development and applications of CRISPR-Cas9 for genome engineering. *Cell* **157**, 1262–1278.
- Huang KP (1989). The mechanism of protein kinase C activation. *Trends Neurosci* **12**, 425–432.
- Hussain M, Wareham AC & Head SI (1994). Mechanism of action of a K<sup>+</sup> channel activator BRL 38227 on ATP-sensitive K<sup>+</sup> channels in mouse skeletal muscle fibres. *J Physiol* **478**, 523–532.
- Huxley AF (1974). Muscular contraction. *J Physiol* **243**, 1–43.
- Ibrahim M, Gorelik J, Yacoub MH & Terracciano CM (2011). The structure and function of cardiac t-tubules in health and disease. *Proc Biol Sci* **278**, 2714–2723.
- Imanishi S & Surawicz B (1976). Automatic activity in depolarized guinea pig ventricular myocardium. Characteristics and mechanisms. *Circ Res* **39**, 751–759.
- Inagaki N, Gono T, Clement JP, Namba N, Inazawa J, Gonzalez G, Aguilar-Bryan L, Seino S & Bryan J (1995). Reconstitution of IKATP: an inward rectifier subunit plus the sulfonylurea receptor. *Science* **270**, 1166–1170.
- Inagaki N, Gono T, Clement IV JP, Wang CZ, Aguilar-Bryan L, Bryan J & Seino S (1996). A family of sulfonylurea receptors determines the pharmacological properties of ATP-sensitive K<sup>+</sup> channels. *Neuron* **16**, 1011–1017.

- Inagaki N, Gono T & Seino S (1997). Subunit stoichiometry of the pancreatic  $\beta$ -cell ATP-sensitive K<sup>+</sup> channel. *FEBS Lett* **409**, 232–236.
- Inserte J, Garcia-Dorado D, Ruiz-Meana M, Padilla F, Barrabés JA, Pina P, Agulló L, Piper HM & Soler-Soler J (2002). Effect of inhibition of Na<sup>(+)</sup>/Ca<sup>(2+)</sup> exchanger at the time of myocardial reperfusion on hypercontracture and cell death. *Cardiovasc Res* **55**, 739–748.
- Insuk SO, Chae MR, Choi JW, Yang DK, Sim JH & Lee SW (2003). Molecular basis and characteristics of KATP channel in human corporal smooth muscle cells. *Int J Impot Res* **15**, 258–266.
- Irisawa H (1978). Comparative physiology of the cardiac pacemaker mechanism. *Physiol Rev* **58**, 461–498.
- Isidoro Tavares N, Philip-Couderc P, Papageorgiou I, Baertschi AJ, Lerch R & Montessuit C (2007). Expression and function of ATP-dependent potassium channels in late post-infarction remodeling. *J Mol Cell Cardiol* **42**, 1016–1025.
- Isomoto S, Kondo C, Yamada M, Matsumoto S, Higashiguchi O, Horio Y, Matsuzawa Y & Kurachi Y (1996). A novel sulfonylurea receptor forms with BIR (Kir6.2) a smooth muscle type ATP-sensitive K<sup>+</sup> channel. *J Biol Chem* **271**, 24321–24324.
- Ivanov S V., Ward JM, Tessarollo L, McAreavey D, Sachdev V, Fananapazir L, Banks MK, Morris N, Djurickovic D, Devor-Henneman DE, Wei M-H, Alvord GW, Gao B, Richardson JA, Minna JD, Rogawski MA & Lerman MI (2004). Cerebellar Ataxia, Seizures, Premature Death, and Cardiac Abnormalities in Mice with Targeted Disruption of the *Cacna2d2* Gene. *Am J Pathol* **165**, 1007–1018.
- Jafri MS (2012). Models of Excitation–Contraction Coupling in Cardiac Ventricular Myocytes. *Methods Mol Biol* **531**, 588.
- Jespersen T, Grunnet M & Olesen S-P (2005). The KCNQ1 potassium channel: From gene to physiological function. *Physiology* **20**, 408–416.
- Jiao J, Garg V, Yang B, Elton TS & Hu K (2008). Protein kinase C- $\epsilon$ ; Induces

- caveolin-dependent internalization of vascular adenosine 5'-triphosphate-sensitive K<sup>+</sup> channels. *Hypertension* **52**, 499–506.
- Jones PP, Guo W & Chen SRW (2017). Control of cardiac ryanodine receptor by sarcoplasmic reticulum luminal Ca<sup>2+</sup>. *J Gen Physiol* **149**, 867–875.
- Jovanović S, Ballantyne T, Du Q, Blagojević M & Jovanović A (2016). Phenylephrine preconditioning in embryonic heart H9c2 cells is mediated by up-regulation of SUR2B/Kir6.2: A first evidence for functional role of SUR2B in sarcolemmal KATP channels and cardioprotection. *Int J Biochem Cell Biol* **70**, 23–28.
- Kakkar R, Ye B, Stoller DA, Smelley M, Shi N-QQ, Galles K, Hadhazy M, Makielski JC & McNally EM (2006). Spontaneous coronary vasospasm in KATP mutant mice arises from a smooth muscle-extrinsic process. *Circ Res* **98**, 682–689.
- Kane GC, Lam C-F, O'Coilain F, Hodgson DM, Reyes S, Liu X-K, Miki T, Seino S, Katusic ZS & Terzic A (2006). Gene knockout of the KCNJ8-encoded Kir6.1 K(ATP) channel imparts fatal susceptibility to endotoxemia. *FASEB J* **20**, 2271–2280.
- Kang G, Leech CA, Chepurny OG, Coetzee WA & Holz GG (2008). Role of the cAMP sensor Epac as a determinant of K ATP channel ATP sensitivity in human pancreatic  $\beta$ -cells and rat INS-1 cells. *J Physiol* **586**, 1307–1319.
- Kanno S, Kovacs A, Yamada KA & Saffitz JE (2003). Connexin43 as a determinant of myocardial infarct size following coronary occlusion in mice. *J Am Coll Cardiol* **41**, 681–686.
- Karck M, Tanaka S, Bolling SF, Simon a, Su TP, Oeltgen PR & Haverich a (2001). Myocardial protection by ischemic preconditioning and delta-opioid receptor activation in the isolated working rat heart. *J Thorac Cardiovasc Surg* **122**, 986–992.
- Karschin C, Ecke C, Ashcroft FM & Karschin A (1997). Overlapping distribution of K(ATP) channel-forming Kir6.2 subunit and the sulfonylurea receptor SUR1 in rodent brain. *FEBS Lett* **401**, 59–64.
- Karuppasamy P, Chaubey S, Dew T, Musto R, Sherwood R, Desai J, John L, Shah AM,

- Marber MS & Kunst G (2011). Remote intermittent ischemia before coronary artery bypass graft surgery: A strategy to reduce injury and inflammation? *Basic Res Cardiol* **106**, 511–519.
- Katz AM (2001). A growth of ideas: Role of calcium as activator of cardiac contraction. *Cardiovasc Res* **52**, 8–13.
- Katzung BG & Morgenstern J a (1977). Effects of extracellular potassium on ventricular automaticity and evidence for a pacemaker current in mammalian ventricular myocardium. *Circ Res* **40**, 105–111.
- Kaul S, Bolger AF, Herrington D, Giugliano RP & Eckel RH (2010). Thiazolidinedione Drugs and Cardiovascular Risks. A Science Advisory From the American Heart Association and American College of Cardiology Foundation. *J Am Coll Cardiol* **55**, 1885–1894.
- Kavak S, Emre M, Tetiker T, Kavak T, Kolcu Z & Günay I (2008). Effects of rosiglitazone on altered electrical left ventricular papillary muscle activities of diabetic rat. *Naunyn Schmiedebergs Arch Pharmacol* **376**, 415–421.
- Kawano T, Zoga V, Kimura M, Liang M-Y, Wu H-E, Gemes G, McCallum JB, Kwok W-M, Hogan QH & Sarantopoulos CD (2009). Nitric Oxide Activates ATP-Sensitive Potassium Channels in Mammalian Sensory Neurons: Action by Direct S-Nitrosylation. *Mol Pain* **5**, 1744-8069-5–12.
- Kefaloyianni E, Bao L, Rindler MJ, Hong M, Patel T, Taskin E & Coetzee WA (2012). Measuring and evaluating the role of ATP-sensitive K<sup>+</sup> channels in cardiac muscle. *J Mol Cell Cardiol* **52**, 596–607.
- Keusch G, Boengler K & Schulz R (2008). Cardioprotection: Nitric oxide, protein kinases, and mitochondria. *Circulation* **118**, 1915–1919.
- Khaliulin I, Parker JE & Halestrap AP (2010). Consecutive pharmacological activation of PKA and PKC mimics the potent cardioprotection of temperature preconditioning. *Cardiovasc Res* **88**, 324–333.

- Kibos AS, Knight BP, Essebag V, Fishberger SB, Slevin M & Țintoiu IC eds. (2014). *Cardiac Arrhythmias*. Springer London, London.
- Kim S-J, Zhang H, Khaliulin I, Choisy SCM, Bond R, Lin H, El Haou S, Milnes JT, Hancox JC, Suleiman MS & James AF (2012). Activation of Glibenclamide-Sensitive ATP-Sensitive K<sup>+</sup> Channels During  $\alpha$ -Adrenergically Induced Metabolic Stress Produces a Substrate for Atrial Tachyarrhythmia. *Circ Arrhythmia Electrophysiol* **5**, 1184–1192.
- Kim VN (2003). RNA Interference in Functional Genomics and Medicine. *J Korean Med Sci* **18**, 309–318.
- Kinnally KW, Peixoto PM, Ryu SY & Dejean LM (2011). Is mPTP the gatekeeper for necrosis, apoptosis, or both? *Biochim Biophys Acta - Mol Cell Res* **1813**, 616–622.
- Kirsch GE, Codina J, Birnbaumer L & Brown AM (1990). Coupling of ATP-sensitive K<sup>+</sup> channels to A<sub>1</sub> receptors by G proteins in rat ventricular myocytes. *Am J Physiol* **259**, H820-6.
- Kleber AG & Saffitz JE (2014). Role of the intercalated disc in cardiac propagation and arrhythmogenesis. *Front Physiol* **5**, 404.
- Kloor D et al. (1999). ATP-Sensitive K<sup>+</sup> channel modulator binding to sulfonylurea receptors SUR2A and SUR2B: opposite effects of MgADP. *Mol Pharmacol* **55**, 832–840.
- Kobayashi S, Murakami W, Myoren T, Tateishi H, Okuda S, Doi M, Nao T, Wada Y, Matsuzaki M & Yano M (2014). A low-dose  $\beta$ <sub>1</sub>-blocker effectively and safely slows the heart rate in patients with acute decompensated heart failure and rapid atrial fibrillation. *Cardiology* **127**, 105–113.
- Kobertz WR (2014). Stoichiometry of the cardiac IKs complex. *Proc Natl Acad Sci* **111**, 5065–5066.
- Kono Y, Horie M, Takano M, Otani H, Xie L-H, Akao M, Tsuji K & Sasayama S (2000). The properties of the Kir6.1–6.2 tandem channel co-expressed with SUR2A. *Pflügers*

*Arch* **440**, 692–698.

- Kovalev H, Quayle JM, Kamishima T & Lodwick D (2004). Molecular analysis of the subtype-selective inhibition of cloned KATP channels by PNU-37883A. *Br J Pharmacol* **141**, 867–873.
- Kowaltowski J, Seetharaman S, Paucek P & Garlid KD (2001). Bioenergetic consequences of opening the ATP-sensitive K(+) channel of heart mitochondria. *Am J Physiol Heart Circ Physiol* **280**, H649–H657.
- Krieg T, Qin Q, McIntosh EC, Cohen M V & Downey JM (2002). ACh and adenosine activate PI3-kinase in rabbit hearts through transactivation of receptor tyrosine kinases. *Am J Physiol Heart Circ Physiol* **283**, H2322–30.
- Kristiansen SB, Henning O, Kharbanda RK, Nielsen-Kudsk JE, Schmidt MR, Redington AN, Nielsen TT & Bøtker HE (2005). Remote preconditioning reduces ischemic injury in the explanted heart by a KATP channel-dependent mechanism. *Am J Physiol Heart Circ Physiol* **288**, H1252–H1256.
- Kubo Y, Baldwin TJ, Nung Jan Y & Jan LY (1993). Primary structure and functional expression of a mouse inward rectifier potassium channel. *Nature* **362**, 127–133.
- Kuniyasu A, Kaneko K, Kawahara K & Nakayama H (2003). Molecular assembly and subcellular distribution of ATP-sensitive potassium channel proteins in rat hearts. *FEBS Lett* **552**, 259–263.
- Lacerda L, Somers S, Opie LH & Lecour S (2009). Ischaemic postconditioning protects against reperfusion injury via the SAFE pathway. *Cardiovasc Res* **84**, 201–208.
- Lacza Z (2003). Heart mitochondria contain functional ATP-dependent K<sup>+</sup> channels. *J Mol Cell Cardiol* **35**, 1339–1347.
- Lagranha CJ, Deschamps A, Aponte A, Steenbergen C & Murphy E (2010). Sex differences in the phosphorylation of mitochondrial proteins result in reduced production of reactive oxygen species and cardioprotection in females. *Circ Res* **106**, 1681–1691.

- Lang SC, Elsässer A, Scheler C, Vetter S, Tiefenbacher CP, Kübler W, Katus HA & Vogt AM (2006). Myocardial preconditioning and remote renal preconditioning. Identifying a protective factor using proteomic methods. *Basic Res Cardiol* **101**, 149–158.
- Laurita KR, Girouard SD & Rosenbaum DS (1996). Modulation of Ventricular Repolarization by a Premature Stimulus: Role of Epicardial Dispersion of Repolarization Kinetics Demonstrated by Optical Mapping of the Intact Guinea Pig Heart. *Circ Res* **79**, 493–503.
- Lawrence CL, Proks P, Rodrigo GC, Jones P, Hayabuchi Y, Standen NB & Ashcroft FM (2001). Gliclazide produces high-affinity block of K ATP channels in mouse isolated pancreatic beta cells but not rat heart or arterial smooth muscle cells. *Currents* 1019–1025.
- Lawrence KM, Chanalaris A, Scarabelli T, Hubank M, Pasini E, Townsend PA, Comini L, Ferrari R, Tinker A, Stephanou A, Knight RA & Latchman DS (2002). KATP channel gene expression is induced by urocortin and mediates its cardioprotective effect. *Circulation* **106**, 1556–1562.
- Lederer WJ & Nichols CG (1989). Nucleotide modulation of the activity of rat heart ATP-sensitive K<sup>+</sup> channels in isolated membrane patches. *J Physiol* **419**, 193–211.
- Lederer WJ, Nichols CG & Smith GL (1989). The mechanism of early contractile failure of isolated rat ventricular myocytes subjected to complete metabolic inhibition. *J Physiol* **413**, 329–349.
- Lee CH, Lee CY, Tsai TS & Liou HH (2008). PKA-mediated phosphorylation is a novel mechanism for levetiracetam, an antiepileptic drug, activating ROMK1 channels. *Biochem Pharmacol* **76**, 225–235.
- Lee K, Dixon a K, Richardson PJ & Pinnock RD (1999). Glucose-receptive neurones in the rat ventromedial hypothalamus express K ATP channels composed of Kir6.1 and SUR1 subunits. *J Physiol* **515**, 439–452.
- Lee KPK, Chen J & MacKinnon R (2017). Molecular structure of human KATP in

- complex with ATP and ADP. *Elife* **6**, 5–9.
- Li A, Knutsen RH, Zhang H, Osei-Owusu P, Moreno-Dominguez A, Harter TM, Uchida K, Remedi MS, Dietrich HH, Bernal-Mizrachi C, Blumer KJ, Mecham RP, Koster JC & Nichols CG (2013a). Hypotension due to Kir6.1 gain-of-function in vascular smooth muscle. *J Am Heart Assoc* **2**, e000365.
- Li GR, Du XL, Siow YL, Karmin O, Tse HF & Lau CP (2003). Calcium-activated transient outward chloride current and phase 1 repolarization of swine ventricular action potential. *Cardiovasc Res* **58**, 89–98.
- Li J, Kline CF, Hund TJ, Anderson ME & Mohler PJ (2010a). Ankyrin-B regulates Kir6.2 membrane expression and function in heart. *J Biol Chem* **285**, 28723–28730.
- Li N, Wu J-XX, Ding D, Cheng J, Gao N & Chen L (2017). Structure of a Pancreatic ATP-Sensitive Potassium Channel. *Cell* **168**, 101–110.e10.
- Li RA, Leppo M, Miki T, Seino S & Marbán E (2000). Molecular Basis of Electrocardiographic ST-Segment Elevation. *Circ Res* **87**, 837 LP-839.
- Li X, Rapedius M, Baukrowitz T, Liu GX, Srivastava DK, Daut J & Hanley PJ (2010b). 5-Hydroxydecanoate and coenzyme A are inhibitors of native sarcolemmal KATP channels in inside-out patches. *Biochim Biophys Acta - Gen Subj* **1800**, 385–391.
- Li Y, Lu J, Han Y, Fan X & Ding S-W (2013b). RNA interference functions as an antiviral immunity mechanism in mammals. *Science* **342**, 231–234.
- Liang X, Evans SM & Sun Y (2015). Insights into cardiac conduction system formation provided by HCN4 expression. *Trends Cardiovasc Med* **25**, 1–9.
- Liem DA, Verdouw PD, Ploeg H, Kazim S & Duncker DJ (2002). Sites of action of adenosine in interorgan preconditioning of the heart. *Am J Physiol Heart Circ Physiol* **283**, H29-37.
- Light PE, Bladen C, Winkfein RJ, Walsh MP & French RJ (2000). Molecular basis of protein kinase C-induced activation of ATP-sensitive potassium channels. *Proc Natl*

*Acad Sci* **97**, 9058–9063.

- Light PE, Kanji HD, Fox JE & French RJ (2001). Distinct myoprotective roles of cardiac sarcolemmal and mitochondrial KATP channels during metabolic inhibition and recovery. *Faseb J* **15**, 2586–2594.
- Lim KHH, Javadov SA, Das M, Clarke SJ, Suleiman M-S & Halestrap AP (2002). The effects of ischaemic preconditioning, diazoxide and 5-hydroxydecanoate on rat heart mitochondrial volume and respiration. *J Physiol* **545**, 961–974.
- Liss B & Roeper J (2001). Molecular physiology of neuronal K-ATP channels (review). *Mol Membr Biol* **18**, 117–127.
- Litovsky SH & Antzelevitch C (1988). Transient outward current prominent in canine ventricular epicardium but not endocardium. *Circ Res* **62**, 116–126.
- Liu D-W & Antzelevitch C (1995). Characteristics of the Delayed Rectifier Current (IKr and IKs) in Canine Ventricular Epicardial, Midmyocardial, and Endocardial Myocytes : A Weaker IKs Contributes to the Longer Action Potential of the M Cell. *Circ Res* **76**, 351–365.
- Liu GS, Thornton J, Van Winkle DM, Stanley a W, Olsson R a & Downey JM (1991). Protection against infarction afforded by preconditioning is mediated by A1 adenosine receptors in rabbit heart. *Circulation* **84**, 350–356.
- Liu Y, Gao WD, O'Rourke B, Marban E, Dong Gao W, O'Rourke B, Marban E, Gao WD, O'Rourke B & Marban E (1996). Synergistic modulation of ATP-sensitive K<sup>+</sup> currents by protein kinase C and adenosine. Implications for ischemic preconditioning. *Circ Res* **78**, 443–454.
- Liu Y, Ren G, O'Rourke B, Marbán E, Seharaseyon J, Marban E, Seharaseyon J, O'Rourke B, Marbán E, Seharaseyon J, O'Rourke B, Marbán E & Seharaseyon J (2001). Pharmacological comparison of native mitochondrial K(ATP) channels with molecularly defined surface K(ATP) channels. *Mol Pharmacol* **59**, 225–230.
- Liu Y, Sato T, Marban E, O'Rourke B & Marban E (1998). Mitochondrial ATP-dependent

- potassium channels: novel effectors of cardioprotection? *Circulation* **97**, 2463–2469.
- Lochner A, Genade S, Tromp E, Podzuweit T & Moolman JA (1999). Ischemic preconditioning and the beta-adrenergic signal transduction pathway. *Circulation* **100**, 958–966.
- Lodwick D, Rainbow RD, Rubaiy HN, Al JM, Vuister GW & Norman RI (2014). Sulphonylurea receptors regulate the channel pore in ATP-sensitive potassium channels via an inter-subunit salt bridge. *Biochem J* **354**, 343–354.
- Lopaschuk GD (1997). Alterations in Fatty Acid Oxidation During Reperfusion of the Heart After Myocardial Ischemia. *Am J Cardiol* **80**, 11A–16A.
- Lopes CMB, Zhang H, Rohacs T, Jin T, Yang J & Logothetis DE (2002). Alterations in conserved Kir channel-PIP2 interactions underlie channelopathies. *Neuron* **34**, 933–944.
- Lu C & Halvorsen SW (1997). Channel activators regulate ATP-sensitive potassium channel (Kir6.1) expression in chick cardiomyocytes. *FEBS Lett* **412**, 121–125.
- Lu HR, Hermans AN & Gallacher DJ (2012). Does terfenadine-induced ventricular tachycardia/fibrillation directly relate to its QT prolongation and Torsades de Pointes? *Br J Pharmacol* **166**, 1490–1502.
- Lu L, Reiter MJ, Xu Y, Chicco A, Greyson CR & Schwartz GG (2008). Thiazolidinedione drugs block cardiac KATP channels and may increase propensity for ischaemic ventricular fibrillation in pigs. *Diabetologia* **51**, 675–685.
- Lu Z (2004). Mechanism of rectification in inward-rectifier K<sup>+</sup> channels. *Annu Rev Physiol* **66**, 103–129.
- Lucchinetti E, Bestmann L, Feng J, Freidank H, Clanachan AS, Finegan BA & Zaugg M (2012). Remote Ischemic Preconditioning Applied during Isoflurane Inhalation Provides No Benefit to the Myocardium of Patients Undergoing On-pump Coronary Artery Bypass Graft Surgery. *Anesthesiology* **116**, 296–310.

- Ludwig LM, Weihrauch D, Kersten JR, Pagel PS & Warltier DC (2004). Protein kinase C translocation and Src protein tyrosine kinase activation mediate isoflurane-induced preconditioning in vivo: potential downstream targets of mitochondrial adenosine triphosphate-sensitive potassium channels and reactive oxygen species. *Anesthesiology* **100**, 532–539.
- M. Ashcroft F & M. Gribble F (2000). New windows on the mechanism of action of KATP channel openers. *Trends Pharmacol Sci* **21**, 439–445.
- Madhvani R V, Xie Y, Pantazis A, Garfinkel A, Qu Z, Weiss JN & Olcese R (2011). Shaping a new Ca<sup>2+</sup> conductance to suppress early afterdepolarizations in cardiac myocytes. *J Physiol* **589**, 6081–6092.
- Mahaffey KW, Puma JA, Barbagelata NA, Dicarli MF, Leesar MA, Browne KF, Eisenberg PR, Bolli R, Casas AC, Molina-Viamonte V, Orlandi C, Blevins R, Gibbons RJ, Califf RM & Granger CB (1999). Adenosine as an adjunct to thrombolytic therapy for acute myocardial infarction - Results of a multicenter, randomized, placebo-controlled trial: The acute myocardial infarction Study of ADenosine (AMISTAD) trial. *J Am Coll Cardiol* **34**, 1711–1720.
- Maillard P V, Ciaudo C, Marchais A, Li Y, Jay F, Ding SW & Voinnet O (2013). Antiviral RNA interference in mammalian cells. *Science* **342**, 235–238.
- Marban E, Robinson SW & Wier WG (1986). Mechanisms of arrhythmogenic delayed and early afterdepolarizations in ferret ventricular muscle. *J Clin Invest* **78**, 1185–1192.
- Marks AR (2013). Calcium cycling proteins and heart failure: Mechanisms and therapeutics. *J Clin Invest* **123**, 46–52.
- Marmar V & Shivkumar K (2008). The Role of the Autonomic Nervous System in Sudden Cardiac Death. *Prog Cardiovasc Dis* **50**, 404–419.
- Marx SO, Gaburjakova J, Gaburjakova M, Henrikson C, Ondrias K & Marks AR (2001). Coupled gating between cardiac calcium release channels (ryanodine receptors). *Circ Res* **88**, 1151–1158.

- Marx SO, Kurokawa J, Reiken S, Motoike H, D'Armiento J, Marks AR & Kass RS (2002). Requirement of a macromolecular signaling complex for beta adrenergic receptor modulation of the KCNQ1-KCNE1 potassium channel. *Science* **295**, 496–499.
- Matar W, Nosek TM, Wong D & Renaud J-M (2000). Pinacidil suppresses contractility and preserves energy but glibenclamide has no effect during muscle fatigue. *Am J Physiol Cell Physiol* **278**, C404–C416.
- Matsuo M, Tanabe K, Kioka N, Amachi T & Ueda K (2000). Different binding properties and affinities for ATP and ADP among sulfonylurea receptor subtypes, SUR1, SUR2A, and SUR2B. *J Biol Chem* **275**, 28757–28763.
- Matsushita K, Kinoshita K, Matsuoka T, Fujita A, Fujikado T, Tano Y, Nakamura H & Kurachi Y (2002). Intramolecular interaction of SUR2 subtypes for intracellular ADP-Induced differential control of K(ATP) channels. *Circ Res* **90**, 554–561.
- McPherson CD, Pierce GN & Cole WC (1993). Ischemic cardioprotection by ATP-sensitive K<sup>+</sup> channels involves high-energy phosphate preservation. *Am J Physiol* **265**, H1809–H1818.
- Medeiros-Domingo A, Kaku T, Tester DJ, Iturralde-Torres P, Itty A, Ye B, Valdivia C, Ueda K, Canizales-Quinteros S, Tusié-Luna MT, Makielski JC & Ackerman MJ (2007). SCN4B-encoded sodium channel  $\beta$ 4 subunit in congenital long-QT syndrome. *Circulation* **116**, 134–142.
- Medeiros-domingo A, Tan B, Crotti L, Tester DJ, Eckhardt L, Cuoretti A, Kroboth SL, Song C, Zhou Q, Kopp D, Schwartz PJ, Makielski JC & Ackerman MJ (2010). Gain-of-Function Mutations, S422L, in the KCNJ8-Encoded Cardiac K-ATP Channel Kir6.1 as a Pathogenic Substrate for J Wave Syndromes. *Hear Rhythm* **7**, 1466–1471.
- Mewton N, Bochaton T & Ovize M (2013). Postconditioning the Heart of ST-Elevation Myocardial Infarction Patients. *Circ J* **77**, 1123–1130.
- Miake J, Marbán E & Nuss HB (2003). Functional role of inward rectifier current in heart probed by Kir2.1 overexpression and dominant-negative suppression. *J Clin Invest*

**111**, 1529–1536.

Mihaylova MM & Shaw RJ (2011). The AMPK signalling pathway coordinates cell growth, autophagy and metabolism. *Nat Cell Biol* **13**, 1016–1023.

Mikhailov M V, Mikhailova E a & Ashcroft SJ (2001). Molecular structure of the glibenclamide binding site of the beta-cell K(ATP) channel. *FEBS Lett* **499**, 154–160.

Miki T, Liss B, Minami K, Shiuchi T, Saraya A, Kashima Y, Horiuchi M, Ashcroft F, Minokoshi Y, Roeper J & Seino S (2001). ATP-sensitive K<sup>+</sup> channels in the hypothalamus are essential for the maintenance of glucose homeostasis. *Nat Neurosci* **4**, 507–512.

Miki T, Minami K, Zhang L, Morita M, Gonoï T, Shiuchi T, Minokoshi Y, Renaud J-M & Seino S (2002a). ATP-sensitive potassium channels participate in glucose uptake in skeletal muscle and adipose tissue. *Am J Physiol - Endocrinol Metab* **283**, E1178–E1184.

Miki T, Suzuki M, Shibasaki T, Uemura H, Sato T, Yamaguchi K, Koseki H, Iwanaga T, Nakaya H & Seino S (2002b). Mouse model of Prinzmetal angina by disruption of the inward rectifier Kir6.1. *Nat Med* **8**, 466–472.

Miki T, Tashiro F, Iwanaga T, Nagashima K, Yoshitomi H, Aihara H, Nitta Y, Gonoï T, Inagaki N, Miyazaki JI & Seino S (1997). Abnormalities of pancreatic islets by targeted expression of a dominant-negative KATP channel. *Proc Natl Acad Sci U S A* **94**, 11969–11973.

Minami K, Miki T, Kadowaki T & Seino S (2004). Roles of ATP-Sensitive K<sup>+</sup> Channels as Metabolic Sensors. *Diabetes* **53**, 1–5.

Mitcheson J (1998). Cultured adult cardiac myocytes Future applications, culture methods, morphological and electrophysiological properties. *Cardiovasc Res* **39**, 280–300.

Morales MJ, Castellino RC, Crews AL, Rasmusson RL & Strauss HC (1995). A Novel  $\beta$  Subunit Increases Rate of Inactivation of Specific Voltage-gated Potassium Channel  $\alpha$  Subunits. *J Biol Chem* **270**, 6272–6277.

- Moreau C, Jacquet H, Prost AL, D'hahan N & Vivaudou M (2000). The molecular basis of the specificity of action of KATP channel openers. *EMBO J* **19**, 6644–6651.
- Morimoto S, Harada K & Ohtsuki I (1999). Roles of troponin isoforms in pH dependence of contraction in rabbit fast and slow skeletal and cardiac muscles. *J Biochem* **126**, 121–129.
- Morrissey A, Parachuru L, Leung M, Lopez G, Nakamura TY, Tong X, Yoshida H, Srivastava S, Chowdhury PD, Artman M & Coetzee WA (2005a). Expression of ATP-sensitive K<sup>+</sup> channel subunits during perinatal maturation in the mouse heart. *Pediatr Res* **58**, 185–192.
- Morrissey A, Rosner E, Lanning J, Parachuru L, Dhar Chowdhury P, Han S, Lopez G, Tong X, Yoshida H, Nakamura TY, Artman M, Giblin JP, Tinker A & Coetzee W a (2005b). Immunolocalization of KATP channel subunits in mouse and rat cardiac myocytes and the coronary vasculature. *BMC Physiol* **5**, 1.
- Muntean D, Kiss L, Jost N & Baczko I (2014). ATP-Sensitive Potassium Channel Modulators and Cardiac Arrhythmias: An Update. *Curr Pharm Des* **21**, 1091–1102.
- Murry CE, Jennings RB & Reimer KA (1986). Preconditioning with ischemia: a delay of lethal cell injury in ischemic myocardium. *Circulation* **74**, 1124–1136.
- Naga Prasad S V., Esposito G, Mao L, Koch WJ & Rockman HA (2000). Gβγ-dependent Phosphoinositide 3-Kinase Activation in Hearts with in Vivo Pressure Overload Hypertrophy. *J Biol Chem* **275**, 4693–4698.
- Nakajo K, Ulbrich MH, Kubo Y & Isacoff EY (2010). Stoichiometry of the KCNQ1 - KCNE1 ion channel complex. *Pnas* **107**, 18862–18867.
- Nakamura M, Nakakimura K, Matsumoto M & Sakabe T (2002). Rapid tolerance to focal cerebral ischemia in rats is attenuated by adenosine A1 receptor antagonist. *J Cereb Blood Flow Metab* **22**, 161–170.
- Nakaya H (2014). Role of ATP-sensitive K<sup>+</sup> channels in cardiac arrhythmias. *J Cardiovasc Pharmacol Ther* **19**, 237–243.

- Nakazawa H, Nakaya H & Sato T (2001). Opening of Mitochondrial K. *Sci Technol* 856–858.
- Nelson CP, Rainbow RD, Brignell JL, Perry MD, Willets JM, Davies NW, Standen NB & Challiss RAJ (2011). Principal role of adenylyl cyclase 6 in K<sup>+</sup> channel regulation and vasodilator signalling in vascular smooth muscle cells. *Cardiovasc Res* **91**, 694–702.
- Ng K-E, Schwarzer S, Duchon MR & Tinker A (2010). The intracellular localization and function of the ATP-sensitive K<sup>+</sup> channel subunit Kir6.1. *J Membr Biol* **234**, 137–147.
- Nichols CG (2006). KATP channels as molecular sensors of cellular metabolism. *Nature* **440**, 470–476.
- Nichols CG, Singh GK & Grange DK (2013). KATP channels and cardiovascular disease: Suddenly a syndrome. *Circ Res* **112**, 1059–1072.
- Nielsen MS, Axelsen LN, Sorgen PL, Verma V, Delmar M & Holstein-Rathlou N-H (2012). Gap Junctions. *Compr Physiol* **2**, 1981–2035.
- NOBLE D & COHEN I (1978). The interpretation of the T wave of the electrocardiogram. *Cardiovasc Res* **12**, 13–27.
- Node K, Kitakaze M, Sato H, Minamino T, Komamura K, Shinozaki Y, Mori H & Hori M (1997). Role of intracellular Ca<sup>2+</sup> in activation of protein kinase C during ischemic preconditioning. *Circulation* **96**, 1257–1265.
- Noma A (1983). ATP-regulated K<sup>+</sup> channels in cardiac muscle. *Nature* **305**, 147–148.
- Novakovic R, Ilic B, Beleslin-Cokic B, Radunovic N, Heinle H, Scepanovic R & Gojkovic-Bukarica L (2013). The effect of resveratrol on contractility of non-pregnant rat uterus: the contribution of K<sup>(+)</sup> channels. *J Physiol Pharmacol* **64**, 795–805.
- Novalija E, Kevin LG, Camara AK, Bosnjak ZJ, Kampine JP & Stowe DF (2003). Reactive oxygen species precede the epsilon isoform of protein kinase C in the anesthetic preconditioning signaling cascade. *Anesthesiology* **99**, 421–428.

- O'Rourke B (2000). Myocardial KATP Channels in Preconditioning. *Circ Res* **87**, 845–855.
- Oldenburg O, Qin Q, Krieg T, Yang X-M, Philipp S, Critz SD, Cohen M V & Downey JM (2004). Bradykinin induces mitochondrial ROS generation via NO, cGMP, PKG, and mitoKATP channel opening and leads to cardioprotection. *Am J Physiol Heart Circ Physiol* **286**, H468-76.
- Olson TM, Alekseev AE, Moreau C, Liu XK, Zingman L V, Miki T, Seino S, Asirvatham SJ, Jahangir A & Terzic A (2007). KATP channel mutation confers risk for vein of Marshall adrenergic atrial fibrillation. *Nat Clin Pract Cardiovasc Med* **4**, 110–116.
- Ortiz D, Gossack L, Quasts U & Bryan J (2013). Reinterpreting the action of ATP analogs on KATP channels. *J Biol Chem* **288**, 18894–18902.
- Ovize M, Baxter GF, Di Lisa F, Ferdinandy P, Garcia-Dorado D, Hausenloy DJ, Heusch G, Vinten-Johansen J, Yellon DM, Schulz R & Working Group of Cellular Biology of Heart of European Society of Cardiology (2010). Postconditioning and protection from reperfusion injury: where do we stand? Position paper from the Working Group of Cellular Biology of the Heart of the European Society of Cardiology. *Cardiovasc Res* **87**, 406–423.
- Oxman T, Arad M, Klein R, Avazov N & Rabinowitz B (1997). Limb ischemia preconditions the heart against reperfusion tachyarrhythmia. *Am J Physiol* **273**, H1707–H1712.
- Paddison PJ, Caudy AA, Bernstein E, Hannon GJ & Conklin DS (2002). Short hairpin RNAs (shRNAs) induce sequence-specific silencing in mammalian cells. *Genes Dev* **16**, 948–958.
- Patel HH, Hsu AK, Peart JN & Gross GJ (2002). Sarcolemmal KATP channel triggers opioid-induced delayed cardioprotection in the rat. *Circ Res* **91**, 186–188.
- Patel SP & Campbell DL (2005). Transient outward potassium current, “Ito”, phenotypes in the mammalian left ventricle: underlying molecular, cellular and biophysical mechanisms. *J Physiol* **569**, 7–39.

- Pelletier MR, Pahapill PA, Pennefather PS & Carlen PL (2000). Analysis of single K(ATP) channels in mammalian dentate gyrus granule cells. *J Neurophysiol* **84**, 2291–2301.
- Pelzmann B, Hallström S, Schaffer P, Lang P, Nadlinger K, Birkmayer GD, Vrecko K, Reibnegger G & Koidl B (2003). NADH supplementation decreases pinacidil-primed I K ATP in ventricular cardiomyocytes by increasing intracellular ATP. *Br J Pharmacol* **139**, 749–754.
- Perez-Reyes E (2003). Molecular physiology of low-voltage-activated t-type calcium channels. *Physiol Rev* **83**, 117–161.
- Petitprez S, Jespersen T, Pruvot E, Keller DI, Corbaz C, Schläpfer J, Abriel H & Kucera JP (2008). Analyses of a novel SCN5A mutation (C1850S): Conduction vs. repolarization disorder hypotheses in the Brugada syndrome. *Cardiovasc Res* **78**, 494–504.
- Piper DR, Hinz WA, Tallurri CK, Sanguinetti MC & Tristani-Firouzi M (2005). Regional specificity of human ether-a'-go-go-related gene channel activation and inactivation gating. *J Biol Chem* **280**, 7206–7217.
- Plant LD, Xiong D, Dai H & Goldstein SAN (2014). Individual IKs channels at the surface of mammalian cells contain two KCNE1 accessory subunits. *Proc Natl Acad Sci* **111**, E1438–E1446.
- Pountney DJ, Sun ZQ, Porter LM, Nitabach MN, Nakamura TY, Holmes D, Rosner E, Kaneko M, Manaris T, Holmes TC & Coetzee WA (2001). Is the molecular composition of K(ATP) channels more complex than originally thought? *J Mol Cell Cardiol* **33**, 1541–1546.
- Pratt EB, Zhou Q, Gay JW & Shyng S-L (2012). Engineered interaction between SUR1 and Kir6.2 that enhances ATP sensitivity in KATP channels. *J Gen Physiol* **140**, 175–187.
- Pu JL, Ye B, Kroboth SL, McNally EM, Makielski JC & Shi NQ (2008). Cardiac sulfonylurea receptor short form-based channels confer a glibenclamide-insensitive KATP activity. *J Mol Cell Cardiol* **44**, 188–200.

- Puhl S-L, Kazakov A, Müller A, Fries P, Wagner DR, Böhm M, Maack C & Devaux Y (2016). Adenosine A<sub>1</sub> receptor activation attenuates cardiac hypertrophy and fibrosis in response to  $\alpha_1$ -adrenoceptor stimulation *in vivo*. *Br J Pharmacol* **173**, 88–102.
- Rahman IA, Mascaro JG, Steeds RP, Frenneaux MP, Nightingale PG, Gosling P, Townsend P, Townend J, Green D & Bonser R (2009). Abstract 3372: Remote Ischaemic Pre-conditioning in Human Coronary Artery Bypass Surgery: From Promise to Disappointment. *Circulation*. Available at: [http://circ.ahajournals.org/content/120/Suppl\\_18/S797.4.short](http://circ.ahajournals.org/content/120/Suppl_18/S797.4.short) [Accessed February 5, 2018].
- Rainbow RD, Lodwick D, Hudman D, Davies NW, Norman RI & Standen NB (2004). SUR2A C-terminal fragments reduce KATP currents and ischaemic tolerance of rat cardiac myocytes. *J Physiol* **557**, 785–794.
- Rainbow RD, Norman RI, Hudman D, Davies NW & Standen NB (2005). Reduced effectiveness of HMR 1098 in blocking cardiac sarcolemmal K ATP channels during metabolic stress. *J Mol Cell Cardiol* **39**, 637–646.
- Rana A, Goyal N, Ahlawat A, Jamwal S, Reddy BVK & Sharma S (2014). Mechanisms involved in attenuated cardio-protective role of ischemic preconditioning in metabolic disorders. *Perfusion* **30**, 1–12.
- Rao DD, Vorhies JS, Senzer N & Nemunaitis J (2009). siRNA vs. shRNA: Similarities and differences. *Adv Drug Deliv Rev* **61**, 746–759.
- Rassaf T, Totzeck M, Hendgen-Cotta UB, Shiva S, Heusch G & Kelm M (2014). Circulating nitrite contributes to cardioprotection by remote ischemic preconditioning. *Circ Res* **114**, 1601–1610.
- Raulf A, Horder H, Tarnawski L, Geisen C, Ottersbach A, Röhl W, Jovinge S, Fleischmann BK & Hesse M (2015). Transgenic systems for unequivocal identification of cardiac myocyte nuclei and analysis of cardiomyocyte cell cycle status. *Basic Res Cardiol* **110**, 33.

- Razeghi P, Young ME, Alcorn JL, Moravec CS, Frazier OH & Taegtmeyer H (2001). Metabolic gene expression in fetal and failing human heart. *Circulation* **104**, 2923–2931.
- Recchia FA, McConnell PI, Bernstein RD, Vogel TR, Xu X & Hintze TH (1998). Reduced nitric oxide production and altered myocardial metabolism during the decompensation of pacing-induced heart failure in the conscious dog. *Circ Res* **83**, 969–979.
- Reiken S, Lacampagne A, Zhou H, Kherani A, Lehnart SE, Ward C, Huang F, Gaburjakova M, Gaburjakova J, Rosemblyt N, Warren MS, He K lun, Yi G hua, Wang J, Burkhoff D, Vassort G & Marks AR (2003). PKA phosphorylation activates the calcium release channel (ryanodine receptor)-in skeletal muscle: Defective regulation in heart failure. *J Cell Biol* **160**, 919–928.
- Reimann F, Gribble FM & Ashcroft FM (2000). Differential response of K(ATP) channels containing SUR2A or SUR2B subunits to nucleotides and pinacidil. *Mol Pharmacol* **58**, 1318–1325.
- Reimann F, Proks P & Ashcroft FM (2001). Effects of mitiglinide (S 21403) on Kir6.2/SUR1, Kir6.2/SUR2A and Kir6.2/SUR2B types of ATP-sensitive potassium channel. *Br J Pharmacol* **132**, 1542–1548.
- Repunte VP, Nakamura H, Fujita A, Horio Y, Findlay I, Pott L & Kurachi Y (1999). Extracellular links in Kir subunits control the unitary conductance of SUR/Kir6.0 ion channels. *EMBO J* **18**, 3317–3324.
- Ribalet B, John SA & Weiss JN (2003). Molecular basis for Kir6.2 channel inhibition by adenine nucleotides. *Biophys J* **84**, 266–276.
- Ripoll C, Lederer WJ & Nichols CG (1993). On the mechanism of inhibition of KATP channels by glibenclamide in rat ventricular myocytes. *J Cardiovasc Electrophysiol* **4**, 38–47.
- Rocchetti M, Besana A, Gurrola GB, Possani LD & Zaza A (2001). Rate dependency of delayed rectifier currents during the guinea-pig ventricular action potential. *J Physiol*

**534**, 721–732.

- Rodrigo GC, Davies NW & Standen NB (2004). Diazoxide causes early activation of cardiac sarcolemmal KATP channels during metabolic inhibition by an indirect mechanism. *Cardiovasc Res* **61**, 570–579.
- Rodrigo GC & Samani NJ (2007). Ischemic preconditioning of the whole heart confers protection on subsequently isolated ventricular myocytes. *AJP Hear Circ Physiol* **294**, H524–H531.
- Roh S, Choi S & Lim I (2007). Involvement of protein kinase A in nitric oxide stimulating effect on a BK(Ca) channel of human dermal fibroblasts. *J Invest Dermatol* **127**, 2533–2538.
- Rohr S (2004). Role of gap junctions in the propagation of the cardiac action potential. *Cardiovasc Res* **62**, 309–322.
- Rorabaugh BR, Ross SA, Gaivin RJ, Papay RS, McCune DF, Simpson PC & Perez DM (2005).  $\alpha$ 1A- but not  $\alpha$ 1B-adrenergic receptors precondition the ischemic heart by a staurosporine-sensitive, chelerythrine-insensitive mechanism. *Cardiovasc Res* **65**, 436–445.
- Ross AM, Gibbons RJ, Stone GW, Kloner RA & Alexander RW (2005). A randomized, double-blinded, placebo-controlled multicenter trial of adenosine as an adjunct to reperfusion in the treatment of acute myocardial infarction (AMISTAD-II). *J Am Coll Cardiol* **45**, 1775–1780.
- Ruscic KJ, Miceli F, Villalba-Galea CA, Dai H, Mishina Y, Bezanilla F & Goldstein SA (2013). IKs channels open slowly because KCNE1 accessory subunits slow the movement of S4 voltage sensors in KCNQ1 pore-forming subunits. *Proc Natl Acad Sci U S A* **110**, E559-66.
- Russ U, Hambrock a, Artunc F, Löffler-Walz C, Horio Y, Kurachi Y & Quast U (1999). Coexpression with the inward rectifier K(+) channel Kir6.1 increases the affinity of the vascular sulfonylurea receptor SUR2B for glibenclamide. *Mol Pharmacol* **56**,

955–961.

Ryding ADS, Sharp MGF & Mullins JJ (2001). Conditional transgenic technologies. *J Endocrinol* **171**, 1–14.

Sah R, Oudit GY, Nguyen TTT, Lim HW, Wickenden AD, Wilson GJ, Molkenin JD & Backx PH (2002). Inhibition of calcineurin and sarcolemmal Ca<sup>2+</sup> influx protects cardiac morphology and ventricular function in Kv4.2N transgenic mice. *Circulation* **105**, 1850–1856.

Saksena S & Marchlinski FE (2015). *Interventional Cardiac Electrophysiology: A Multidisciplinary Approach*. Cardiotext Publishing.

Samie FH, Mandapati R, Gray R a, Watanabe Y, Zuur C, Beaumont J & Jalife J (2000). A mechanism of transition from ventricular fibrillation to tachycardia : effect of calcium channel blockade on the dynamics of rotating waves. *Circ Res* **86**, 684–691.

Sanada S, Asanuma H, Tsukamoto O, Minamino T, Node K, Takashima S, Fukushima T, Ogai A, Shinozaki Y, Fujita M, Hirata A, Okuda H, Shimokawa H, Tomoike H, Hori M & Kitakaze M (2004). Protein kinase A as another mediator of ischemic preconditioning independent of protein kinase C. *Circulation* **110**, 51–57.

Sanada S, Kitakaze M, Asanuma H, Harada K, Ogita H, Node K, Takashima S, Sakata Y, Asakura M, Shinozaki Y, Mori H, Kuzuya T & Hori M (2001). Role of mitochondrial and sarcolemmal K(ATP) channels in ischemic preconditioning of the canine heart. *Am J Physiol Heart Circ Physiol* **280**, H256-63.

SANDOW A (1952). Excitation-contraction coupling in muscular response. *Yale J Biol Med* **25**, 176–201.

Sanguinetti MC, Curran ME, Zou A, Shen J, Specter PS, Atkinson DL & Keating MT (1996). Coassembly of KVLQT1 and minK (IsK) proteins to form cardiac IKS potassium channel. *Nature* **384**, 80–83.

Sanguinetti MC, Jiang C, Curran ME & Keating MT (1995). A mechanistic link between an inherited and an acquired cardiac arrhythmia: HERG encodes the IKr potassium

- channel. *Cell* **81**, 299–307.
- Sansom MSP, Shrivastava IH, Bright JN, Tate J, Capener CE & Biggin PC (2002). Potassium channels: Structures, models, simulations. *Biochim Biophys Acta - Biomembr* **1565**, 294–307.
- Santana LF, Cheng EP & Lederer WJ (2010). How does the shape of the cardiac action potential control calcium signaling and contraction in the heart? *J Mol Cell Cardiol* **49**, 901–903.
- Sasaki N, Murata M, Guo Y, Jo SH, Ohler A, Akao M, O'Rourke B, Xiao RP, Bolli R & Marbán E (2003). MCC-134, a single pharmacophore, opens surface ATP-sensitive potassium channels, blocks mitochondrial ATP-sensitive potassium channels, and suppresses preconditioning. *Circulation* **107**, 1183–1188.
- Sato T, O'Rourke B & Marban E (1998). Modulation of Mitochondrial ATP-Dependent K<sup>+</sup> Channels by Protein Kinase C. *Circ Res* **83**, 110–114.
- Satoh E, Yamada M, Kondo C, Repunte VP, Horio Y, Iijima T & Kurachi Y (1998). Intracellular nucleotide-mediated gating of SUR/Kir6.0 complex potassium channels expressed in a mammalian cell line and its modification by pinacidil. *J Physiol* **511**, 663–674.
- Satoh H (1995). Role of T-type Ca<sup>2+</sup> channel inhibitors in the pacemaker depolarization in rabbit sino-atrial nodal cells. *Gen Pharmacol* **26**, 581–587.
- Schmidt MR, Smerup M, Konstantinov IE, Shimizu M, Li J, Cheung M, White P a, Kristiansen SB, Sorensen K, Dzavik V, Redington a N & Kharbanda RK (2007). Intermittent peripheral tissue ischemia during coronary ischemia reduces myocardial infarction through a KATP-dependent mechanism: first demonstration of remote ischemic preconditioning. *Am J Physiol Heart Circ Physiol* **292**, H1883-90.
- Schmitt N, Grunnet M & Olesen S-P (2014). Cardiac potassium channel subtypes: new roles in repolarization and arrhythmia. *Physiol Rev* **94**, 609–653.
- Schoemaker RG & van Heijningen CL (2000). Bradykinin mediates cardiac

- preconditioning at a distance. *Am J Physiol Heart Circ Physiol* **278**, H1571-6.
- Schwartz LM, Reimer KA, Crago MS & Jennings RB (2007). Pharmacological preconditioning with diazoxide slows energy metabolism during sustained ischemia. *Exp Clin Cardiol* **12**, 139–147.
- Sciarovsky S, Rechavia E, Strasberg B, Sagie A, Bassevich R, Kusniec J, Mager A & Agmon J (1988). Unstable angina: ST segment depression with positive versus negative T wave deflections--clinical course, ECG evolution, and angiographic correlation. *Am Heart J* **116**, 933–941.
- Seharaseyon J, Ohler A, Sasaki N, Fraser H, Sato T, Johns DC, O'Rourke B & Marbán E (2000a). Molecular composition of mitochondrial ATP-sensitive potassium channels probed by viral Kir gene transfer. *J Mol Cell Cardiol* **32**, 1923–1930.
- Seharaseyon J, Sasaki N, Ohler A, Sato T, Fraser H, Johns DC, O'Rourke B, Marbán E & Marban E (2000b). Evidence against functional heteromultimerization of the K(ATP) channel subunits Kir6.1 and Kir6.2. *J Biol Chem* **275**, 17561–17565.
- Seino S & Miki T (2004). Gene targeting approach to clarification of ion channel function: studies of Kir6.x null mice. *J Physiol* **554**, 295–300.
- Shaffer F, Mccraty R, Zerr CL & Medical DVA (2014). A healthy heart is not a metronome: an integrative review of the heart's anatomy and heart rate variability. *Front Psychol* **5**, 1040.
- Shi NQ, Ye B & Makielski JC (2005). Function and distribution of the SUR isoforms and splice variants. *J Mol Cell Cardiol* **39**, 51–60.
- Shi W-W, Yang Y, Shi Y & Jiang C (2012). K(ATP) channel action in vascular tone regulation: from genetics to diseases. *Sheng Li Xue Bao* **64**, 1–13.
- Shi W, Cui N, Shi Y, Zhang X, Yang Y & Jiang C (2007a). Arginine vasopressin inhibits Kir6.1/SUR2B channel and constricts the mesenteric artery via V1a receptor and protein kinase C. *Am J Physiol Regul Integr Comp Physiol* **293**, R191–R199.

- Shi W, Cui N, Wu Z, Yang Y, Zhang S, Gai H, Zhu D & Jiang C (2010). Lipopolysaccharides up-regulate Kir6.1/SUR2B channel expression and enhance vascular KATP channel activity via NF- $\kappa$ B-dependent signaling. *J Biol Chem* **285**, 3021–3029.
- Shi Y, Wu Z, Cui N, Shi W, Yang Y, Zhang X, Rojas A, Ha BT & Jiang C (2007b). PKA phosphorylation of SUR2B subunit underscores vascular KATP channel activation by beta-adrenergic receptors. *Am J Physiol Regul Integr Comp Physiol* **293**, R1205–R1214.
- Shieh C-C, Coghlan M, Sullivan JP & Gopalakrishnan M (2000). Potassium Channels: Molecular Defects, Diseases, and Therapeutic Opportunities. *Pharmacol Rev* **52**, 557–594.
- Shinbo A & Iijima T (1997). Potentiation by nitric oxide of the ATP-sensitive K<sup>+</sup> current induced by K<sup>+</sup> channel openers in guinea-pig ventricular cells. *Br J Pharmacol* **120**, 1568–1574.
- Shindo T, Yamada M, Isomoto S, Horio Y & Kurachi Y (1998). SUR2 subtype (A and B)-dependent differential activation of the cloned ATP-sensitive K<sup>+</sup> channels by pinacidil and nicorandil. *Br J Pharmacol* **124**, 985–991.
- Shyng S & Nichols CG (1997). Octameric stoichiometry of the KATP channel complex. *J Gen Physiol* **110**, 655–664.
- Sicouri S & Antzelevitch C (1991). A subpopulation of cells with unique electrophysiological properties in the deep subepicardium of the canine ventricle. The M cell. *Circ Res* **68**, 1729–1741.
- Sims MW, Winter J, Brennan S, Norman RI, Andre Ng G, Squire IB & Rainbow RD (2014). PKC-mediated toxicity of elevated glucose concentration on cardiomyocyte function. *AJP Hear Circ Physiol* **307**, H587–H597.
- Singh H, Hudman D, Lawrence CL, Rainbow RD, Lodwick D & Norman RI (2003). Distribution of Kir6.0 and SUR2 ATP-sensitive potassium channel subunits in isolated

- ventricular myocytes. *J Mol Cell Cardiol* **35**, 445–459.
- Skyschally A, van Caster P, Iliodromitis EK, Schulz R, Kremastinos DT & Heusch G (2009). Ischemic postconditioning: Experimental models and protocol algorithms. *Basic Res Cardiol* **104**, 469–483.
- Smith KA & Bigham MT (2013). Cardiogenic Shock. *Open Pediatr Med Journal* **7**, 19–27.
- Solenkova N V. (2005). Endogenous adenosine protects preconditioned heart during early minutes of reperfusion by activating Akt. *AJP Hear Circ Physiol* **290**, H441–H449.
- Sollini M, Frieden M & Bény J-L (2002). Charybdotoxin-sensitive small conductance K(Ca) channel activated by bradykinin and substance P in endothelial cells. *Br J Pharmacol* **136**, 1201–1209.
- Soundarapandian MM, Wu D, Zhong X, Petralia RS, Peng L, Tu W & Lu Y (2007). Expression of functional Kir6.1 channels regulates glutamate release at CA3 synapses in generation of epileptic form of seizures. *J Neurochem* **103**, 1982–1988.
- Sparrow JC & Schöck F (2009). The initial steps of myofibril assembly: integrins pave the way. *Nat Rev Mol Cell Biol* **10**, 293–298.
- Stephan D, Winkler M, Kühner P, Russ U & Quast U (2006). Selectivity of repaglinide and glibenclamide for the pancreatic over the cardiovascular KATP channels. *Diabetologia* **49**, 2039–2048.
- Stoller D a, Fahrenbach JP, Chalupsky K, Tan B-H, Aggarwal N, Metcalfe J, Hadhazy M, Shi N-Q, Makielski JC & McNally EM (2010). Cardiomyocyte sulfonylurea receptor 2-KATP channel mediates cardioprotection and ST segment elevation. *Am J Physiol Heart Circ Physiol* **299**, H1100–H1108.
- Storey NM, Stratton RC, Rainbow RD, Standen NB & Lodwick D (2013). Kir6.2 limits Ca(2+) overload and mitochondrial oscillations of ventricular myocytes in response to metabolic stress. *Am J Physiol Heart Circ Physiol* **305**, H1508-18.
- Suga S, Kanno T, Ogawa Y, Takeo T, Kamimura N & Wakui M (2000). cAMP-

independent decrease of ATP-sensitive K<sup>+</sup> channel activity by GLP-1 in rat pancreatic β-cells. *Pflügers Arch - Eur J Physiol* **440**, 566–572.

Suga S, Wu J, Ogawa Y, Takeo T, Kanno T & Wakui M (2001). Phorbol ester impairs electrical excitation of rat pancreatic beta-cells through PKC-independent activation of KATP channels. *BMC Pharmacol* **1**, 3.

Sukhodub A, Jovanović S, Du Q, Budas G, Clelland A, Shen M, Sakamoto K, Tian R & Jovanović A (2007). AMP-activated protein kinase mediates preconditioning in cardiomyocytes by regulating activity and trafficking of sarcolemmal ATP-sensitive K<sup>+</sup> channels. *J Cell Physiol* **210**, 223–236.

Sun H & Feng Z (2013). Neuroprotective role of ATP-sensitive potassium channels in cerebral ischemia. *Acta Pharmacol Sin* **34**, 24–32.

Sun X & Wang H-S (2005). Role of the transient outward current (I<sub>to</sub>) in shaping canine ventricular action potential--a dynamic clamp study. *J Physiol* **564**, 411–419.

Surah-Narwal S, Xu SZ, McHugh D, McDonald RL, Hough E, Cheong A, Partridge C, Sivaprasadarao A & Beech DJ (1999). Block of human aorta Kir6.1 by the vascular K ATP channel inhibitor U37883A. *Br J Pharmacol* **128**, 667–672.

Surawicz B & Parikh SR (2003). Differences between ventricular repolarization in men and women: Description, mechanism and implications. *Ann Noninvasive Electrocardiol* **8**, 333–340.

Suzuki M, Fujikura K, Kotake K, Inagaki N, Seino S & Takata K (1999). Immunolocalization of sulphonylurea receptor 1 in rat pancreas. *Diabetologia* **42**, 1204–1211.

Suzuki M, Kotake K, Fujikura K, Inagaki N, Suzuki T, Gono T, Seino S & Takata K (1997). Kir6.1: a possible subunit of ATP-sensitive K<sup>+</sup> channels in mitochondria. *Biochem Biophys Res Commun* **241**, 693–697.

Suzuki M, Li RA, Miki T, Uemura H, Sakamoto N, Ohmoto-Sekine Y, Tamagawa M, Ogura T, Seino S, Marbán E, Nakaya H, Marban E & Nakaya H (2001). Functional roles of cardiac and vascular ATP-sensitive potassium channels clarified by Kir6.2-

knockout mice. *Circ Res* **88**, 570–577.

Suzuki M, Sasaki N, Miki T, Sakamoto N, Ohmoto-Sekine Y, Tamagawa M, Seino S, Marbán E & Nakaya H (2002). Role of sarcolemmal K(ATP) channels in cardioprotection against ischemia/reperfusion injury in mice. *J Clin Invest* **109**, 509–516.

Szentandrassy N, Harmati G, Bárándi L, Simkő J, Horváth B, Magyar J, Bányász T, Lorincz I, Szebeni A, Kecskeméti V & Nánási PP (2011). Effects of rosiglitazone on the configuration of action potentials and ion currents in canine ventricular cells. *Br J Pharmacol* **163**, 499–509.

Szentmiklosi AJ, Szentandrassy N, Hegyi B, Horvath B, Magyar J, Bányász T & Nanasi PP (2015). Chemistry, physiology, and pharmacology of  $\beta$ -adrenergic mechanisms in the heart. Why are  $\beta$ -blocker antiarrhythmics superior? *Curr Pharm Des* **21**, 1030–1041.

Tajada S, Ciudad P, Moreno-Domínguez A, Pérez-García MT & López-López JR (2012). High blood pressure associates with the remodelling of inward rectifier K<sup>+</sup> channels in mice mesenteric vascular smooth muscle cells. *J Physiol* **590**, 6075–6091.

Takahashi N, Morishige K, Jahangir a, Yamada M, Findlay I, Koyama H & Kurachi Y (1994). Molecular cloning and functional expression of cDNA encoding a second class of inward rectifier potassium channels in the mouse brain. *J Biol Chem* **269**, 23274–23279.

Takano M, Xie LH, Otani H & Horie M (1998). Cytoplasmic terminus domains of Kir6.x confer different nucleotide-dependent gating on the ATP-sensitive K<sup>+</sup> channel. *J Physiol* **512**, 395–406.

Tan B-H, Pundi KN, Van Norstrand DW, Valdivia CR, Tester DJ, Medeiros-Domingo A, Makielski JC & Ackerman MJ (2010). Sudden infant death syndrome-associated mutations in the sodium channel beta subunits. *Hear Rhythm* **7**, 771–778.

Tan JH, Al Abed A & Brock J a (2007). Inhibition of KATP channels in the rat tail artery by neurally released noradrenaline acting on postjunctional  $\alpha_2$ -adrenoceptors. *J*

*Physiol* **581**, 757–765.

Tang C, Skibsbye L, Yuan L, Bentzen BH & Jespersen T (2015). Biophysical characterization of inwardly rectifying potassium currents (I(K1) I(K,ACh), I(K,Ca)) using sinus rhythm or atrial fibrillation action potential waveforms. *Gen Physiol Biophys* **34**, 383–392.

Tang Y, Long C-L, Wang R-H, Cui W & Wang H (2010). Activation of SUR2B/Kir6.1 subtype of adenosine triphosphate-sensitive potassium channel improves pressure overload-induced cardiac remodeling via protecting endothelial function. *J Cardiovasc Pharmacol* **56**, 345–353.

Tarasov A, Dusonchet J & Ashcroft F (2004). Metabolic Regulation of the Pancreatic Beta-Cell ATP-Sensitive K<sup>+</sup> Channel: A Pas de Deux. *Diabetes* **53**, S113–S122.

Teramoto N (2006a). Physiological roles of ATP-sensitive K<sup>+</sup> channels in smooth muscle. *J Physiol* **572**, 617–624.

Teramoto N (2006b). Pharmacological profile of U-37883A, a channel blocker of smooth muscle-type ATP-sensitive K<sup>+</sup> channels. *Cardiovasc Drug Rev* **24**, 25–32.

Teramoto N, Aishima M, Zhu HL, Tomoda T, Yunoki T, Takahashi-Yanaga F, Brading AF & Ito Y (2004). Effects of U-37883A on intracellular Ca<sup>2+</sup>-activated large-conductance K<sup>+</sup> channels in pig proximal urethral myocytes. *Eur J Pharmacol* **506**, 1–7.

Tester DJ, Tan BH, Medeiros-Domingo A, Song C, Makielski JC & Ackerman MJ (2011). Loss-of-function mutations in the KCNJ8-Encoded Kir6.1 KATP channel and sudden infant death syndrome. *Circ Cardiovasc Genet* **4**, 510–515.

Thomzig A, Prüss H & Veh RW (2003). The Kir6.1-protein, a pore-forming subunit of ATP-sensitive potassium channels, is prominently expressed by giant cholinergic interneurons in the striatum of the rat brain. *Brain Res* **986**, 132–138.

Thorneloe KS, Maruyama Y, Malcolm a T, Light PE, Walsh MP & Cole WC (2002). Protein kinase C modulation of recombinant ATP-sensitive K(+) channels composed

- of Kir6.1 and/or Kir6.2 expressed with SUR2B. *J Physiol* **541**, 65–80.
- Tian C, Zhu R, Zhu L, Qiu T, Cao Z & Kang T (2014). Potassium channels: Structures, diseases, and modulators. *Chem Biol Drug Des* **83**, 1–26.
- Tinker A, Aziz Q, Thomas A & Harvey W (2014). The role of ATP-sensitive potassium channels in cellular function and protection in the cardiovascular system. *Br J Pharmacol* **171**, 12–23.
- Tokuno S (2002). Spontaneous Ischemic Events in the Brain and Heart Adapt the Hearts of Severely Atherosclerotic Mice to Ischemia. *Arterioscler Thromb Vasc Biol* **22**, 995–1001.
- Tomai F, Crea F, Gaspardone A, Versaci F, De Paulis R, Penta de Peppo A, Chiariello L & Gioffrè PA (1994). Ischemic preconditioning during coronary angioplasty is prevented by glibenclamide, a selective ATP-sensitive K<sup>+</sup> channel blocker. *Circulation* **90**, 700–705.
- Tong H, Chen W, Steenbergen C & Murphy E (2000). Ischemic Preconditioning Activates Phosphatidylinositol-3-Kinase Upstream of Protein Kinase C. *Circ Res* **87**, 309–315.
- Tong H, Rockman HA, Koch WJ, Steenbergen C & Murphy E (2004). G Protein-Coupled Receptor Internalization Signaling Is Required for Cardioprotection in Ischemic Preconditioning. *Circ Res* **94**, 1133–1141.
- Tong X, Porter LM, Liu G, Dhar-Chowdhury P, Srivastava S, Pountney DJ, Yoshida H, Artman M, Fishman GI, Yu C, Iyer R, Morley GE, Gutstein DE & Coetzee W a (2006). Consequences of cardiac myocyte-specific ablation of KATP channels in transgenic mice expressing dominant negative Kir6 subunits. *Am J Physiol Heart Circ Physiol* **291**, H543–H551.
- Töpert C, Döring F, Wischmeyer E, Karschin C, Brockhaus J, Ballanyi K, Derst C & Karschin A (1998). Kir2.4: a novel K<sup>+</sup> inward rectifier channel associated with motoneurons of cranial nerve nuclei. *J Neurosci* **18**, 4096–4105.
- Toyoda Y, Friehs I, Parker R a, Levitsky S & McCully JD (2000). Differential role of

- sarcolemmal and mitochondrial K(ATP) channels in adenosine-enhanced ischemic preconditioning. *Am J Physiol Heart Circ Physiol* **279**, H2694–H2703.
- Trudeau MC, Warmke JW, Ganetzky B & Robertson GA (1995). HERG, a human inward rectifier in the voltage-gated potassium channel family. *Science* **269**, 92–95.
- Tsai C-H (2002). Differential Effects of Sarcolemmal and Mitochondrial KATP Channels Activated by 17beta -Estradiol on Reperfusion Arrhythmias and Infarct Sizes in Canine Hearts. *J Pharmacol Exp Ther* **301**, 234–240.
- Tsuchida A, Liu Y, Liu GS, Cohen M V & Downey JM (1994). alpha 1-adrenergic agonists precondition rabbit ischemic myocardium independent of adenosine by direct activation of protein kinase C. *Circ Res* **75**, 576–85.
- Tu Z, Yang W, Yan S, Guo X & Li X-J (2015). CRISPR/Cas9: a powerful genetic engineering tool for establishing large animal models of neurodegenerative diseases. *Mol Neurodegener* **10**, 35.
- Turrens JF, Beconi M, Barilla J, Chavez UB & McCord JM (1991). Mitochondrial generation of oxygen radicals during reoxygenation of ischemic tissues. *Free Radic Res Commun* **12–13 Pt 2**, 681–689.
- Um SY & McDonald T V. (2007). Differential Association between HERG and KCNE1 or KCNE2 ed. Valdivia R. *PLoS One* **2**, e933.
- Unniyampurath U, Pilankatta R & Krishnan MN (2016). RNA Interference in the Age of CRISPR: Will CRISPR Interfere with RNAi? *Int J Mol Sci* **17**, 291.
- Vandenberg JI, Bett GC & Powell T (1997). Contribution of a swelling-activated chloride current to changes in the cardiac action potential. *Am J Physiol* **273**, C541-7.
- Varró A, Lathrop DA, Hester SB, Nánási PP, Papp JGY, Varró A, Lathrop DA, Hester SB, Nánási PP & Papp JGY (1993). Ionic currents and action potentials in rabbit, rat, and guinea pig ventricular myocytes. *Basic Res Cardiol* **88**, 93–102.
- Van Veen TAB, Van Rijen HVM & Opthof T (2001). Cardiac gap junction channels:

- Modulation of expression and channel properties. *Cardiovasc Res* **51**, 217–229.
- Veldhuis MG (2015). A Little Too Much: Cardiac Electrophysiological Effects of Elevated Inward Rectifying Current Carried by the K<sub>v</sub>(IR)2.1 Ion Channel Protein. *Adapt Med* **7**, 1–8.
- Verkerk AO, Wilders R, van Borren MMGJ, Peters RJG, Broekhuis E, Lam K, Coronel R, de Bakker JMT & Tan HL (2007). Pacemaker current (I<sub>f</sub>) in the human sinoatrial node. *Eur Heart J* **28**, 2472–2478.
- Vincent GM, Timothy K, Fox J & Zhang L (1999). The inherited long QT syndrome: from ion channel to bedside. *Cardiol Rev* **7**, 44–55.
- Wang Q, Curran ME, Splawski I, Burn TC, Millholland JM, VanRaay TJ, Shen J, Timothy KW, Vincent GM, de Jager T, Schwartz PJ, Toubin JA, Moss AJ, Atkinson DL, Landes GM, Connors TD & Keating MT (1996). Positional cloning of a novel potassium channel gene: KVLQT1 mutations cause cardiac arrhythmias. *Nat Genet* **12**, 17–23.
- Wang S, Cone J & Liu Y (2001a). Dual roles of mitochondrial K(ATP) channels in diazoxide-mediated protection in isolated rabbit hearts. *Am J Physiol Hear Circ Physiol* **280**, H246-55.
- Wang S, Long C, Chen J, Cui W, Zhang Y, Zhang H & Wang H (2016). Pharmacological evidence : a new therapeutic approach to the treatment of chronic heart failure through SUR2B / Kir6 . 1 channel in endothelial cells. *Nat Publ Gr* **38**, 41–55.
- Wang S, Song L, Lakatta EG & Cheng H (2001b). Ca<sup>2+</sup> signalling between single L-type Ca<sup>2+</sup> channels and ryanodine receptors in heart cells. *Nature* **410**, 592–596.
- Wang X, Wu J, Li L, Chen F, Wang R & Jiang C (2003). Hypercapnic acidosis activates KATP channels in vascular smooth muscles. *Circ Res* **92**, 1225–1232.
- Wang Y, Yu L, Cui N, Jin X, Zhu D & Jiang C (2013). Differential sensitivities of the vascular KATP channel to various PPAR activators. *Biochem Pharmacol* **85**, 1495–1503.

- Warren M, Guha PK, Berenfeld O, Zaitsev A, Anumonwo JMB, Dhamoon AS, Bagwe S, Taffet SM & Jalife J (2003). Blockade of the Inward Rectifying Potassium Current Terminates Ventricular Fibrillation in the Guinea Pig Heart. *J Cardiovasc Electrophysiol* **14**, 621–631.
- Watanabe H, Darbar D, Kaiser DW, Jiramongkolchai K, Chopra S, Donahue BS, Kannankeril PJ & Roden DM (2009). Mutations in Sodium Channel 1- and 2-Subunits Associated With Atrial Fibrillation. *Circ Arrhythmia Electrophysiol* **2**, 268–275.
- Watanabe H, Koopmann TT, Scouarnec S Le, Yang T, Ingram CR, Schott J, Demolombe S, Probst V, Anselme F, Escande D & Wiesfeld ACP (2008). Sodium channel  $\beta$ 1 subunit mutations associated with Brugada syndrome and cardiac conduction disease in humans. *Structure* **118**, 268–275.
- Watanabe T, Delbridge LM, Bustamante JO & McDonald TF (1983). Heterogeneity of the action potential in isolated rat ventricular myocytes and tissue. *Circ Res* **52**, 280–290.
- Wellman GC, Barrett-Jolley R, Köppel H, Everitt D & Quayle JM (1999). Inhibition of vascular K(ATP) channels by U-37883A: a comparison with cardiac and skeletal muscle. *Br J Pharmacol* **128**, 909–916.
- Winslow RL, Cortassa S, O'Rourke B, Hashambhoy YL, Rice JJ & Greenstein JL (2011). Integrative modeling of the cardiac ventricular myocyte. *Wiley Interdiscip Rev Syst Biol Med* **3**, 392–413.
- Wojtovich AP, Nadtochiy SM, Brookes PS & Nehrke K (2012). Ischemic preconditioning: the role of mitochondria and aging. *Exp Gerontol* **47**, 1–7.
- Wojtovich AP, Urciuoli WR, Chatterjee S, Fisher AB, Nehrke K & Brookes PS (2013). Kir6.2 is not the mitochondrial KATP channel but is required for cardioprotection by ischemic preconditioning. *Am J Physiol - Hear Circ Physiol* **304**, H1439–H1445.
- Wojtovich AP, Williams DM, Karcz MK, Lopes CMB, Gray DA, Nehrke KW & Brookes PS (2010). A novel mitochondrial KATP channel assay. *Circ Res* **106**, 1190–1196.
- Woodcock EA, Kistler PM & Ju YK (2009). Phosphoinositide signalling and cardiac

- arrhythmias. *Cardiovasc Res* **82**, 286–295.
- Woodcock EA & Matkovich SJ (2005). Cardiomyocytes structure, function and associated pathologies. *Int J Biochem Cell Biol* **37**, 1746–1751.
- Workman AJ et al. (2001). The contribution of ionic currents to changes in refractoriness of human atrial myocytes associated with chronic atrial fibrillation. *Cardiovasc Res* **52**, 226–235.
- Workman AJ (2010). UKPMC Funders Group Author Manuscript Cardiac adrenergic control and atrial fibrillation. *Cardiovasc Res* 1–23.
- Workman AJ, Marshall GE, Rankin AC, Smith GL & Dempster J (2012). Transient outward K<sup>+</sup> current reduction prolongs action potentials and promotes afterdepolarisations: a dynamic-clamp study in human and rabbit cardiac atrial myocytes. *J Physiol* **590**, 4289–4305.
- Wu G, Ai T, Kim JJ, Mohapatra B, Xi Y, Li Z, Abbasi S, Purevjav E, Samani K, Ackerman MJ, Qi M, Moss AJ, Shimizu W, Towbin JA, Cheng J & Vatta M (2008). -1- Syntrophin Mutation and the Long-QT Syndrome: A Disease of Sodium Channel Disruption. *Circ Arrhythmia Electrophysiol* **1**, 193–201.
- Wu Q, Shen T, Shao L, Ma H & Wang J (2012). Ischemic Postconditioning Mediates Cardioprotection Via PI3K/GSK-3 $\beta$ / $\beta$ -Catenin Signaling Pathway in Ischemic Rat Myocardium. *Shock* **38**, 165–169.
- Xu H, Li H & Nerbonne JM (1999). Elimination of the transient outward current and action potential prolongation in mouse atrial myocytes expressing a dominant negative Kv4  $\alpha$  subunit. *J Physiol* **519**, 11–21.
- Yamada K, Ji JJ, Yuan H, Miki T, Sato S, Horimoto N, Shimizu T, Seino S & Inagaki N (2001). Protective role of ATP-sensitive potassium channels in hypoxia-induced generalized seizure. *Science* **292**, 1543–1546.
- Yamada M, Isomoto S, Matsumoto S, Kondo C, Shindo T, Horio Y & Kurachi Y (1997). Sulphonylurea receptor 2B and Kir6.1 form a sulphonylurea-sensitive but ATP-

- insensitive K<sup>+</sup> channel. *J Physiol* **499 (Pt 3)**, 715–720.
- Yamada M, Isomoto S, Matsumoto S, Kondo C, Shindo T, Horio Y & Kurachi Y (2011). sensitive but ATP-insensitive K<sup>+</sup> channel. *Physiology* 715–720.
- Yamada S, Kane GC, Behfar A, Liu X-K, Dyer RB, Faustino RS, Miki T, Seino S & Terzic A (2006). Protection conferred by myocardial ATP-sensitive K<sup>+</sup> channels in pressure overload-induced congestive heart failure revealed in KCNJ11 Kir6.2-null mutant. *J Physiol* **577**, 1053–1065.
- Yang C, Talukder MAH, Varadharaj S, Velayutham M & Zweier JL (2013). Early ischaemic preconditioning requires Akt- and PKA-mediated activation of eNOS via serine1176 phosphorylation. *Cardiovasc Res* **97**, 33–43.
- Yang X, Cohen M V & Downey JM (2010). Mechanism of cardioprotection by early ischemic preconditioning. *Cardiovasc drugs Ther* **24**, 225–234.
- Yang XM, Philipp S, Downey JM & Cohen M V. (2006). Atrial natriuretic peptide administered just prior to reperfusion limits infarction in rabbit hearts. *Basic Res Cardiol* **101**, 311–318.
- Yang XM, Proctor JB, Cui L, Krieg T, Downey JM & Cohen M V. (2004). Multiple, brief coronary occlusions during early reperfusion protect rabbit hearts by targeting cell signaling pathways. *J Am Coll Cardiol* **44**, 1103–1110.
- Yang Y, Shi Y, Guo S, Zhang S, Cui N, Shi W, Zhu D & Jiang C (2008). PKA-dependent activation of the vascular smooth muscle isoform of KATP channels by vasoactive intestinal polypeptide and its effect on relaxation of the mesenteric resistance artery. *Biochim Biophys Acta - Biomembr* **1778**, 88–96.
- Yasuda S, Kobayashi H, Iwasa M, Kawamura I, Sumi S, Narentuoya B, Yamaki T, Ushikoshi H, Nishigaki K, Nagashima K, Takemura G, Fujiwara T, Fujiwara H & Minatoguchi S (2009). Antidiabetic drug pioglitazone protects the heart via activation of PPAR-gamma receptors, PI3-kinase, Akt, and eNOS pathway in a rabbit model of myocardial infarction. *Am J Physiol Hear Circ Physiol* **296**, H1558-65.

- Ye Y, Keyes KT, Zhang C, Perez-Polo JR, Lin Y & Birnbaum Y (2010). The myocardial infarct size-limiting effect of sitagliptin is PKA-dependent, whereas the protective effect of pioglitazone is partially dependent on PKA. *AJP Hear Circ Physiol* **298**, H1454–H1465.
- Yin H, Chao L & Chao J (2008). Nitric oxide mediates cardiac protection of tissue kallikrein by reducing inflammation and ventricular remodeling after myocardial ischemia/reperfusion. *Life Sci* **82**, 156–165.
- Yoshida H, Feig JE, Morrissey A, Ghiu IA, Artman M & Coetzee WA (2004a). KATP channels of primary human coronary artery endothelial cells consist of a heteromultimeric complex of Kir6.1, Kir6.2, and SUR2B subunits. *J Mol Cell Cardiol* **37**, 857–869.
- Yoshida M, Nakakimura K, Cui YJ, Matsumoto M & Sakabe T (2004b). Adenosine A(1) receptor antagonist and mitochondrial ATP-sensitive potassium channel blocker attenuate the tolerance to focal cerebral ischemia in rats. *J Cereb Blood Flow Metab* **24**, 771–779.
- Young PJ, Dalley P, Garden A, Horrocks C, La Flamme A, Mahon B, Miller J, Pilcher J, Weatherall M, Williams J, Young W & Beasley R (2012). A pilot study investigating the effects of remote ischemic preconditioning in high-risk cardiac surgery using a randomised controlled double-blind protocol. *Basic Res Cardiol* **107**, 256.
- Yu L, Jin X, Cui N, Wu Y, Shi Z, Zhu D & Jiang C (2012). Rosiglitazone selectively inhibits K(ATP) channels by acting on the K(IR) 6 subunit. *Br J Pharmacol* **167**, 26–36.
- Yu L, Jin X, Yang Y, Cui N & Jiang C (2011). Rosiglitazone inhibits vascular K ATP channels and coronary vasodilation produced by isoprenaline. *Br J Pharmacol* **164**, 2064–2072.
- Yuan X, Jing S, Wu L, Chen L & Fang J (2014). Pharmacological postconditioning with tanshinone IIA attenuates myocardial ischemia-reperfusion injury in rats by activating the phosphatidylinositol 3-kinase pathway. *Exp Ther Med* **9**, 973–977.

- Yunoki T, Teramoto N & Ito Y (2003). Functional involvement of sulphonylurea receptor (SUR) type 1 and 2B in the activity of pig urethral ATP-sensitive K<sup>+</sup> channels. *Br J Pharmacol* **139**, 652–660.
- Zamore PD, Tuschl T, Sharp PA & Bartel DP (2000). RNAi: double-stranded RNA directs the ATP-dependent cleavage of mRNA at 21 to 23 nucleotide intervals. *Cell* **101**, 25–33.
- Zatta AJ, Kin H, Lee G, Wang N, Jiang R, Lust R, Reeves JG, Mykytenko J, Guyton RA, Zhao ZQ & Vinten-Johansen J (2006). Infarct-sparing effect of myocardial postconditioning is dependent on protein kinase C signalling. *Cardiovasc Res* **70**, 315–324.
- Zeng H, Horie K, Madisen L, Pavlova MN, Gragerova G, Rohde AD, Schimpf BA, Liang Y, Ojala E, Kramer F, Roth P, Slobodskaya O, Dolka I, Southon EA, Tessarollo L, Bornfeldt KE, Gragerov A, Pavlakis GN & Gaitanaris GA (2008). An Inducible and Reversible Mouse Genetic Rescue System ed. Beier D. *PLoS Genet* **4**, e1000069.
- Zeng WZ, Li XJ, Hilgemann DW & Huang CL (2003). Protein kinase C inhibits ROMK1 channel activity via a phosphatidylinositol 4,5-bisphosphate-dependent mechanism. *J Biol Chem* **278**, 16852–16856.
- Zerangue N, Schwappach B, Jan YN & Jan LY (1999). A New ER Trafficking Signal Regulates the Subunit Stoichiometry of Plasma Membrane KATP Channels. *Neuron* **22**, 537–548.
- Zhang C, Miki T, Shibasaki T, Yokokura M, Saraya A & Seino S (2006). Identification and characterization of a novel member of the ATP-sensitive K<sup>+</sup> channel subunit family, Kir6.3, in zebrafish. *Physiol Genomics* **24**, 290–297.
- Zhang DQ & McMahon DG (2000). Direct gating by retinoic acid of retinal electrical synapses. *Proc Natl Acad Sci U S A* **97**, 14754–14759.
- Zhang H, Flagg TP & Nichols CG (2010). Cardiac sarcolemmal KATP channels: Latest twists in a questing tale! *J Mol Cell Cardiol* **48**, 71–75.

Zhao Z-Q, Corvera JS, Halkos ME, Kerendi F, Wang N-P, Guyton RA & Vinten-Johansen J (2003). Inhibition of Myocardial Injury by Ischemic Postconditioning During Reperfusion: Comparison with Ischemic Preconditioning. *Am J Physiol* **285**, H579–H588.

Zhou M, Tanaka O, Sekiguchi M, Sakabe K, Anzai M, Izumida I, Inoue T, Kawahara K & Abe H (1999). Localization of the ATP-sensitive potassium channel subunit (Kir6.1/uK(ATP)-1) in rat brain. *Brain Res Mol Brain Res* **74**, 15–25.

Zicha S, Fernández-Velasco M, Lonardo G, L'Heureux N & Nattel S (2005). Sinus node dysfunction and hyperpolarization-activated (HCN) channel subunit remodeling in a canine heart failure model. *Cardiovasc Res* **66**, 472–481.

